# ROCK MASS-TUNNEL SUPPORT INTERACTION ANALYSIS

**A THESIS**

submitted in fulfilment of the
requirements for the award of the degree
of
DOCTOR OF PHILOSOPHY
in
CIVIL ENGINEERING

By

## MANOJ KUMAR VERMAN

**DEPARTMENT OF CIVIL ENGINEERING
UNIVERSITY OF ROORKEE
ROORKEE-247 667 (INDIA)**

**FEBRUARY, 1993**

DEDICATED  TO  MUMMY - PAPA
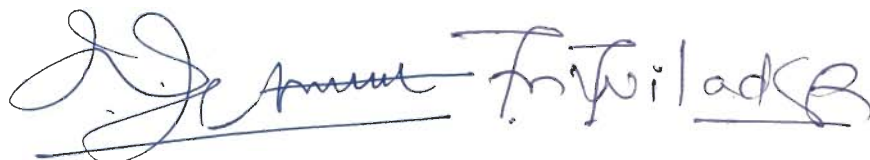
# CANDIDATE'S DECLARATION

I hereby certify that the work which is being presented in the thesis entitled **ROCK MASS - TUNNEL SUPPORT INTERACTION ANALYSIS**, in fulfilment of the requirement for the award of the **Degree of Doctor of Philosophy**, submitted in the Department of Civil Engineering of the University of Roorkee, is an authentic record of my own work carried out during the period from September, 1985 to December, 1992 under the supervision of Dr. Bhawani Singh, Dr. M.N. Viladkar, and Dr. J.L. Jethwa.

The matter embodied in this thesis has not been submitted by me for the award of any other degree.

Dated: February 1, 1993

**(MANOJ KUMAR VERMAN)**

This is to certify that the above statement made by the candidate is correct to the best of our knowledge.
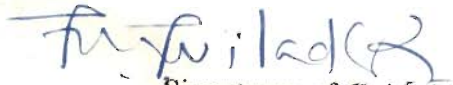
**(Dr. J.L. JETHWA)**
Scientist-in-charge,
Central Mining Research
Station Unit,
**NAGPUR, INDIA**

**(Dr. M.N. VILADKAR)**
Reader,
Deptt. of Civil Engg.,
University of Roorkee,
**ROORKEE, INDIA**

**(Dr. BHAWANI SINGH)**
Professor,
Deptt. of Civil Engg.,
University of Roorkee,
**ROORKEE, INDIA**

The Ph.D. Viva-Voce examination of **Mr. Manoj Kumar Verman, Research Scholar** has been held on....Aug. 21, 1993.......

**Signatures of Guide(s)**

**Signature of External Examiner(s)**
21.8.93

# ACKNOWLEDGEMENTS

## ABSTRACT

The application of the rock mass-tunnel support interaction analysis in designing the tunnel support system is well known. An approach for quick and reliable determination of the ground reaction (response) and the support reaction curves, which are the two essential components of the rock mass-tunnel support interaction analysis, has been proposed. The proposed approach is based on the results of field instrumentation and other related field studies carried out in nine Indian tunnels. Description of the geology and its influence on the tunnelling conditions, as well as the details of the field studies, have been presented for these tunnelling projects located in the lower and middle Himalayas and in the peninsular region of India.

As the first step towards obtaining the ground reaction curve, empirical correlations and a design chart have been proposed for the three types of tunnelling conditions, namely, self-supporting, non-squeezing, and squeezing, on the basis of the analysis of data obtained from the Indian tunnels and some of the case-histories reported by Barton et al. (1974). The correlations show that the ground condition depends on the rock mass quality(Q), height of overburden and the tunnel size. The correlations have important practical benefits, especially with regards to the possibility of achieving a favourable ground condition by changing the tunnel alignment to obtain a better rock mass quality, or a reduced overburden, or both. Alternatively, two or three smaller tunnels may be chosen instead of a larger tunnel to avoid squeezing ground condition, thereby

reducing the support problems and the construction time.

After predicting the expected ground condition, the next step is to determine the ground reaction curve for the predicted ground condition. Determination of the ground reaction curves for the self-supporting and the non-squeezing conditions depends on the modulus of deformation of the rock mass which is normally obtained from expensive and time-consuming uniaxial jacking tests, whose results often have a large scatter. An empirical correlation has, therefore, been proposed for prediction of the modulus of deformation of the rock mass. The correlation indicates that the modulus of deformation of the rock mass increases with RMR and the tunnel depth. This depth dependency of the modulus of deformation is likely to be more pronounced in weaker rock masses and almost absent in strong, brittle rock masses.

For using the correlation for the modulus of deformation, the RMR value may either be obtained in the field or, if one prefers to use the Q-system, from a correlation proposed between RMR and $Q_m$, where $Q_m$ is the modified Q (with SRF equal to 1). This modification has been carried out to overcome the uncertainities in determination of SRF.

A semi-empirical correlation has been proposed for obtaining the value of cohesion of the rock mass. The correlation indicates the mobilisation of a much higher cohesion around the underground openings than the values suggested by Bieniawski (1979) on the basis of the field data of rock slopes. The observation of this

'apparant strength enhancement' on the basis of the field instrumentation data, is well supported by a number of laboratory tests conducted by several investigators on thick-walled hollow cylindrical samples. This apparent strength enhancement may be attributed to anisotropy in strength, statistical variation in strength and confining conditions around tunnels. As such, a strength enhancement factor of 4 to 6 is recommended which should be multiplied with the cohesion parameter from block shear tests on rock mass for obtaining the ground reaction curve in the squeezing ground condition.

The behaviour of the steel rib-backfill support system has been studied at a number of tunnel sections, in order to propose an approach for determination of the support reaction curve. The study shows that the steel rib-backfill support system exhibits a non-linear behaviour under pressure, unlike the normally assumed linear elastic behaviour, due to the continuously changing backfill stiffness. The backfill, though not the main load carrying element, significantly influences the behaviour of the support system under pressure. The behaviour of three types of backfills, viz, concrete, gravel, and tunnel-muck, under pressure, has been studied. The conctete backfill provides a stiffer support than the other two types of backfills and is, therefore, preferable for the elastic ground condition. The tunnel-muck and the gravel backfills may be more suited to the moderately squeezing and the highly squeezing ground conditions respectively, as the latter is relatively more flexible.

With the help of the proposed rock mass-tunnel support

interaction analysis, the effect of charging of the water conductor system on the support pressure has been studied. The study has revealed that the additional support pressure on the final support due to the charging of the water conductor system, could be as high as 80 percent of the insitu stress in elastic ground condition. The proposed rock mass - tunnel support interaction analysis further shows that the short-term support pressure is practically independent of the tunnel size if the $A_s/S$ and $t_b$ values are increased in direct proportion to the tunnel size, where $A_s$ is the cross-section area of the steel rib, S is the rib spacing and $t_b$ is the backfill thickness. This explains the modern concept of support pressure (Barton et al., 1974 and Singh et al., 1992) based on extensive field observations.

Knowledge of the stand-up time of an underground opening helps in determining the time by which the support installation may be delayed and it may, therefore, have a bearing on the selection of the support system. Empirical correlations have been proposed for determination of the stand-up time for underground openings with arch roof and flat roof. The correlations indicate that the stand-up time of an underground opening depends on its span, RMR, and height of overburden, with RMR having the most dominant influence. The influence of the opening size is more pronounced in openings located at deeper depths as compared to the shallow openings. The stand-up time is also influenced by the shape of the underground opening. An opening with an arch roof has a better stand-up time than that

with a flat roof for a given value of RMR. This difference, however, decreases with increase in RMR and ceases to exist for RMR $\geq$ 65.

Finally, it should be added that tunnelling is an art and adventure due to several uncertainities in exploration and behaviour of the rock masses, particularly in the Himalaya. The key to the management of the uncertainities lies in monitoring through instrumentation, contingency plans, and team spirit.

# CONTENTS

## NOTATIONS

| SYMBOL | DESCRIPTION |
|---|---|
| $A_s$ | cross-sectional area of steel rib |
| $a$ | radius of tunnel opening |
| $B$ | width or span of opening |
| $B_s$ | self-supporting span of opening |
| $B', b'$ | material property constants in Eq.2.6 |
| $b$ | i) radius of broken (elastic) zone<br>ii) radius of fractured region in Eq.2.2 |
| $b_i, b_m, b_o$ | radii of inner, middle and outer plastic zones in Fig.2.4 |
| $C_*$ | compressibility ratio defined by Eq.2.13 |
| Ch. | chainage |
| $c$ | i) cohesion of rock mass<br>ii) radius of plastic zone in Fig.2.2 |
| $c_p$ | peak cohesion of rock mass in elastic zone |
| $c_{pm}$ | mobilised cohesion of rock mass |
| $c_r$ | residual cohesion of rock mass in plastic zone |
| $D$ | parameter defined by Eqs.2.9c and 2.17 |
| $E$ | modulus of elasticity of rock mass |
| $E_1, E_2$ | moduli of deformation of rock mass in horizontal and vertical directions respectively |
| ESR | excavation support ratio |
| $E_b$ | modulus of elasticity of backfill |
| $E_c$ | modulus of elasticity of concrete |
| $E_d$ | modulus of deformation of rock mass |
| $E_{dry}$ | modulus of deformation of dry rock mass |

| SYMBOL | DESCRIPTION |
|---|---|
| $E_{min}$ | smaller of the two moduli of deformation of rock mass in horizontal and vertical directions |
| $E_r$ | modulus of elasticity of rock material |
| $E_s$ | modulus of elasticity of steel |
| $E_{sat}$ | modulus of deformation of saturated rock mass |
| $e$ | coefficient of volumetric expansion for failed rock mass |
| $e_{av}$ | average plastic dilation in Eq.2.9 |
| $F_*$ | flexibility ratio defined by Eq.2.14 |
| $f$ | correction factor for effect of tunnel depth on modulus of deformation of rock mass in Eq.6.8 and for effect of overburden on support pressure in Eq.7.11 |
| $f_1, f_2 .. f_n$ | straight line yield functions representing piecewise linear approximation of non-linear yield function in Fig.2.3 |
| | depth on modulus of elasticity of rock mass in Eq.6.7 |
| $f_t$ | ratio of stand-up times of arch and flat openings |
| $f'_w, f'_r$ | normalised observed wall and roof support pressures respectively |
| $G$ | shear modulus of rock mass |
| $H$ | height of overburden |
| $H_p$ | height of rock load |
| $H_t$ | height of opening |
| $I$ | moment of inertia of steel rib |
| $J$ | $(1+\sin\phi)/(1-\sin\phi)$ in Eqs.2.3 and 2.9e |
| $J_a$ | joint alteration number |
| $J_n$ | joint set number |
| $J_r$ | joint roughness number |

| SYMBOL | DESCRIPTION |
|---|---|
| $J_w$ | joint water reduction factor |
| $K$ | $(1+\sin\phi)/(1-\sin\phi)$ in Eq.6.21 |
| $k$ | stiffness of support system |
| $k_b$ | stiffness of backfill |
| $k_c$ | stiffness of concrete lining |
| $k_s$ | stiffness of steel ribs |
| $M$ | parameter defined by Eqs.2.9f, 2.9g and 2.19 |
| $M_\phi, M_\gamma$ | parameters defined by Eqs. 2.11a and 2.11c respectively |
| $m, n$ | Parameters in Fairhurst parabolic failure criterion |
| $m, s$ | material constants for original rock mass in Eqs. 2.17 and 2.19 |
| $m_p$ | $(1+\sin\phi p)/(1-\sin\phi r)$ in Eq. 2.23a |
| $m_r$ | $(1+\sin\phi r)/(1-\sin\phi r)$ in Eq. 2.23b |
| $m_r, s_r$ | material constants for broken rock mass in Eqs. 2.18 and 2.20 |
| $N$ | parameter defined by Eq.2.20 |
| $p$ | support load in Eq.3.1 |
| $p_h$ | short-term support pressure in horizontal |
| $p_i$ | short-term support pressure (or internal pressure) |
| $p_{idry}$ | short-term support pressure in dry condition |
| $p_{if}$ | short-term support pressure at equilibrium |
| $p_{imax}$ | maximum support capacity of steel ribs direction |
| $p_{isat}$ | short-term support pressure in saturated condition |
| $p_o$ | insitu stress magnitude |
| $p_{roof}$ | ultimate support pressure on roof |

| SYMBOL | DESCRIPTION |
|---|---|
| $p_v$ | short-term support pressure in vertical direction |
| $p_w$ | seepage pressure on tunnel lining in Eq.7.17 |
| $p_{wall}$ | ultimate support pressure on wall |
| $p_w, p_r$ | predicted short-term wall and roof support pressures respectively in Eq.7.11 |
| $p_w^{obsd}, p_r^{obsd}$ | measured short-term wall and roof support pressures respectively in Eq.7.11 |
| $Q$ | rock mass quality of Barton et al. |
| $Q_m$ | modified Q (with SRF=1) |
| $Q_w$ | wall factor |
| $q_c$ | uniaxial compressive strength of intact rock |
| RD | relative distance |
| RF | reduction factor in Eqs.7.17 and 7.21 |
| RMR | Bieniawski's Rock Mass Rating |
| RQD | Rock Quality Designation |
| RSR | Rock Structure Rating of Wickham et al. |
| $r_{ic}, r_{ec}$ | inner and outer radii of the ring of concrete lining (Eq.2.7) |
| S | spacing of steel ribs |
| SRF | stress reduction factor |
| $S_a$ | active span |
| $t_{arch}, t_{flat}$ | stand-up time for openings with arch roof and flat roof respectively |
| $t_{arch}^{obsd}, t_{flat}^{obsd}$ | stand-up time for openings with arch roof and flat roof respectively |
| $t_b$ | thickness of backfill |
| $t_c$ | thickness of concrete lining |
| $u_a$ | radial tunnel deformation or tunnel-wall displacement |

| SYMBOL | DESCRIPTION |
|---|---|
| $u_{ao}$ | initial radial tunnel closure before installation of supports |
| $u_b$ | radial displacement of elastic-plastic boundary |
| $u_r$ | tunnel-wall displacement at any point close to the face in Eq. 2.21 |
| $w_1, w_2 .. w_n$ | angles with horizontal of straight line yield functions representing piecewise linear approximation of non-linear yield function in Fig.2.3 |
| $w_e$ | ric/rec in Eq. 2.7 |
| X | proportionality factor defining the ratio of tunnel-wall displacement at any point close to the face to the maximum tunnel-wall displacement far away from the face in Eq.2.21. |
| z | face advance |
| $\alpha$ | (i) power of H in Eqs.6.9,6.11 and 6.27 to 6.30 representing depth or confining pressure dependency of modulus of deformation of rock mass<br>(ii) $2\sin\phi/(1-\sin\phi)$ in Eqs. 2.2 and 2.5 |
| ß | angle of a point from horizontal in Eq.2.3 |
| $\gamma$ | unit weight of rock mass |
| $\Delta$ pisat | additional support pressure due to charging of water conductor system |
| $\epsilon_1$ | major Principal strain |
| $\nu$ | Poisson's ratio of rock mass |
| $\nu_c$ | Poisson's ratio of concrete |
| $\nu_s$ | Poisson's ratio for tunnel support in Eqs.2.13 & 2.14 |
| $\sigma_1$ | major principal stress (yield stress in Eq.2.6) |
| $\sigma_3$ | minor principal stress (confining pressure in Eq.2.6) |
| $\sigma_b$ | radial stress at elastic-plastic interface in Eqs.2.3 and 2.23e |

| SYMBOL | DESCRIPTION |
|--------|-------------|
| $\sigma_{dp}$ | $2cp$ Cos $\phi p/(1-\sin\phi p/(1-\sin\phi p)$ in Eqs.2.23a and 2.23f |
| $\sigma_{dr}$ | $2cr$ Cos $\phi r/(1-\sin \sigma r)$ in Eqs.2.23b, 2.23e, 2.24 and 2.25 |
| $\sigma_{H2}, \sigma_{H1}$ | minimum and maximum applied boundary stresses in Eq.2.26 |
| $\sigma_r$ | radial stress |
| $\sigma_{re}$ | radial stress in elastic zone |
| $\sigma_r^{pl}$ | radial stress in plastic zone |
| $\sigma_{ys}$ | yield strength of steel |
| $\sigma_z$ | axial stress |
| $\sigma_\Theta$ | tangential stress |
| $\sigma_{\Theta e}$ | tangential stress in elastic zone |
| $\sigma_{\Theta f}$ | breakout stress in Eq.2.26 |
| $\sigma_{\Theta pl}$ | tangential stress in plastic zone |
| $\rho$ | rock density in Eq.2.26 |
| $\bar{\tau}_{rz}$ | average shear stress within broken zone in Eq.2.21 |
| $\phi$ | angle of internal friction of rock mass |
| $\phi_p$ | peak angle of internal friction of rock mass in elastic zone |
| $\phi_r$ | residual angle of internal friction of rock mass in plastic zone |

# LIST OF TABLES

# LIST OF FIGURES

# CHAPTER 1

# CHAPTER 1

## INTRODUCTION

### 1.1 GENERAL

Creation of an opening in a rock mass disturbs the natural state of equilibrium which exists before the excavation. In order to achieve the state of equilibrium again, the opening tries to close in. In a competent rock mass, the equilibrium is achieved after certain amount of closure takes place and the opening becomes stable. In a weaker rock mass, the state of equilibrium is achieved through collapse. However, to maintain the required size of the tunnel, closure cannot be permitted to take place beyond a certain amount. It is, therefore, necessary to help the rock mass to support itself. This help is rendered by the installation of an external element, known as the support system, which is placed around the tunnel periphery and is designed to limit the tunnel closure within permissible limits. Rock mass and tunnel support system are, therefore, two of the most important components of a tunnel and the behaviour of a supported tunnel depends, to a great extent, on interaction between the two. This interactive nature may be studied with the help of the ground reaction (response) and the support reaction curves which represent the load-deflection behaviour of the rock mass and the support system respectively. The point of intersection of these curves represents the state of equilibrium, i.e., at this point the support pressure required to limit further deformation of the opening is balanced by the support pressure available from the support system.

## 1.2 ROCK-SUPPORT INTERACTION - THE BASIC CONCEPT

To understand the basic concept of the rock mass-tunnel support interaction, it is worthwhile to reproduce here an excellent explanation of the problem presented by Daemen (1977). Although this has been previously reproduced by some authors (e.g. Hoek & Brown, 1980; Bieniawski, 1984; Sharma, 1985) and a repetition once again may appear to be a little awkward to those familiar with the literature on the subject, it is an effective way of bringing out the importance of the interactive nature of the rock mass and the support system.

Daemen (1977) presented his explanation through a figure, reproduced as Fig.1.1 which shows different steps of tunnel excavation and support (steel ribs) installation. The horizontal and the vertical in situ stresses are assumed to be equal and to have a magnitude $p_o$. All the steps pertain to a tunnel section X-X. In the lower part of the figure, the ground reaction and the support reaction curves for the tunnel section under consideration are presented and points corresponding to different steps, are marked on these curves.

Step 1 pertains to the situation when the tunnel face has not yet reached the section X-X and the rock mass there is still in a state of pre-excavation equilibrium. This situation is denoted by point A on the ground-reaction curve where the pressure required to be supported by the support system is equal to $p_o$. In fact, at this stage, the support is being provided by the rock mass inside the dotted line shown in the cross-section

STEP 1

STEP 2

STEP 3

STEP 4

STEP 5

SECTION X-X

RADIAL DEFORMATION u

EXCAVATED PROFILE

TUNNEL PROFILE

SUPPORT PRESSURE $P_i$

A  $P_i = P_o$

LINEAR-ELASTIC DIFORMATION

START OF FAILURE OF ROCK SURROUNDING TUNNEL

SUPPORT REACTION

LOAD-DEFORMATION CURVE FOR TUNNEL ROOF

LOAD-DEFORMATION CURVE FOR TUNNEL SIDEWALL

RADIAL SUPPORT PRESSURE $P_i$ ⟶

PRESSURE REQUIRED TO LIMIT DEFORMATION

PRESSURE AVAILABLE FROM SUPPORT

RADIAL DEFORMATION u ⟶

Fig.1.1 - Concept  of Rock Mass-Tunnel Support Interaction
(after Daemen, 1977)

in step 1.

In step 2, the rock mass from within the dotted line is excavated as the tunnel face advances beyond section X-X. Removal of the rock mass which was acting as a support means that the available support pressure has now become equal to zero. However, this will not result in a collapse of the tunnel as the support is now being provided by the restraint available due to the proximity of the tunnel face to Section X-X. The support pressure now available due to this restraint, denoted by points B & C (on ground reaction curves for tunnel roof and side walls respectively), limits the deformation to a value on X-axis corresponding to these points. The support pressure required to limit the tunnel roof deformation is higher than that required to limit the sidewall deformation because the weight of the loosened rock mass above the tunnel roof is added to the support pressure required to limit the tunnel roof deformation.

In step 3, the steel ribs have been installed at section X-X. However, since the tunnel face has not advanced further, no further deformation has taken place (assuming that there is no time-dependent deformation). The supports at section X-X, therefore, carry no load and this situation is denoted by point D which is the starting point for the support-reaction curve.

Step 4 shows that the tunnel face has moved about 1.5 times the tunnel diameter beyond section X-X and the restraint provided by the proximity of the tunnel face is now considerably reduced. This results in an additional radial deformation of the

tunnel (indicated by curves BFH and CEG) which, in turn, induces load on the support system. The support system, acting as a stiff spring, provides more and more support pressure with increasing tunnel deformation and the support-reaction curve follows the path DEF.

In step 5 the restraint provided by the face at section X-X has totally disappeared as the face has moved much beyond the section. If no supports were installed, the radial tunnel deformation would have continued to increase as indicated by the curves EG and FH. In the case of sidewalls, the support pressure required to limit further deformation drops to zero at point G and, in this case, the sidewalls become stable. For the roof, however, the required support pressure drops to a minimum (denoted by point H) and then begins to rise again. This is because the downward movement of the loosened rock mass above the roof causes more rock mass to become loose. The weight of this additional loose rock mass is added to the required support pressure. The continuously rising trend of the ground-reaction curve for the roof shows that the roof would have collapsed if no support had been installed.

The most important feature of Fig.1.1 is the point of intersection of the ground reaction and the support reaction curves (denoted by E & F for sidewalls and roof respectively). At this point, the support pressure required to limit further deformation is balanced by the pressure available from the support system. Thus, at this point, the supported tunnel attains a state of equilibrium.

The example of Fig.1.1 adequately brings out the importance of considering the interactive nature of the rock mass and the support system for a rational design of the latter. For this, the load-deflection behaviour of both rock mass and support system must be clearly understood and a lot of literature has appeared in this respect.

## 1.3 BRIEF REVIEW OF LITERATURE

For the elastic behaviour of the rock mass, theory of elasticity gives solutions for stresses and displacements. For the elasto-plastic behaviour of the rock mass, many authors have developed expressions for stresses and displacements in the rock mass surrounding the tunnel. The available literature on the subject is mainly devoted to the analysis of the rock mass behaviour in an axisymmetric tunnel. The Mohr-Coulomb yield criterion has been the favourite of a majority of authors since Fenner (1938) made the first major attempt to calculate elasto-plastic stresses for determining support pressures and displacements. Hobbs (1966a) was the first to use a non-linear yield criterion and was followed by Ladanyi (1974) who used Fairhurst's second degree parabola as the yield criterion, Korbin (1976) and Kennedy & Lindberg (1978) who used a piece-wise linear Coulomb approximation of the non-linear Mohr envelope, and Hoek & Brown (1980) and Brown et al.(1983) who used Hoek & Brown's empirical non-linear criterion.

The early theories assumed elastic-perfectly plastic stress-strain model of the rock mass. Morrison & Coates (1955) were the

first to assume a reduced strength of the rock mass in the plastic zone and used an elastic-brittle plastic model. Later, several authors assumed an elastic-strain softening behaviour of the rock mass using a tri-linear stress-strain law (Diest,1967; Daemen & Fairhurst,1971; Handron & Aiyer,1972; Egger,1974; Panet,1976; Korbin,1976; Nguyen Minh & Berest,1979; Brown et al., 1983 and Sharma,1985). Fritz (1984) assumed that the behaviour in the the plastic zone is mainly governed by the properties of the plastic St. Venant element. Senseny et al. (1989) presented a closed-form solution for elasto-plastic response of a circular hole subjected to repeated loading. Brown et al. (1989) developed solutions for stresses and strains around axisymmetric excavation in an infinite media, considering power law and exponential variation of the elastic modulus with the minor principal stress. Histake et al. (1989) incorporated newly developed peak and residual strength criteria and non-linear stress-strain relations which change with the confining pressure. Carter and Booker (1990) studied the influence of the rate of excavation on stress distribution around circular tunnels and concluded that a rapid excavation may result in a significant difference between the short-term and long-term stress distribution.

Early solutions proposed by Fenner (1938), Kastner (1949), Morrison & Coates (1955), Hobbs (1966a), Bray (1967), and Diest (1967), did not include any treatment of the plastic volumetric strains,although some of them allowed for a strength reduction in the plastic zone. Labasse (1949), however, evaluated an average plastic dilation in the rock mass. His concept was later used by

others, including Lombardi (1970), Daemen & Fairhurst (1971), Ladanyi (1974), and Jethwa (1981). Effects of face advance and shear stress on support pressure were studied by Jethwa (1981) who modified Daemen's (1975) equation for short-term support pressure to include these effects.

The analysis of the tunnel support behaviour received much less attention. Various authors (e.g. Lombardi,1970; Daemen,1975; Hoek & Brown,1980) generally presented similar expressions for support stiffness for different types of support systems considering a linear elastic behaviour. More recently, Stille et al. (1989) and Indraratna & Kaiser (1990) presented elasto-plastic analyses for rock mass supported with grouted rock bolts, and Mitri and Hassan (1990) studied the behaviour of the steel supports in coal mines with the help of a non-linear finite element analysis.

The convergence-confinement method of tunnel design, which is based on the rock mass-tunnel support interaction concept or, in other words, on the ground reaction and the support reaction curves, was discussed in detail by Gesta et al. (1980), Duddeck (1980) and Lombardi (1980). Recently, Eisenstein and Branco (1991), based on a comparison of the analytical results with field measurements, concluded that while the method is applicable to deep tunnels, it is not suitable for shallow tunnels due to the non-axisymmetric mode of deformation and development of plasticity in the latter. Corbetta et al. (1991) incorporated the effect of the distance from the tunnel face at the time of support installation in the convergence-confinement method and

applied it to an elastic-perfectly plastic ground. Stimpson (1991) extended the method to the case of a rectangular opening in horizontal layered strata considering linear elastic behaviour and the classical beam theory.

A large number of authors have reported the use of field instrumentation in tunnels of varying sizes and in different ground conditions. Many of these have drawn significant conclusions regarding the ground and the support behaviour, support requirements, method of support design, method of excavation, sequence of excavation, and benefits of the New Austrian Tunnelling Method (NATM).

## 1.4 STATEMENT OF PROBLEM

The ground reaction and the support reaction curves are now fully established as effective tools for developing the understanding of the tunnel mechanics. The practical utility of these curves lies in designing the tunnel support system.

Determination of the ground reaction curve in elastic and squeezing grounds, using the approaches suggested earlier, depends on a number of input parameters, some of which are difficult to determine reliably, thus affecting the reliablity of the analytical results. Cross-checking of theoretical results with field observations has also not been reported much.

Determination of the support reaction curve has not received adequate attention. The support behaviour has been assumed to be linear elastic which is not realistic due to the non-linear

behaviour of the support backfill. The variation in backfill stiffness with support pressure has also not been studied. The influence of the parameters, viz the face advance, tunnel size and saturation of the rock mass due to charging of the water conductor system, on support pressure, has not been studied from the point of view of the rock mass-tunnel support interaction.

Finally, the analytical solutions suggested are not very easy to use by the field engineers at the site for quick estimation and revision, if required, of the support requirements during construction.

Due to the above reasons, there is a need to develop a simple, yet reliable, approach for the determination of the ground reaction and the support reaction curves directly from the data of instrumented tunnels.

## 1.5 ORGANISATION OF THESIS

The thesis is divided into eight chapters. Chapter 2 contains a review of literature. Some important rock mass classifiction systems are described in Chapter 3. Chapter 4 is devoted to the geology, and its influence on the tunnelling conditions in case of the tunnelling projects for which the data has been obtained and used in this study. Chapter 5 contains the details of the field instrumentation. In Chapters 6 and 7, based on the data analysis, an approach is presented for determining the ground reaction and the support reaction curves. The conclusions drawn from the present study and the recommendations for the future work are presented in Chapter 8.

# CHAPTER 2

## CHAPTER 2

## REVIEW OF LITERATURE

### 2.1 GENERAL

The objective of the present study is to propose a simple, yet reliable, approach for determining the ground reaction and the support reaction curves for (i) self-supporting tunnels,(ii) tunnels in elastic ground condition, and (iii) tunnels in squeezing (or elasto-plastic) ground condition. While a lot of literature has been devoted to the ground behaviour, the literature on the support behaviour is limited. The present study is based on several field observations. Therefore, a review of literature on field observations in undrground openings has also been included. The available literature on the subject has thus been classified into the following four categories:

(i) The elastic ground behaviour, covering both the self-supporting tunnels and the tunnels in elastic ground condition,

(ii) tunnels in squeezing ground condition considering the elasto-plastic ground behaviour,

(iii) behaviour of the supports, and

(iv) field instrumentation in underground openings.

## 2.2 EARLIER WORK

### 2.2.1 Ground and Support Behaviour

For the purpose of obtaining the ground reaction (response) curve for the elastic ground behaviour (or the elastic part of the elasto-plastic ground reaction curve), various authors have used the following standard expression obtained from the theory of elasticity:

$$u_a/a = (1+v)(p_o-p_i)/E \qquad (2.1)$$

where,

$u_a$ = tunnel-wall displacement,

$a$ = radius of tunnel opening,

$v$ = Poisson's ratio of rock mass,

$E$ = modulus of elasticity of rock mass,

$p_o$ = insitu stress magnitude, and

$p_i$ = short-term support pressure.

Several authors have presented solutions for obtaining elasto-plastic (including elastic-perfectly plastic, Fig.2.1a; elastic-brittle-plastic, Fig.2.1b; and elastic-plastic with strain softening, Fig.2.1c) stress distribution for determining support pressures and displacements in the rock mass surrounding tunnels. Some of the authors have obtained the ground reaction curve, while the others have stopped short of that by terminating at the final expressions for the stresses and displacements. Comparatively fewer authors have extended their analyses to include the determination of the support reaction curve. The review of literature has been restricted to the closed-form

13
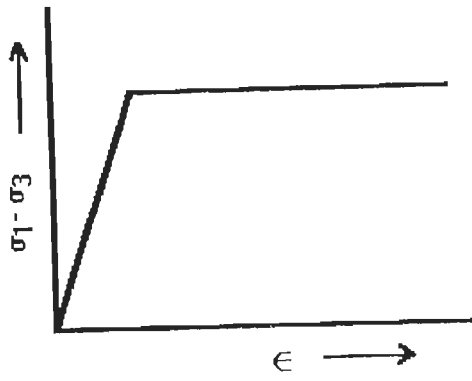


(a) Elastic-Perfectly Plastic
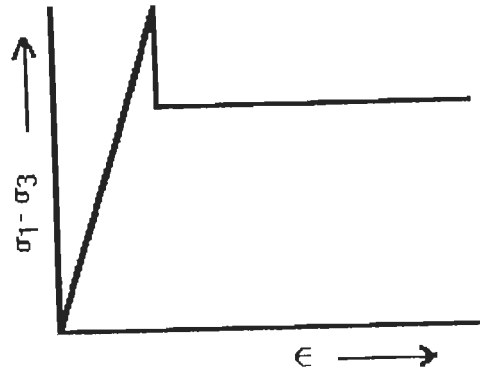
(b) Elastic-Brittle-Plastic
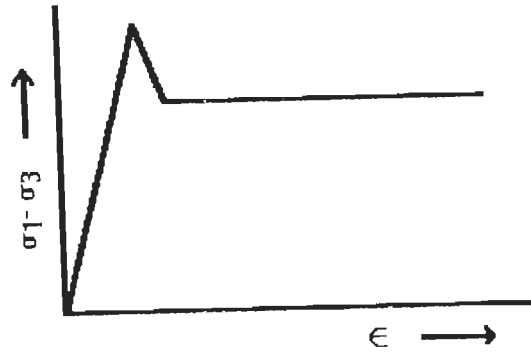
(c) Elastic-Strain Softening

Fig.2.1 – Stress-Strain Models Used In Elasto-Plastic Analyses

solutions, as the scope of the present work does not include the use of numerical methods.

Terzaghi (1919, 1925, 1943) was, perhaps, the first to perform calculations for elasto-plastic stress distribution around a cylindrical underground opening. However, these calculations did not perhaps found field application for the design of tunnel supports.

The first major attempt to use elasto-plastic stress calculations for determining support pressures was made by Fenner (1938) who used the Mohr-Coulomb yield criterion and attempted to prove theoretically that any cylindrical underground opening can stand on its own without supports, provided the plastic zone can be allowed to propagate to a large distance into the rock mass. This conclusion was drawn as the term including cohesion always appeared in the calculations. In order to attain the 'natural equilibrium state' by allowing the plastic zone to propagate, large displacements should be allowed or large amounts of rock mass should be removed. Fenner (1938) demonstrated, through numerical examples, that the extent of plastic zone required to ensure tunnel stability without supports was several times larger than the tunnel radius and concluded that it was desirable to install supports rather than remove the large amounts of rock mass. The short-term support pressure due to Fenner (1938) is given by:

$$p_i = [p_o(1-\sin \phi) + c \cot \phi] (a/b)^{\alpha} - c \cot \phi \qquad (2.2)$$

where,

$p_i$ = short-term support pressure,

$p_o$ = insitu stress magnitude,

a = radius of tunnel opening,

b = radius of broken (plastic) zone,

$\phi$ = angle of internal friction of rock mass,

c = cohesion of rock mass, and

$\alpha$ = 2 sin $\phi$/(1-sin $\phi$).

Labasse (1949) may be credited with being one of the firsts to consider the rock mass-tunnel support interaction. The importance of the equilibrium state between rock mass and support system over rock load and support pressure was highlighted and it was concluded that the relative displacement was an important factor. Labasse (1949), therefore, recognized the necessity of considering the influence of volume increase associated with rock failure and plastic deformation. The analysis considers the Mohr-Coulomb yield criterion with zero cohesion and evaluates an average volumetric strain in the plastic zone. For the case of non-hydrostatic pre-tunnelling stress field, the short-term support pressure is given by:

$$p_i = \sigma_b(a/b)^{J-1} - [(3/2)\tau a/(J-2)][1-(a/b)^{J-2}]\cos \beta \qquad (2.3)$$

where,

$\beta$ = angle from horizontal of the point under consideration,

$\sigma_b$ = radial stress at elastic-plastic interface corresponding to the point under consideration,

J = (1+sin $\phi$)/(1-sin $\phi$), and

$\tau$ = unit weight of rock mass.

The tunnel-wall displacement due to squeezing is given by:

$$u_a = a - [a^2 - e(b^2-a^2)]^{1/2} \qquad (2.4)$$

where,

$u_a$ = tunnel-wall displacement, and

e = coefficient of volumetric expansion for failed rock mass, defined as ratio of increase in volume of failed rock mass to its original volume.

Kastner (1949) also used the Mohr-Coulomb yield criterion but did not consider the influence of volume increase associated with rock failure. Like Labasse (1949), Kastner too presented solution for the non-hydrostatic case and paid attention to the importance of rock mass-tunnel support interaction. The analysis predicts a potential fracture zone from the elastic stress distribution and imposes some arbitrary limits, for the purpose of designing the support, on the extent to which such a zone can be allowed to propagate. It was pointed out that the broken zone widens with the increase in the ratio of the primitive stress to the insitu compressive strength of the rock mass, and decreases with an increase in the support capacity. The effect of gravity was, however, neglected. The short-term support pressure is given by:

$$p_i = [p_o(1-\sin \phi) - c \cos \phi + c \cot \phi] (a/b)^\alpha - c \cot \phi \qquad (2.5)$$

Eq. 2.5 differs from the equation proposed by Fenner (Eq.2.2) by the term $-c \cos \phi$.

Morrison and Coates (1955) examined and corrected a number of basic errors in Fenner's (1938) analysis. Mohr-Coulomb peak

and residual yield criteria with a constant friction angle and zero residual cohesion were chosen. It appers that these authors were the first to use a reduced strength, in this case zero cohesion, for the plastic zone. An elastic-brittle-plastic model (Fig.2.1 b) was preferred to the elastic-perfectly plastic model (Fig.2.1a)used by Fenner (1938), Labasse(1949) and Kastner(1949).

Pacher (1964) presented a detailed qualitative discussion on rock mass-tunnel support interaction and brought out convincingly the importance of time of support installation and the necessity to avoid the development of 'loosening' of the rock mass in order to limit the loosening pressure. Pacher (1964) cautioned that a very weak support system could lead to a collapse of the ground arch. Pacher's contribution was duly acknowledged and the ground reaction and the support reaction curves came to be known as Fenner-Pacher curves in Austria (Duddeck, 1980)

Sirieys (1964) suggested the existence of a 'broken' zone of zero cohesion within the plastic zone around the support, with the rest of the plastic zone having a finite cohesion. Serata (1964) also considered the existence of a series of annular zones within the plastic zone and suggested different material models for these annular zones.

Based on the results of the triaxial tests carried out on broken cylinders of a single rock - calcareous silty mudstone - Hobbs (1966 a) proposed the following non-linear power law as the yield criterion:

$$\sigma_1 = B'\sigma_3{}^{b'} + \sigma_3 \tag{2.6}$$

where, $\sigma_1$ is the yield stress, $\sigma_3$ is the confining pressure, and B' and b' are the material property constants.

Hobbs (1966 a) used the above relationship to obtain stresses, approximate deformations, and movement paths around a circular roadway in fractured rock mass subjected to a uniformly distributed pressure. Different values of Young's modulus and Poisson's ratio were used for the plastic and elastic zones.

Hobbs (1966 b) performed hollow cylinder tests on coal samples and observed an apparant strength enhancement. The hollow cylindrical samples failed at much higher compressive strength than measured.

Richter (1966) considered different values of the modulus of elasticity within the broken zone and suggested the existence of a series of annular rings around the tunnel periphery having low modulus, followed by another series of annular rings upto the elastic-plastic interface having higher modulus, and finally the elastic zone having the highest value of the modulus of elasticity which remains unchanged at its original value during tunnelling.

Bray (1967) reverted back to the linear Mohr-Coulomb yield criterion after Hobbs (1966a) used a non-linear power law and performed the calculations considering slip along the fracture planes.

Diest (1967) was the irst to allow for strain-softening

behaviour (Fig.2.1 c) of the rock mass but did not treat the plastic volumetric strains. The analysis assumes a zero residual strength and is based on the Mohr-Coulomb yield criterion.

Salencon (1969) employed Tresca and Mohr-Coulomb yield criteria and applied associted flow rule of the theory of plasticity. The rate of plastic volumetric change was assumed to be independent of strain.

Hoskins (1969), Daemen and Fairhurst (1971), and Haimson and Edl (1972) also reported, like Hobbs (1966 b), an apparant strength enhancement around boreholes, on the basis of laboratory tests. Daemen and Fairhurst (1971) found no indication of fracturing around the borehole when the external hydrostatic pressure, applied to thick-walled hollow cylinders of Indiana limestone and concrete, reached levels at which linear elastic analysis gives tangential stress at the borehole wall of at least four times the measured uniaxial compressive strength of the material. Final collapse occurred at even higher pressure.

Lombardi (1966) considered two limiting points only to denote the ground characteristics, one giving the transition from elastic to plastic state, and the other representing failure. Later, Lombardi (1970) pointed out the stabilizing effect of the volume increase due to failure, inspite of increasing the tunnel-wall displacement. Lombardi (1970, 1977, 1980) used mohr-Coulomb yield criterion with different values of peak and residual cohesion and friction angle, estimated average volumetric strain in plastic zone and used different values of

Young's modulus and Poisson's ratio in the plastic zone. Lombardi (1970, 1973) discussed the load-deformation characteristics of various types of linings and supports, and presented expressions for support stiffnesses considering a linear elastic support behaviour. The following expression was given for the stiffness of concrete lining, $k_C$:

$$k_C = \frac{E_C(1-w_e{}^2)}{(1+\nu_C)\ (1-2\nu_C+w_e{}^2)}$$ (2.7)

where,

$E_C$ = modulus of elasticity of concrete,

$w_e = r_{ic}/r_{ec}$, $r_{ic}$ and $r_{ec}(\approx a)$ being the inner and outer radii of concrete ring, and

$\nu_C$ = Poisson's ratio of concrete.

Eq.2.7 may, as well, be written as:

$$k_C = \frac{E_C[a^2 - (a-t_C{}^2)]}{(1+\nu_C)\ [(1-2\nu_C)a^2 + (a-t_C)^2]}$$ (2.8)

where,

$t_C$ = thickness of concrete lining

Sakurai (1970) based his calculations for stress distribution on a modified von Mises yield criterion. By adopting this criterion, three different regions concerning stresses appear around a tunnel, i.e., a region defined as 'fractured region' existing in the vicinity of tunnel surface, 'plastic region' located behind the fractured region, and 'elastic region' located farthest from the tunnel surface (Fig.2.2). These three

regions do not always appear, but their existence depends upon the state of initial stresses and mechanical properties of the medium. Sakurai presented expressions for stresses and displacements for three different possible cases - a) existence of elastic, plastic and fractured regions, b) existence of elastic and fractured regions, and c) existence of elastic region only.

Hendron and Aiyer (1972) used the Mohr-Coulomb yield criterion with constant angle of friction and considered three cases of constant, varying, and zero cohesion in the plastic zone. The stress-strain models chosen by them were - elastic-plastic (Fig.2.1 a), elastic-brittle-plastic (Fig.2.1 b), and elastic-strain softening (Fig.2.1 c). Solutions were presented for several different cases using the associated flow rule over the entire plastic zone and different values of Young's modulus and Poisson's ratio in the plastic zone in some of the solutions.

Ladanyi (1974) realised that the investigations carried out till 1973 had failed to produce a viable closed-form solution for the determination of the support pressure, i.e., a method that would enable the ground pressure on tunnel lining to be estimated on the basis of the most probable field stress conditions and rock mass properties. A solution was, therefore, presented which, although valid for a simple tunnel geometry and field stress condition, has the advantage of taking into account a number of significant characteristics of the rock mass, in particular its plastic volumetric dilation and strength decrease with time. At failure, two different forms of Mohr

failure criterion were used - i) Coulomb straight line, and ii) Fairhurst (1964) second-degree parabola. In the post-failure region, the rock mass was assumed to be perfectly plastic and Mohr-Coulomb failure theory was assumed to be valid for broken rock mass. As far as the volumetric strain is concerned, Ladanyi applied associated flow rule of the theory of plasticity over limited range of post-peak strain. A word of caution was also given that an indiscriminate use of this rule could lead to predicting volumetric strains much in excess of reality. According to the theory, the ground reaction curve may be determined using the expression:

$$u_a/a = 1 - [(1-e_{av})/(1+A)]^{1/2} \qquad (2.9)$$

where,

$e_{av}$ = average plastic dilation

$$= \frac{2(u_b/b)(b/a)^2}{[(b/a)^2-1][1+1/2D \ln(b/a)]} \qquad \text{for } b/a < \sqrt{3} \qquad (2.9a)$$

$$= \frac{2(u_b/b)(b/a)^2}{[(b/a)^2-1][1+1/1.1D]} \qquad \text{for } b/a > \sqrt{3}, \qquad (2.9b)$$

$u_b$ = radial displacement of elastic-plastic boundary,

$D$ = $-\sin \phi$     (for Coulomb straight line failure criterion)

$$= -\frac{(m-1)}{2(1+n\sigma_3/q_c)^{1/2}+m-1} \qquad \begin{array}{l}\text{(for Fairhurst parabolic} \\ \text{failure criterion)}\end{array} \qquad (2.9c)$$

The expressions for $u_b/b$ and the radius of broken zone, b, are as follows:

$$u_b/b = \frac{(1+v)}{E} Mq_c, \text{ and} \qquad (2.9d)$$

$$b = a[(p_o+H-Mq_c)/(p_i+H)]^{1/(J-1)} \qquad (2.9e)$$

where,

$$M = [1+ \frac{2\sin \phi}{1-\sin \phi}(p_o/q_c)]/[\frac{2}{1-\sin \phi}] \quad \text{(for Coulomb straight line failure criterion)} \quad (2.9f)$$

$$= [1+np_o/q_c - (1/4)(m-1)^2]^{1/2}/(m+1) \quad \text{(for Fairhurst parabolic failure criterion)} \quad (2.9g)$$

$$J = (1 + \sin \phi)/(1 - \sin \phi), \text{ and} \quad (2.9h)$$

$q_c$ = uniaxial compressive strength of intact rock.

The broken zone exists for all values of $p_i$ smaller than $p_{icr}$, which is given as $p_o-Mq_c$. Eq.2.9 will be applicable in this case. For values of $p_i$ greater than $p_{icr}$, however, no broken zone exists and the ground response curve may be obtained from the following relationship for elastic deformation:

$$u_a/a = (1+\nu)(p_o-p_i)/E \quad (2.10)$$

Ladanyi (1974) assumed all the parameters to be time-dependent but used only their limiting, i.e., short-term and long-term, values in the analysis. Expressions were obtained for both long-term and short-term ground-reaction curves considering the reduction in rock mass strength with time. Later, Ladanyi (1980) attempted to fill the time gap between the short-term and the long-term rock mass response, by assuming a non-linear Maxwell (power law) creep model and calculated the time-dependent tunnel-wall displacement and increase in support pressure. The effect of the loading history was, however, not considered . This was subsequently accounted for by Gill and Ladanyi (1987). For determination of the support reaction curve, Ladanyi (1974) used the linear elastic support behaviour, as suggested by Lombardi (1970, 1973).

Egger (1974) took into account the post-failure behaviour of the rock mass characterised by the disintegration and the loosening rate. The analysis considers the Mohr-Coulomb peak and residual yield criteria and elastic-strain softening stress-strain model (Fig.2.1 c) and assumes a constant angle of internal friction and zero residual cohesion. The plastic volumetric strain was linearly related to the major and minor principal plastic strains by a variable parameter. Egger evaluated, for the cases of axial and central symmetry, the dependence of support pressure on the radial displacement of the tunnel wall. It was shown that a 'critical' post-failure characteristic can be indicated, for both the cases, which separates 'heavy' rock mass behaviour from the rock mass 'tending to overbreak'.

Daemen (1975) accounted for the effect of gravity and obtained the following closed-form solution for the short-term tunnel support pressure, considering strength reduction and strain softening in the broken zone:

$$p_i = [p_o(1-\sin \phi_p) - c_p\cos \phi_p + c_r\cot \phi_r]M_\phi$$
$$- c_r\cot \phi_r \pm \gamma (b-a)M_\gamma \qquad (2.11)$$

where,

$\phi_p$ =peak angle of internal friction of rock mass in elastic zone,

$\phi_r$ =residual angle of internal friction of rock mass in plastic zone,

$c_p$ = peak cohesion of rock mass in elastic zone,

$c_r$ = residual cohesion of rock mass in plastic zone,

$M_\phi = (a/b)^\alpha,$ \qquad (2.11a)

$\alpha = 2 \sin \phi_p/(1-\sin \phi_p)$ \qquad (2.11b)

$$M_r = \frac{a}{b-a} \frac{1-\sin \phi_r}{1-3\sin \phi_r}[(a/b)^{\alpha-1}-1] \tag{2.11c}$$

The positive and the negative signs pertain to the support pressure on the tunnel roof and the floor respectively.

Daemen (1975) also performed a finite element analysis to study the influence of face advance on support pressure and concluded that the supports installed close to the face attract higher support pressure. For obtaining the support reaction curve, expressions similar to those suggested by Lombardi (1970, 1973) were used for different types of support systems. The expression for the stiffness of the concrete lining is given by:

$$k_C = \frac{E_C(2a-t_C)}{(1+\nu_C)[(1-2\nu_C)a^2 + (a-t_C)^2]} \tag{2.12}$$

which may be rewritten as:

$$k_C = \frac{E_C[a^2 - (a-t_C^2)]}{(1+\nu_C)[(1-2\nu_C)a^2 + (a-t_C)^2]} \tag{2.12a}$$

which is the same as Eq.2.8 given by Lombardi (1970, 1973).

Panet (1976) used the same yield criterion, stress-strain model, and treatment of plastic volumetric strains as Egger (1974). The influence of the tunnel face was, however, allowed. It was assumed that upon failure, the rock mass looses its initial strength and undergoes a volume increase. It was pointed out that the tunnel may remain stable if the total loss of the residual strength of rock mass in close proximity of the tunnel periphery is prevented.

Korbin (1976) assumed a non-linear strain softening stress-strain model and considered a piecewise linear Coulomb approximation of the non-linear Mohr envelope. Use was made of Hendron's and Aiyer's (1971) application of the associated flow rule for treating the plastic volumetric strains.

Kennedy and Lindberg (1978) investigated the effect of the non-linearity of the yield function in the problem of the elastic-plastic (Fig.2.1 a) closure of a cylindrical opening in rock mass subjected to an axisymmetric load. Realising that the behaviour of a rock mass is best represented by a non-linear yield function, they considered the yield function to be represented by a series of straight line segments (Fig.2.3). This representation enabled them to arrive at a closed-form solution using a non-linear yield criterion (decreasing friction angle with increasing mean normal stress) which otherwise invariably requires use of a numerical technique. A piecewise linear Coulomb approximation of non-linear Mohr envelope was used as the yield criterion and the associated flow rule was applied over the entire plastic zone. An alternative incompressible flow solution was presented using the non-associated flow rule. It was shown, with the help of an example, that the tunnel closure is sensitive to plastic behaviour nearest the tunnel, where stresses are the lowest. Kennedy and Lindberg (1978) concluded, therefore, that the low stress part of the yield function, where the non-linearity is usually the greatest, should be represented as accurately as possible.

Florence and Schwer (1978) considered the rock mass behaviour as elastic-perfectly plastic (Fig.2.1 a), obeying the Mohr-Coulomb yield condition and associated flow rule which was applied over the entire plastic zone. The significant feature of the analysis was, however, the influence of axial stress resulting in up to three different plastic zones depending on the relative magnitudes of tangential $(\sigma_\Theta)$, radial $(\sigma_r)$ and axial $(\sigma_z)$ stresses which, in turn, depend on the values of Poisson's ratio and the friction angle. Development of different plastic ‾ zones is shown to be taking place with increase in axial stress. The inner plastic zone pertains to the situation when $\sigma_\Theta < \sigma_z < \sigma_r$, the middle plastic zone occurs when $\sigma_\Theta < \sigma_z = \sigma_r$, and the outer plastic zone is formed when $\sigma_\Theta < \sigma_r < \sigma_z$ (Fig.2.4).

Einstein and Schwartz (1979) proposed two dimensionless parameters, the compressibility and flexibility ratios, to incorporate the relative stiffness between the rock mass and the tunnel support into the solution. The compressibility ratio, $C^*$, and the fliexibility ratio, $F^*$, were defined as:

$$C^* = \frac{Ea(1-\nu_s^2)}{E_s A_s(1-\nu^2)} \qquad (2.13)$$

and

$$F^* = \frac{Ea^3(1-\nu_s^2)}{E_s I_s(1-\nu^2)} \qquad (2.14)$$

in which,

$E, \nu$ and $E_s, \nu_s$ = elastic constants for rock mass and tunnel support respectively,

$A_s$ = average cross-sectional area of tunnel support per unit length of tunnel
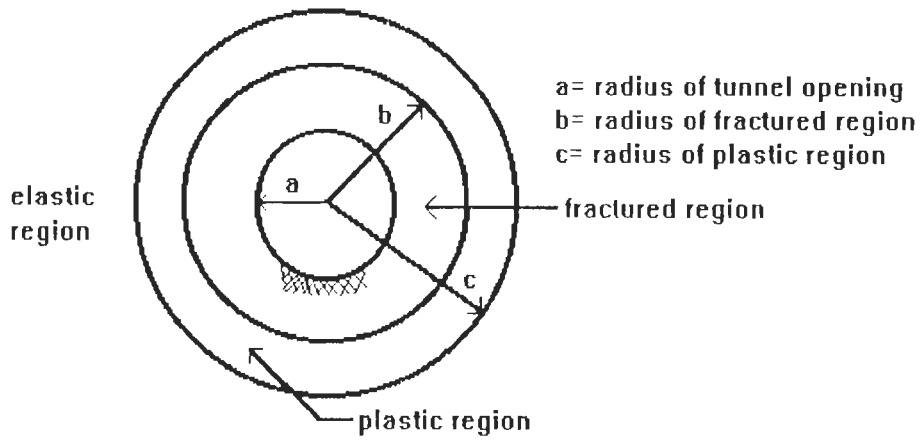
Fig.2.2- Three Different Regions Around Tunnnel *[after Sakurai, 1970]*

a= radius of tunnel opening
b= radius of fractured region
c= radius of plastic region



$f_1, f_2..f_n$ = straight line yield functions with slopes $\tan w_1$, $\tan w_2$.. $\tan w_n$ and valid for $\sigma_3 < p_1, p_2..p_n$
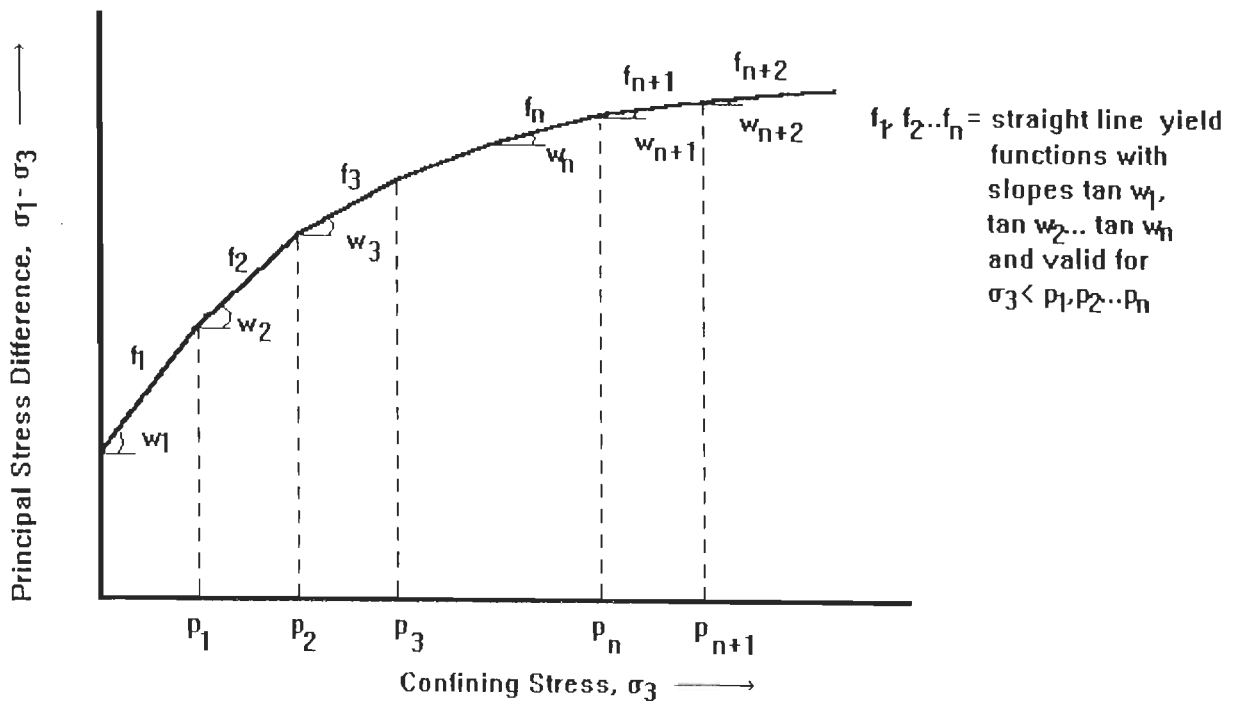
Fig. 2.3 - Piecewise Linear Approximation of Non-linear Yield Function
*[after Kennedy and Lindberg, 1978]*

$I_s$ = moment of inertia of tunnel support per unit length of tunnel

$C^*$ and $F^*$ are the measures of the relative stiffness of the rock mass-tunnel support system under a symmetric and an antisymmetric loading condition respectively. Using these parameters, Einstein and Schwartz (1979) obtained solutions for normalized support thrust, moment and displacement considering a linear elastic ground and support behaviour, and assuming that the support is installed simultaneously with the excavation.

Minh and Berest (1979) used the Mohr-Coulomb peak and residual yield criteria with constant angle of friction and allowed for strain softening behaviour (Fig.2.1 c) of the rock mass. The major and minor principal plastic strains were related linearly by a variable parameter, as was done by Egger (1974) and Panet (1976). Like Florence and Schwer (1978),the analysis allows for the influence of axial stress. In this case, however, this influence results in two different plastic zones depending upon the relative magnitudes of tangential, radial and axial stresses.

Dube (1979) considered the non-hydrostatic primary stress field and modified Eq.2.11 proposed by Daemen (1975) for hydrostatic stress field. Accordingly, the following expressions for the short-term support pressures were obtained:

$$p_v = [p_o/2 \ (3 \ \lambda -1)(1-\sin \ \phi_p) - c_p \cos \ \phi_p + c_r \cot \ \phi_r](a/b)^{\alpha} \\ -c_r \cot \ \phi_r \pm \tau \ (b-a) \ ^p M_\tau \tag{2.15}$$

and

$$p_h = [p_o/2 \ (3- \ \lambda)(1-\sin \ \phi_p) - c_p \cos \ \phi_p + c_r \cot \ \phi_r](a/b)^{\alpha} \\ -c_r \cot \ \phi_r \pm \tau \ (b-a) \ M_\tau \tag{2.16}$$

where,

$p_v$ = short-term support pressure in the vertical direction,

$p_h$ = short-term support pressure in the horizontal direction, and

$\lambda$ = ratio of the horizintal and vertical primary stresses.

Approximate expressions were also derived for the elastic radial displacement at the broken zone boundary, and a graphical method was suggested to obtain the radius of the broken zone from the results of the borehole extensometers.

Egger (1980) suggested that the three-dimensional character of the stresses and the deformations around the tunnel face could be simulated by using a hypothesis of spherical symmetry. Thus, the ground response curve for the face may be determined by analogy to that for sections behind the face. It was concluded that the progressive or brittle rupture, partial or total loss of cohesion at fracture, dilation or deformation at constant volume, could all be taken into account. Egger (1980) further suggested to determine the cohesion of the rock mass by back-calculating it from the observations of the borehole extensometers installed in the tunnel to avoid the scale effect, which results in an underestimation of the cohesion value obtained from tests on small specimens.

Hoek and Brown (1980a) used Ladanyi's solution but incorporated their own empirical non-linear peak and residual failure criteria (Hoek and Brown, 1980b) into it. The assosiated flow rule was used over a limited range of post-peak strain and steps for performing the complete ground-support interaction

analysis were presented. Various parameters of Ladanyi's equation (Eq.2.9) were rederived. Accordingly, the parameter D (in Eqs.2.9a and 2.9b), and radius of broken zone, b, are given by:

$$D = \frac{-m}{m+4[(m/q_c)(p_o-Mq_c) + s]^{1/2}} \qquad (2.17)$$

and

$$b = a.e^{[N - 2\sqrt{\{(p_i/m_r q_c) + (s_r/m_r^2)\}}]} \qquad (2.18)$$

where,

$m,s$ and $m_r,s_r$ = material constants for original and broken rock mass respectively,

$$M = 1/2[(m/4)^2 + mp_o/q_c + s]^{1/2} - m/8, \text{ and} \qquad (2.19)$$

$$N = 2[\frac{p_o-Mq_c}{m_r q_c} + \frac{s_r}{m_r^2}]^{1/2} \qquad (2.20)$$

Hoek and Brown (1980a) suggested similar expressions as those given by Lombardi (1970, 1973) and Daemen (1975), for obtaining the stiffness of the different types of supports. Thus, the support reaction curve was considered to be linear elastic.

Kaiser (1980, 1981) recognised the necessity of considering the effect of the loading history on the rock mass response in the analysis of stresses around the underground openings. This effect for the case of support loading resulting from the advance of the tunnel face through an imperfectly elastic rock mass, was considered using the rate-dependent Mohr-Coulomb peak and residual criteria for an elastic-brittle-plastic (Fig.2.1 b) rock mass. Emphasis was laid on allowing different values of elastic constants in the elastic and broken zones and it was suggested that the modulus reduction, associated with progressive

failure of the rock mass, can alone account for the displacements observed at the tunnel boundaries.

Jethwa (1981) modified Daemen's equation (Eq.2.11) to account for the effect of face advance and shear stresses mobilised as a result of the differential displacement within the broken zone, for obtaining the short-term tunnel support pressure, and proposed the equation:

$$p_i = [p_o X(1-\sin \phi_p) - c_p \cos \phi_p + c_r \cot \phi_r]M_\phi$$

$$- c_r \cot \phi_r \pm \tau(b-a)M_\tau - M_\tau(b-a)\frac{d\overline{\tau}_{rz}}{dz} \qquad (2.21)$$

where,

$X$ = proportionality factor = $u_r/u_a$,

$u_r$ = tunnel-wall displacement at any point close to the face,

$z$ = face advance, and

$\overline{\tau}_{rz}$ = average shear stress for $a<r<b$.

Jethwa (1981) adopted the values of $X$ suggested by Daemen (1975) on the basis of a three-dimensional FEM analysis for elastic ground (Fig.2.5). A semi-empirical theory was also proposed for ultimate creep pressure and a safety factor of 3 was suggested for designing permanent tunnel lining on the basis of comparison of the theoretical estimates of ultimate creep pressures with the capacities of the existing tunnel linings.

Brown, Bray, Ladanyi and Hoek (1983) extended Hoek and Brown's (1980a) work to a more complex material behaviour model. Using Hoek & Brown's failure criteria, they obtained a closed-
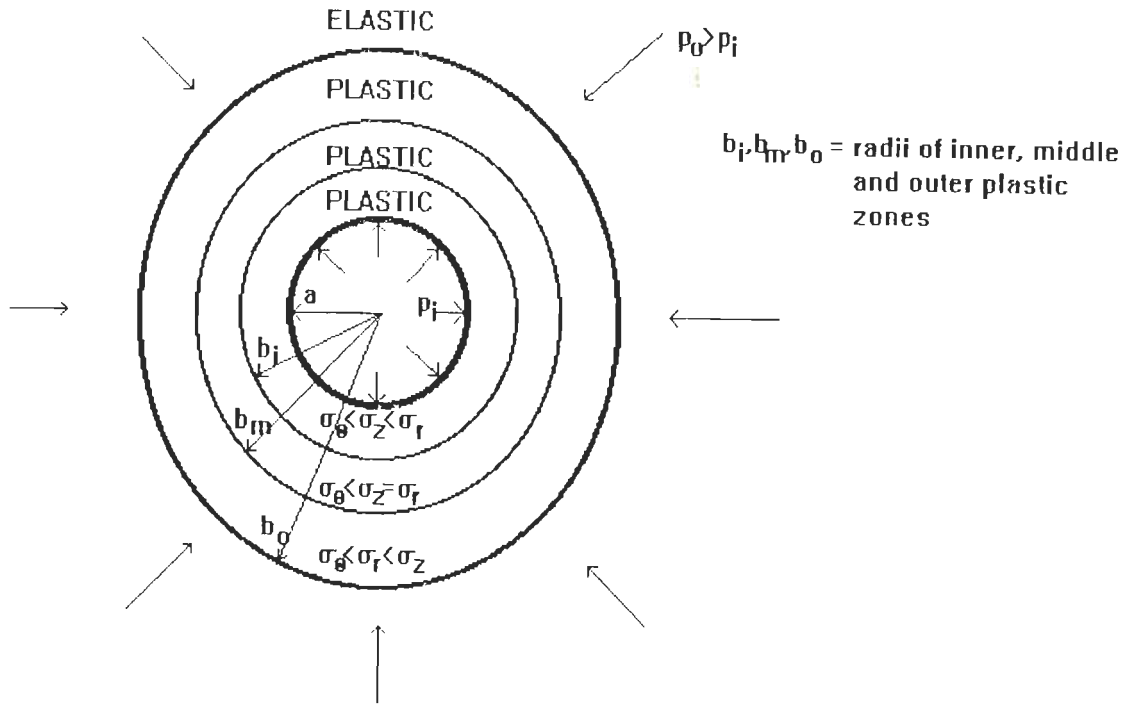
Fig.2.4 - Outer Elastic and Three Plastic Zones *(after Florence & Shwer, 1978)*
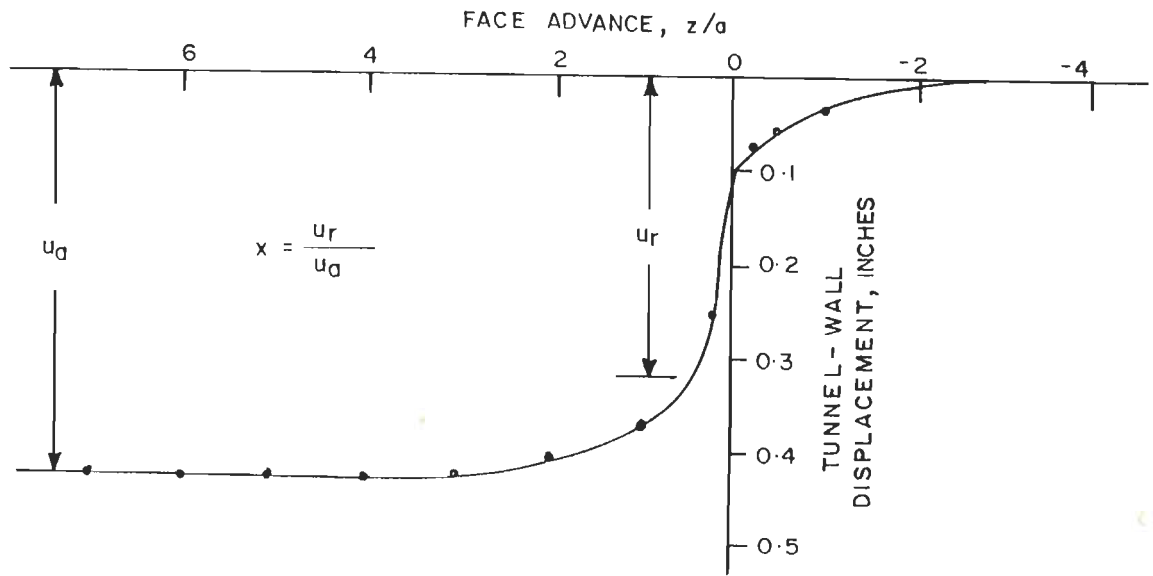


Fig.2.5 - Determination of Proportionality Factor `X' in Elastic Ground (after Daemen, 1975)

form solution for the simpler case of an elastic-brittle-residual plastic model (Fig.2.1 b) with post-peak dilation occuring at a constant rate with major principal strain in the residual plastic zone. A step-wise numerical solution was then presented for the more complex tri-linear elastic-strain softening-residual plastic stress-strain model (Fig.2.1 c) with post-peak dilation occuring at a lower rate with major principal strain in the constant strength plastic zone than in the strain-softening zone. The ground-reaction curves were obtained for both the solutions.

Gill and Ladanyi (1983) and Ladanyi and Gill (1984) showed that the conventional characteristic line concept (or, the rock mass-tunnel support interaction concept) generally understimated both the support pressure and the tunnel convergence, when applied to a rock mass showing creep of a Maxwell type (both linear and non-linear). Later, Gill and Ladanyi (1987), by using a Zener-type creep model to account for the loading history, demonstrated that this underestimate decreases with time and tends to zero when the time tends to infinity. It was found that this behaviour supports the long-term strength concept proposed by Ladanyi (1974).

Fritz (1984) performed the elasto-plastic analysis assuming that the behaviour in the plastic zone is governed mainly by the properties of the plastic St. Venant element (as modified by Fritz, 1982). The element starts to deform when its stress reaches, for the first time, the peak strength. The initiated deformational process is then characterized by the residual strength. Modified Mohr-Coulomb yield criterion, characterising

both the peak and the residual strengths, was used to represent the rock mass behaviour. This is given in terms of the principal stresses $\sigma_r$ and $\sigma_\theta$ for peak condition as:

$$F_p = \sigma_\theta - m_p\sigma_r - \sigma_{dp} = 0 \qquad \text{for } r=b \qquad (2.22a)$$

and

$$F_r = \sigma_\theta - m_r\sigma_r - \sigma_{dr} = 0 \qquad \text{for } r<b \qquad (2.22b)$$

where,

$$m_p = (1+\sin \phi_p)/(1-\sin \phi_p), \quad m_r = (1+\sin \phi_r)/(1-\sin \phi_r) \qquad (2.22c)$$

$$\sigma_{dp} = 2 c_p\cos \phi_p/(1-\sin \phi_p) \text{ and } \sigma_{dr} = 2 c_r\cos \phi_r/(1-\sin \phi_r) \qquad (2.22d)$$

According to this theory, the radius of the elasto-plastic boundary is given by:

$$b = a[\sigma_{dr} + (m_r-1)\sigma_b]/[\sigma_{dr} + (m_r-1)p_i] \qquad (2.22e)$$

where $p_i$ is the internal pressure.

The radial stress at r=b, i.e., $\sigma_b$ is given by:

$$\sigma_b = (2p_o-\sigma_{dp})/(m_p+1) \qquad (2.22f)$$

and the stresses in the plastic zone are given by:

radial stress, $$\sigma_r^{pl} = \frac{\sigma_{dr} + (m_r-1)p_i}{(m_r-1)} (r/a)^{mr-1} - \frac{\sigma_{dr}}{(m_r-1)} \qquad (2.23)$$

and

tangential stress, $$\sigma_\theta^{pl} = m_r\frac{\sigma_{dr}+(m_r-1)p_i}{(m_r-1)}(r/a)^{mr-1} - \frac{\sigma_{dr}}{(m_r-1)} \qquad (2.24)$$

Sharma (1985) showed that for the complex tri-linear stress-strain model of Brown et al. (1983), a simpler solution, using a combination of analytical and numerical methods, may be employed to obtain the same results as achieved by them (Brown et al.,

1983) using a step-wise numerical solution.

Lu (1986) considered the strain hardening behaviour of the rock mass and performed his analysis using the modified Mohr-Coulomb yield criterion. It was pointed out that consideration of the strain hardening behaviour results in a higher value of tangential stress at the tunnel periphery, and a smaller radius of broken zone.

Detournay and Fairhurst (1987) proposed a semi-analytical elasto-plastic model for the case of non-hydrostatic loading of a long, cylindrical cavity. Realising that the analysis of the case where the insitu stress field is non-hydrostatic had received only limited attention and the available solutions were largely based on purely numerical techniques, an explicit solution was presented for the stress field and the displacement in the elastic region, with a numerical calculation of the displacement in the plastic region. The solution is applicable for stress conditions for which the problem is statically determined. The range of deviation from a hydrostatic stress condition that can be analysed with the model is, therefore, limited. The analysis has highlighted the role played by the obliquity, m, which is defined as the ratio of the far-field stress deviator to its yield limit in characterising deviation from hydrostatic conditions. It was found that the shape of the broken zone, the ellipticity of the cavity caused by non-uniform closure, and the condition of statical determinancy were all controlled by the obliquity, m. It was concluded, however, that the average closure and the average radius of the plastic zone

are both well predicted by the solution for the hydrostatic case. A significant prediction, based on the model, is that the direction of maximum convergence becomes perpendicular to the direction of the maximum insitu compressive stress if the rock fails in a large enough region around the underground cavity. This provides a possible explanation of the large lateral displacements which are often observed in tunnels driven in severe squeezing ground conditions.

Santarelli and Brown (1987) and Brown, Bray and Santarelli (1989) loaded hollow cylinders of sandstone externally with hydrostatic pressures and observed the initiation of fracture at the borehole wall at about three times the failure pressure predicted by the classical (constant modulus) theory of elasticity. It was, therefore, suggested that the use of classical theory of elasticity in porous rocks may lead to erroneous predictions of the deformation and initiation and extent of failure around underground excavations. Solutions for elastic stresses and strains induced around circular excavations in rock mass subjected to initially axisymmetric stress fields were presented considering power law and exponential variations of elastic modulus with minor principal stress. It was concluded that the maximum stress concentrations do not occur at the excavation boundaries and are less than the constant value of 2.0 given by constant modulus elasticity. Guenot (1989) also observed similar apparant strength enhancement around borehole walls.

Senseny, Lindberg and Schwer (1989) performed a closed-form analysis for elasto-plastic response of a circular hole in an

infinite Mohr-Coulomb medium subjected to repeated loading. Results of the analysis show how the deformation of the hole is influenced by the magnitude of the internal pressure, the Mohr-Coulomb parameters, and the pressure at which the load is cycled. The results, however, have limited practical applications as these pertain to only those underground openings which are subjected to repeated loading, such as, buried facilities which undergo repetitive weapons loading.

Stille, Holmberg and Nord (1989) and Indraratna and Kaiser (1990) presented closed-form elasto-plastic solutions for underground openings supported with grouted rock bolts. Using modified Mohr-Coulomb failure criterion and non-associated flow rule, the ground reaction curves for the rock mass after installation of the grouted rock bolts were obtained. Stille et al. (1989) considered two different support systems, one with grouted bolts alone and the other with grouted bolts and shotcrete. The analytical results show good consistency with the measured results of the Kielder experimental tunnel for two of the four different theoretical solutions presented. Indraratna and Kaiser (1990) verified the results by laboratory simulation with physical models. The solution was applied to a case-history and was compared with the empirical design method based on Rock Mass Rating.

Histake, Cording, Ito, Sakurai and Phien-Weja (1989) incorporated newly developed peak and residual strength criteria and non-linear stress-strain which change with the confining pressure, and presented a new solution to calculate stresses,

strains and displacements around a circular tunnel under an initially hydrostatic insitu stress field.

Carter and Booker (1990) studied the influence of the rate of excavation on stress distribution around a circular tunnel excavated in an elastic rock mass. It was demonstrated that for rapid excavation, the dynamic effects may result in significant differences between the short-term and long-term stress distributions, and that a more gradual excavation reduces this difference. Carter and Booker (1990) concluded that for most rock masses, the stress removal at the tunnel walls must occur over a period of about 0.1 sec. or less for the dynamic effects to have a significant influence.

Mitri and Hassan (1990) studied the strength and stiffness characteristics of steel supports in coal mines with the help of a non-linear finite element analysis and obtained a good agreement between the numerical and the experimental results. They carried out a parametric study to examine the influence of load distribution, support diameter, splay leg angle and the section size.

Eisenstein and Branco (1991) used the formulation presented by Kaiser (1980) for the determination of the ground reaction curves to employ the convergence-confinment method (or, the rock mass-tunnel support interaction analysis) for design of two tunnels, one shallow and the other deep, in stiff clay, and compared the results with field measurements. The deep tunnel showed good agreement between the analysis and the field data.

The shallow tunnel did not. The discrepancy was attributed to the fact that the mode of deformation and development of plasticity in the soil surrounding the shallow tunnel was not axisymmetric, as assumed in the analytical method.

Corbetta, Bernaud and Minh (1991) developed a method to account for the effect of distance from the tunnel face at the time of support installation on the tunnel convergence for using the convergence-confinement method for elastic-perfectly plastic (Fig.2.1 a) ground. The support pressure and tunnel convergence were evaluated considering plasticity of ground and distance from the face where the support is installed.

Stimpson (1991) extended the existing rock mass-tunnel support analysis to the case of a rectangular opening in horizontal layered strata, considering linear elastic behaviour and classical beam theory. The influence of factors, such as, time of support installation; roof failure; number, thickness and stiffness of strata; bolt type, length and spacing; roof span and roof beam thickness, on the bolt load was evaluated.

Fuenkajorn and Daemen (1992) conducted biaxial borehole stability tests on cylindrical tuff samples and, depending upon the rock density, observed the breakout stress (tangential compressive stress at the borehole wall where breakouts are induced) to be higher than the measured uniaxial compressive strength of tuff. The empirical equation suggested for breakout stress, $\sigma_{\Theta f}$, is:

$$\sigma_{\Theta f} = (949 \rho - 1994) \exp(2.05 \, \sigma_{H2}/\sigma_{H1}) \qquad \text{MPa} \qquad (2.25)$$

where,

$\sigma_{H2}, \sigma_{H1}$ = minimum and maximum applied boundary stresses, and

$\rho$      = rock density (g/cc)

## 2.2.2 Field Observations

Terzaghi (1942) was the first to realise the importance of field observation in tunnels and estimated rock loads from the observation of progressive failure of wooden blocks placed between the steel arch supports and the surrounding rock mass in several railroad tunnels in the eastern Alps. On the basis of the observations, Terzaghi strongly recommended the reduction in the amount of steel used for supports and advocated the measurement of support pressures and tunnel closures by systematic instrumentation. Later, Terzghi (1946) proposed the classical method of rock load estimation (discussed in Art.3.2 of Chapter 3) on the basis of the observations in eastern Alps.

Ward (1955) devised techniques for measuring pressures and deformations in underground excavations. These techniques were used by Ward and Chaplin (1957) in several old London tubes. On the basis of these measurements, they concluded that in shallow tunnels, the support pressure is equal to the full cover pressure.

Tattersall, Wakeling and Ward (1955) monitored a pressure tunnel driven through London clays. They measured radial pressure, hoop load, and tunnel deformation and reported that the diameter of the steel liner changed by only 0.3 to 1.5 mm over a period of one year.

Lane (1957) instrumented the Garrison Dam tunnels and concluded that a stiffer support attracts higher support pressure as compared to a relatively flexible support, an observation which is confirmed by the rock mass-tunnel support interaction analysis.

Rabcewicz (1964) demonstrated, through field observations, the effectiveness of the New Austrian Tunnelling Method (NATM) in controlling the tunnel deformations. On the basis of the observations, the stabilizing effect of early installation of the invert was also established. In fact, the NATM approach introduced by Rabcewicz (1964) is based on continuous monitoring of support pressures and tunnel closures. Later in 1969, Rabcewicz brought out the advantage of providing a flexible lining over a rigid lining which attracts unecessarily high radial stresses, on the basis of measurements carried out on models.

Ward and Thomson (1965) instrumented shallow tunnels through London clays to study the behaviour of tunnel linings. Based on six years of monitoring, during which the support pressure approached the cover pressure, they concluded that the deformations of the cast iron liner and the concrete lining were nearly equal.

Grosvenor and Abel (1966) observed that in the 7m diameter twin road Straight Creek tunnel, the build up of support pressure was initially fast and reached its peak close to the face, before dropping to lower stable values at about 60 m behind the face.

The peak support pressures were observed to be 3 to 5 times the stable support pressures. These observations are contrary to the normal observations which do not indicate any drop in support pressure without yielding of the support. Although it has been reported by them that the steel ribs in the Straight Creek tunnel underwent severe buckling and bending, the reason for the drop in support pressures has not been specified.

Golser (1973), on the basis of the measurement of tunnel-wall displacements in underground excavations, recommended continuous monitoring of dispacements to reduce the support costs.

Hills, Szalay, Rourke and Smith (1974) measured support pressures and tunnel-wall displacements in Tarbela Dam tunnels in Pakistan and found their data to support Terzaghi's classification system (discussed in Art.3.2 of Chapter 3).

Dunnicliff and Schmidt (1974) emphasized the need for careful planning of the instrumentation scheme through all the steps and pointed out the benefits of field monitoring in tunnels, such as improvement in tunnelling practice and reduction in tunneling risks and costs.

Lane (1975) showed, through instrumentation at test sections, how field observations result in cost saving in tunnel supports.

Ward, Coates and Tedd (1976) carried out an interesting study of different support systems by extensively monitoring the

3.3m diameter    Kielder experimental tunnel. They demonstrated that  the rock bolt-sprayed concrete combination allows the least tunnel-wall displacement and the steel ribs, the most (Fig. 2.6). They also showed that the tunnel-wall displacements are less in a machine  excavated tunnel as compared to a tunnel excavated using the drill-and-blast method.

Dube  (1979) instrumented the Giri Hydel Tunnel in the lower Himalaya  in  India  and  reported  large  tunnel closures in the squeezing  ground  condition.  On  the  basis  of  the  borehole extensometer  observations,  a  graphical  method was proposed to estimate the radius of the broken zone.

Jethwa  (1981)  carried  out detailed instrumentation of the Chhibro-Khodri  Tunnel  located  in  the lower Himalaya  in India. The  data  obtained  from this and the other tunnels were used to evaluate  the  rock  mass classification systems by comparing the predicted  and  observed  support pressures in both squeezing and non-squeezing  ground  conditions.  On  the  basis  of  the  data obtained  from  multi-point borehole extensometers, the graphical method,  proposed by Dube (1979) to estimate the radius of broken zone, was modified. A good agreement was found between the short-term  support  pressure  predicted  by  the  analytical  approach proposed  by  Jethwa  (1981,  Eq.  2.21) and the observed support pressure  in squeezing ground condition. Jethwa (1981) discovered the  existence  of a compaction zone within the broken zone where the  volume  reduces  with  time.  Thus,  he  postulated that the ultimate  support  pressures would be 2 to 3 times the short-term support pressures in squeezing ground.

Sakurai (1983) carried out field instrumentation using the sliding micrometers, inclinometers, and borehole extensometers in two transport tunnels and an undersea tunnel, with a view to demonstrate the applicability of the back-analysis methods proposed earlier by the author (Sakurai). The back-analysis method was aimed at determining the initial stresses, Young's modulus, and cohesion and friction angle of the rock mass around tunnels, from the measured tunnel convergence.

Singh and Aziz (1983) described various rock mechanics instruments used by them for strata control investigations in coal mines and demonstrated the use of instrumentation in evaluating the stability of coal mine road ways with the help of case-histories.

Stillborg, Pekkari and Pekkari (1983) presented details of a comprehensive instrumentation scheme adopted in the Research Mine in Kiruna, Sweden. The instruments installed included sliding micrometers, borehole extensometers and distometers. All the instruments were connected to a computerised data acquisition system.

Takino, Kimura, Kamemura and Kawamoto (1983) measured the support pressures and the tunnel closures at tunnel intersections in Enasan Tunnel in Japan, and observed a close relationship between the face advance and the tunnel closure. The effect of poor geological conditions on the tunnel closures, was also observed.

TIME AFTER EXCAVATION, DAYS
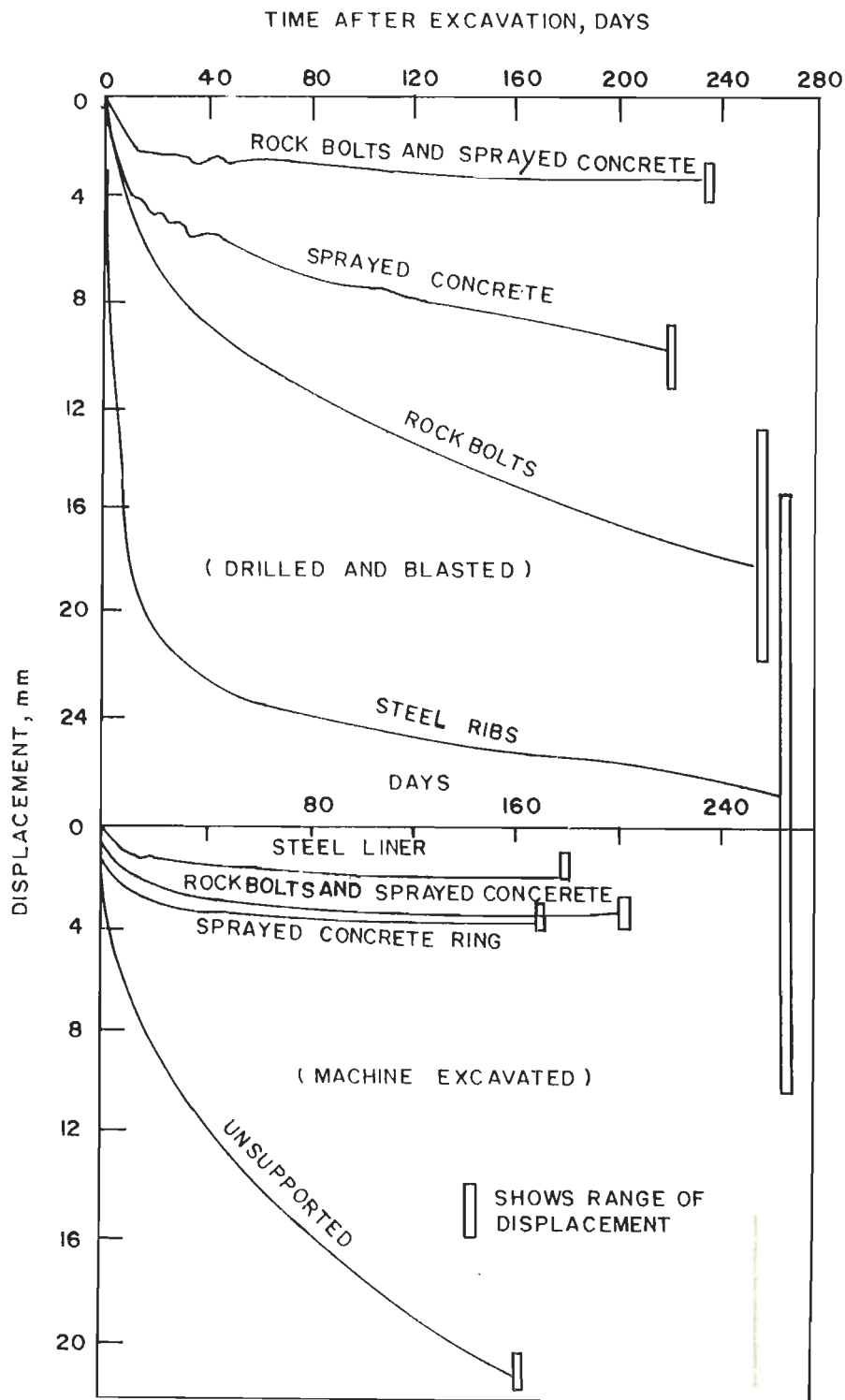


Fig.2.6 – Observed Radial Displacements for Various
Support Systems  in  Kielder Experimental
Tunnel  (after Ward et al., 1976)

Ueng, Kao, Chi and Huang (1983) presented the results of an extensive field monitoring programme carried out in a powerhouse cavern in Taiwan. The instruments installed were 30 three-point borehole extensometers, 24 convergence bolts, and 30 load cells. The significant contribution of the instrumentation was that some stability problems, which were leading to a collapse, were detected in time and remedial measures taken. The instrumentation was then helpful in verifying the effectiveness of the remedial measures.

Whittaker, Hassani, Bonsall and White (1983) carried out field monitoring of three mine tunnels in Britain with the help of borehole extensometers to investigate into the development of the yield zones around the tunnels. The effect of lithology and rock mass strength on the extent of the yield zone, was studied. The instrumentation results indicated that while in competent rock masses the yield zone developed after a relatively short period of time and tunnel advance (3 days and 9m respectively), the complete development of the yield zone in the weaker rock formations was found to be time-dependent.

Yoshimura, Yuki, Yamada and Kokubun (1986) carried out the monitoring of Miyana Tunnel in Japan as a part of the New Austrian Tunnelling Method (NATM) and found the application of NATM to be benefitial in limiting the tunnel convergence to very small values as compared to the high convergence recorded in other Japanese tunnels in similar rock mass conditions. They observed the effect of face advance on the tunnel convergence and concluded that the maximum convergence at a tunnel section occurs

within a distance of 2 to 3 times the tunnel diameter between the section and the advancing face.

Dutro and Perry (1987) presented details of tunnel instrumentation comprising of convergence monitoring instruments, borehole extensometers and borehole inclinometers, and examined the performance requirements of the instruments. They further discussed the advantages and disadvantages of various instruments.

Douglas and Alexander (1989) presented results of instrumentation carried out in the underground caverns of the Dinorwig Power station. Results of monitoring during a nearby earthquake measuring 5.4 on the Richter scale have also been included.

Chang (1990) discussed the advantages and the limitations of borehole extensometers on the basis of field instrumentation in railway tunnels in Taiwan and presented details of installation, analysis of the data obtained, and suggested a method of back analysis to obtain the unrecorded data.

Boisen (1990) presented the instrumentation results, and described the benefits thereof, obtained from four underground projects in different geological conditions - a 25 m diameter soft ground tunnel excavated in multiple drifts, a powerhouse cavern in unstable jointed rock, tunnels in squeezing ground, and a twin tunnel project in sedimentary rocks.

Verman, Jethwa and Singh (1991) presented details of a comprehensive instrumentation scheme for monitoring of the underground power house cavity of the Sardar Sarovar Project in India. The author reported the results of the instrumentation, mainly consisting of 31 multi-point and 17 single-pont borehole extensometers, and brought out its usefulness with an example of timely warning of an unstable zone which was gradually heading for a possible collapse. Remedial measures were taken up and their effectiveness was reflected in the observations of the instruments which started showing a stable trend. Later, on the basis of the six years of monitoring in this cavern, which established the adequacy of the supports installed in the cavern roof, Verman, Jethwa and Goel (1993) worked out the support requirements for the sidewalls and found these to compare favourably with the results of the existing approaches.

## 2.3 EXISTING GAPS

The following gaps have been identified in the present knowledge on the subject:

(i)   Determination of the ground reaction curve in elastic and squeezing ground condition, using the various approaches discussed, depends on a number of input parameters, some of which are difficult to determine reliably without much time and effort. There is a need to develop an approach for quick, easy, and reliable estimation of these parameters.

(ii)  No approach, based on quick and easy to use field parameters, has been suggested for prediction of ground condition.

(iii) Most of the analytical approaches, suggested for obtaining the support pressure, have not been adequately supported by field observations.

(iv) Laboratory experiments on cylindrical samples, such as those conducted by Hobbs (1966b), Hoskins (1969), Daemen and Fairhurst (1971), Haimson and Edl (1972), Santarelli and Brown (1987), Guenot (1989), and Fuenkajorn and Daemen (1992), indicate the mobilisation of a much higher strength at the periphery of an underground opening than the measured uniaxial compressive strength of the material. This observation has significant implications with regard to the design of underground openings. However, this has not been verified by actual field observations in the case of tunnels.

(v) The effect of parameters, such as, tunnel size and saturation of the rock mass due to charging of the water conducter system, on support pressure, has not been studied.

(vi) One of the most significant gaps in the knowledge is that the realistic (observed) non-linear behaviour of the supports under pressure has not been considered, and the analyses have been carried out with the theoretical assumption of a linear elastic load-deflection characteristic of the supports. The variation in the support backfill stiffness, responsible for the non-linear support behaviour in steel-supported tunnels, with support pressure has not been studied.

(vii) The analytical solutions suggested are not very easy to use at site by field engineers for quick estimation and revision, if required, of support requirements during construction.

(viii) The effect of shape of the opening roof (flat or arch) on the stand-up time has not been evaluated. In the civil engineering works, arch shaped roof is used.

## 2.4 JUSTIFICATION OF PROBLEM

During the course of the present study, an attempt has been made to close the above gaps in order to suggest a reliable and easy to use approach for determination of the ground reaction and the support reaction curves for self-supporting tunnels, tunnels in elastic ground condition, and tunnels in squeezing ground condition.

# CHAPTER 3

# CHAPTER 3

# ROCK MASS CLASSIFICATION FOR TUNNELS

## 3.1 INTRODUCTION

Rock Mass classification systems are the mainstay of the widely used empirical approach of tunnel design which, in essence, is the application of the experience acquired at previous tunnelling projects to the design of supports for the tunnel under consideration. Begining with the classical rock load classification of Terzaghi (1946), several rock mass classification systems have been proposed to date, most notable amongst them being those proposed by Bieniawski (1973) and Barton et al. (1974). These and some of the other classification systems of practical significance are described in the following paragraphs.

## 3.2 TERZAGHI'S ROCK LOAD CLASSIFICATION

Based on field observations on the steel-supported railroad tunnels through eastern Alps, Terzaghi (1942, 1946) developed his classification system which has been in use for over four decades now, particularly in the USA and India. The rock mass was divided in nine categories (Table 3.1) on the basis of the rock mass condition and the values of rock load for each category in the form of certain height of the loosened rock mass were suggested. This loosening pressure has been assumed to increase directly with the tunnel size.

Table 3.1 - Terzaghi's Rock Load Table

Rock load $H_p$ on tunnel roof with width B and height $H_t$ at depth of more than $1.5(B+H_t)$.

| | Rock Condition | Rock Load $H_p$ | Remarks |
|---|---|---|---|
| i) | Hard and intact | Zero | Light lining required only if spalling or popping occurs |
| ii) | Hard stratified or schistose | 0 to 0.5B | Light support, mainly for protection against spalls. Load may change erratically from point to point |
| iii) | Massive, moderately jointed | 0 to 0.25B | |
| iv) | Moderately blocky & seamy | 0.25B to $0.35(B+H_t)$ | No side pressure |
| v) | Very blocky and seamy | 0.35 to $1.10(B+H_t)$ | Little or no side pressure |
| vi) | Completely crushed | $1.10(B+H_t)$ | Considerable side pressure. Softening effects of seepage towards bottom of tunnel require either continuous support for lower ends of ribs or circular ribs |
| vii) | Squeezing rock, moderate depth | 1.10 to $2.10(B+H_t)$ | Heavy side pressure, invert struts required. Circular ribs are recommended |
| viii) | Squeezing rock, great depth | 2.10 to $4.50(B+H_t)$ | |
| ix) | Swelling rock | Upto 250 feet, irrespective of value of $(B+H_t)$ | Circular ribs are required. In extreme cases use yielding support |

Although Terzaghi's classification may not be suitable for the modern construction techniques and support systems, it is still being successfully employed for the purpose for which it was developed due to its ease of application and suitability to the steel-supported tunnels. The practical importance of Terzaghi's classification, despite Cecil's observation (1970) that the classification is too general to permit an objective evaluation of rock quality and that it provides no quantitative information on the properties of rock masses, has attracted the attention of several researchers who have proposed modifications in the classification. Deere et al. (1970) interchanged the rock load values for Terzaghi's rock mass categories (ii) and (iii) of Table 3.1. Another modification of Terzaghi's classification by Singh and Jethwa (1993) is in the offing. They have proposed modification to incorporate all ground conditions and constant support pressures for all types of underground structures ranging from small to large sized openings, in order to develop a comprehensive, yet easy to use, classification system.

## 3.3 DEERRE'S ROCK QUALITY DESIGNATION

Deere (1964) proposed a numerical index of the rock mass quality and termed this as Rock Quality Designation (RQD). The RQD was defined as the ratio of the cumulative length of pieces longer than or equal to 10 mm in a core, to the total core length. The relationship proposed between RQD and the engineering quality of rock mass is presented in Table 3.2.

Table 3.2 - Deere's (1964) Correlation of RQD with Rock Core Quality

| RQD (Percent) | Rock core quality |
|---------------|-------------------|
| <25 | Very poor |
| 25-50 | Poor |
| 50-75 | Fair |
| 75-90 | Good |
| 90-100 | Excellent |

Later in 1970, Deere et al. related the RQD with support requirement, both for the conventional and the machine excavation methods (Table 3.3). Cording et al. (1972) found a reasonable correlation between RQD and Terzaghi's rock load factor for steel-supported tunnels. They, however, could not arrive at an acceptable correlation for tunnels supported by rock bolts. Thus, Cording and Deere (1972) concluded that Terzaghi's concept was suitable for steel-supported tunnels only.

The utility of RQD is limited to a quick preliminary judgement of the quality of rock core. The RQD alone is insufficient to provide an adequate description of the rock mass as it does not include the influence of joint fillings, as pointed out by Merritt (1972), and other joint properties. The influence of clay seams and fault gouge on the tunnel stability was discussed by Brekke and Howard (1972).

## 3.4 LAUFFER'S CLASSIFICATION

Lauffer (1958), on the basis of Stini's work (1950) on the importance of structural defects of rock masses, related the

## Table 3.3 - Support Recommendations for Tunnels (6m to 12m) Based on RQD (after Deere et al., 1970)

| Rock quality | Tunneling method | Alternative support systems | | |
|---|---|---|---|---|
| | | Steel sets[2] | Rockbolts[3] | Shotcrete |
| **Excellent[1]**<br>RQD > 90 | Boring machine | None to occ. light set. Rock load $(0.0-0.2)B$ | None to occasional | None to occ. local application |
| | Conventional | None to occ. light set. Rock load $(0.0-0.3)B$ | None to occasional | None to occ. local application 2 in. to 3 in. |
| **Good[1]**<br>75 < RQD < 90 | Boring machine | Occ. light sets to pattern on 5-ft to 6-ft ctr. Rock load $(0.0$ to $0.4)B$ | Occasional to pattern on 5-ft to 6-ft centers | None to occ. local application 2 in. to 3 in. |
| | Conventional | Light sets, 5-ft to 6-ft ctr. Rock load $(0.3$ to $0.6)B$ | Pattern 5-ft to 6-ft centers | Occ. local application 2 in. to 3 in. |
| **Fair**<br>50 < RQD < 75 | Boring machine | Light to medium sets, 5-ft to 6-ft ctr. Rock load $(0.4-1.0)B$ | Pattern, 4-ft to 6-ft ctr. | 2 in. to 4 in. crown |
| | Conventional | Light to medium sets, 4-ft to 5-ft ctr. Rock load $(0.6-1.3)B$ | Pattern 3-ft to 5-ft ctr. | 4 in. or more crown and sides |
| **Poor[2]**<br>25 < RQD < 50 | Boring machine | Medium circular sets on 3-ft to 4-ft ctr. Rock load $(1.0-1.6)B$ | Pattern, 3-ft to 5-ft ctr. | 4 in. to 6 in. on crown and sides. Combine with bolts |
| | Conventional | Medium to heavy sets on 2-ft to 4-ft ctr. Rock load $(1.3-2.0)B$ | Pattern, 2-ft to 4-ft ctr. | 6 in. or more on crown and sides. Combine with bolts |
| **Very poor[3]**<br>RQD < 25 (Excluding squeezing or swelling ground) | Boring machine | Medium to heavy circular sets on 2-ft ctr. Rock load $(1.6$ to $2.2)B$ | Pattern, 2-ft to 4-ft ctr. | 6 in. or more on whole section. Combine with medium sets |
| | Conventional | Heavy circular sets on 2-ft ctr. Rock load $(1.6$ to $2.2)B$ | Pattern, 3-ft center | 6 in. or more on whole section. Combine with medium to heavy sets |
| **Very poor[3]**<br>(Squeezing or swelling) | Boring machine | Very heavy circular sets on 2-ft ctr. Rock load up to 250-ft. | Pattern, 2-ft to 3-ft ctr. | 6 in. or more on whole section. Combine with heavy sets |
| | Conventional | Very heavy circular sets on 2-ft ctr. Rock load up to 250-ft. | Pattern, 2-ft to 3-ft ctr. | 6 in. or more on whole section. Combine with heavy sets |

Notes:
1. In good and excellent rock, the support requirement will be, in general, minimal but will be dependent upon joint geometry, tunnel diameter, and relative orientations of joints and tunnel.
2. Lagging requirements will usually be zero in excellent rock and will range from up to 25% in good rock to 100% in very poor rock.
3. Mesh requirements usually will be zero in excellent rock and will range from occasional mesh (or straps) in good rock to 100% mesh in very poor rock.
4. $B$ = tunnel width

stand-up time to the active span of the tunnel and the rock mass class (Fig.3.1). The active span of a tunnel is defined as the distance of the last support from the tunnel face, and the tunnel width, whichever is less. The stand-up time is the duration for which a tunnel will stand on its own without support after the excavation. Lauffer also pointed out the influence of orientation of tunnel axis, shape of cross-section of tunnel, method of excavation, and the support system.

Lauffer's classification was later modified by other followers of the 'Austrian School' of tunnelling and rock mechanics. Among these, the contribution of Pacher et al. (1974) is considered significant. They illustrated the effect of the tunnel size on the stand-up time and concluded that an increase in the former leads to a substantial reduction in the stand-up time. This explains why a larger tunnel requires the multi-drift or the heading and bench method of excavation in a fair rock mass, whereas a smaller tunnel (such as a pilot tunnel) is successfully driven through the same rock mass by using the full face method of excavation. The qualitative nature of this classification system, however, poses practical difficulties in assessing both the stand-up time and the active span. The classification system, nevertheless, introduced the stand-up time and the active span as parameters relevent to the tunnel stability and influenced the development of the more recent classification systems.

## 3.5 ROCK STRUCTURE RATING METHOD

The Rock Structure Rating (RSR) method of rock mass classification was developed by Wickham, Tiedmann and Skinner (1972, 1974) primarily for the steel-supported tunnels. On the basis of observations at 190 tunnel sections in 53 tunnels, the authors developed a 'ground support prediction model'. The RSR concept takes into account the following two broad categories of parameters influencing the rock mass behaviour around tunnels:

**a)    Geologic parameters -**

i)   Type of rock mass,

ii) joint pattern (average spacing of joints),

iii)joint orientation (dip and strike),

iv) type of discontinuities,

v)   major faults, shears and folds,

vi) rock material properties, and

vii)weathering or alteration.

**b)    Construction parameters -**

i)    Size of tunnel,

ii)   direction of drive, and

iii) method of excavation.

All  the above factors were grouped into the following three basic parameters:

a)   Parameter  A - general  appraisal of a rock structure on  the basis of :

i)   rock type origin (igneous, metamorphic, sedimentary),

ii)  rock hardness (hard, medium, soft, decomposed), and

iii) geologic   structure   (massive,   slightly   faulted/folded,
     moderately faulted/folded, intensely faulted/folded).

b)   Parameter  B - effect of discontinuity pattern with  respect
     to the direction of tunnel drive on the basis of:

i)   joint spacing,

ii)  joint orientation (strike and dip), and

iii) direction of tunnel drive.

c)   Parameter C - effect of groundwater inflow on the basis of:

i)   overall  rock  mass  quality  due  to  parameters  A  and  B
     combined,

ii)  joint condition (good, fair, poor), and

iii) amount of water inflow.

     Ratings  were  assigned to these three basic parameters, the
sum  of which gives the RSR value which is related to the quality
of  rock  mass. Charts were prepared for the determination of the
support  requirements  from  the RSR value for 3m, 6m, 7m and 10m
diameter tunnels.

     In  the  RSR  method, the support pressure has been taken to
increase  in direct proportion to the tunnel size. The method may
be  more  suited  to the steel-supported tunnels, excavated using
the  conventional  method  as  147  of  the  164 supported tunnel
sections,  considered  for  developing the method, were supported
with steel ribs and excavated by the drill- and-blast method.

## 3.6 GEOMECHANICS CLASSIFICATION (RMR SYSTEM)

Bieniawski (1973) proposed a rock mass classification system in South Africa, based on ratings assigned to parameters expected to influence the rock mass behaviour around tunnels, and called it the Geomechanics classification. The classification system, which is also known as the rock mass rating (RMR) system, takes into account the following six parameters:

i) Uniaxial compressive strength of intact rock material,

ii) rock quality designation (RQD),

iii) spacing of discontinuities,

iv) condition of discontinuities,

v) groundwater conditions, and

vi) orientation of discontinuities.

The ratings have been assigned to the first five of the above classification parameters in accordance with the ranges of their values. This is followed by an adjustment of the ratings to account for the sixth parameter for very favourable to very unfavourable discontinuity orientation. Finally, the ratings for all the parameters are summed up to arrive at the total rating, called the rock mass rating (RMR), which is related to five rock mass classes, ranging from very good to very poor (Table 3.4; Bieniawski,1979). Ranges of average stand-up time, and cohesion and friction angle of the rock mass were suggested for each of these rock mass classes (Table 3.4). The suggested cohesion and friction angle values are based on the data of rock slopes compiled by Hoek and Bray (1977). The stand-up

Table 3.4 - Rock Mass Classes Determined from Total RMR Ratings (after Bieniawski, 1979)

| Rating | 100-81 | 80-61 | 60-41 | 40-21 | <20 |
|---|---|---|---|---|---|
| Class No. | I | II | III | IV | V |
| Description | Very good rock | Good rock | Fair rock | Poor rock | Very poor rock |
| Average stand-up time | 10 years for 15m span | 6 months for 8m span | 1 week for 5m span | 10 hours for 2.5m span | 30 mints. for 1m span |
| Cohesion of rock mass (kPa) | >400 | 300-400 | 200-300 | 100-200 | <100 |
| Friction angle of rock mass | >45° | 35°-45° | 25°-35° | 15°-25° | <15° |

time and the maximum unsupported span may be obtained from Fig.3.2 (Bieniawski, 1989) for a given rock mass rating.

Bieniawski (1975) recommended the excavation methods and the support systems for a 10 m diameter tunnel, but did not suggest any value of support pressure. In 1983, Unal proposed the following correlation for determination of the support load from RMR:

$$P = \frac{100 - RMR}{100} \gamma B = \gamma H_p \qquad (3.1)$$

where,

$P$ = support load in $kg/m^2$,

$H_p = [\frac{100 - RMR}{100}] B$ is the rock load height in meters,

$B$ = tunnel width in meters, and

$\gamma$ = unit weight of rock in $kg/m^3$

Bieniawski (1978) and Serafim and Pereira (1983) obtained the following correlations (Fig.3.3) for determination of the insitu modulus of deformation, $E_d$, in the case of rock foundations:

$$E_d = 2RMR - 100 \quad GPa \qquad \text{(for RMR < 50; Bieniawski, 1978)} \qquad (3.2)$$

$$E_d = 10^{(RMR - 10)/40} \quad GPa \qquad \text{(Serafim and Pereira, 1983)} \qquad (3.3)$$

Bieniawski (1976) found a reasonable correlation between RMR and Barton's rock mass quality (Q), on the basis of 117 case histories (68 Scandinavian, 28 South African, and 21 others) as shown in Fig.3.4.

## 3.7 Q-SYSTEM

Based on a detailed study of over 200 case histories in the Scandinavian region, Barton, Lien and Lunde (1974) of the Norwegian Geotechnical Institute, developed the Q-system of rock mass Classification and proposed the following equation to determine the rock mass quality, denoted by Q:

$$Q = \frac{RQD}{J_n} \times \frac{J_r}{J_a} \times \frac{J_w}{SRF} \qquad (3.4)$$

where,

RQD = rock quality designation (to be taken equal to 10 for RQD < 10),

$J_n$ = joint set number,

$J_r$ = joint roughness number,

$J_a$ = joint alteration number,

$J_w$ = joint water reduction factor, and

SRF = stress reduction factor.

A - VERY GOOD ROCK ;    G - VERY POOR ROCK
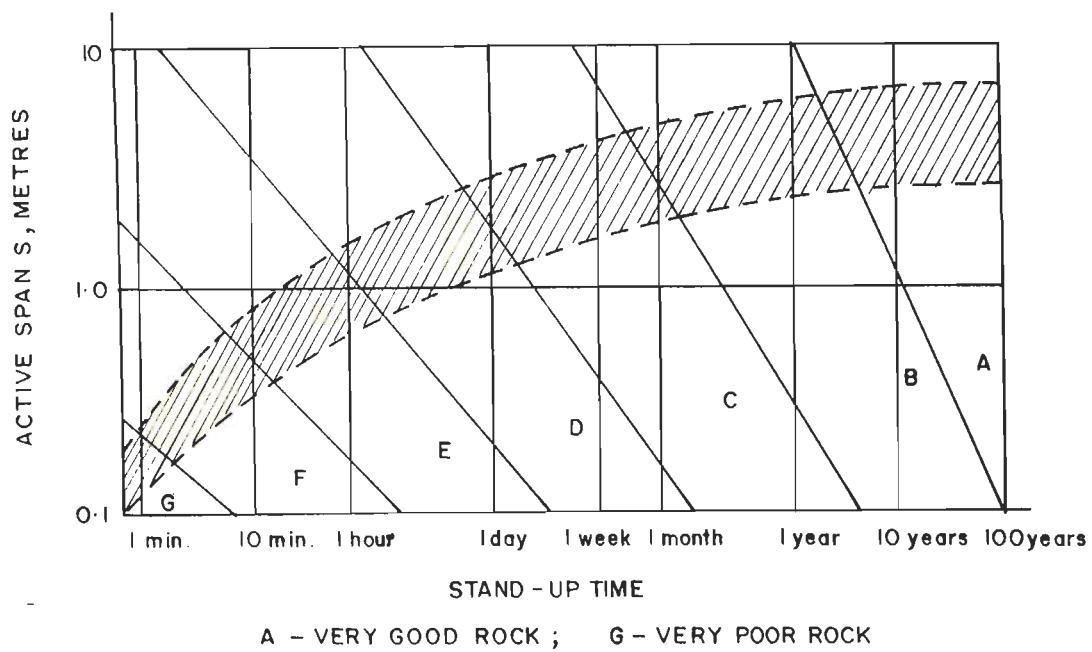
Fig.3.1 - Relationship Between Active Span and
Stand-up Time (after Lauffer, 1958)
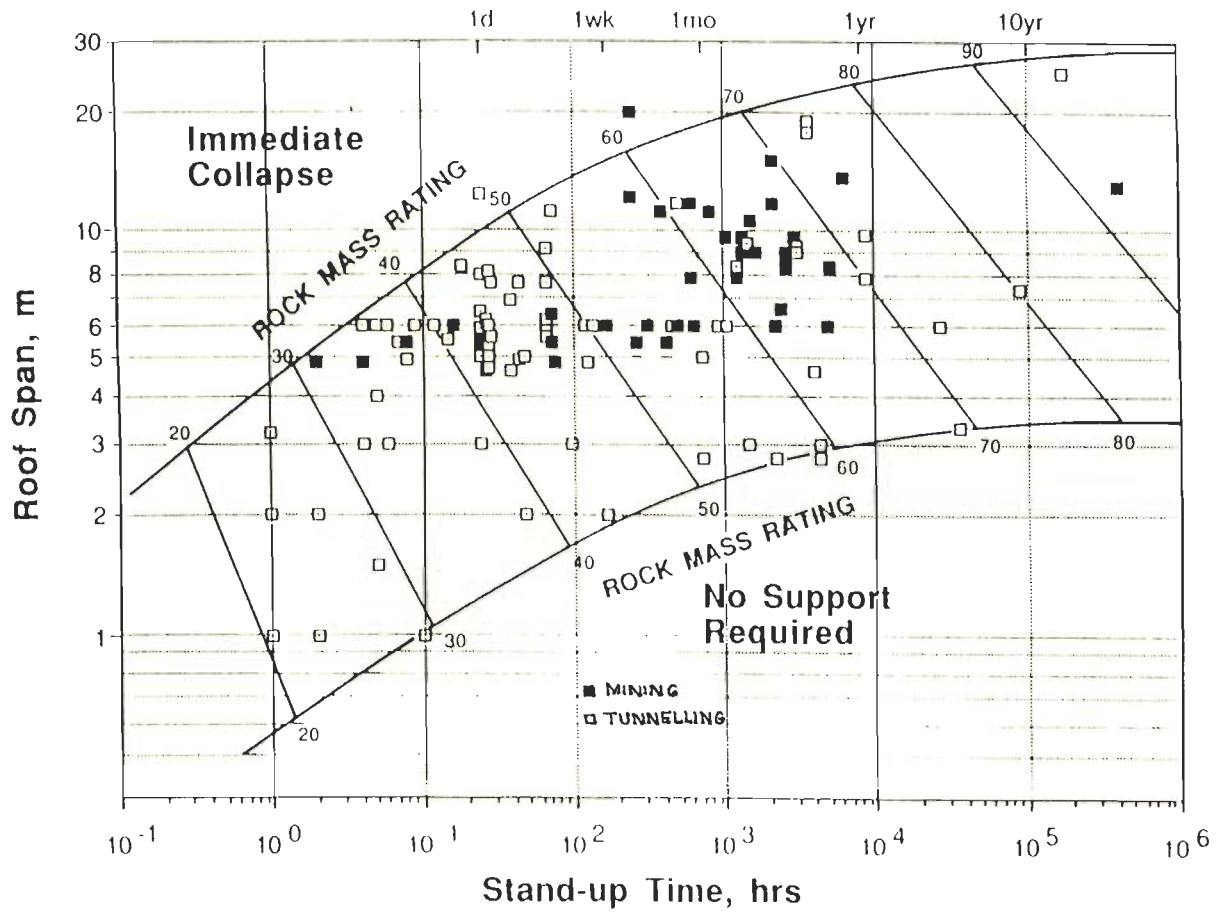


Fig.3.2 - Relationship Between Stand-up Time and Roof Span for
Various Rock Mass Classes (after Bieniawski, 1989)
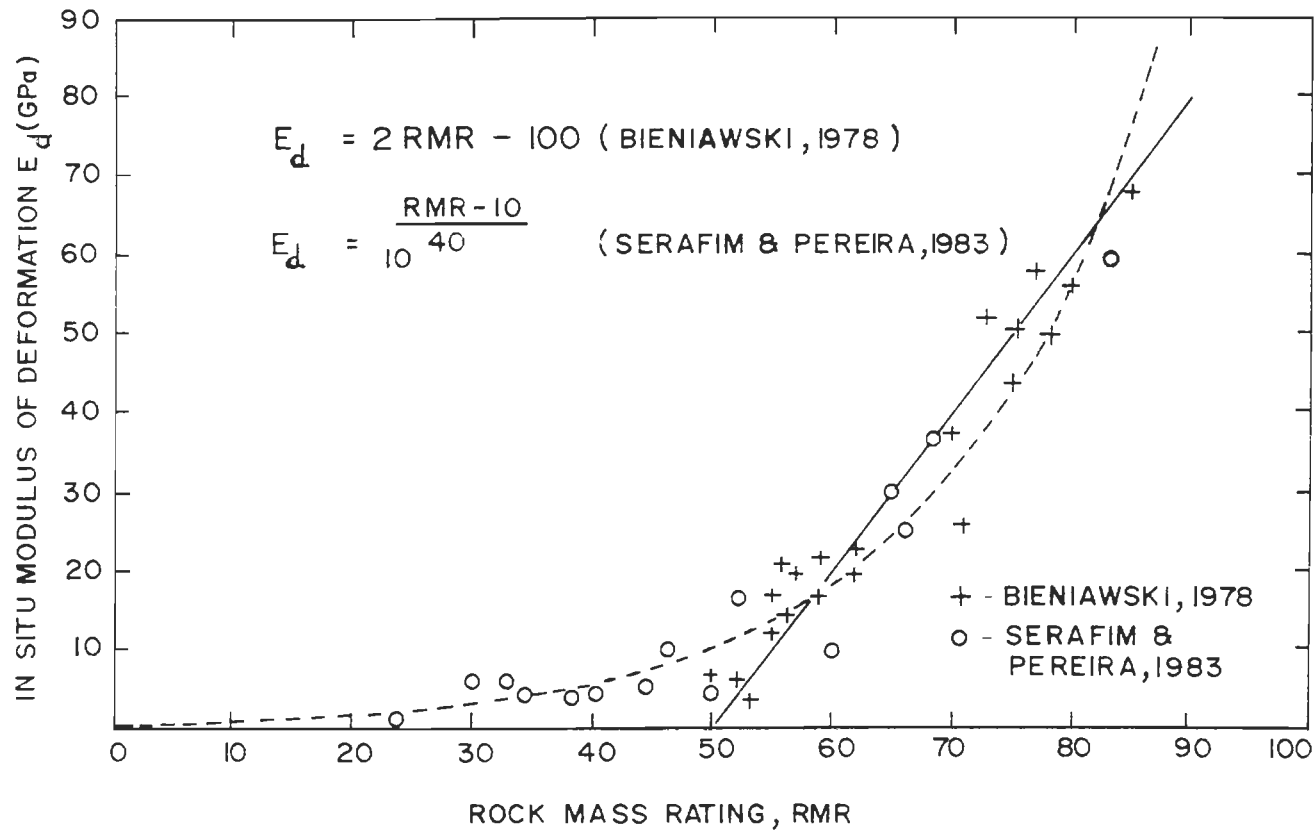
Fig.3.3 - Correlation Between Insitu Modulus of Deformation and RMR

The figure shows a plot of IN SITU MODULUS OF DEFORMATION $E_d$ (GPa) versus ROCK MASS RATING, RMR with the following correlations:

$$E_d = 2\,RMR - 100 \quad (BIENIAWSKI, 1978)$$

$$E_d = 10^{\frac{RMR-10}{40}} \quad (SERAFIM\ \&\ PEREIRA, 1983)$$

Legend:
+ - BIENIAWSKI, 1978
o - SERAFIM & PEREIRA, 1983
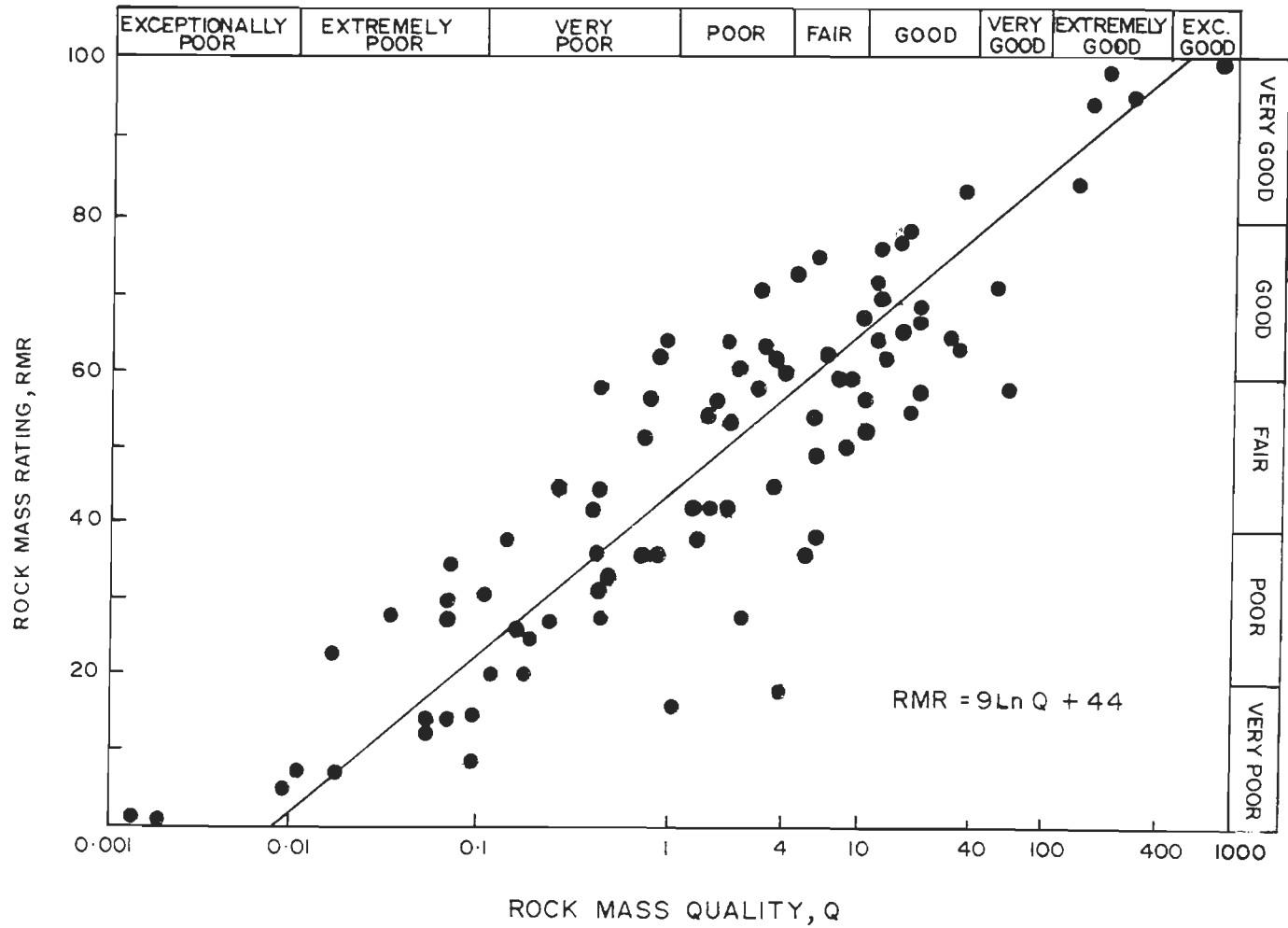
Fig.3.4 - Correlation Between RMR and Q (after Bieniawski, 1976)

The rock mass quality may, therefore, be considered as consisting of only three parameters which are crude measures of:

i)   block size (RQD/Jn),

ii)  inter-block shear strength (Jr/Ja), and

iii) active stress ($J_w$/SRF).

Barton et al. (1974) related the Q-value with tunnel support requirements on the basis of the equivalent dimension of the excavation, which they defined as:

$$\text{Equivalent dimension} = \frac{\text{Excavation span, diameter or height (m)}}{\text{ESR}}$$

where ESR is the excavation support ratio. Barton et al. (1974) suggested the values of ESR according to the use for which the excavation is intended and the required degree of safety. The equivalent dimension was related with the support requirement and 38 support categories were suggested for estimation of the permanent support. For temporary support, they suggested to either increase Q to 5Q or ESR to 1.5 ESR. The following equation for the determination of the maximum unsupported span was suggested:

$$\text{Maximum unsupported span} = 2(\text{ESR})^{0.4} \tag{3.5}$$

To estimate the ultimate support pressure, Barton et al. (1974, 1975) suggested the following correlations:

$$p_{roof} = (2/J_r)\ Q^{-1/3} \tag{3.6}$$

$$p_{wall} = (2/J_r)\ Q_w^{-1/3} \tag{3.7}$$

Table 3.5 – Correlation Between Rock Mass Quality and Wall Factor

| Range of Q | Wall factor $Q_w$ |
|:---:|:---:|
| > 10 | 5.0 Q |
| 0.1 – 10 | 2.5 Q |
| < 0.1 | 1.0 Q |

where,

$p_{roof}$ = ultimate support pressure on roof,

$p_{wall}$ = ultimate support pressure on walls, and

$Q_w$    = wall factor.

The wall factor may be obtained from Table 3.5.

For the case when the number of joint sets is less than three, the following correlations have been suggested:

$$p_{roof} = (2/3) \ J_n^{1/2} \ J_r^{-1} \ Q^{-1/3} \qquad (3.8)$$

$$p_{wall} = (2/3) \ J_n^{1/2} \ J_r^{-1} \ Q_w^{-1/3} \qquad (3.9)$$

Figure 3.5 depicts the plot between Q and the ultimate support pressure. For determination of the short-term pressure, Barton et al. (1975) suggested multiplication of the estimated value of Q by a factor of 5.0. From Eq. 3.6, the ultimate support pressure is, therefore, 1.7 times the short-term support pressure.

Singh et al. (1992) have suggested correction factors for overburden f (Eq.7.12) and for tunnel closure f' (Eq.7.11) in the case of squeezing ground. Details are discussed in Art.7.3.2 of Chapter 7.
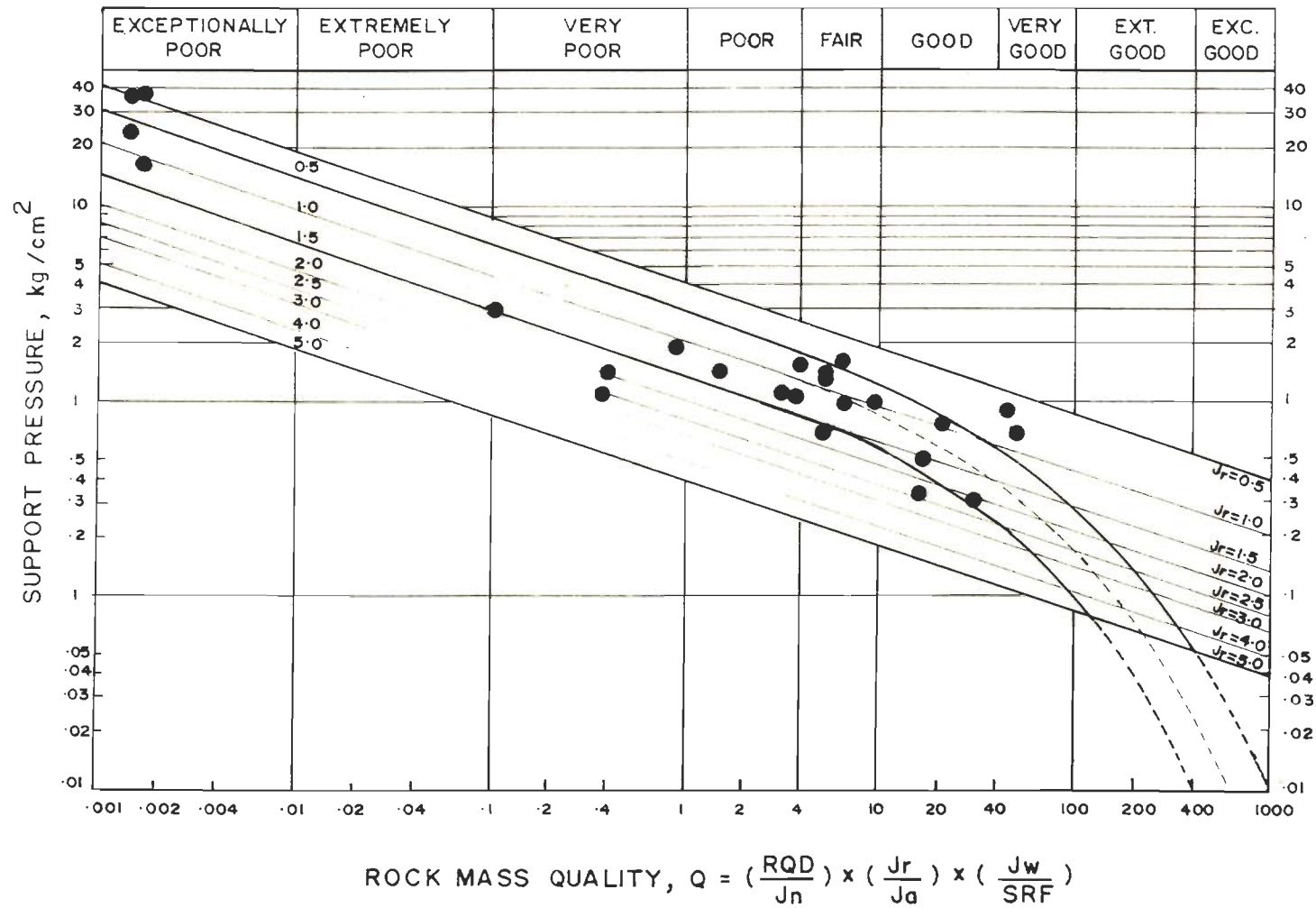
Fig.3.5 - Relationship Between Q and Ultimate Support Pressure
(after Barton et al., 1974)

# CHAPTER 4

# CHAPTER 4

## GEOLOGY AND ITS INFLUENCE ON TUNNELLING CONDITIONS

### 4.1 GENERAL

Almost every aspect of a tunnelling project, from its conception to commissioning, is influenced by the geology of the area. Reliability of the predicted geology, therefore, plays an important role in the success of the project. On the other hand, inadequate geological investigation and poor anticipation of the nature and the magnitude of problems catch the tunnelling engineers unawares, resulting in delays and higher cost of construction. Inadequate investigations are, however, not necessarily due to an inadequate effort by the geologists. At many places, such as the Himalaya, the terrain does not permit desired numbers of boreholes upto the tunnel grade. Moreover, the pilot tunnels do not adequately represent the tunnelling problems to be faced in the main tunnel which is bigger in size and has a much greater height of overburden. Often the equipment is an outdated one and has its limitations.

Several irrigation and hydro-electric projects involving tunnelling are located in India. The Central Mining Research Station, Dhanbad, India, has been involved in rock mechanical studies in many of these tunnels, located in the tectonically active lower and middle Himalayas as well as in the peninsular India, for well over two decades. The author has been associated with seven of these tunnels for instrumentation and other field studies. The present work is based on the field studies carried

out in ten tunnels (Tables 5.1 and 5.2), including two mine inclines. No report of any field work related to tunnelling is complete without a mention of the geology of the area. The following paragraphs contain details of the geology pertaining to the tunnels considered for the present work, and the influence thereof on the tunnelling conditions.

## 4.2 GEOLOGICAL DETAILS OF TUNNELLING PROJECTS

As stated earlier, the present work is based on field studies carried out in tunnels located in the Himalaya and the peninsular India. The tunnelling difficulties encountered in the fragile rock masses and frequently changing ground conditions of the tectonically active lower and middle Himalayas are well known to the tunnelling engineers. Similarly, the geologists are well aware of the numerous problems faced during geological investigations in the Himalaya due to difficult terrains and high overburden. Design of supports for tunnels in weak rock masses under high overburden, often leading to squeezing ground condition, is regarded as a formidable task by the rock mechanics engineers. As a result of all this, tunnelling through the lower and the middle Himalayas becomes a challenging operation. The description of geology of tunnels located in these regions, therefore, deserves a more detailed treatment as compared to those driven through the relatively stable and less problematic peninsular region of India.

**4.2.1 Chhibro-Khodri Tunnel (Uttar Pradesh)**

**4.2.1.1 General features**

In stage-I of the Yamuna Hydro-electric Scheme, located in the lower Himalaya in the state of Uttar Pradesh, the water of Tons river is taken from a diversion dam, located at Ichari, to the underground powerhouse of 240 MW capacity at Chhibro (Fig.4.1) through a 6.25 km long pressure tunnels of 7.0 m diameter for utilizing a drop of 120 m. The Chhibro-Khodri tunnel was constructed in Stage-II of this scheme to utilize the discharge from the Chhibro underground power house. The 5.6 km long tunnel of 7.5 m diameter carries the water from Chhibro to Khodri, where a surface power house of 120 MW capacity has been constructed to utilize a drop of 64 m (Fig.4.1).

Construction of the Chhibro-Khodri tunnel was started from both Chhibro and Khodri ends. An inspection gallery, in the form of a small incline (2.0 x 2.5 m), was driven to the tunnel grade near Kalawar, situated midway between the two ends, to observe the rock mass behaviour in the Krol-Nahan intra-thrust zone. To excavate the main tunnel through this zone, two additional headings, one towards Chhibro and the other towards Khodri, were opened through the Kalawar inspection gallery.

**4.2.1.2 Regional geology and structural features**

The Chhibro-Khodri tunnel passes through various formations from north to south (Shome et al., 1973 ; Fig.4.2) as shown in Table 4.1.

Table 4.1 – Geological Formations Along Chhibro-Khodri Tunnel

| Formation | Rock Mass Description |
|---|---|
| **NORTH (Inlet)** | |
| Mandhali series (Palaeozoic) | - boulder slates,<br><br>- graphitic and quartzitic slates,<br><br>- Bhadraj quartzite unit with 5-10 m thick crushed quartzites along the Krol thrust |
| ---------------------- Krol thrust ---------------------- | |
| Subathu-Dagshai series (Lower Miocene) | - 1-3 m thick plastic black clays along the thrust,<br><br>- red and purple shales and siltstones,<br><br>- minor grey and green quartzites,<br><br>- 20-22m thick black clays with thin bands of quartzites,<br><br>- 5-10m thick soft and plastic black clays along the Nahan thrust |
| ---------------------- Nahan thrust ---------------------- | |
| Nahan series (Upper Tertiary) | - greenish grey to grey micaceous sandstones,<br><br>- purple siltstones,<br><br>- red, purple, grey and occasional mottled blue concrationary clays |
| **SOUTH (Outlet)** | |

The regional strike of these formations is almost normal to the tunnel alignment with their dips ranging from $20^{\circ}$ to $60^{\circ}$ in NNW to NNE direction, i.e., towards the upstream.

Two main boundary faults, running from Punjab to Assam along the foothills of the Himalaya, are the major structural features of the area. These low angle reverse faults, locally termed as
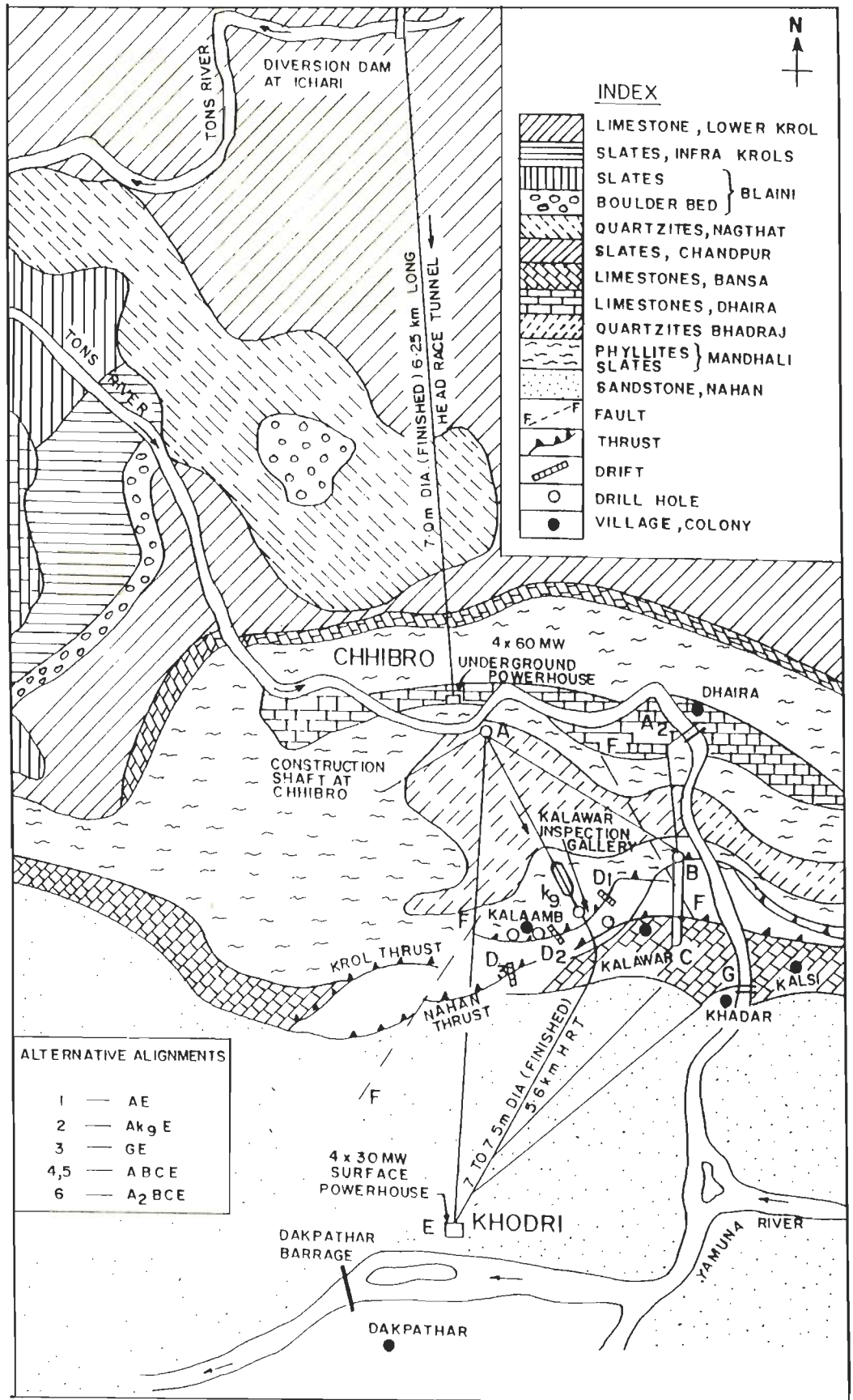
Fig. 4.1—LAYOUT OF CHHIBRO-KHODRI TUNNEL

the Krol and the Nahan thrusts, are dipping at $26^O$ due N $26^O$ and $27^O$ to $30^O$ due N $10^O$ respectively and have their strikes almost normal to the tunnel alignment. The outcrops of the thrusts were spotted across river Tons near Khadar and at a few nullah exposures. The intra-thrust zone was further explored with the help of a few drill holes, drifts, and trenches (indicated in Fig.4.1) near the villages of kalawar and Kala-Amb.

## 4.2.1.3 Influence of geology on tunnelling conditions

The influence of geology in the Chhibro-Khodri tunnel was evident in the selection of the layout and in the tunnelling problems encountered.

### a) Predicted width of intra-thrust zone and selection of layout

Presence of the intra-thrust zone was expected to pose several tunnelling difficulties. Krishnaswami (1967) predicted the existence of large quantities of locked-up water in this zone. Several alternative layouts (Fig.4.1) were proposed by Krishnaswami and Jalote (1968) to either eliminate completely or reduce appreciably the tunnel length through the intra-thrust zone. Layout no.2 ($Ak_9E$, Fig. 4.1) was ultimately selected to achieve a reduction of the tunnel length through the intra-thrust zone from 800 m, in the case of the straight alignment (AE), to 230 m with only nominal increase in the cost. The resulting increase in the tunnel length was to be 0.4 km. The original and the revised geological sections (after Auden, 1942 and Jain et al.,1975 respectively) are shown in Figs.4.2 and 4.3.

## b) Actual width of intra-thrust zone along selected layout

In addition to their presence at Kalawar, the Subathu-Dagshai red shales were encountered between 1139 m and 1297m from the inlet end at Chhibro (Fig.4.3), indicating the existence of the intra-thrust zone there also. A hole, drilled at 1130 m from inlet through the tunnel roof and inclined at 60° due east, established the presence of the Krol thrust over the tunnel. The existing geological data was then interpreted afresh by Jain et al. (1975) who predicted the presence of a series of tear faults between Chhibro and kalawar (Fig.4.3). They also predicted the existence of a third intra-thrust zone between 1861 m and 2166 m from inlet. The total anticipated width of the intra-thrust zones was thus to be 695 m as compared to the previously estimated width of 230 m along the selected tunnel layout.

## c) Trifurcation of tunnel to tackle squeezing ground condition

As expected, tunnelling through the intra-thrust zones proved to be an arduous task. The multi-drift method was adopted to prevent frequent rock falls at the face. In the top heading, a central pilot tunnel had to be excavated by forepoling at many places. Heavy steel arches (300x140 mm and 150x150 mm at 0.25-0.5 m spacing) were provided to cope up with high squeezing pressures.

Due to the tunnelling difficulties, the rate of advance of the tunnel through the intra-thrust zones was very poor (5 to 6 m per month). Construction of the tunnel, which was already lagging behind by six years in the year 1975, would have taken
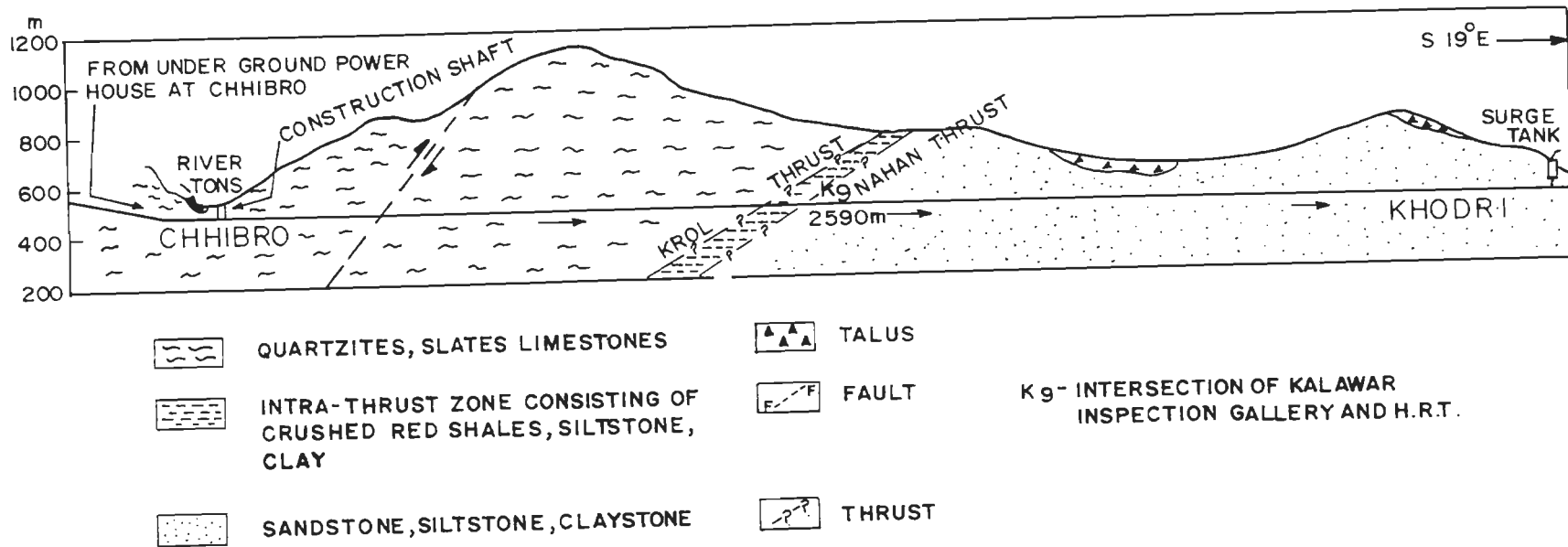
Fig.4.2 - Original Geological Section of Chhibro-Khodri Tunnel
(after Auden, 1942)
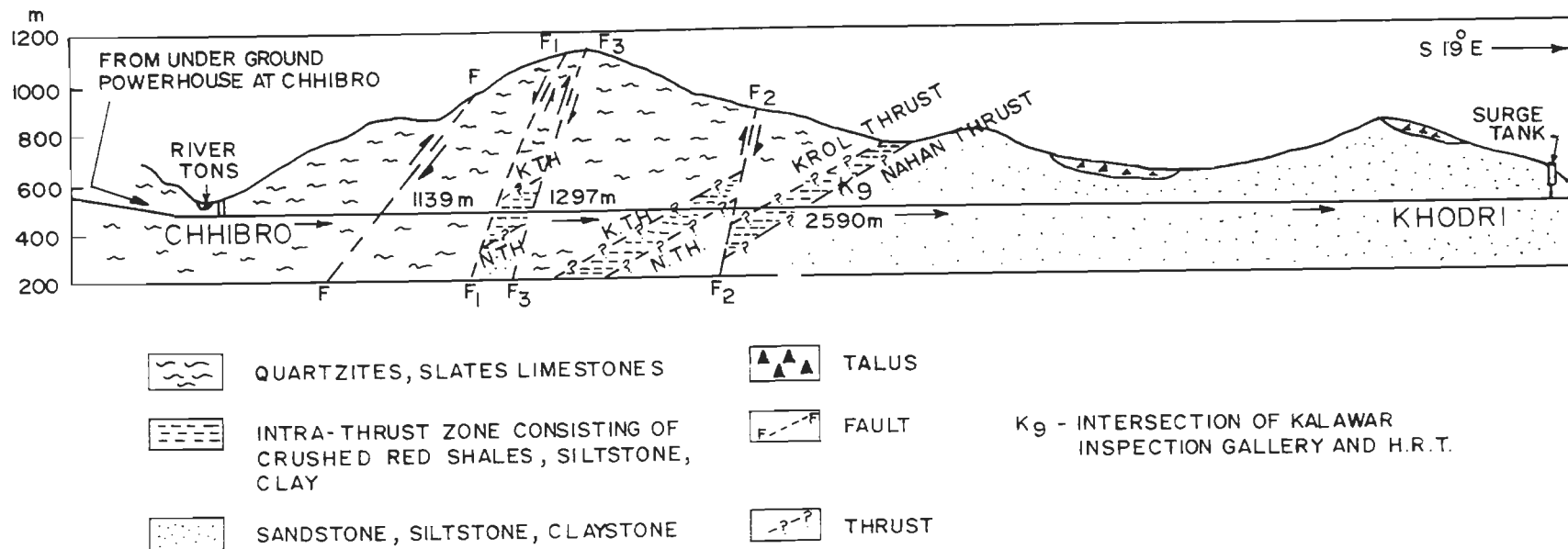
Fig.4.3 – Revised   Geological   Section   of   Chhibro-Khodri   Tunnel
(after Jain et al., 1975)

another five and a half years through the remaining 800 m length (between P and Q in Fig. 4.3) from the two ends at this rate. It was, therefore, decided to divide the remaining portion of the tunnel into three smaller tunnels of about 5.0 m excavated diameter each. Reduction in the tunnel size lessened the tunnelling problems and the central tunnel was completed in two and a half years (from the end of 1976 to mid-1979). **The quantitative effect of the tunnel size was, however, not known then, although the relationship between the tunnel size and the squeezing ground condition had been realized in a qualitative way. This is, therefore, one of the objectives of the present work for which a solution has been presented in Art.6.2 of Chapter 6.** The full benefit of the trifurcation, however, could not be achieved in the Chhibro- Khodri tunnel as the excavation of all the three smaller tunnels was not taken up simultaneously.

**d) Heavy water inflow at Kalawar**

The impervious layer of the argillaceous black clays along the Krol thrust was suddenely punctured by the perched water of the hill in November 1972. As a result, the water gushed into the main tunnel from the crown at a point located at 182m upstream of the point of intersection ($K_9$) of the Kalawar inspection gallery and the main tunnel, at a rate of about 1.2 cumecs. The local geology near the point of the water inflow is shown in Fig.4.4 (Shome et al., 1973).

## 4.2.2 Giri Tunnel (Himachal Pradesh)

### 4.2.2.1 General features

The 7.2 km long Giri Tunnel, with a finished diameter of 3.6m is the head race tunnel of the Giri Hydroelectric Project located in the lower Himalaya in the state of Himaachal Pradesh. The tunnel excavation started simultaneously from four faces - one each at the inlet and the outlet ends, and two from an intermediate adit at Marar (Fig. 4.5) located at about 5.5 km downstream from the inlet. Two additional faces were created later through a 365 m long inclined approach, with a gradient of 1 in 3, at Tanlog at 2.632 km from the inlet (fig.4.6).

### 4.2.2.2 Regional geolgy and structural features

Auden (1942) mapped the regional geology of the area and indicated the presence of three thrusts - Renuka, Krol and Nahan. The detailed geological study of the area was later carried out by Shome and Dayal (1965, 1966, 1967), and Dayal and Mandwal (1969). They proposed a number of alternative alignments for the Giri tunnel to either reduce, or eliminate completely the tunnel length through the intra-thrust zone. The alignment finally selected (alignment no. 4; Fig.4.5) had the tunnel passing through the intra-thrust zone for a length of 2.4 km.

The accepted alignment was again changed to avoid the major portion of the intra-thrust zone by giving it a deviation from the straight line (final alignment; Fig.4.5). This was done to take care of the apprehensions regarding the presence of high
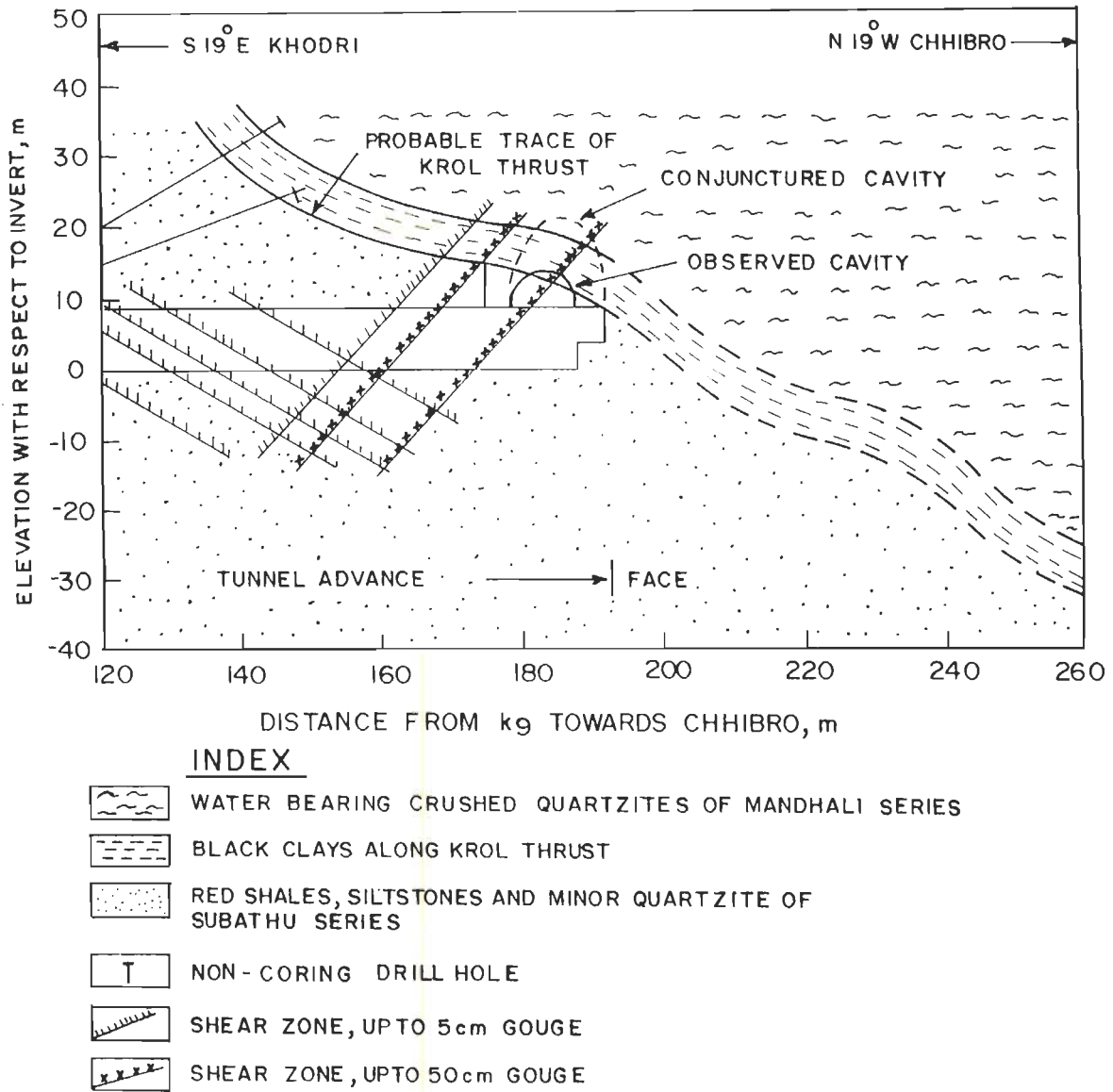
Fig.4.4 – Geological Set-up Causing Inrush of Water in Main Tunnel at 182m Upstream of $K_9$ (after Shome et al., 1973)
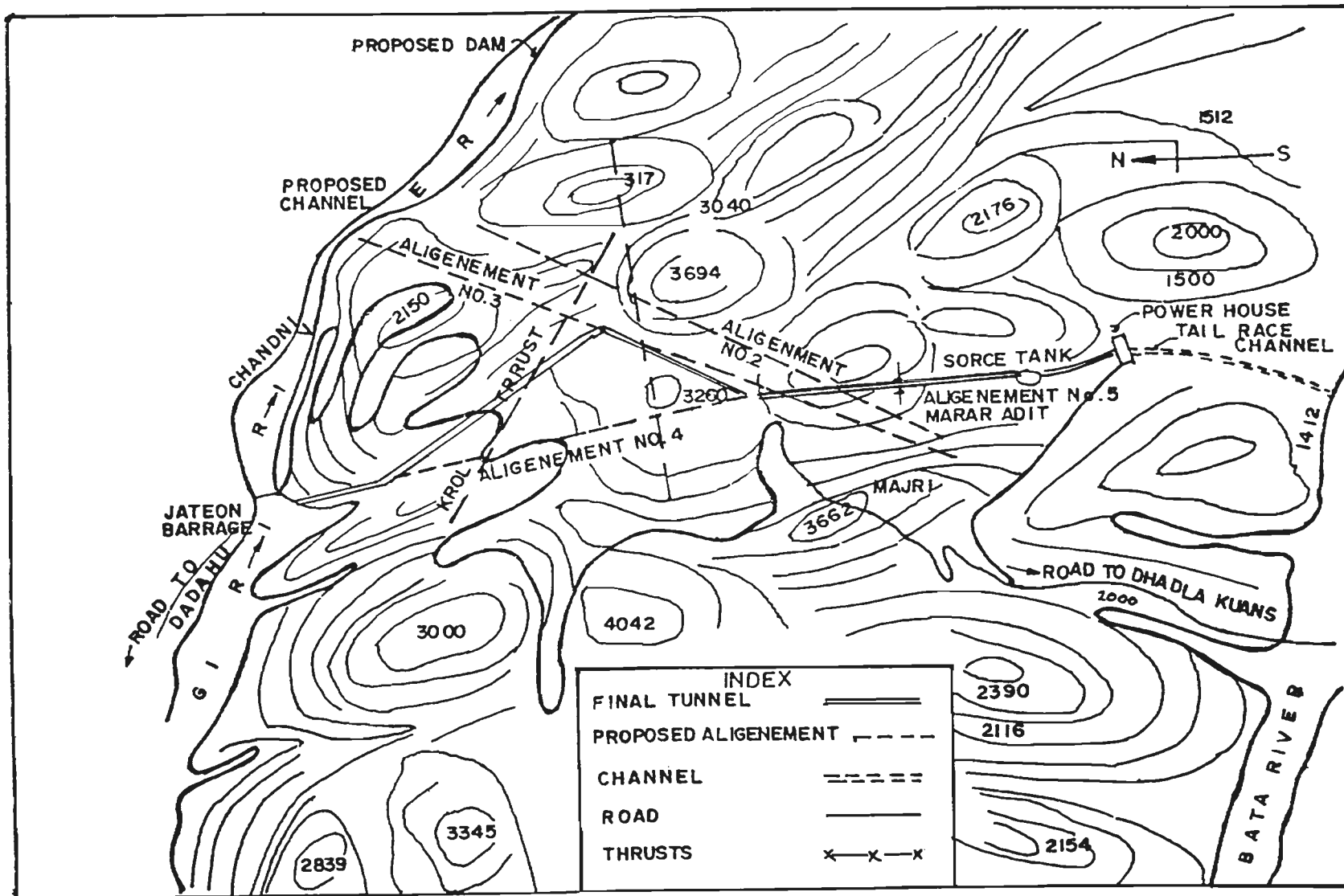
Fig.4.5 - Lay-out of Giri Hydroelectric Project

residual stresses in the intra-thrust zone which were likely to result in high squeezing pressures (Shome and Dayal, 1969). It was also anticipated that crustal movements along the faults could pose a danger to the tunnel after its commissioning. The changed alignment reduced the tunnel length through the intra-thrust zone to only 600 m, although the total tunnel length increased by 1 km.

The changed tunnel alignment passes through various formations from the north to the south, as shown in Table 4.2.

## 4.2.2.3 Influence of geology on tunnelling conditions

The accepted alignment of the Girl tunnel was deviated from straight line to reduce its length through the intra-thrust zone However, contrary to the expectations, the tunnelling problems started dramatically after the deviatiion. As it turned out, the phyllites/slates of infra-Krols, through which the tunnel length was increased following the change in the alignment and which were considered safer tunnelling media, proved to be more problematic and hazardous than the intra-thrust zone. As the tunnel progressed with difficulty through this zone, a few more faults, which were not anticipated earlier, were detected. The actual positions of some of the main geological features were also found to be different than their predicted positions. The predicted and the actual geological sections along the tunnel alignment are shown in Figs.4.6 and 4.7a. A comparison between

4.2 - Geological Formations Along Giri Tunnel

| Age of Formation | Local Name | Description of Rock Mass |
|---|---|---|
| **NORTH** | | |
| Permo-Carboniferous | Blaini's | Boulder beds, siliceous and dolomitic limestones, red, grey and greenish shales |
| | Infra-Krols | Grey and bleached arenaceous slates/phyllites interbedded with quartzites |
| ---------DADAHU FAULT--------- | | |
| Not known, either Tertiary or Pre-Tertiary | Dadahus | Purple and green shales with bands of dolomite limestones |
| Not known, either Tertiary or Pre-Tertiary | Tarwalis | Grey limestones with black slates |
| ---------KROL THRUST--------- | | |
| Eocene,Mid-Miocene | Subathus | Olive green and red shales with limestones, basic dykes |
| --------NAHAN THRUST--------- | | |
| Mid-Miocene | Nahans | Sandstones, pseudo-conglomerate claystones and siltstones |
| **SOUTH** | | |

the predicted and the actual features is presented in Table 4.3. The contact between the Blaini's slates and the infra-Krol formations turned out to be faulted at RD (relative distance) 1312 m instead of RD 1600 m as predicted. In addition, the tunnel encountered the infra-Krols about 300 m ahead of the anticipated location. Similarly, the Krol and the Nahan thrusts were encounterd 200-580 m and 115 m ahead of their predicted positions.

FIG. 4.6 _ GEOLOGICAL CROSS- SECTION OF POWER TUNNEL AT GIRI HYDEL PROJECT AS PREDICTED FROM SURFACE MAPPING (After GHOSH, 1970)
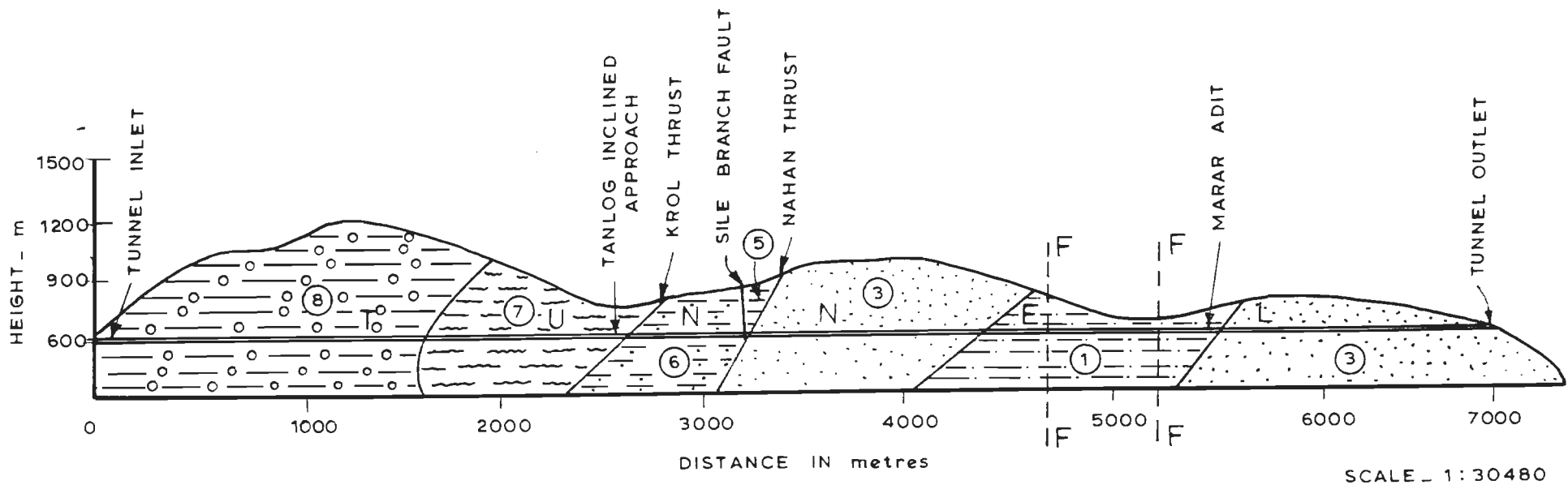
INDEX

(INDEX IS COMMON TO ALL SKETCHES OF GIRI TUNNEL)

1  CLAY/SILTSTONES

2  PSEUDOCONGLOMERATES

3  SAND STONES

4  BASIC ROCK

5  SHALE

6  SHALE WITH QUARTZITES

7  PHYLLITES/SLATES

8  BLAINI'S SLATES

9  SHEAR ZONES
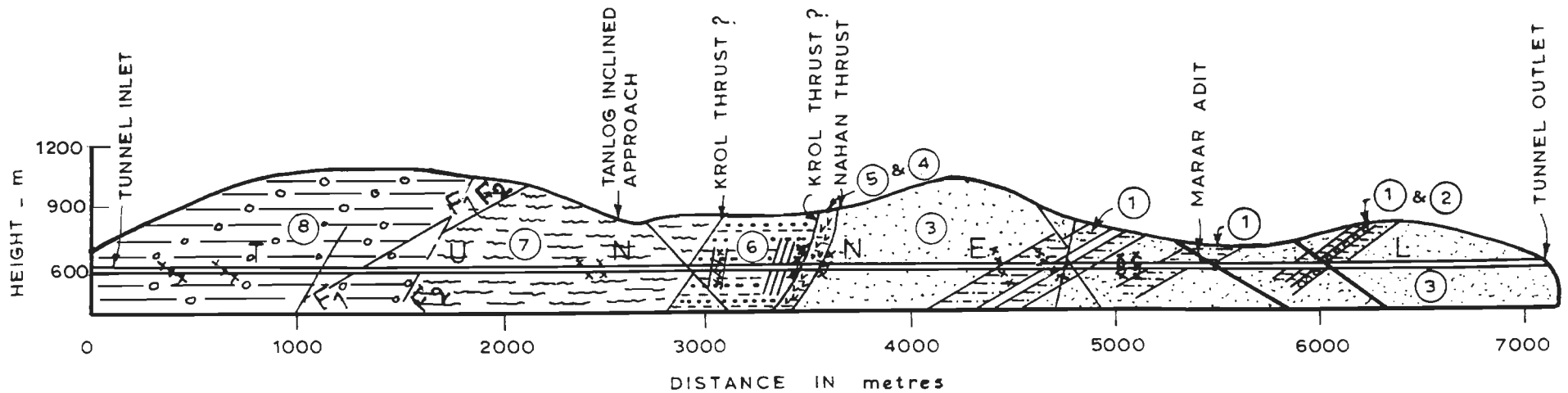
FIG.4.7 a — Actual Geological Cross Section Along the Giri Tunnel Alignment
(After G.S.I., 1977)
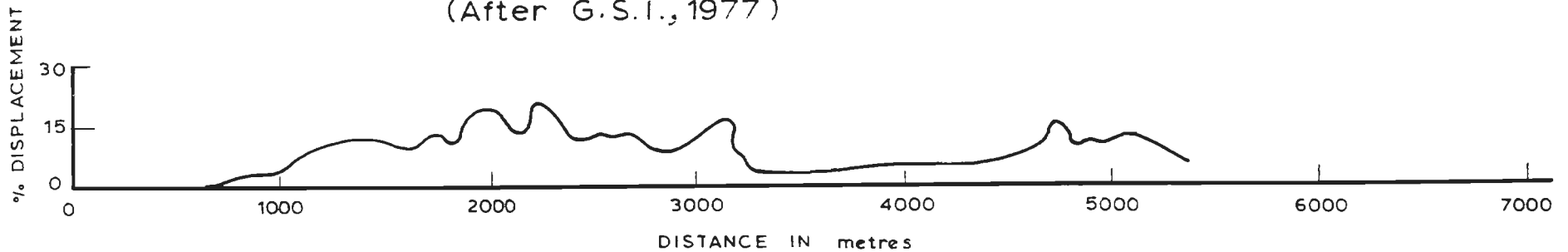


SCALE — 1:30480

FIG. 4.7 b — VARIATION OF SUPPORT DISPLACEMENT ALONG THE ACTUAL GEOLOGICAL
CROSS-SECTION OF THE GIRI TUNNEL ALIGNMENT

Table 4.3 - Comparison Between Predicted and Actual Geology
Along Giri Tunnel

| S.No. | Description of feature | Predicted* | Actual* | Difference in meters |
|-------|------------------------|------------|---------|----------------------|
| 1. | Krol Thrust | R.D. 2780m | (a) R.D.[+]3360m | 580 |
|  |  |  | (b) R.D. 2980m | 200 |
| 2. | Nahan Thrust | R.D. 3405m | R.D. 3520m | 115 |
| 3. | Sile Branch Fault | R.D. 3350m | (a) R.D. 3196m | 154 |
|  |  |  | (b) R.D. 3296m | 114 |
|  |  |  | (c) R.D. 3266m | 84 |
| 4. | Marar Fault | R.D. 4959.5m | (a) R.D. 4780m | 169.5 |
|  |  |  | (b) R.D. 4860m | 89.5 |
| 5. | Length of Blaini's formations | 1710m | 1312m | 398 |
| 6. | Length of Infra-Krols | 1070m | 1660m | 590 |
| 7. | Length of Dadahus | 625m | 384m | 241 |
| 8. | Length of Nahans | 3710m | 3595m | 115 |

*The distances are approximate
+R.D. - Relative Distance

The large differences between the predicted and the actual geology were the results of inadequate geological investigations. The main sources of geological information were the meagre surface data which were extrapolated to the tunnel grade. This was not supported by any detailed bore hole investigations before the start of the tunnelling operations. A borehole, driven to ascertain the location of the Krol thrust, was terminated before reaching the tunnel grade. Thus, for prediction of the geological features along the tunnel alignment, the geologists were handicapped in the absence of the adequate borehole data upto the

tunnel grade. Moreover, a comprehensive surface data was difficult to obtain on account of a thick cover of vegetation and top soil and this, perhaps, accounted for some of the missed faults. The geology played a dominating role during excavation of the Giri tunnel. Some of the tunnelling problems faced are discussed below.

**a) Frequently changing lithology**

The tunnel exprerienced a frequently changing lithology along its alignment. In absence of the adequate data to assess the support requirements for various rock mass types, the supports were designed on the basis of a broad categorisation of the rock mass expected to be encountered during the excavation. Thus, the support pressures were estimated from Terzaghi's rock mass classification (1946) for three broad rock mass categories. The supports designed on this basis, however, could not cope with the frequently changing lithology encountered during excavation. Abrupt changes in the ground conditions necessiated changes in the support requirements also. This however, could not be done due to the limitations of the construction technology and the very nature of the installation of the steel supports. Consequently, the supports designed for a fair rock mass were provided in a poor rock mass as well, resulting in support failures at a number of locations.

Thus, the vulnerability of the steel supports in frequently changing ground conditions was exposed. The steel supports are not only 'passive', it takes considerable time and effort to

change the support density frequently. On the other hand, the 'active' support system, consisting of shotcrete and rock bolts, is not only quick to apply but is also easily adaptable to the changing ground conditions, except perhaps in highly squeezing ground.

## b) Poor anticipation of geological features

The unanticipated changes in the geology along the tunnel alignment accounted for a number of supporting problems. While excavating through the Blaini's slates, which were otherwise found to be safer tunnelling media, severe buckling and twisting of ribs took place. This occurred in a length of about 50 m around RD 1000 m, where the Blaini's slates are affected by two parallel faults (Fig.4.7a) which had not been predicted (Fig.4.6). Within a week's time after installation, the supports, consisting of horse-shoe shaped 150x80 mm ribs spaced at 0.5 m, experienced severe buckling and twisting. The situation improved when heavier 150x150 mm ribs spaced at 0.5 m were installed. The butt joints of these ribs, however, failed.

The twisting and buckling of ribs, associated with oozing out of the backfill concrete, continued for a length of about 50m (between RD 990 to 1040m ) in the fault zone between faults F1-F1 and F2-F2 (Fig.4.7a). The problem was considerably reduced immediately after the fault zone was crossed and installation of the lighter supports was resumed.

## c) Squeezing problems

Squeezing problems were encountered at a number of places in the Giri tunnel. One such instance is the buckling and twisting of ribs, discussed earlier, in the fault zone between faults F1-F1 and F2-F2 (Fig.4.7a) in the Blaini's slates. In this fault zone, the rock mass was poor and the over burden high, resulting in the occurrance of the squeezing ground condition.

The phyllites of the infra-krols proved to be the most difficult tunnelling media. Occurrance of squeezing ground conditions resulted in large displacements of the supports, ranging from 50 mm to 430 mm, i.e., 2.2 to 17.5 percent of the average tunnel radius, in 300 days. To tackle the problem of large displacements, it was decided to observe the effect of different types of support backfills on the tunnel-wall displacements. Initially, a flexible backfill, using gravel or just 'nothing ' between the ribs and the rock mass, was used. After proceeding for about a kilometer, it was decided to stop the tunnelling on account of large displacements and restart it only after rectification of already excavated reach with 150x75 mm ribs with backfill concreting upto the flange (Madhavan, 1982). Dube (1979), who carried out detailed instrumentation of the Giri tunnel, measured the tunnel-wall displacements in test-sections of 10 to 15 m lengths, constructed using different types of support backfills (concrete backfill, gravel backfill, and 'no' backfill). On the basis of his observations, Dube (1979) concluded, that although the final tunnel-wall displacement was same in both the cases, the flexible gravel backfill behaved

better than the stiffer concrete backfill. In the case of the flexible backfill, the displacements reduced gradually, probably causing less damage to the rock mass within the broken zone. The displacement in the case of the concrete backfill, on the other hand, reduced drastically initially. **A detailed study of the different types of support backfills is one of the main objectives of the present work and this aspect will be covered under chapter 7.**

The clay/siltstone of the Nahans also posed squeezing problems and the displacements there varied from a few millimeters to about 300 mm, i.e., 13 percent of the tunnel radius in the most problematic section.

Variatiion of support displacements along the tunnel alignment is shown in Fig.4.7b (after Dube, 1979).

### 4.2.3 Maneri-Uttarkashi Tunnel (Maneri Bhali Project, Stage-I), Uttar Pradesh

#### 4.2.3.1 General features

Under stage-I of the Maneri Bhali Hydroelectric Project, located in the middle Himalaya in the state of Uttar Pradesh, a 41m high concrete dam has been constructed across river Bhagirathi, a major tributary of river Ganga, near Maneri village to divert the river water. The diverted water is carried through a 8.56 km long circular tunnel of 4.75m finished diameter, to a surface power house at Uttarkashi for generating 80 MW of hydro-power utlilizing a head of 184 m. The tunnel excavation commenced

by opening four faces - one each at the intake (at Maneri) and at the outlet (at Tiloth near Uttarkashi) ends, and two at Heena through an intemediate adit (Figs. 4.8 and 4.9).

## 4.2.3.2 Regional geology and structural features

The rock masses exposed in the area are quartzites, quartzites interbedded with minor slate bands, chlorite schists, phyllites, metabasics, and basic intrusives belonging to the Garhwal group (Jain et al., 1976 ). These rock formations are affected by a thrust, locally termed as the main central thrust, towards the north and the northeast of the porject area. The Garhwal group of formations are separated from the Chandpur group, lying towards the south and the south-west of the project area, by another thrust, called the Srinagar thrust (or the north Almora thrust ).

The general strike and dip directions of the rock formations in the region are presented in Table 4.4.

Table 4.4 - General Strike and Dip Directions in the Region of Maneri-Uttarkashi Tunnel

| Area | Strike | Dip | Dip Direction |
|------|--------|-----|---------------|
| Maneri area | N15$^O$-20$^O$W | 25$^O$-35$^O$ | S70$^O$-75$^O$W |
| Heena area | N40$^O$W | 30$^O$-45$^O$ | S50$^O$W |
| Tiloth area | N20$^O$W to N20$^O$E | 35$^O$-45$^O$ | NE to SE |

The Maneri-Uttarkashi tunnel passes through various formations from north to south (Jain et al.,1976, Fig. 4.9) as shown in Table 4.5.

Fig.4.8 – Alternative Alignments of Maneri-Uttarkashi Tunnel

Fig.4.9 - Geological Section of Maneri-Uttarkashi Tunnel

Table 4.5 - Geologocal Formations Along Maneri-Uttarkashi Tunnel

| Rock Type | Local Name |
|---|---|
| **NORTH**<br>Quartzites<br><br>Metabasics<br><br>Quartzites with minor slate bands<br>**SOUTH** | Garhwal group |

The tectonic disturbances in the area have resulted in intense folding and faulting of these lithological units and have created close joints, brecciation and shearing.

## 4.2.3.3 Influence of geology on tunnelling conditions

Due to the geological features of the Maneri-Uttarkashi tunnel, the following problems were encountered during excavation.

### a) water inrush at Ch. 3549 m

A heavy inrush of water at a rate of 6 cusecs (0.17 cumecs) accompnied the sudden collapse of the face and a fall of about 300 $m^3$ of loose rock at Ch. 3549 m on October 19, 1974. This was followed by sliding of 400 $m^3$ of muck on November 22, 1974 and 200 $m^3$ of muck on December 18, 1974. The water discharge reduced gradually and stabilized at 1.28 cusecs (0.04 cumecs) in February 1975.

The cause of the water inrush may be traced to the structural features of the rock formations around Ch. 3549. The tunnel passes through metabasic and basic chlorite schists upto

Ch.3530 m and then enters the jointed and blocky quartzites which are folded in a synclinal form (Fig. 4.10). The quartzites, surrounded by relatively impervious metabasic chlorite schist formations, were heavily charged with a water head of 80 m. The situation was made worse by the presence of the two 40 cm wide cross shear zones intersecting the tunnel crown (Fig. 4.10). The cumulative effect of these factors was the triggering off of the collapse of the tunnel face, associated with sliding of huge quantities of muck and heavy water inflow.

As a corrective measure it was decided to divert the tunnel slightly, after six months of continuous effort to retrieve the face failed to produce any result. Three alternative tunnel alignments, shown as Alt I, Alt II, and Alt III in Fig. 4.8, were proposed with a view to reduce (by 280 m-Alt I and III) or eliminate (Alt II) the tunnel length through the water charged area (Table 4.6). The proposed alignments also meant an increase in tunnel length by 0.875, 2.105 and 0.47 km respectively for Alt I,II and III. The added advantage of selecting Alt I and II was the availability of the two additional faces through an intermediate adit of approximately 200 m length (point C2-Fig.4.8). Fig.4.11 shows the geological section along the original straight line alignment passing through the water charged quartzites and the alternative alignment Alt II which completely avoids the quartzites.

The tunnel was diverted into the chlorite schists from Ch.3492 m, i.e., 57 m behind the collapsed face. During excavation, deep drilling was carried out to probe for a suitable
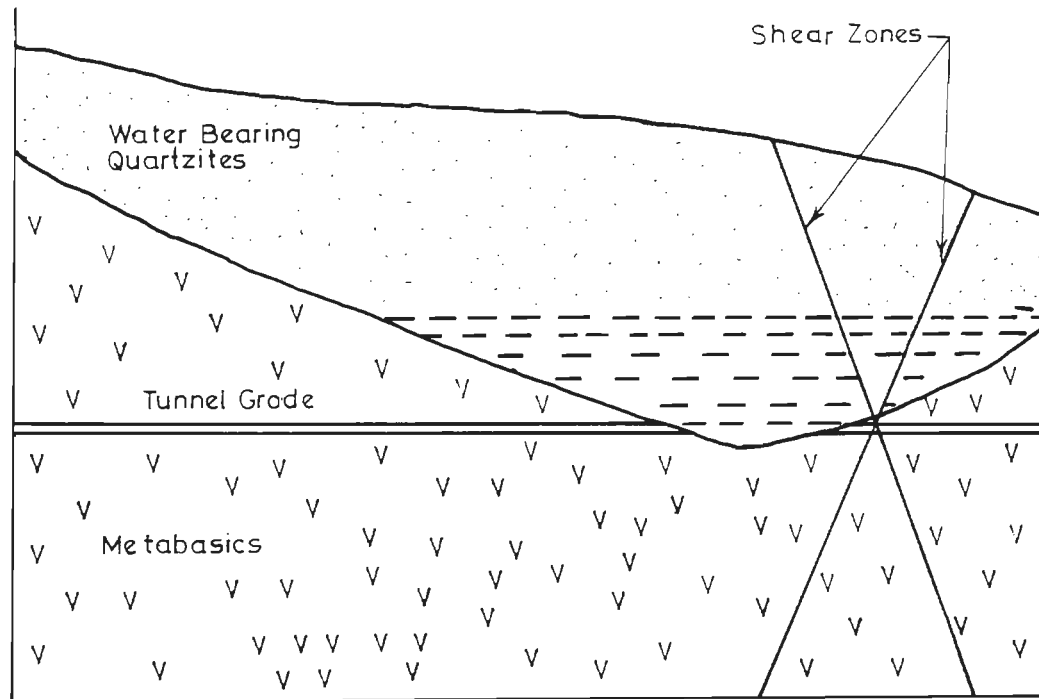
Fig. 4·10–Geological Features Around Chainage 3549m Causing Water Inrush
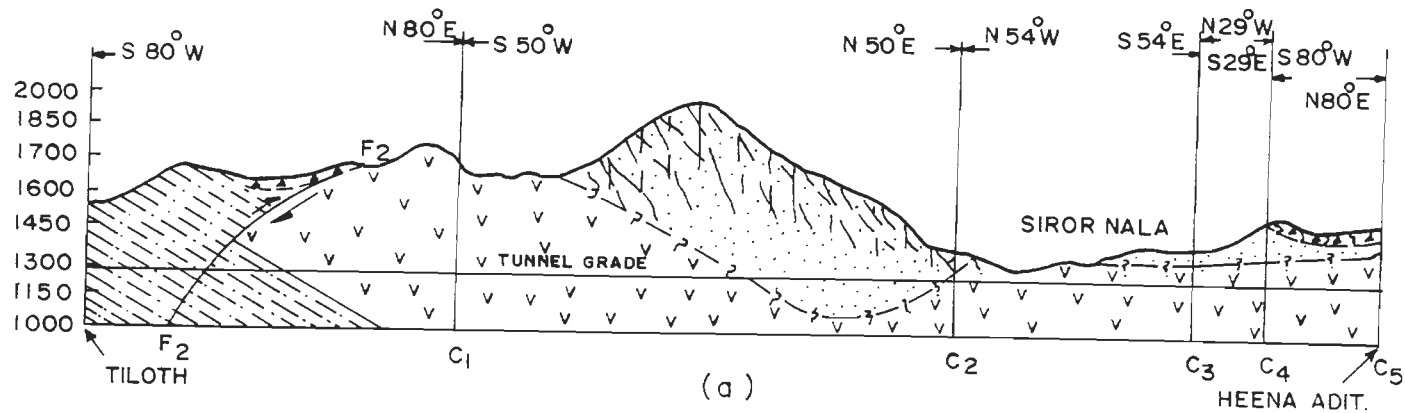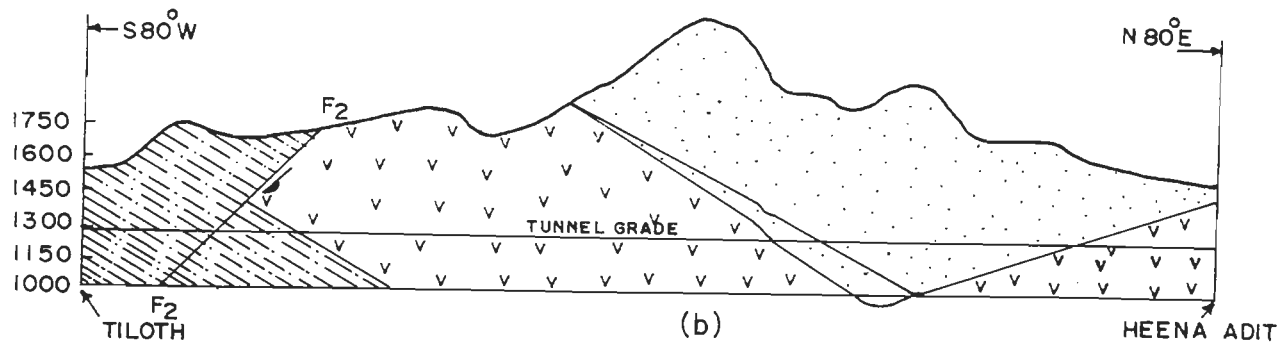
Fig.4.11 – Geological Section of Maneri-Uttarkashi Tunnel Between Heena and Tiloth
(a)   along original straight line alignment
(b)   along alternative alignment Alt II

Table 4.6 - Tunnel Length Along Various Alternative Alignments of Maneri-Uttarkashi Tunnel

| S.No. | Proposed Alignment | Total Tunnel Length Between Heena & Tiloth (m) | Tunnel Length through Water Charged Quartzites (m) | Increase in Tunnel Length from Original Alignment (m) |
|-------|-----------|-----------|-----------|-----------|
| 1 | Original | 5065 | 1200 | - |
| 2 | Alt I | 5940 | 920 | 875 |
| 3 | Alt II | 7170 | - | 2105 |
| 4 | Alt III | 5535 | 920 | 470 |

place to enter the quartzite zone, if possible, to avoid the much longer alternative alignments, Alt I, II and III (Fig. 4.12). After, driving the tunnel parallel to the plane of contact of the chlorite schists and the quartzites for a length of about 75 m, the probe drilling indicated the suitability of the quartzite zone for accepting the grout. The tunnel was then diverted into the quartzites and the excavation progressed cautiously with advance probe holes ahead of the tunnel face (Fig. 4.12). Umbrella grouting was carried out when the face reached within 5m of the contact plane. After establishing, through advance probe holes, that the grouted zone had become a solid mass and there was no inrush of water, the tunnel was driven wihtout difficulty leaving a 5m thick bulkhead (similar to the one shown in Fig.4.14) in the front.

## b) Cavity formation at Ch.5038-5055 m

The tunnel excavation witnessed the formation of a number of cavities, both small and big in size. Formation of a major cavity took place between Ch. 5038 m and 5050 m due to the presence of a shear zone consisting of heavily water charged crushed quartzites which crossed the tunnel crown at Ch. 5050 m. The total volume of the cavity was estimated to be 813 $m^3$. The mucking had to be abandoned due to continuous inflow of muck. As a part of the remedial measures, the tunnel face was sealed with forepoling using rolled steel joists, and drainage holes were provided on the tunnel sides to drain off the seepage water. The cavity above the forepoles was then blocked with concrete. This was followed by grouting of the cavity. This operation, which consumed $67m^3$ of blocking concrete and 3295 bags of cement (for grouting) did not succeed in completely stopping the flow of muck and water. A side drift was then excavated on the left to drain off the water. The drift intersected the main tunnel beyond the shear zone in good metabasic rock mass. The operation was then started at the face by opening the bulkhead and excavating the heading. This proved futile, however, due to a renewed inflow of crushed material and seepage water. The face was sealed again and drainage pipes were provided through the new bulkhead. The muckpile was then grouted. This was followed by excavation using the multi-drift method from the tunnel face as well as from the point of intersection of the drainage drift and the tunnel in the opposite direction. The task was, thus, successfully accomplished.
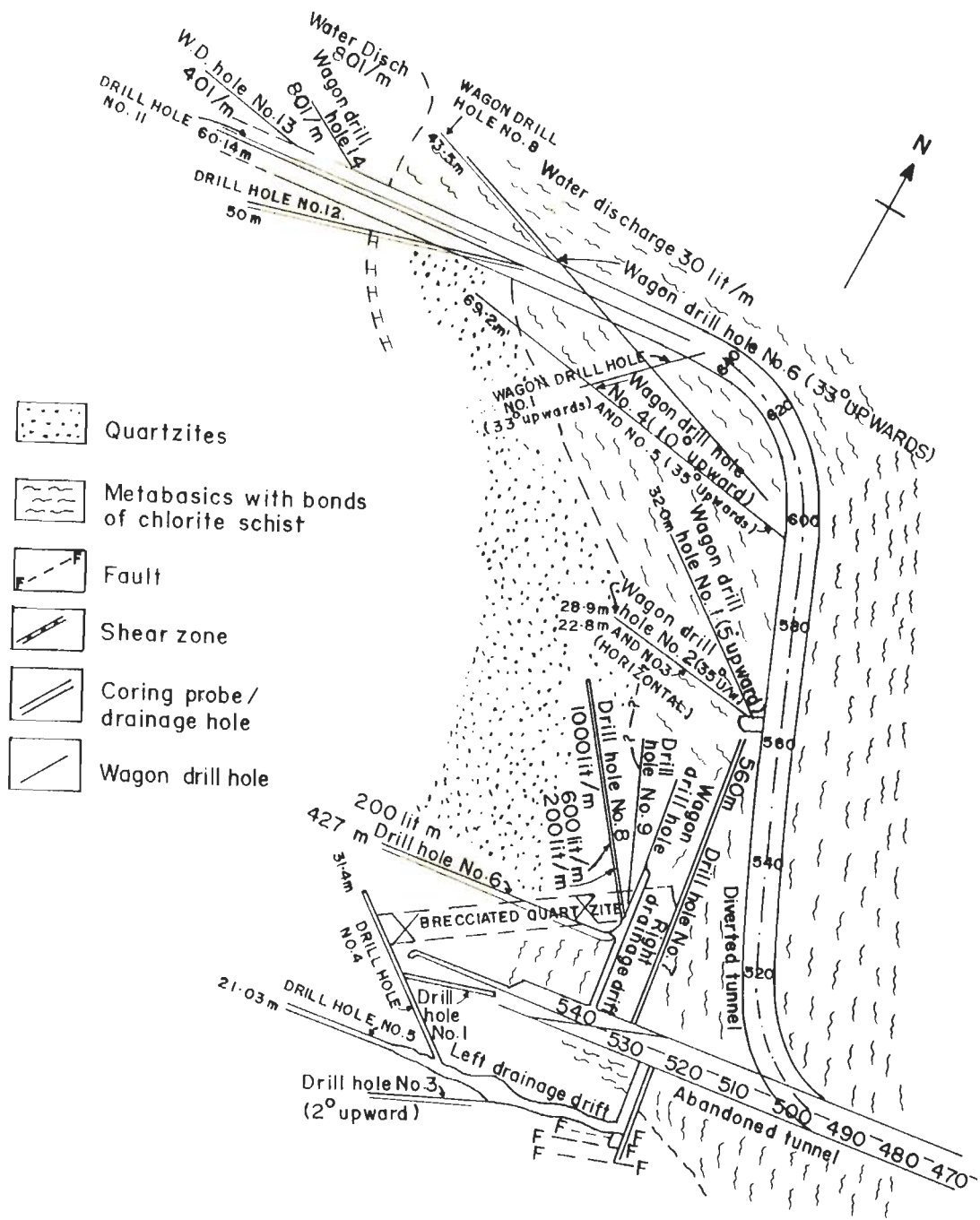
Fig.4.12 - Diversion of Maneri-Uttarkashi Tunnel

## c) Squeezing problems at Ch.5250-5550 m

The tunnel passed under high overburden, ranging from 700 to 900 m, from Ch. 5550 to 5250 m (while tunnelling from the outlet end) through partially wet and thinly foliated metabasics, resulting in highly squeezing ground conditions. In this reach, the tunnel was supported by ISMB 150x150mm ribs spaced at 810 mm to 965 mm, with blocking concrete upto their outer flanges. The excavation and the support installation carried out in July 1978, went on without any difficulty. It was after a period of 5-6 months that the squeezing problems became apparent when the blocking concrete began to crack accompnied by buckling of steel ribs.

Strengthening of the steel ribs with ISMB 150x150x75 mm laggings and extension of the blocking concrete upto the inner flanges, proved to be a useful remedial measure in controlling further buckling of the ribs. However, at the time of providing the final concrete lining, it was observed that the extent of deformation of the ribs required their removal in order to achieve the required size of the tunnel. The invert had heaved by as much as 80 cm. Removal of the twisted ribs and the blocking concrete, trimming of the rockmass, and erection of ISHB 150x150 mm ribs spaced at 750 mm, was then carried out to achieve the required finished diameter of 4.75 m. While this arrangement worked well for most of the affected tunnel reach, a heavy rock fall occurred while removing the twisted ribs between Ch.5509 m and 5517m, resulting in the formation of a cavity with an estimated volume of 430m$^3$. The problem was tackled by forepoling,

grouting of muck above the forepoles, re-excavation to achieve the required tunnel size, and supporting with ISMB 150x150 mm spaced at 600 mm.

The required finished tunnel size had to be sacrificed in some reaches affected by squeezing for a fear of complete collapse. The finished tunnel diameter was reduced to 4.00 m in a length of about 200m and to 4.20 m in a length of 80m.

### 4.2.4 Maneri Bhali Stage-II Tunnel (Uttar Pradesh)

### 4.2.4.1 General features

The Maneri Bhali Stage-II Project involves construction of a barrage at Uttarkashi to divert the water of the river Bhagirathi through a 16 km long head race tunnel of 6.0 m finished diameter to utilize a drop of 285 m between Uttarkashi and Dharasu for genration of 304 MW of power. The head race tunnel shall carry 142 cumecs of water with an average velocity of 4.75 m/sec. The project is located in the middle Himalaya in the state of Uttar Pradesh.

The head race tunnel is being excavated from four faces - two from the inlet (Joshiyara, Uttarkashi) and the outlet (Dharasu) ends, and two from an intermediate adit located almost midway between the two ends at Dhanarigad (Fig.4.13). The major portion (7.5 km) of the tunnel is to be excavated through the Dhanarigad adit using the upstream and downstream faces.

## 4.2.4.2 Regional geology and structural features

The Geological Survey of India (GSI) mapped the geology of the project area and along the tunnel alignment. The tunnel alignment passes through quartzites, metavolcanics, limestones, dolomites and epidiorites of the Garhwal group, and phyllites, slates and greywackes of the Tehri formations (Fig. 4.13). Towards the tunnel outlet, the Garhwal group is thrusted over the Tehri formations at approximately 13800 m from the Joshiyara (Uttarkashi) inlet. The thrust is locally called the Srinagar thrust and runs through the Himalaya over a distance of about 100 km. Other important structural features along the tunnel alignment are the numerous faults of localised nature. The rock masses along the alignment are moderately jointed, having a large number of open joints and cross shear zones.

Excavation of tunnel from the four faces has revealed more details of the types of rock mass encountered. From the inlet, the tunnel has been driven through moderately foliated, jointed and sheared metabasics and quartzites. The rock mass encountered during tunnelling on the upstream side from the Dhanarigad adit, mainly consists of massive to foliated, jointed and saturated metabasics (amygdaloidal andesite). Occassionaly, phyllite bands have also been observed. The metabasics were found to be heavily crushed and pulverised beyond Ch.793m (from Dhanarigad on the upstream side). The quartzites, encountered during excavation, were also heavily crushed and charged with water. On the downstream side of the Dhanarigad adit, sheared and jointed metabasics, massive to moderately jointed quartzites,

pyretiferrous slates with thin intercalation of quartzites, and jointed limestones, have been encountered. Excavation from the Dharasu outlet end has been carried out through massive phyllites and greywackes with calcareous lenses. Thinly foliated phyllites and thinly bedded greywackes, which are occassionally brecciated, have also been encountered.

## 4.2.4.3 Influence of geology on tunnelling conditions

The influence of geology on the tunneling conditions was evident at many places during excavation. A number of tunnelling problems were faced due to the occurrance of squeezing ground conditions on account of adverse geological conditions, poor rock masses, and high overburden. Some of the problems faced in the squeezing zones are discussed below.

Excavation of the tunnel from Dhanarigad adit on the upstream side was accompanied by squeezing ground conditions almost throughout the metabasics, which are affected by faults, folds and shear zones with gauge. The height of overburden is considerable in this reach and varies between 400 to 500m. The metabasics are heavily crushed and pulverised at their contact with the qartzites near Ch.793m (Fig. 4.13). The quartzites, which followed, were also heavily crushed and charged with water, causing high pressures. The metabasics are believed to be highly strained due to accumulated tectonic strains. The combination of these factors resulted in severe squeezing conditions, particularly in the last 40m length, and triggered off the tunnel collapse at Ch.793m. The problems encountered are discussed

U/s    D/s

DHANERIGAD

ADIT

2000 m
1500 INLET                                                                    OUTLET
1000
500
0        F F    2000      4000      6000      8000   F    F 10,000 F    12000   T 14000   16000 m

103

Fig.4.13 - Geological Section Along Maneri-Bhali Stage-II Tunnel

in the following paragraphs.

**a) Side collapse at Ch. 766m, upstream of Dhanarigaad adit**

Under high side pressure due to squeezing ground condition, the right side of the tunnel collapsed at Ch.766m. The tunnel face (heading) was at Ch.772 m at the time of the collapse. The void created behind the steel rib supports due to the collapse, was filled up with backfill concrete and the heading was advanced cautiously. No difficulty was faced upto Ch. 785m.

**b) Cavity formation at Ch.785m, upstream of Dhanarigad adit**

At Ch.785m, a cavity appeared on the left side of the tunnel and kept on advancing. The spacing of 150x150 mm steel ribs was reduced to 500 mm, and forepoling and concrete backfilling of the cavity was resorted to in an effort to control its advancement. Only the tunnel heading was excavated further, leaving the bench behind at Ch.785m. The heading was,thus, advanced to Ch.791m.

**c) Collapse of tunnel at Ch.793m, upstream of Dhanarigad adit**

At Ch. 791m, the orepoles were extended 2 m ahead of the heading, i.e., upto Ch.793 m. Before the advancing cavity, thus supported with forepoles, could be filled with concrete through the placer pipes, the muck started flowing from the heading, leaving the forepoles in a cantilever shape (Fig. 4.14; Varshney, 1988). This prevented the placing of concrete as the placer pipes got choked. The cantilevered forepoles were supported with a bulkhead of sand bags. Further efforts for concreting by new placer pipes were abandoned as another flow of

muck took place. Later, the flow of muck and water disturbed the bulkhead also. Finally, on December 7, 1984, the muck flow disturbed the heading supports and covered the last 28m of the excavated tunnel (i.e. from Ch.793 to Ch.765m). This was followed by another heavy loose fall on December 13, 1984. This time, the muck flowed down to Ch.753m, i.e., 40m behind Ch. 793m.

The mucking and the operation to salvage the buried equipments were started on December 20, 1984. Till the begining of January, 1985, mucking had been carried out in the major portion of the affected tunnel length. On January 5, 1985, however, yet another collapse, this time on the right side at Ch.772m, occurred. The collapse, accompnied with loud sounds of rolling boulders was followed by inrush of water. Finally, the tunnel totally collapsed between Ch.775 and 779m on January 22, 1985. As a result of the collapses and high squeezing pressures, the steel rib supports were badly damaged. Figure 4.15 shows schematically the collapse of the supports. The amount by which the supports yielded under high squeezing pressures is indicated by Fig.4.16.

## d) Squeezing ground condition in small-sized drift

As a remedial measure, a drift of 2.5x2.5 m size was excavated from Ch.745m parallel to the tunnel on the right side at a distance of 20m from the tunnel for facilitating the grouting of the affected tunnel length and for providing deep drainage holes to release the hydrostatic pressure. Even the drift, smaller in size than the tunnel, experienced highly
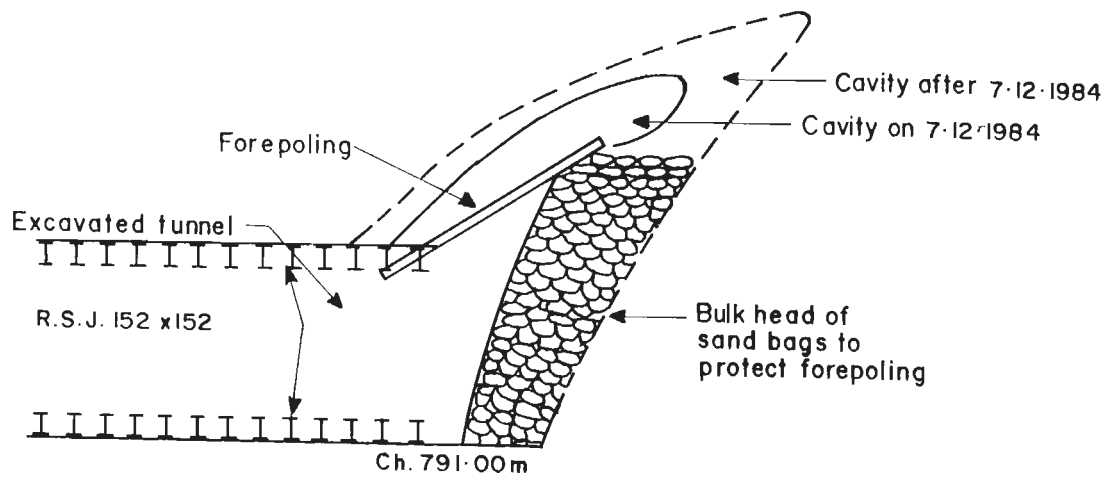
Fig.4.14 - Cavity Formation in Maneri Bhali Stage-II
Tunnel (after Varshney, 1988)

107
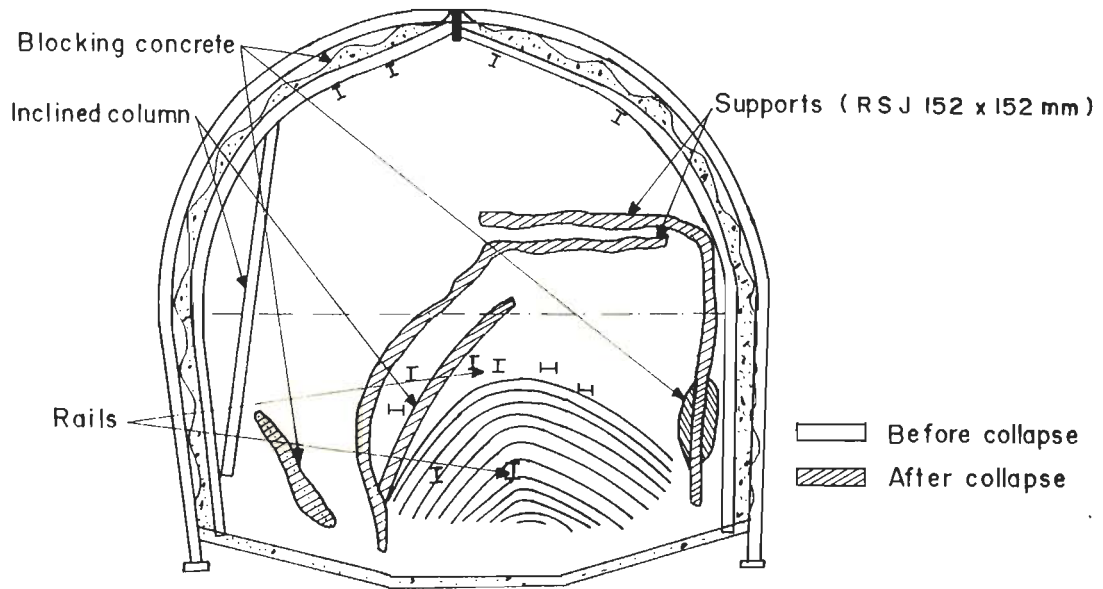


a) Chainage 778m Upstream of Dhanarigad Adit
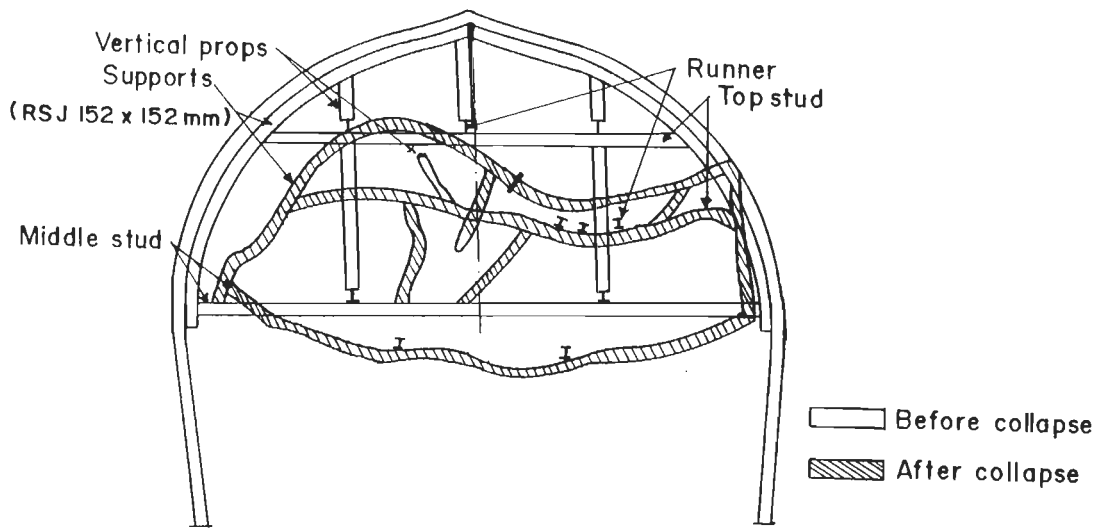


b) Chainage 785m Upstream of Dhanarigad Adit

Fig.4.15 - Collapse of Steel Supports due to Squeezing Ground Conditions in Maneri Bhali Stage-II Tunnel
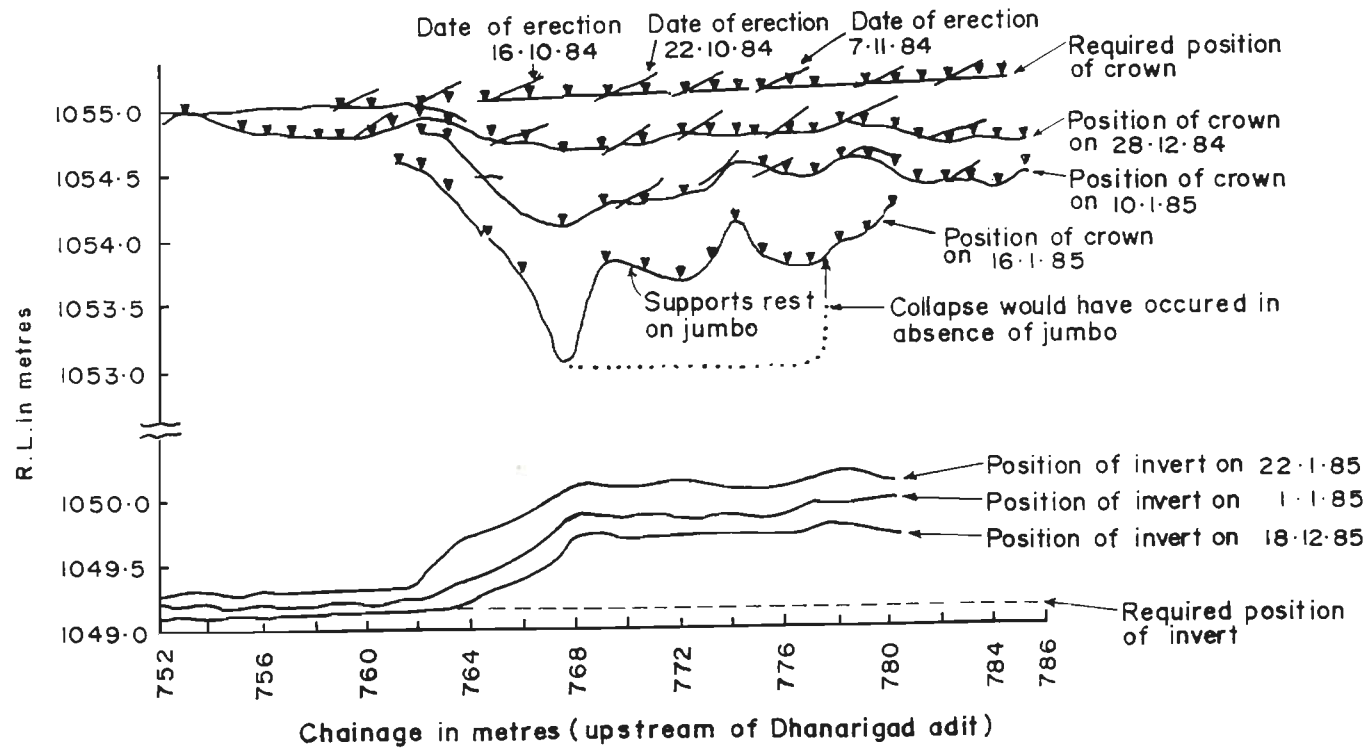
Fig.4.16 - Collapse of Crown under Squeezing Pressures in
Maneri Bhali Stage-II Tunnel

squeezing conditions. On several occassions, the section excavated on the previous day was found squeezed and collapsed the next day. Till May 1985, only 45m length of the drift could be excavated when it collapsed completely due to upheavel of invert.

The affected tunnel reach was finally rectified by umbrella grouting, forepoling, erection of braced secondary supports, and removal of the collapsed supports.

## 4.2.5 Loktak Tunnel (Manipur State)

### 4.2.5.1 General features

The Loktak Hydroelectric Project, located in the state of Manipur, comprises of a barrage across the Imphal river at Ithai to regulate the water of the Loktak lake, and a 10.268 km long water conductor system to carry the water from the Loktak lake to the Leimatak power house, located across the hills in the Leimatak valley. The water conductor system consists of 2.26 km long open channel, a 1.22 km long and 5.0 m diameter horse-shoe shaped cut-and-cover section, a 6.50 km long and 3.81 m diameter horse-shoe shaped head race tunnel and a 0.27 km long and 3.65 m diameter circular pipe tunnel (Fig.4.17). The water conductor system is designed to carry a 58.8 cumecs of water, out of which 16.8 cumecs is meant for lift irrigation scheme and the balance of 42 cumecs for generation of 105 MW (3x35 MW) of power utilizing a drop of 312 m.

The head race tunnel was excavated from eight faces - one from a vertical shaft at the intake, two each from two

intermediate vertical construction shafts, two from an intermediate adit, and one from the outlet (Fig.4.17). The tunnel was constructed over a period of ten years from 1971 to 1981.

## 4.2.5.2 Regional geology and structural features

The Geological Survey of India (Ray, 1968; Singh and Choudhury, 1975) conducted the geological investigations in the project area. The geology along the tunnel alignment was predicted mainly on the basis of the surface mapping as the sub-surface data were meagre due to the difficulties faced and costs involved in drilling boreholes down to the tunnel grade. The maximum height of overburden above the tunnel is 460m. The availability of even the surface data was limited due to the paucity of the rock exposures, and the observatinons were limited to the road and 'nullah' cuttings only (Chaudhury and Chattopadhyay, 1982).

The tunnel passes through the various lithological units mentioned in Table 4.7 from the inlet to the outlet (Fig. 4.18). One of the major structural features along the tunnel alignment is a N-S trending syncline. Thick layers of sandstones and siltstones occupy the trough of the syncline whereas splintary shales with thin bands of sandstones and siltstones exist on the flanks at the tunnel grade. The axial portion of the syncline has been refolded into several N-W trending cross-folds. The syncline limbs are affected by a number of faults and several vertical or steeply dipping joints.
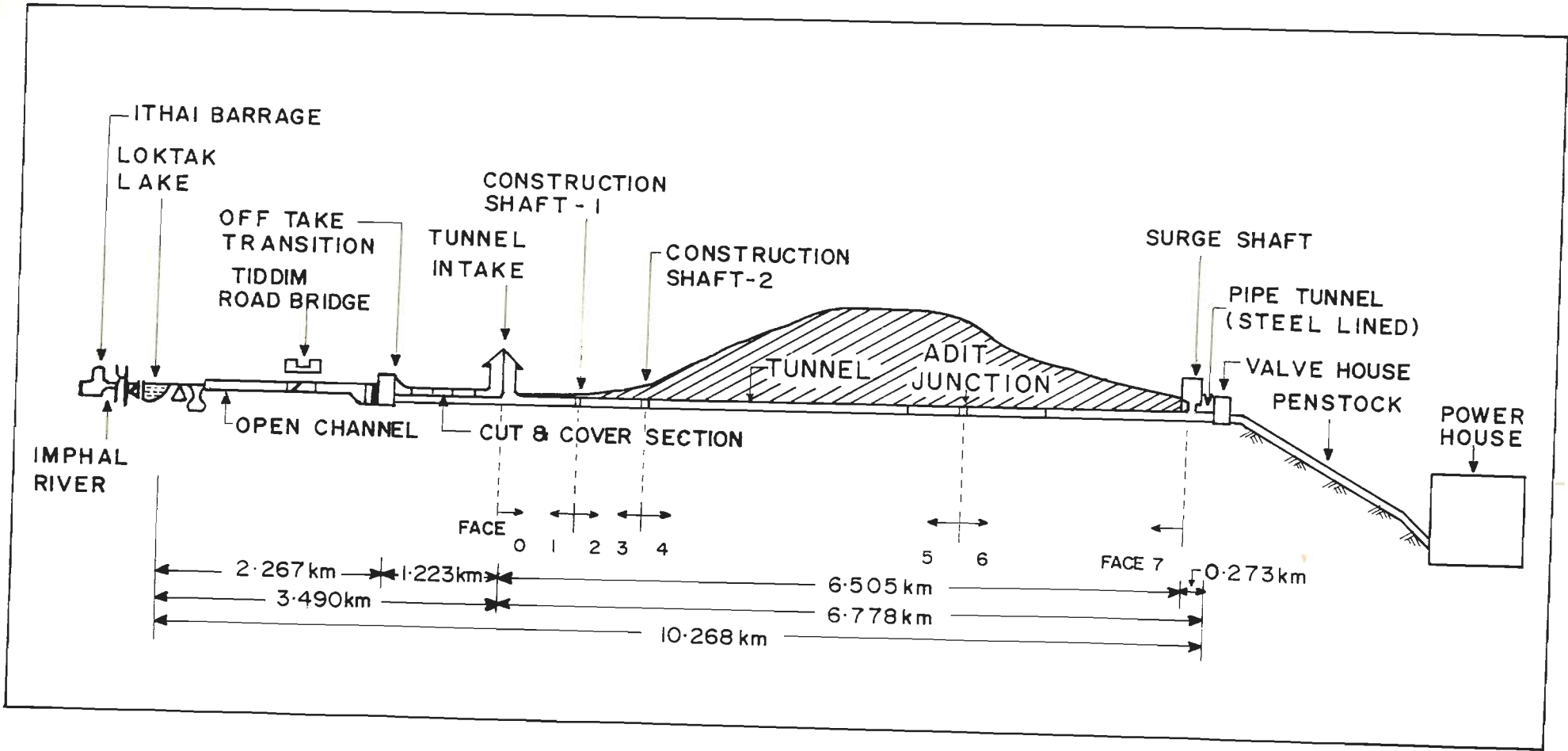
Fig.4.17 - Water Conductor System of Loktak Hydroelectric Project
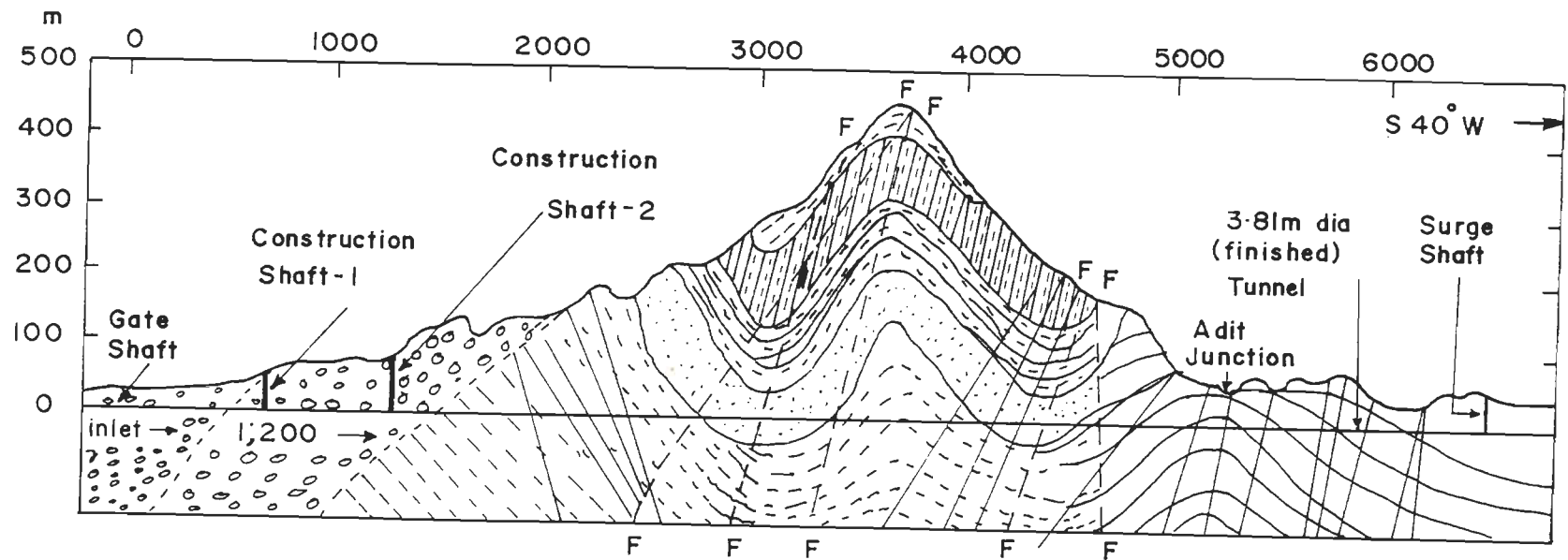
Fig.4.18 - Tentative Geological Section of Loktak Tunnel
(after GSI as in Jan., 1979)

Table 4.7 - Lithology of Loktak Tunnel

| Lithological Unit | Constituents |
|---|---|
| lake deposits | silt, sand, pebbles in varying proportions |
| unconsolidated terrace deposits | broken rock fragments, large sized boulders, silky and sandy fractions |
| Disang (Eocene) group | Fine grained sandstones with thin calcite veins, silt-stones, grey to black soft and splintary shales |

## 4.2.5.3 Influence of geology on tunnelling conditions

As expected, the complicated geological set-up of the region significantly influenced the tunneling conditions in the form of a number of tunneling problems.

### (i) Flowing ground conditions

Flowing ground conditions posed a lot of problems while tunnelling through the lake and terrace deposits in the initial stages, primarily due to the unconsolidated nature of these deposits and high water table condition. The highly saturated condition, specially in the lake deposits, made the tunnelling operations proceed with difficulty through this reach. The lake deposits were encountered from inlet for a length of 830 m, followed by the terrace deposits from 830 m to 1250 m.

### (ii) Squeezing ground conditions

The terrace deposits were followed by splintary shales with bands of sandstones and siltstones. This reach, lying mainly betweeen the construction shaft no.2 and the adit, posed the most

difficult tunnelling conditions on account of moderately to highly squeezing ground. Intensely folded strata, having a number of faults and joints, with frequently encountered water pockets and high overburden, resulted in the occurrance of squeezing ground conditions. The steel arches deformed considerably while tunnelling through the shales below an overburden of 200m and above, resulting in a very slow rate of tunnelling. A change over to the New Austrian Tunnelling Method (NATM) improved the situation.

The use of NATM in Loktak tunnel helped a great deal in tackling the squeezing ground conditions. The approach consisted of excavation by road-header (Alpine Miner-50, manufactured by Voest-Alpine) and supporting with shotcrete and rock bolts. The tunnel behaviour was continuously monitored by measuring the convergence with a tape extensometer, and the support capacity was accordingly revised. This empirical dimensioning of the support is an important feature of NATM. In very poor reaches with practically no stand-up time, the shotcrete and the rock bolts were used in combination with the steel ribs. The details of the use of NATM in Loktak tunnel have been given by Malhotra et al. (1982).

The experience of Loktak tunnel has brought out the advantage of employing NATM over the conventional approach of tunnelling. Initially, steel ribs with concrete backfill were erected to support the squeezing rock mass. However, due to large tunnel closures, the whole steel-supported reach had to be

rectified to achieve the required excavated size of the tunnel. In comparison, the NATM worked much better as, out of a tunnel length of 2000 M excavated using this approach, only 500 m length had to be rectified to achieve the required tunnel size. However, while using the NATM, considerable deformations had to be allowed in order to optimize the support requirements. In fact, in highly squeezing ground condition, the tunnel was excavated to a width of 5300 mm instead of the required 4600 mm, to allow for a total tunnel convergence of 750 mm.

### 4.2.6 Tehri Tunnels (Tehri Dam Project), Uttar Pradesh

### 4.2.6.1 General features of Tehri Dam Project

Tehri Dam Project, presently under construction in the middle Himalaya in the state of Uttar Pradesh, is the first multipurpose development scheme in the Ganga Valley. The main components of the scheme (Fig.4.19) are:

i)   A 260.5 m high earth and rock fill dam across river Bhagirathi near the town of Tehri at about 1.5 km downstream of its confluence with river Bhilangana,

ii)  four diversion tunnels, two on each river bank, of horse-shoe shape and 11 m finished diameter each,

iii) a chute spillway on the right bank to discharge 12,000 cumecs of water and to negotiate a fall of 205m,

iv)  four head race tunnels of circular shape and 8.5 m finished diameter each,

v)   an  underground power house with four conventional  turbines
     on  the  left bank for generation of 1000  MW  (4x250mw)  of
     power in stage-I of the project,

vi)  another  power  house with four reversible turbines  of  the
     same capacity for stage-II of the project,

vii) a  104m high concrete dam across the same river at Koteshwar
     about 22 km downstream of the main dam to create a balancing
     reservoir, and

viii) a surface power house for generation of 400 MW (4x100MW)  of
     power.

When  completed,  the  project will create a live storage of
2615  million  cubic  meter,  provide  irrrigation  water for 270
thousand  hectares  of  land,  and generate 2900 million units of
power  annually,  apart  from  helping  in  moderation of floods,
development of tourism, etc.

## 4.2.6.2 The tunnels

The  four horse-shoe shaped diverson tunnels of 11m diameter
each  are  designed  for a routed flood discharge of 7300 cumecs.
The  two  left bank diversion tunnels, T-1 and T-2 (Fig.4.19) are
1778m  and  1774m long respectively. The remaining two right bank
diverson  tunnels,  T-3 and T-4 (Fig.4.19) have a length of 1298 m
and  1429  m respectively. The construction of the four diversion
tunnels  has  been  completed. Out of the four circular head race
tunnels  of  8.5m diameter each, two are meant to carry the water
from  the  reservoir  to  the  power  house  of  stage-I, and the
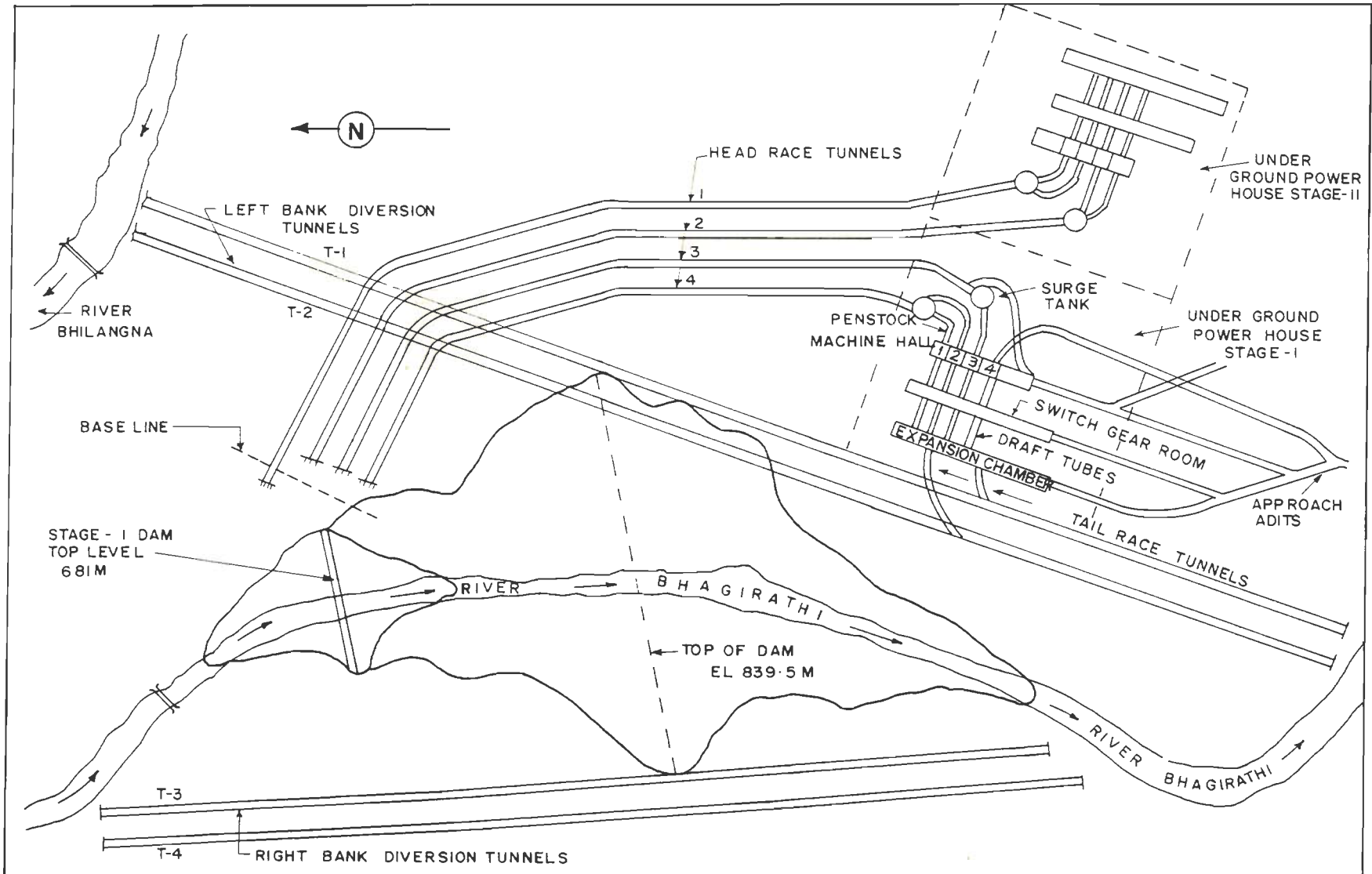
FIG. 4.19 — GENERAL LAY-OUT PLAN OF TEHRI DAM PROJECT

remaining two  to the stage-II power house.

## 4.2.6.3 Regional geology and structural features

A detailed geological study of the project area was carried out by the  Geological Survey of India. The rockmass around the project  area belongs to the phyllites of Chandpur series (Auden, 1939). These are in contact with Simla slates on the eastern side of  the dam, and with the younger dolomites and quartzites of the Garhwal group at some places. The project area is affected by the Srinagar thrust which is a regional feature and is traceable over a  distance of 100 km through the Himalaya. A number of faults of localised  nature are also found. Some of these, such as Gadolia, Deul, Tehri and Marh faults, are tear faults. The project lies in a siesmically active zone.

The  Chandpur phyllites are banded  in appearance and are constituted  of  argillaceous  and  arenaceous  materials.  The phyllites have been classified into three categories on the basis of their lithological composition, physical competance and degree of  tectonism  (Shome  &  Kumar, 1979). These categories have been termed  as  grade  I,  II and III. The most competent and the best quality  of  phyllites represent grade I, and the poorest type of phyllites  is  designated as grade III. The Tehri gorge, which is the  main  area  of  the  projet activity, contains 45 percent of grade  I,  25  percent  of  grade II, and 30 percent of grade III phyllites (Pant  et  al.,  1982). The description of these three grades of phyllites is as follows:

## a) Grade I phyllites

The grade I phyllites are predominantly arenaceous, massive in character and distinctly jointed, at places pyritiferrous, and having lenticular elongated streaks of brown coloured calcareous material. The foliation planes are least developed. A number of bands of grade I phyllites, varying in width from a few millimeters to about a meter, occupy the Tehri gorge as pronounced ribs. In thin sections, the grade I phyllites are seen to be mainly composed of detrital quartz grains. The foliation banding is not much pronounced and the only effect of metamorphism is the elongation of quartz and muscovite crystals.

## b) Grade II phyllites

The grade II phyllites are conspicuously banded on account of rapid alterations of arenaceous and argillaceous materials. These contain a number of quartz veins, both along and across the foliation planes. The band width varies from a few millimeters to 100 mm. The main constituent of these phyllites in thin sections is also quartz but well developed sericitic bands are present. Oriented layers of sericite, muscovite and chlorite, giving a banded apperance to the rock mass, are found.

## c) Grade III phyllites

The grade III phyllites are composed mainly of the argillaceous component and contain arenaceous material in a lesser proportion. These phyllites contain quartz veins and are traversed by closely spaced foliation planes, cleavages and

joints. Minor folds and puckers are also present. The composition of these phyllites in thin sections is the same as in the case of the grade II phyllites.

The right bank diversion tunnels pass mostly through the grade II phyllites which constitute 60 percent of the rock mass encountered. Grade I and III phyllites are also present and constitute 30 percent and 10 percent respectively of the rock mass encountered. The grade II phyllites are highly jointed and have as many as five joint sets. The general strike of the phyllites is N55$^O$W-S55$^O$E to N70$^O$W-S70$^O$E and the dip is 35$^O$-55$^O$ due south west, i.e., along the downstream side. The right bank diversion tunnels are aligned in N6$^O$W-S6$^O$E direction. The tunnels are driven across the strike and are, therefore, favourably oriented. Fig.4.20 shows the predicted geological section along the alignment of the right bank diversion tunnels.

The left bank diversion tunnels have also been excavated through a rock mass predominated by the grade II phyllites. Towards the outlet, the grade III phyllites have been encounterd. A few bands of grade I and grade III phyllites are present along the alignment. The predicted geological section along the alignment of the left bank diversion tunnels is shown in Fig.4.21.

The diversion tunnels pass through a number of shear zones which constitute 5 percent of the tunnelling media encountered by the diversion tunnels. The remaining 95 percent of the rock mass is shared by Grade I (35 percent), grade II (40 percent) and grade III (20 perecent) phyllites (Verma and Rajvanshi, 1988).

The head race tunnels are located in grade I and grade II phyllites, with bands of grade III phyllites at places.

## 4.2.6.4 Influence of geology on tunnelling conditions

Construction of the Tehri tunnels has not experienced the tunnelling problems of the magnitude of those faced in Chhibro-Khodri, Maneri-Uttarkashi, Maneri Bhali Stage-II, and Loktak Tunnels, on account of relatively better geological conditions, lesser cover, and more favourable tunnel oreintation. The Tehri tunnels, especially the diversion tunnels, on the other hand, have a much larger excavated diameter.

The tunnelling work for the left bank diversion tunnel commenced from both the ends in the year 1979. A huge land slide near the outlet portal in the year 1980, however, delayed the tunnelling work from this end. The outlet portal could be established only in the year 1981. From the inlet end, tunnel driving for the first 250m length had to be done very carefully due to the presence of highly jointed grade II and grade III phyllites.

The excavation of the right bank diversion tunnel also was taken up simultaneously from both the ends. Due to a large excavated diameter (13 m) of the left bank and the right bank diversion tunnels, the excavation was carried out by the heading and bench approach using the conventional drill-and-blast method. The following sequence of construction was adopted (Rajvanshi, 1985):
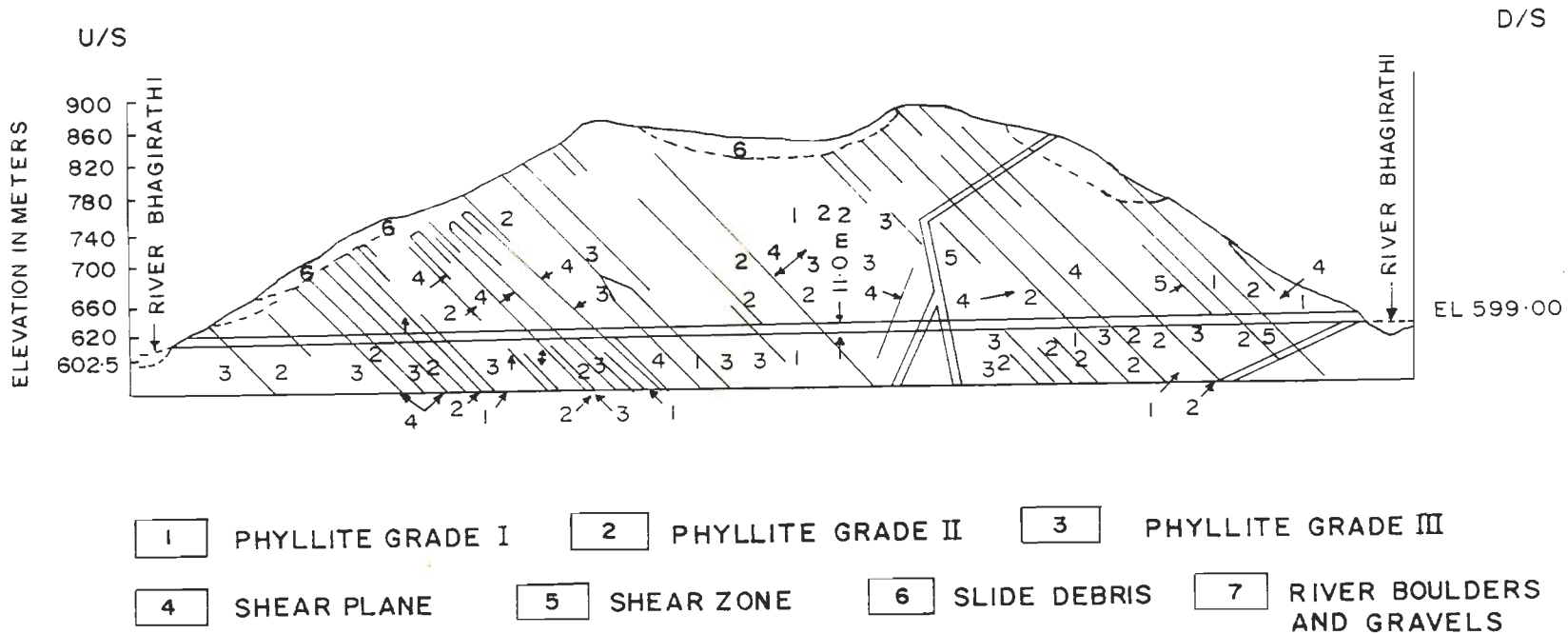
Fig. 4.20 - Geological Section Along Right Bank Diversion Tunnels

**Legend:**

| 1 | PHYLLITE GRADE I | 2 | PHYLLITE GRADE II | 3 | PHYLLITE GRADE III |

| 4 | SHEAR PLANE | 5 | SHEAR ZONE | 6 | SLIDE DEBRIS | 7 | RIVER BOULDERS AND GRAVELS |

U/S

D/S

980
900
820
740
660
632
580

ELEVATION IN METERS

EL. 596·00

123

| ▲▲▲ | DEBRIS | ∘∘∘∘ | RIVER BOULDER | ⠿⠿ | PHYLLITE GRADE-I | ⊟⊟ | PHYLLITE GRADE-II |

PHYLLITE GRADE III    UNDIFFRENTIATE PHYLLITE    ˣˣˣ SHEAR ZONE
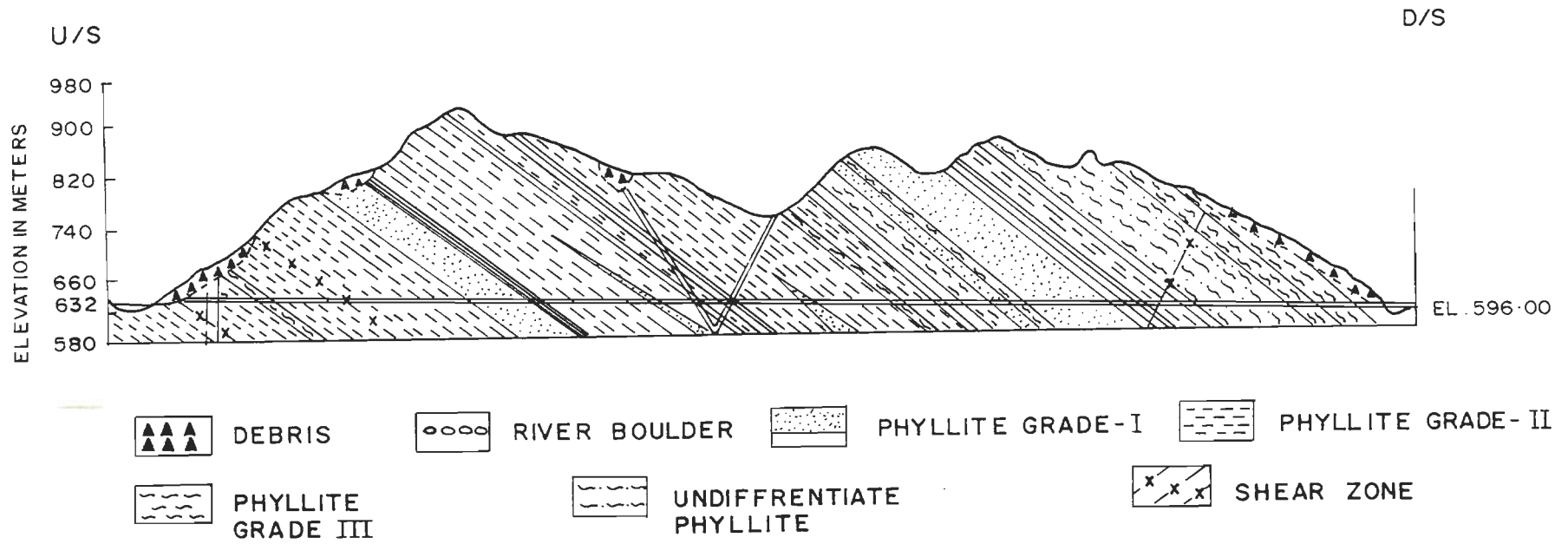
Fig.4.21 – Geological Section Along Left Bank Diversion Tunnels

i)   Heading excavation and immediate supporting,

ii)  overt lining with M250 concrete, 2.5 to 3 months after  the
     heading excavation,

iii) bench excavation, and

iv)  invert lining,  followed  by the lining on the  sides,  with
     M250 concrete.

The  only major problem encounted during the construction of
the  diversion tunnels, using the above sequence, was the failure
of  the  rock  mass on the right side in a length of 30m (527m to
557  m  from  the  inlet) in the right bank diversion tunnel, T-4
(Fig.4.19)  while  the  bench  excavation  was  in progress. This
resulted  in sliding of the rock mass from beneath the overt kerb
which,  in  turn,  caused  undermining  of  the  overt  lining
(Fig.4.22).  The  cause of the failure has been attributed to the
presence  of a shear zone in the above 30m reach, and complacency
shown  during  the  bench  excavation  (because of a problem-free
heading  excavation  which  was  carried out at a faster pace) in
leaving  the  bench  unsupported for a longer period of time than
the low stand-up time (estimated to be 48 hours) of the rock mass
(Rajvanshi, 1985).

## 4.2.7 Bagur-Navile  Tunnel  (Hemavathy  Irrigation  Project), Karnataka State

### 4.2.7.1 General features

The  9.76  km  long  D-shaped  Bagur-Navile  tunnel has been
constructed in Hassan district in the state of Karnataka to carry
the  waters  of the Hemavathy river across the ridge between the

Hemavathy and the Shimsha valleys mainly for irrigation purposes. The tunnel, with a finished width of 5.4m, is designed to carry a discharge of 70.79 cumecs for irrigating 2,55,000 hectares of land in Tumkur and Mandya districts of Karnataka, and for supplying drinking water to several towns in the Shimsha sub-basin. The tunnel was constructed using ten faces - one each at the inlet and the outlet ends, and eight through four intermediate vertical shafts (Fig.4.23). The tunnel was constructed over a period of about nine years from December 1980 onwards.

## 4.2.7.2 Geological features

The tunnel is driven through schistose gneiss. The predicted geology along the tunnel alignment did not reveal the presence of any fault. During construction, however, a collapse occurred in the approach adit. This led to further investigations by geophysical methods which revealed the presence of four major and two minor faults along the tunnel alignment. When actually encountered, the positions of the major faults were found to be slightly shifted from those predicted. The locations of the faults are given in Table 4.8.

The tunnel passes through a schist belt for a length of 1100m between Ch.13100m and Ch.14200m (Fig.4.23). The formation in this region is micaceous schist which was found to be quite unpredictable while tunnelling. Undisturbed samples taken from the Honnenahally fault zone indicate that the fault gouge is sand containing 10 to 15 percent of clay. The Honnenahally fault
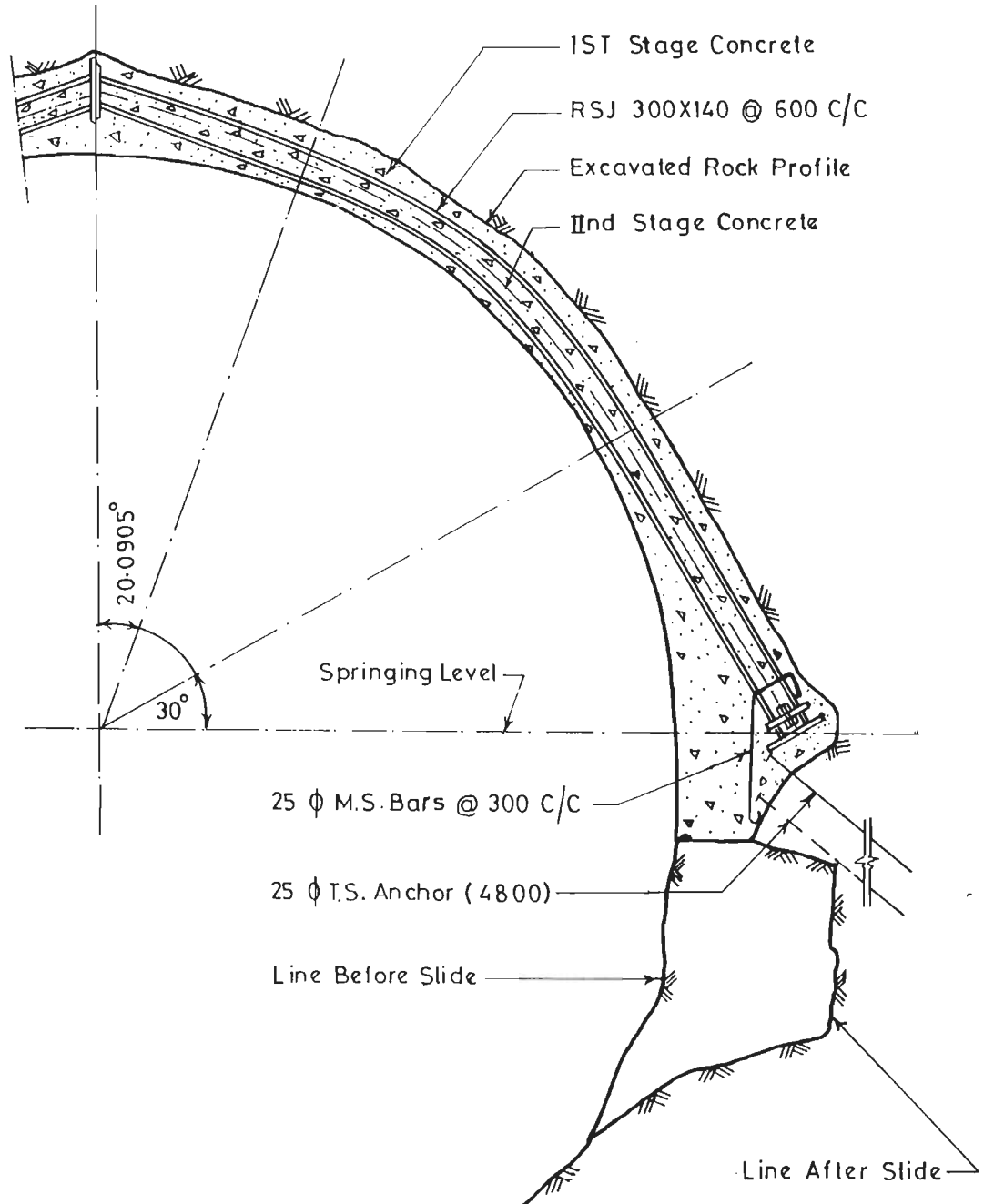
Fig. 4·22 – Undermining Of Overt Lining In Right Bank Diversion Tunnel T-4

A - Bagur Fault

B - Honnennahally Fault

C - Obalapura Fault

D - Kallasomahahally Fault

E - Minor faults in Nuggenhally schist belt

GENERAL ROCK TYPE ALONG THE TUNNEL IS SCHISTOSE GNEISS
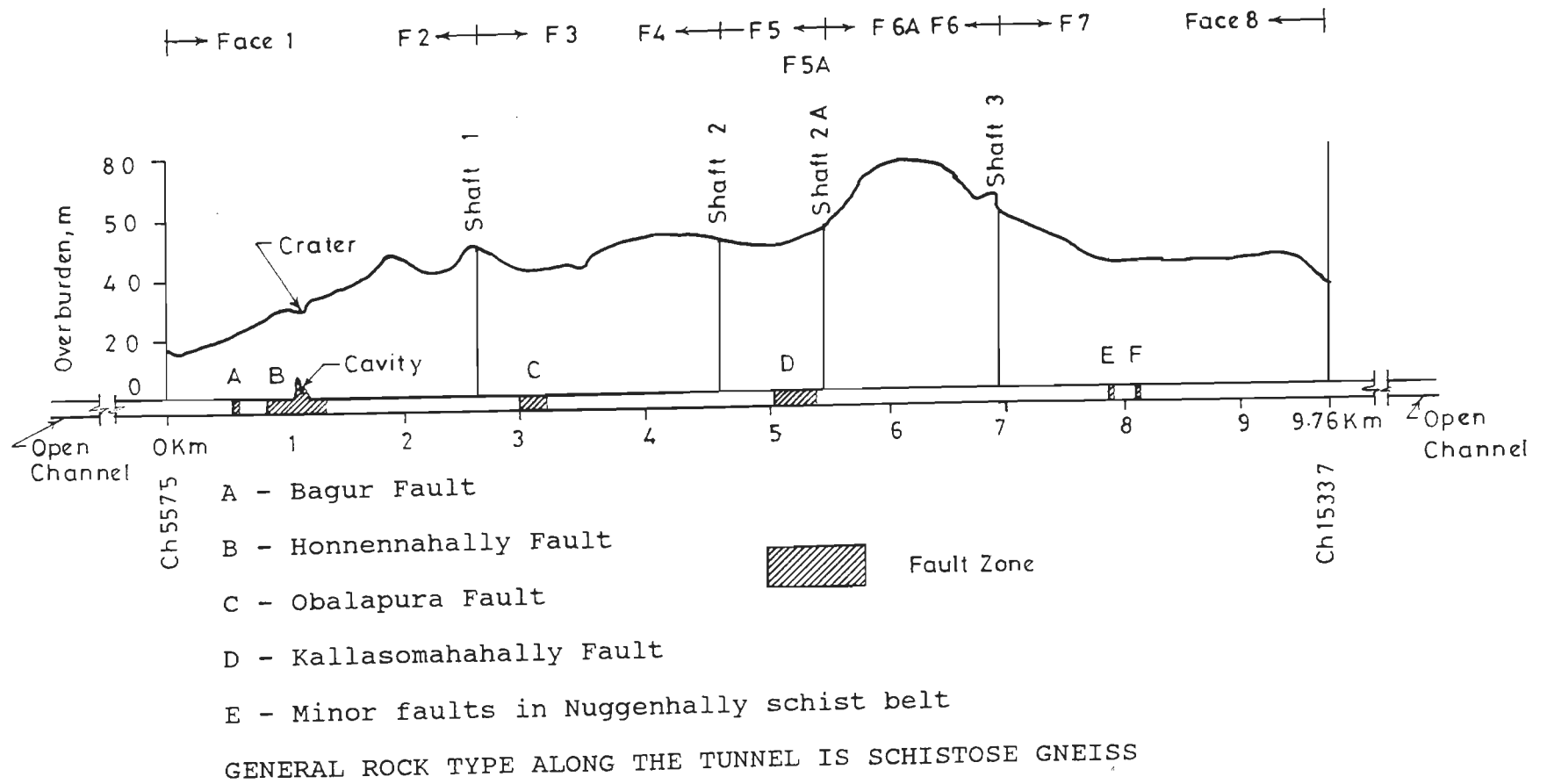
Fig.4.23 - Longitudinal Section of Bagur-Navile Tunnel

Table 4.8 - Predicted and Encountered Locations of Fault Zones in Bagur-Navile Tunnel

| S. No. | Fault | Location (chainage, m) | | Thickness, m | |
|---|---|---|---|---|---|
| | | Predicted | Encountered | Predicted | Encountered |
| 1. | Bagur Fault | 6129-6181m | 6129-6204m | 52 | 75 |
| 2. | Honnennahally Fault | 6460-6535m | 6385-6865m | 75 | 480 |
| 3. | Obalapura Fault | 8550-8635m | 8523-8685m | 85 | 162 |
| 4. | Kallasomaha-hally Fault | 10760-10930m | 10627-10974m | 170 | 347 |
| 5. | Minor faults in Nuggenh-ally schist belt | 13475-13500m and 13675-13700m | as predicted as predicted | 25 25 | 25 25 |

zone, which is the largest in width along the tunnel alignment, is composed of banded gneiss with quartzo-felspathic veins, as may be seen in the outcrops near Honnenahally village to the west of the tunnel alignment. The outcrops show a N30$^{O}$W trend with a general dip of 75$^{O}$ due west. Three sets of joints were observed in these outcrops. Gneisses in the region are subjected to intense fracturing.

## 4.2.7.3 Influence of geology on tunnelling conditions

The presence of the fault zones along the tunnel alignment had a significant influence on the tunnelling operations. In addition to the fault zones, there were zones of heavy water discharge and overbreakage which posed tunnelling problems. The micaceous schist (Ch.13100m to 14200m) posed roof stability problems at several locations because of a low stand-up time.

Most of the tunnelling problems were, however, faced in the fault zones. During construction of the tunnel, four collapses took place in the fault zones. Details of these collapses are given in Table 4.9 and in the following paragraphs in a chronological order.

## a) First collapse, face 1, chainage 6129m

The first collapse at Ch.6129m came as a surprise as good rock mass condition had been predicted in this reach on the basis of the geological investigations. The strata, suddenly met with at this chainage, contained fractured micaceous gouge associated with the Bagur fault, whereas the geological predictions had not indicated any fault along the whole of the tunnel alignment. The suddenly encountered fault zone at Ch.6129m resulted in a collapse on October 8, 1981, requiring rectification in a length of 61m. The collapse was associated with sliding of 47725 $m^3$ of muck into the tunnel. the rectification work was carried out by the cut-and-cover method at a cost of Rs.8.5 lacs (0.85 million) and consumed 24 months. The 'discovery' of the fault zone led to the geophysical methods for further investigations and, consequently, several fault zones were predicted.

## b) Second collapse, face 3, chainage 8523m

The geophysical investigations, commissioned as a result of the first collapse predicted the presence of the obalapura fault zone between Ch.8550m and 8635m. The fault zone was, however, suddenly encountered at Ch.8523m, resulting in a collapse on

Table 4.9 - Details of Collapses in Bagur-Navile Tunnel

| Collapse No. | I | II | III | IV |
|---|---|---|---|---|
| Face No. | 1 | 3 | 1 | 1 |
| Date of collapse | 22.7.81 | 22.12.82 | 4.7.84 | 17.5.87 |
| Affected chainages,m | 6129 to 6190 | 8523 to 8553 | 6441 to 6477 | 6640 to 6670 |
| Rectified length,m | 61 | 30 | 36 | 30 |
| Fault name | Bagur Fault | Oblapura Fault | Honnenhally Fault | Honnenahally Fault |
| Ovderburden,m | 21 | 50 | 25 | 28 |
| Ground water condition | Low to moderate seepage | Moderate to heavy seepage | Moderate to heavy seepage | Low seepage |
| Rectification method | Cut & cover | Cement and chemical grouting through holes from ground surface | Cement grouting through holes from ground surface | Consolidation of 6m thick cylinder around tunnel by cement grouting radial holes from inside the tunnel |
| Rectification time, months | 24 | 12 | 13 | 4 |
| Rectification cost,millions of Rupees | 8.536 | 3.528 | 4.64 | 3.500 |
| Rectification cost, millions of Rupees at 1989 level | 14.564 | 5.652 | 7.433 | 3.500 |
| Rectification cost,millions of Rupees per meter of tunnel | 0.239 | 0.188 | 0.206 | 0.117 |
| Rectification time, days/m | 12 | 12 | 11 | 4 |

December 22,1982 associated with heavy seepage of water and sliding of 810 m$^3$ of muck consisting of micaceous gouge. The affected tunnel reach was rectified by cement and chemical grouting from the ground surface and consumed 12 months and Rs. 35.28 lacs.

## c) Third collapse, face 1, chainage 6441m

While tunnelling from face 1, another collapse occurred on July 4, 1984 at Ch.6441m in the Honnenahally fault zone which was intercepted at Ch.6385m instead of the predicted location of Ch.6460m. In fact, contrary to the prediction of a 75m thick Honnenahally fault zone, a 480m thick fault zone was encountered from Ch.6385m to 6865m. The collapse was associated with a muck flow of 160 m$^3$. The rectification work spanned over 13 months and was accomplished at a cost of Rs.46.4 lacs. The rectification method involoved construction of bulkheads and cement grouting from the ground surface. This was followed by excavation through the grouted zone using forepoles and steel arch supports.

## d) Fourth collapse, face 1, Ch.6640m

The last collapse occurred in a 30m length from Ch.6640m to 6670m in the Honnenahally fault zone on May 17,1987, 12 days after completion of the support erection. The presence of this fault zone had been predicted upto Ch.6535m only. The collapse resulted in sliding of 1,100 m$^3$ of muck. Later, formation of a pot-hole took place on the ground surface above the collapsed

portion on July 22, 1988. The author was a member of the CMRS team which was entrusted with the job of suggesting the remedial measures (Jethwa,Verman,Goel,Prabhakar and Singh, 1988). An inspection of the collapsed zone, before starting the rectification work, revealed that a cavity had formed in the roof due to the flowing of sand-like loose debris (Fig. 4.24). The slided material was cohesionless and was intermingled with boulders of varying sizes. The boulders and the broken rock pieces were poor in strength and could be converted into powder when manually pressed between the palms. The debris were generally dry but the occurrance of considerable seepage in this zone during the heading excavation was reported by the site engineers. The rate of seepage had gradully reduced and then ceased completely after sometime, indicating the presence of accumulated water in the fault zone. Figure 4.25 shows a view of the collapsed zone.

The remedial measures included construction of bulkheads and excavation of heading in short lengths by multi-drift method, followed immediately by supporting and forepoling. This was followed by cement grouting in all the directions with a view to create a 6m thick consolidated zone around the tunnel. Bench excavation and supporting was then carried out in small lengths in two drifts. The immediate supporting was then followed up with final concreting.

It was observed that the collapse occurred due to excessive buckling of the steel ribs under heavy side pressures (Fig.4.24). Interestingly, although the steel ribs had

been correctly designed according to the category 6 of Terzaghi's rock load table (Table 3.1) for 'completely crushed but chemically intact' material, the designers overlooked one importanat remark of Terzaghi, pertaining to this category, which says 'considerable side pressures expected' and did not provide for any invert struts. Cosequently, the ribs buckled badly and a major collapse occurred 12 days after the supports were erected. Absence of any instrumentation in critical tunnel reaches, such as the fault zones, meant that there was to be no advance warning of the collapse. Even the simple closure measurements would have been sufficient to give enough indication of the impending collapse and suitable measures would have been taken to prevent it.

## 4.2.8 Lower Periyar Tunnel (Kerala State)

### 4.2.8.1 General features

Construction of the 12.80 km long Lower Periyar Tunnel along the left bank of the Periyar river in Idukki district in the state of Kerala is nearing completion. The 6.05m finished diameter tunnel is located in the peninsular region of India and is an important part of the Lower Periyar Hydro-electric Project. The tunnel was excavated from the inlet and eight additional faces opened through four intermediate adits (Fig.4.26). Most of the construction work is over and the only work left is placing of the final concrete lining in some reaches.

A ←

B ←

30 m.

Ch 6140 m

Ch 6170 m

L- SECTION

Ribs before
buckling

Ribs after
buckling

CROSS- SECTION A-B
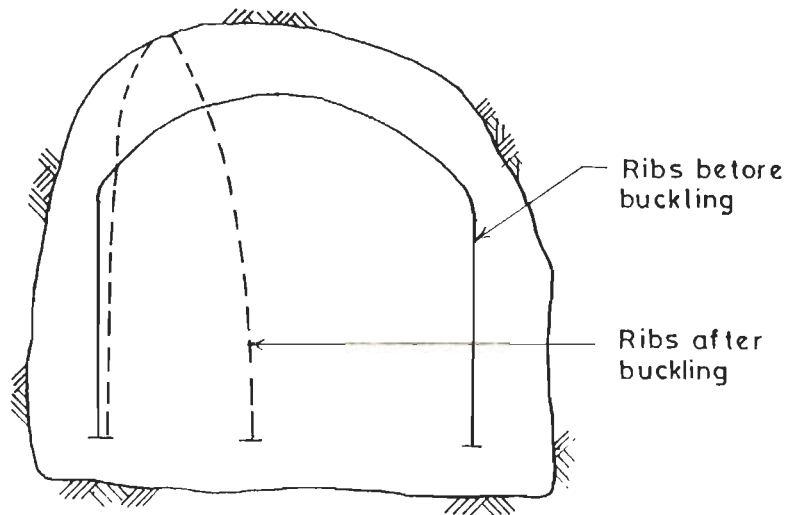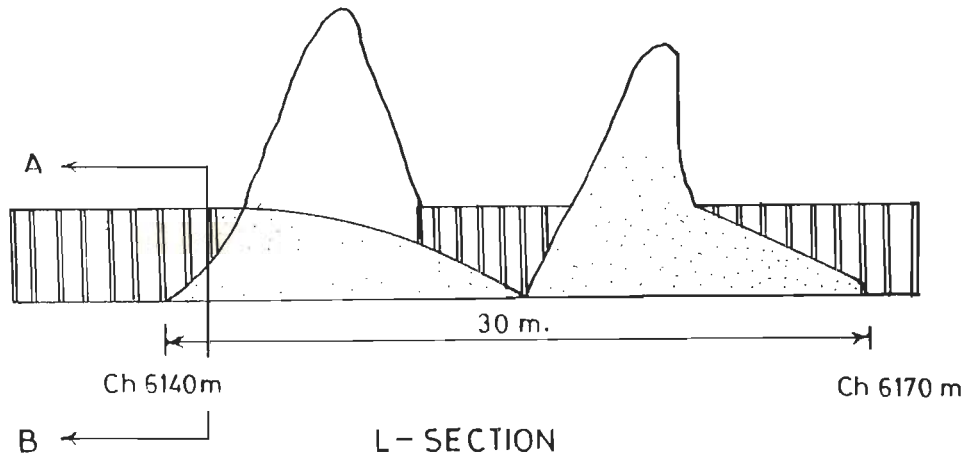
Fig.4.24 - Formation of Cavities and Buckling of
Steel Ribs in Bagur-Navile Tunnel

Fig.4.25 - A View of Collapsed Portion in
           Honnenahally Fault Zone (4th
           Collapse) of Bagur-Navile Tunnel

## 4.2.8.2 Regional geology and structural features

Detailed geological mapping of the area was carried out by the Geological Survey of India (GSI). According to GSI, the project area lies in the Archaen terrain consisting of composite gneisses and intermediate acid charnockites with intrusions of amphibolites. Most of the tunnel is aligned in a N60$^O$W direction. Initially, however, a small length of the tunnel, i.e., from the inlet to Ch.42.5m and from Ch.42.5m to Ch.1205.2m, is aligned in N35$^O$W and N85$^O$W directions respectively (Fig. 4.26). The tunnel passes under an overburden varying in height from 38m to 285m, the maximum being at Ch.3200m near a place called Arrathukadavuthodu. The tunnel alignment passes through massive to jointed composite gneisses comprising of migmatised charnockites with lenses and stringes of amphibolites and granite-gneisses belonging to the archaen super group. According to the GSI reports, drag folds associated with migmatisation are seen throughout the length. Pegmatite veins appear to have been injected along some of the major joint planes. The foliation of the composite gneiss varies in strike from NE-SW to N70$^O$E-S70$^O$W having a dip of 20$^O$-50$^O$ in the SE direction. Upto Ch.42.5m, the strike of the foliation, however, is in the NW-SE direction with a dip of 70$^O$ in the SW direction. Two shear zones of 1 to 2m thickness intercept the tunnel alignment at Ch.10500m and 11410m.

## 4.2.8.3 Influence of geology on tunnelling conditions

The geological features along the tunnel alignment were by and large favourable for tunnelling except for two shear zones

and low cover zones. The rock mass quality was fair to good along most of the tunnel length and the ground conditions were practically uniform except in the shear zones. The influence of geology in the case of the Lower Periyar tunnel, therefore, was reflected in the form of a practically problem-free tunnelling operations, notwithstanding the normal tunnelling problems associated with the construction of a tunnel. It is, however, not the geology alone which creates problems. Sometimes, poor anticipation of tunnelling problems and the absence of a planned approach to tackle the likely problems enhances the tunnelling difficulties. Such eventualities were carefully avoided in the Lower Periyar tunnel. Under advice from the Central Mining Researh Station, the zones likely to pose tunnelling problems were identified in advance, and approaches worked out to avoid such problems. As a result, the tunnel construction through these zones was almost free of problems. On the basis of the geological reports, geological logs and other parameters, such as Q and RMR, the following four zones were identified for careful consideration.

(i)   Low cover zone I from Ch.1110 m to 1130 m,
(ii)  low cover zone II from Ch.9630 m to 9650 m,
(iii) shear zone I from Ch.10500 m to 10610 m, and
(iv)  shear zone II from Ch.11410 m to 11490 m

Suitable supporting measures were suggested for these zones.
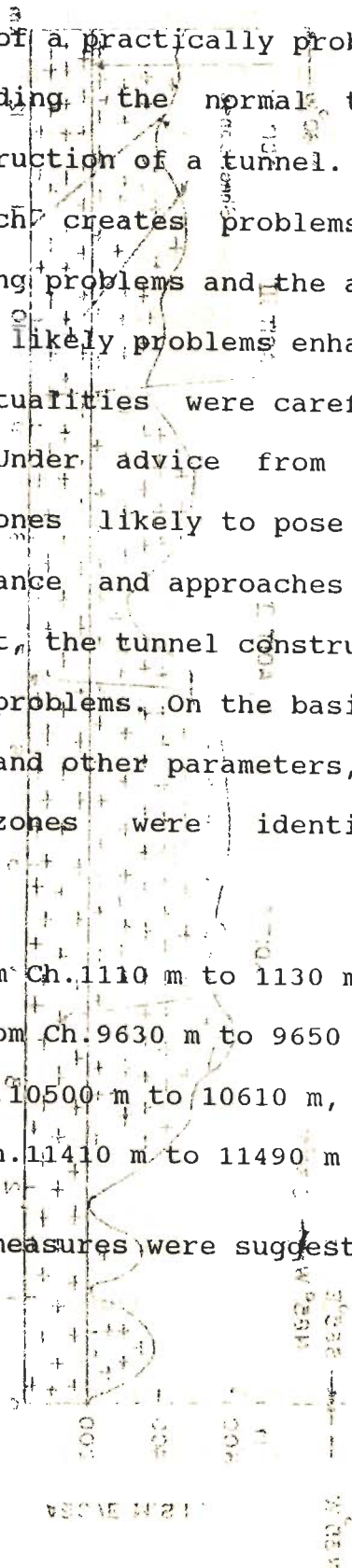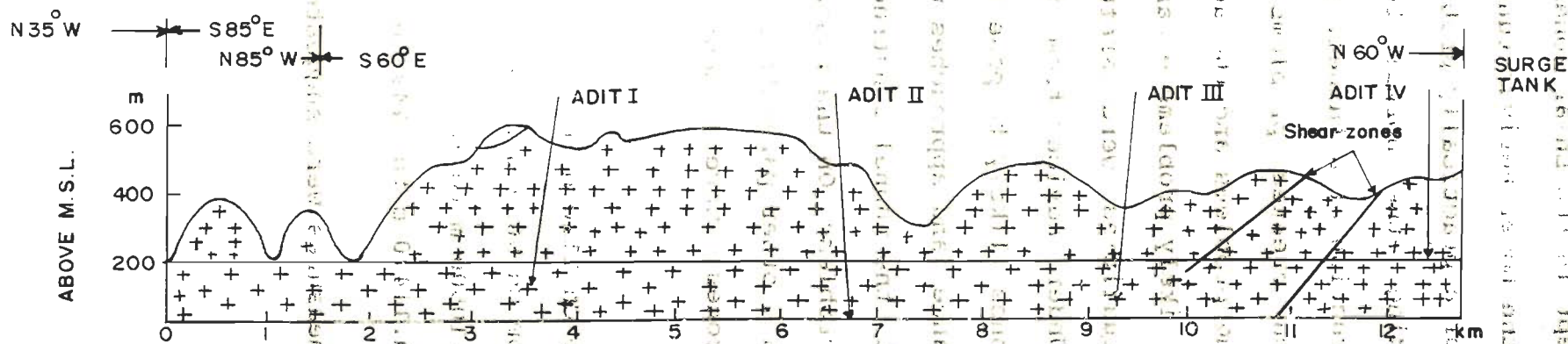
Fig. 4.26 — Geological Section of Lower Periyar Tunnel

## 4.2.9 Tandsi Inclines (Tandsi Mine Project), Madhya Pradesh

### 4.2.9.1 General features

Western Coalfields Limited (WCL), a subsidiary of Coal India Limited (CIL) has started a new mining project, called the Tandsi Project, in Kanhan area located in Chhindwara district in the state of Madhya Pradesh in Central India. Access to the coal seam, lying at a depth of about 220m, will be provided through six inclines. These inclines are proposed to be constructed in two sets of three inclines each. The length of each of the inclines will be 1.05 km with a gradient of 1 in 4.65. The inclines will serve as permanent life lines of the mine. Construction of two of the inclines is in progress.

### 4.2.9.2 Regional geology

The main rock formations in the area are Talchirs, Barakars and Moturs. Talchirs consist of hard, dark grey arenaceous shales with bands of granites and quartzites, greenish grey splintary shales, and sandstones. These Talchir formations lie unconformably above the archaen rocks. The Motur formations of the middle Permian age consist of medium to coarse grained sandstones with greenish grey clays. The Barakars are comprised of fine to medium grained sandstones with bands of shales and carbonaceous shales. The Barakar formations contain the coal seams. A geological cross-section along Incline no. 2 is shown in Fig.4.27. Occurrance of five faults along the inclines has been predicted. The Talchirs, as observed at the surface, are highly weathered and jointed.

## 4.2.9.3 Influence of geology on tunnelling conditions

Roof falls and formation of cavities occurred in June 1990 in both the inclines which are under construction due to the encoun-tering of soft sandstone strata. In the affected zone, massive roof falls started taking place about 20 hours after blasting, and finally culminated into formation of dome shaped cavities. It is, however, felt that despite the soft strata, the roof falls could be avoided by taking proper supporting measures. Erection of the steel ribs was not only delayed but the backfill between the ribs and the rock mass was also not provided. The delayed and ineffective support system resulted in the roof falls.

Rectification of the affected incline length (Ch.308 to 326m in Incline no. 2, Fig. 4.27) was carried out under the advice of the Central Mining research station (CMRS), by strengthening of the existing supports, construction of the bulkhead and grouting of the cavity, and excavation of the affected zone in short pulls of 0.5m in 3-4m lengths, followed by erection of supports and placing of the backfill.

Subsequently, under CMRS's advice, the NATM approach has been followed for construction of the inclines. This is for the first time that this approach has been adopted in the coal mines in India. The controlled blasting technique of excavation and the shotcrete-rock bolt support system have resulted in minimising the overbreaks, reducing the additional support requirements, and optimising the rate of drivage and cost of construction.

F1   F3   F4   F5   F6

Incline 1 in 4.65 (Total Length 1056 m)

500

400

300

200

330   F1  F3  F4   660   F5   F6   990   1320

INDEX

| ✓ ✓ | Soil |

| " = " | Moturs |

Barakars

Talchirs

Coal Seams

Scale—1:5450
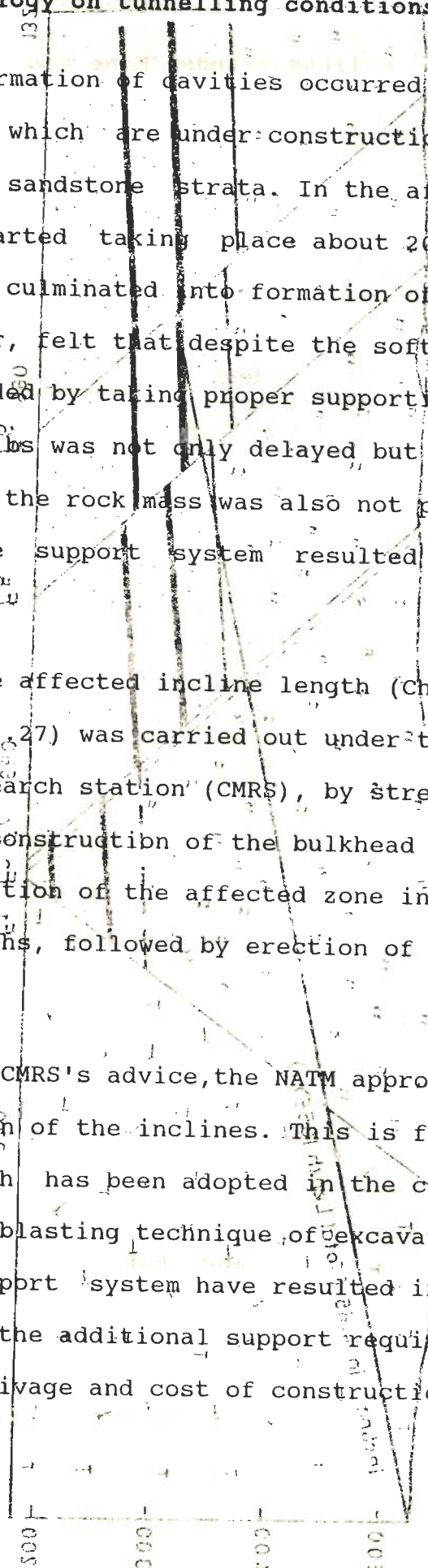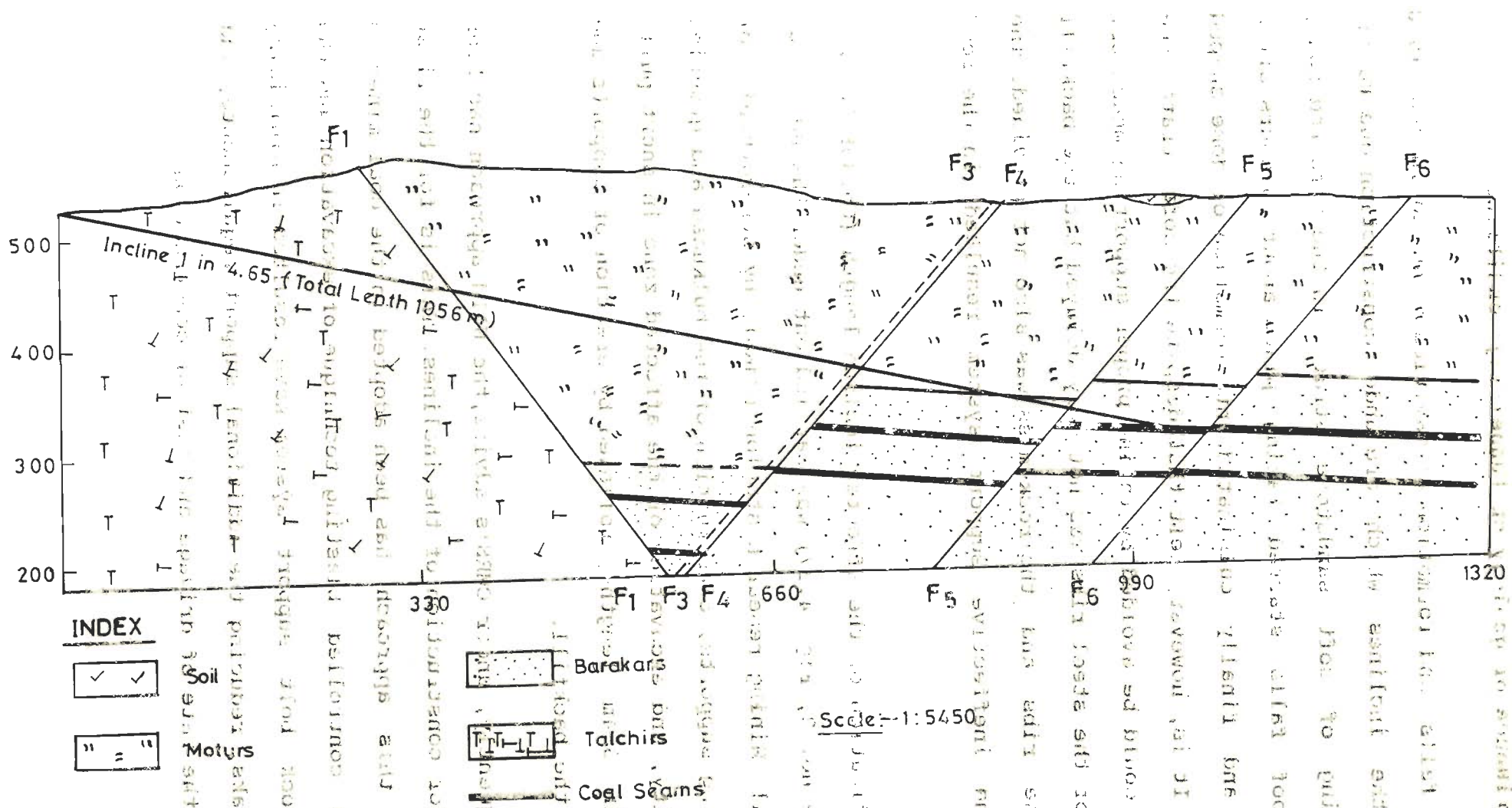
Fig.4.27 Geological Section Along Tandsi Incline No.2 (Mine 1)

# CHAPTER 5

# CHAPTER 5

## FIELD INSTRUMENTATION AND MONITORING OF TUNNELS

### 5.1 INTRODUCTION

Monitoring of the rock mass behaviour by field instrumentation is an important part of the design and construction process of the underground excavations. This is the backbone of the observational method of tunnel support design which is based on the 'build-as-you-go' philosophy. The modern tunnelling approach of the New Austrian Tunnelling Method relies heavily on continuous field monitoring. The present study is substantially influenced by the results of extensive field monitoring carried out in several Indian tunnels over the last two decades. A few important aspects of field instrumentation and other field studies carried out in nine Indian tunnels, described in Chapter 4, form the contents of this chapter.

### 5.2 ROCK MASS-TUNNEL SUPPORT INTERACTION ANALYSIS AND TUNNEL INSTRUMENTATION

The observational method of tunnel support design, based on field instrumentation, laid the foundation for the development of what is called the 'convergence-confinement method'. The convergence-confinement method is based on the concept of the rock mass-tunnel support interaction introduced in Chapter 1. The method is aimed at estimating the support pressure from the point of intersection of the ground reaction and the support reaction curves (Fig.5.1).

The application of the convergence-confinement method depends on tunnel instrumentation to a great extent. The predicted ground reaction and support reaction curves (using the approach discussed later in Chapters 6 and 7) are revised continuously throughout the tunnelling process on the basis of the actual measurements during construction, and the amount of support is accordingly increased or decreased, so as to achieve the desirable point of intersection or, in other words, a safe and economical support system. The point of intersection should neither be beyond the minimum value (denoted by point D in Fig. 5.1) of the required support pressure, nor be much ahead of this value. In the former case, the support will be unsafe and in the latter, uneconomical. In fact, the curves may not intersect at all in the former case.

## 5.3 FIELD STUDY

The tunnel instrumentation programme was an important part of a comprehensisve field study carried out at nine tunnelling projects with a view to develop an approach for determination of the ground reaction and the support reaction curves. The field study comprised of the following:

(i) instrumentation to measure support pressures and tunnel deformations,

(ii) estimation of Barton's Rock Mass Quality, Q, and Bieniawski's Rock Mass Rating, RMR, at the instrumented and other sections,

(iii) collection of other relevant data, such as, type of rock mass, modulus of deformation, uniaxial compressive strength etc., of the rock mass, wherever available,

(iv) collection of tunnel details, such as, direction of tunnel axis, size and shape of tunnel, height of overburden, dates of excavation & support installation for each instrumented section, and

(v) collection of tunnel support details, such as, section of steel rib used, type and thickness of backfill.

The above field study was carried out at 63 sections of the following tunnels:

**(a) Tunnels with instrumented sections in elastic ground condition** (Table 5.1)

(i) Tehri Tunnels, Uttar Pradesh

(ii) Lower Periyar Tunnel, Kerala

(iii) Maneri-Uttarkashi Tunnel, Uttar Pradesh

(iv) Maneri Stage-II Tunnel, Uttar Pradesh

(v) Bagur-Navile Tunnel (Hemavathy Project), Karnataka

(vi) Tandsi Inclines (i.e., inclined tunnels for a mine), Madhya Pradesh

**(b) Tunnels with instrumented sections in squeezing ground condition** (Table 5.2)

(i) Chhibro-Khodri Tunnel, Uttar Pradesh

(ii) Giri Tunnel, Himachal Pradesh

(iii) Maneri Stage-II Tunnel, Uttar Pradesh

(iv) Loktak Tunnel, Manipur

Out of the 63 tunnel sections where the field study was carried out, the details of some of the sections are given in Tables 5.1 and 5.2 for elastic and squeezing ground conditions respectively.

## 5.4 TYPES OF INSTRUMENTS

One of the main purposes of the field work was to study the ground and the support behaviour at various tunnel sections with a view to develop an empirical/semi-empirical approach for predicting the ground reaction and the support reaction curves.

Since these curves represent the relationship between the support pressure and the tunnel closure, the instrumentation scheme consisted of monitoring these two parameters using the following types of insturments:

(i) Load cells to measure the hoop load on steel ribs,
(ii) contact pressure cells to measure the contact pressure at the rock mass-tunnel support interface, and
(iii) tape extensometer to measure the tunnel closure.

In addition to these types of instruments, borehole extensometers (single-point and multi-point) were also installed at some of the tunnel sections to monitor the deep seated displacements in the rock mass around the tunnel periphery radially at different depths. The borehole extensometer data were, however, not used for the specific purpose of the present study.

## Table 5.1 - Tunnel Sections in Elastic Ground Condition

| S. No. | Project | Location of Section | Rock Type | Q | Height of Overburden (m) | Excavated Diameter (m) |
|---|---|---|---|---|---|---|
| 1. | Tehri,U.P. | a)Ch.828m, HRT-3 | Phyllites Grade III | 0.36 | 295 | 9.5 |
| | | b)Ch.829m, HRT-3 | Phyllites Grade III | 0.36 | 295 | 9.5 |
| | | c)Ch.683m, LBDT-1 | Phyllites Grade II | 14 | 225 | 13.0 |
| | | d)Ch.614m, RBDT-1 | Phyllites Grade II with bands of Grade I | 3.2 | 240 | 13.0 |
| | | e)Ch.615m, RBDT-1 | Phyllites Grade II with bands of Grade I | 3.2 | 240 | 13.0 |
| 2. | Lower Periyar, Kerala | a)Ch.2361m | Granite-biotite gniess | 4.4 | 120 | 6.8 |
| | | b)Ch.6218m | Granite-biotite gniess | 5.5 | 197 | 6.8 |
| 3. | Maneri-Uttarkashi, U.P. | a)Ch.789.5m U/S Heena | Metabasics with a 1.5m thick shear zone | 0.66 to 0.10 | 367 | 5.8 |
| | | b)Ch.1060m U/S Heena | Foliated Metabasics | 3.4 to 6.8 | 234 | 5.8 |
| | | c)Ch.738.5m D/S Maneri | Moderately Foliated Quartzites | 1.2 to 6 | 250 | 5.8 |
| | | d)Ch.1310m U/S Uttarkashi | Foliated Metabasics | 3.4 to 6.8 | 467 | 5.8 |

Table 5.1 (contd.)

| S. No. | Project | Location of Section | Rock Type | Q | Height of Overburden (m) | Excavated Diameter (m) |
|--------|---------|---------------------|-----------|---|--------------------------|------------------------|
| 4. | Maneri Stage-II, U.P. | a) Ch.1568.75m U/S Dharasu | Greywackes | 2.75 | 100 | 7.0 |
| | | b) Ch.1780m U/S Dharasu | Greywackes | 1.02 | 175 | 7.0 |
| 5. | Bagur-Navile, Karnataka | a) Ch.6380m | Schistose gneiss | 0.08 | 45 | 6.0 |
| | | b) Ch.10678m | Schistose gneiss | 1.353 | 50 | 6.0 |
| | | c) Ch.8695 | Schistose gneiss | 13.53 | 49 | 6.0 |
| 6. | Tandsi Mine, M.P. | a) Ch.60m | Talchirs | 11.8 | 16 | 5.4 |
| | | b) Ch.80m | Talchirs | 32 | 18 | 5.4 |
| | | c) Ch.220m | Talchirs | 1.1 | 67 | 5.4 |
| | | d) Ch.265 | Talchirs | 9.07 | 88 | 5.4 |

Ch. - Chainage
HRT - Head Race Tunnel
LBDT- Left Bank Diversion Tunnel
RBDT- Right Bank Diversion Tunnel
U/S - Upstream
D/S - Downstream

Table 5.2 - Tunnel Sections in Squeezing Ground Condition

| S. No. | Project | Location of Section | Rock Type | Q | Height of Overburden (m) | Excavated Diameter (m) |
|---|---|---|---|---|---|---|
| 1. | Maneri Stage-II, U.P. | a) Ch.50.5m Dhanarigad drift(U/S) | Metabasics | 0.08 | 710 | 2.5 |
| | | b) Ch.51m Dhanarigad drift(U/S) | Metabasics | 0.08 | 710 | 2.5 |
| | | c) Ch.777.2m U/S Dhanarigad | Crushed Quartzites | 0.18 | 705 | 7.0 |
| 2. | Giri,H.P. | a) Phyllites | Completely crushed to phyllites | 0.06 to 0.32 | 240 | 4.8 |
| | | b) Slates | Very blocky & seamy slates | 0.32 to 0.82 | 380 | 4.8 |
| 3. | Chhibro-Khodri,U.P | a) Ch.2575m | Red shales | 0.025 to 0.1 | 280 | 3.0 |
| | | b) Ch.2621m | Black clays | 0.016 | 280 | 3.0 |
| | | c) Ch.1199m | Crushed red shales | 0.012 to 0.05 | 680 | 9.6 |
| 4. | Loktak, Manipur | | Shales | 0.011 to 0.044 | 300 | 4.8 |

Ch. - Chainage
U/S - Upstream

## 5.4.1 Load Cells

The load cells were installed within the steel ribs as shown schematically in Fig. 5.2 and pictorially in Fig.5.3. The load cells are normally installed at the springing level to measure the vertical load, and at the crown to measure tha horizontal load. Where the side pressure is likely to be a problem, the load cells are installed within the invert (which is provided to counter the side pressures) for monitoring the side pressure. Mainly two types of load cells were used- mechanical load cells and vibrating wire type electrical load cells. These are shown in Fig.5.4. The observations from the mechanical load cells were taken using a mechanical read-out device, such as, a dial gauge (Fig. 5.5). A battery operated portable electrical read-out unit (Fig. 5.5) with digital display was used for the electrical load cells. Figure 5.6 shows an electrical read-out unit being used in a tunnel. The future instrumentation is being planned with the electro-mechanical load cells in mind. As its name suggests, an electro-mechanical load cell contains both mechanical and electrical sensors and facilitates observations using both a mechanical and an electrical read-out unit (Fig.5.5). This enables cross-checking of observations to establish the reliability of the electrical observations. Once this reliability is established, the observations may be continued to be recorded after commisioning of the tunnel by using an electrical read out unit (or a centralised data logging system) when the load cell becomes inaccessible for dial gauge observations.

Fig 5.1— Selection Of Desirable Support From Convergence—Confinement Method
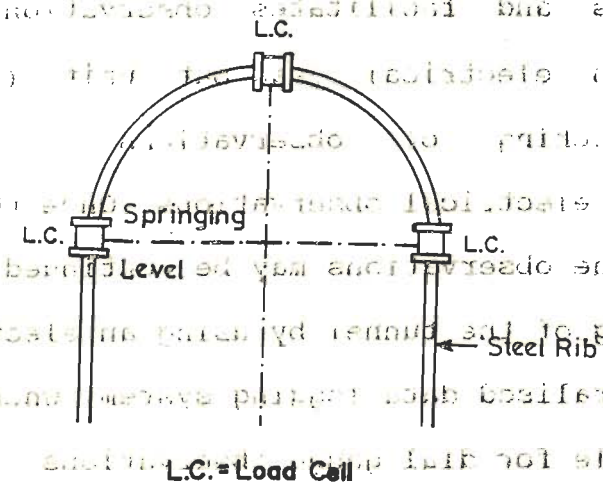
Fig.5.2 — A Typical Array of Installation
of Load Cells within Steel Ribs

(Figure 5.1 labels)

A

$p_i = p_o$

ELASTIC BEHAVIOUR

PLASTIC BEHAVIOUR

Support Pressure $p_i$

PRESSURE REQUIRED TO LIMIT DEFORMATION

PRESSURE AVAILABLE FROM SUPPORT

GROUND REACTION CURVE

SUPPORT REACTION CURVE

TOO STIFF SUPPORT (UNECONOMICAL)

$C_1$

DESIRABLE SUPPORT (ECONOMICAL & SAFE)

$C_2$

TOO FLEXIBLE SUPPORT (UNSAFE)

RADIAL DEFORMATION $U_a$

(Figure 5.2 labels)

L.C.

L.C.      Springing      L.C.

Level

Steel Rib

L.C.= Load Cell

Fig.5.3(a) - Electrical Load Cells Installed within
Steel Ribs at Springing Level



Fig.5.3(b) - A Mechanical Load Cell (with Dial Gauge)
Installed within Steel Rib at Springing
Level

Fig.5.4 - Load Cells
   a) Electrical Load Cell
   b) Mechanical Load Cell
   c) Rock Bolt Load Cell



Fig.5.5 - Read-out Units for Use with load Cells
   a) Electrical Read-out unit
   b) Dial Gauge

**Fig.5.6 - An Electrical Read-out Unit being Used in a Tunnel**

## 5.4.2 Contact Pressure Cells

The contact pressure cells were used at some tunnel sections in combination with the load cells. These cells have the advantage of facilitating the measurement of the radial support pressures in different radial directions. The need for knowing the radial support pressure in a particular direction arises when the local geology, e.g. inclined joints, is expected to affect the support loading in that direction. The load cells facilitate estimation of the average values of the vertical and horizontal support pressures. From the load cell data, it is not easy to determine the variation of the support pressure in a particular radial direction to know the effect of directional loading of the steel ribs. The contact pressure cells are installed on the outer flange of the steel rib before the backfill is placed. The contact pressure cells, which consist of a hollow spherical segment sandwiched between the thick rectangular steel plates, is shown schematically in Fig.5.7. A typical array of the installation of contact pressure cells is shown in Fig.5.8.

## 5.4.3 Measurement of Tunnel Closure

### 5.4.3.1 The instrument

The tunnel closures were measured by using tape extensometers. A tape extensometer (Fig.5.9) is used to measure the variation (reduction or increase) in the distance between two diametrically opposite points on the tunnel periphery (Fig.5.11a). This measuring distance may be inclined at any angle, the most common being the horizontal one. The

diametrically opposite points are fixed in the form of closure bolts (also called closure studs or anchors) of about 1m length grouted in boreholes drilled in the rock mass from the tunnel periphery (Fig.5.11b). The tape extensameter consists of a read-out unit (a dial gauge unit or a battery operated digital display unit) and a steel tape, besides a constant tension device. The read-out unit is connected to the closure bolt at one end and the tape is then unwound to the required length and connected to the closure bolt installed on the diametrically opposite end. For each observation the same amount of tension is applied to the tape using the constant tension device. This eliminates the error due to the sag of the tape. For connecting the tape extensometer to the closure bolts, either a ball and socket arrangement (ball attached to the bolt, as in Fig.5.11b, and socket attached to the tape extensometer) or a hook arrangement (the tape extensometer shown in Fig. 5.9 has hooks on both sides) is provided. Fig.5.12 shows a tape extensometer observation being taken in a tunnel

While the tape extensometer was used at most of the instrumented tunnel sections, another instrument called 'distomat' (make-Telemac, France) was used for measuring tunnel convergence in Bagur-Navile tunnel (Fig 5.10). Instead of a tape, the distomat has a wire with provision to fix a reference point to indicate the tension applied for a particular observation. During the subsequent observations, the reference point is shifted to achieve the same amount of tension. The instrument has a digital display read-out unit. The author faced several practical difficulties while using this instrument and found the
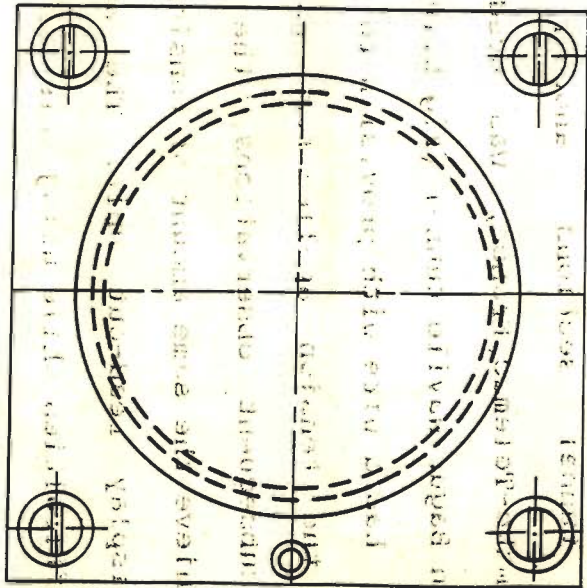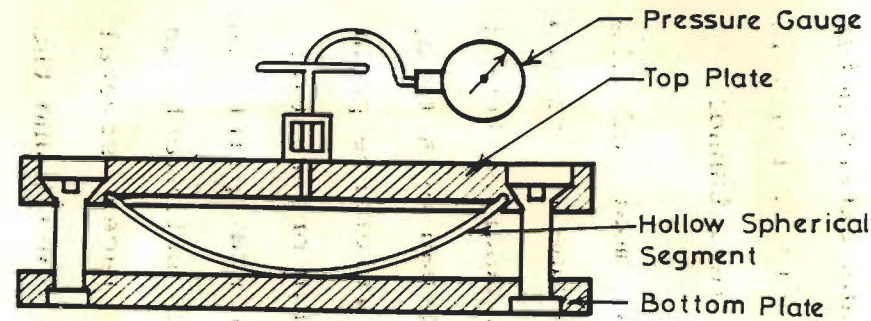
Fig.5.7 - Contact Pressure Cell
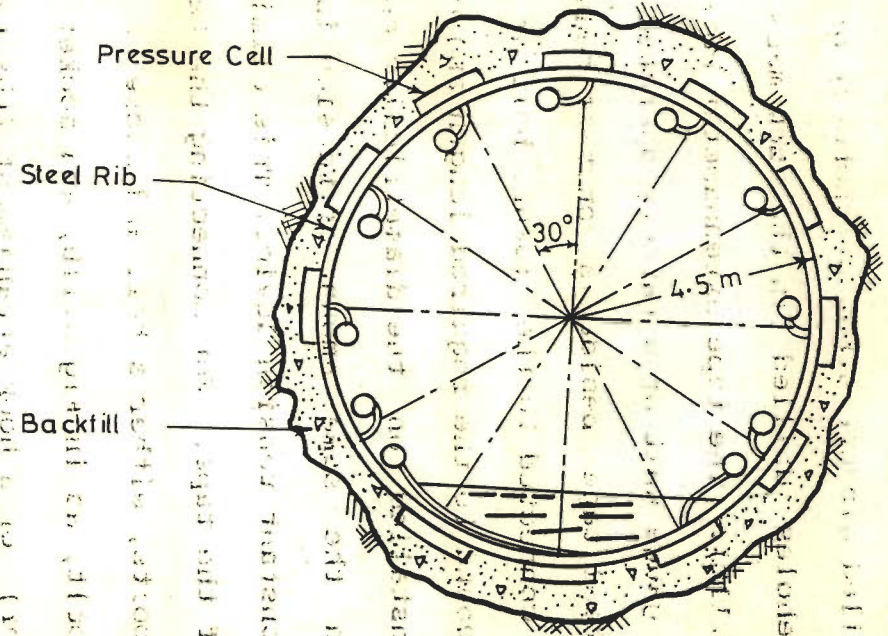
Fig.5.8 - A Typical Installation Array of Contact Pressure Cells in Chhibro-Khodri Tunnel (after Jethwa, 1981)

**Fig.5.9** - Tape Extensometer Used for Measuring
Tunnel Closure



**Fig.5.10** - DISTOMAT Used for Measuring
Tunnel Closure in Bagur-Navile
Tunnel
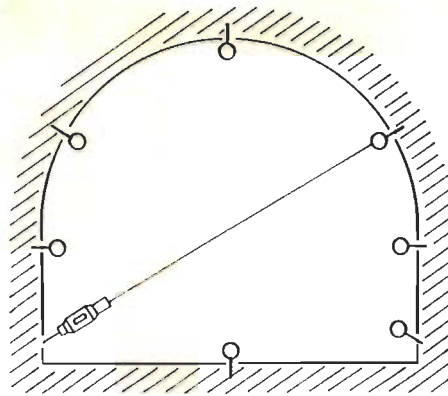
Fig.5.11(a) - Tape Extensometer Connected to Two Diametrically Opposite Points
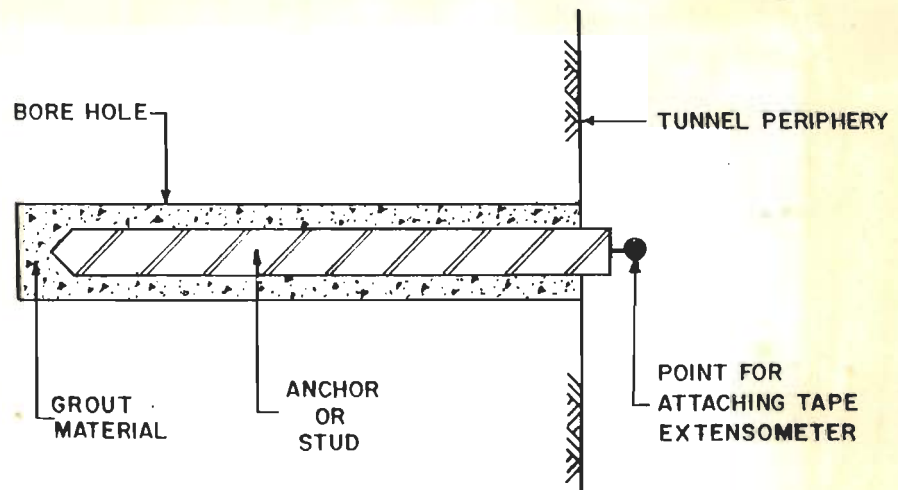


Fig.5.11(b) - Installation of Closure Stud

Fig.5.12(a) - A Tape Extensometer Observation
Being Taken at a Tunnel Section



Fig.5.12(b) - Other End of Tape Extensometer

tape extensometer to be a better convergence measuring device.

## 5.4.3.2 Utility of closure measurements

During his association with field instrumentation in tunnels and underground powerhouse cavities (at Sardar Sarovar Project in Gujarat and Koyna Stage iv Project in Maharashtra - data not reported as the scope of the present work does not cover large cavities) for the past eight years, the author has realised the usefulness of closure measurements. Tunnel closure is a parameter which is not only relatively easy to monitor, but is also easy to interpret as its value is directly available from the tape extensometer data. The support pressure, on the other hand, has to be estimated indirectly from the load measurements. Also, the closure measurements take into account the overall rock mass movement at the instrumented section, as compared to the parameters, such as support loads which are measured at a point. The installation procedure for closure observations does not require much expertise. The closure measurements work out to be much cheaper as the same tape extensometer may be used for several tunnel sections, unlike the other instruments, such as, load cells, contact pressure cells, and borehole extensometers which, once installed, are normally not retrievable. The stability of a tunnel is normally expressed quantitatively in terms of the allowable tunnel closure as a percentage of the tunnel size depending upon the ground condition (see Fig.7.10 and 7.11 in Chapter 7)

Thus, while the measurement of the support pressures is very

important and, in fact, indispensible, the usefulness of the closure observations should be kept in mind when planning an instrumentation scheme. While the cost of taking closure measurements is less, the advantages are many. Therefore, the practice of installing closure bolts at a number of sections was adopted in the tunnels included in Tables 5.1 and 5.2. Closure observations were recorded at a total of 63 sections, including 22 of 29 sections mentioned in Tables 5.1 and 5.2 where the support pressures were also measured. That way, the rock mass behaviour could be observed at many tunnel sections, without adding significantly to the cost of instrumentation, in addition to the limited number of carefully selected sections for detailed instrumentation.

## 5.5 DETERMINATION OF UNRECORDED TUNNEL CLOSURE AND SUPPORT PRESSURE

### 5.5.1 Unrecorded Data

It is often not possible to commence the closure or load cell observations immediately after the excavation or, in other words, right at the face. This is due to the time consumed for installation of closure bolts and the fact that the protruding part (for attaching the tape-extensometer - Fig.5.11b) of the closure bolt is often found bent or broken when installed close to the face as a result of the fly rock hitting the closure bolts during blasting. Same is the case with the load cells which not only take time for installation (the load cells are placed within the steel ribs which are normally not installed immediately after the excavation because of practical difficulties), but, like the

closure bolts, are also exposed to the flying rock pieces during blasting when installed close to the face. The case-histories considered for the present work were no exceptions and the valuable information regarding the initial tunnel closure and support pressure immediately after blasting, was almost always lost. To overcome this problem, a graphical method was adopted to determine the unrecorded closure and support pressure.

## 5.5.2 Estimation of Unrecorded Closure and Support Pressure

The method adopted may be explained with the help of an example of the Maneri Bhali Stage-II tunnel. Fig.5.13 shows a plot of the radial tunnel closure with respect to time at ch.1568.75m. The first observation was taken 12 days after the date of excavation. The missing data of the first 12 days were obtained by first plotting the data on a log-log scale and then by extrapolating the initially straight line portion of the curve (Fig.5.14). Extrapolation of the straight line portion to -12 days (i.e., 12 days before the date of first observation) on log-log scale, and conversion of the extrapolated value to ordinary scale gives the value of the radial tunnel closure on the date of excavation as -0.16 cm. This implies that an additional value of 0.16cm has to be added to the radial closure values to account for the missing data. The original and the extrapolated data are presented in Table 5.3. The complete data (including the extrapolated data) were then replotted in the form of the time versus radial closure curve (Fig.5.15).

### 5.5.3 Significance of Determining Unrecorded Closure and Support Pressure

In the example, pertaining to the extrapolation of closure data, illustrated in Figs.5.13 to 5.15, the unrecorded tunnel closure was found to be 25 percent of the maximum tunnel closure and occurred within 3.25 percent of the time taken for the maximum tunnel closure to take place (Fig.5.15). Similar trends were noticed for most of the remaining cases of tunnel closure and support pressure also. The high ratio of the unrecorded data as a percentage of the maximum data value occurring within a short time after excavation, underlines the importance of estimating these missing data, without which the tunnel closures and the support pressures are likely to be substantially underestimated.

Another important aspect of the unrecorded data is their influence on the observed support reaction curve and, therefore, on the point of intersection of the ground reaction and the suopport reaction curves. This is shown in Fig.5.16. It is often seen that the dates of excavation, support installation, and first observation are different. The correct coordinates of the point of intersection 'C', as is clear from Fig.5.16, are XDOE and XDOSI, where XDOE is the final closure extrapolated to the date of excavation, and XDOSI is the final support pressure extrapolated to the date of support installation. This is because while the ground reaction curve starts at point 'A' immediately after excavation (or even before the excavation; according to Daeman, 1971, some tunnel closure takes place ahead of the face),
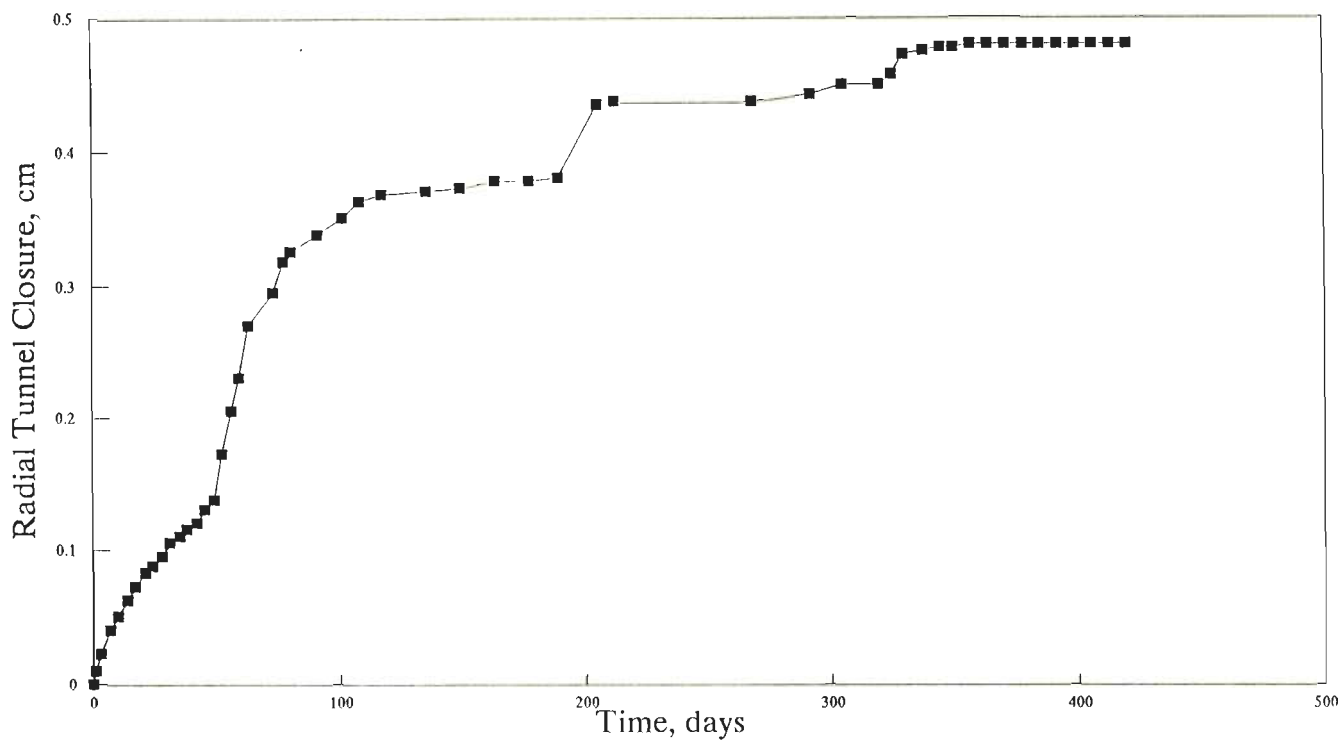
Fig.5.13 – Radial Tunnel Closure Plotted with Time from Date of First Observation Onwards at Ch.1568.75m (from Outlet) in Maneri Bhali Stage–II Tunnel
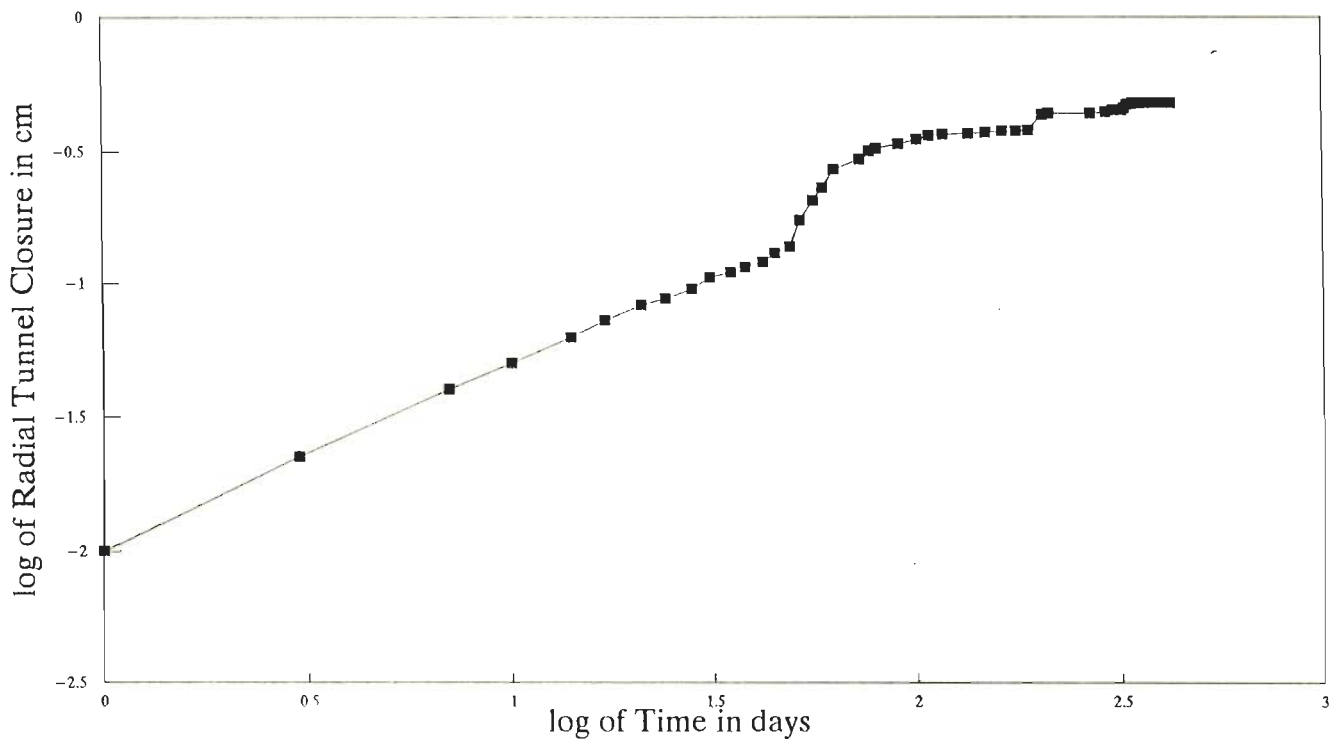


Fig.5.14 – Radial Tunnel Closure Plotted with Time on log–log Scale at Ch.1568.75m (from Outlet) in Maneri Bhali Stage–II Tunnel
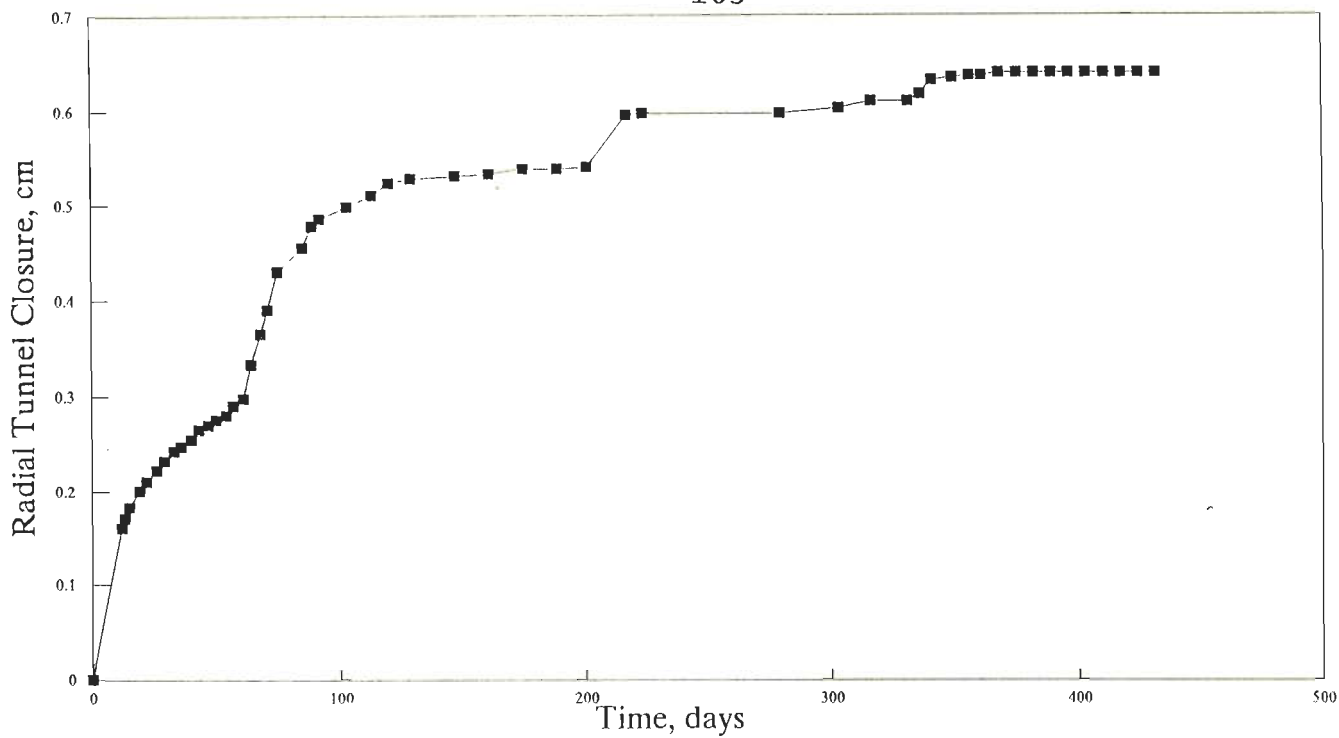
Fig.5.15 – Radial Tunnel Closure Extrapolated to Date of Excavation at Ch.1568.75m (from Outlet) in Maneri Bhali Stage–II Tunnel

Table 5.3 – Extrapolation of Radial Tunnel Closure to Date of Excavation at Ch.1568.75m (from Outlet) in Maneri Bhali Stage-II Tunnel

| Date | Original Data* | | Extrapolated Data | |
|------|------|------|------|------|
| | No.of days | Radial Tunnel Closure, cm | No.of Days | Radial Tunnel Closure, cm |
| 23-4-86[+] | -12 | -0.16 | 0 | 0 |
| 5-5-86[■] | 0 | 0 | 12 | 0.16 |
| 6-5-86 | 1 | 0.01 | 13 | 0.17 |
| 8-5-86 | 3 | 0.0225 | 15 | 0.1825 |
| 12-5-86 | 7 | 0.04 | 19 | 0.2 |
| 15-5-86 | 10 | 0.05 | 22 | 0.21 |
| 19-5-86 | 14 | 0.0625 | 26 | 0.2225 |
| 22-5-86 | 17 | 0.0725 | 29 | 0.2325 |
| 26-5-86 | 21 | 0.0825 | 33 | 0.2425 |
| – | – | – | – | – |
| – | – | – | – | – |
| – | – | – | – | – |
| 4-5-87 | 357 | 0.48 | 369 | 0.64 |
| 22-6-87 | 406 | 0.48 | 418 | 0.64 |
| 29-6-87 | 413 | 0.48 | 425 | 0.64 |
| 6-7-87 | 420 | 0.48 | 432 | 0.64 |

* First row contains data extrapolated to date of excavation
+ Date of excavation
■ Date of first observation

DOE — DATE OF EXCAVATION

DOSI — DATE OF SUPPORT INSTALLATION

X DOE — FINAL DATA VALUE AFTER EXTRAPOLATION
TO DATE OF EXCAVATION

X DOSI — FINAL DATA VALUE AFTER EXTRAPOLATION TO
DATE OF SUPPORT INSTALLATION

UX — FINAL DATA VALUE OF UNEXTRAPOLATED DATA

GRC — GROUND REACTION CURVE

SRC — SUPPORT REACTION CURVE

Radial Tunnel Closure ⟶
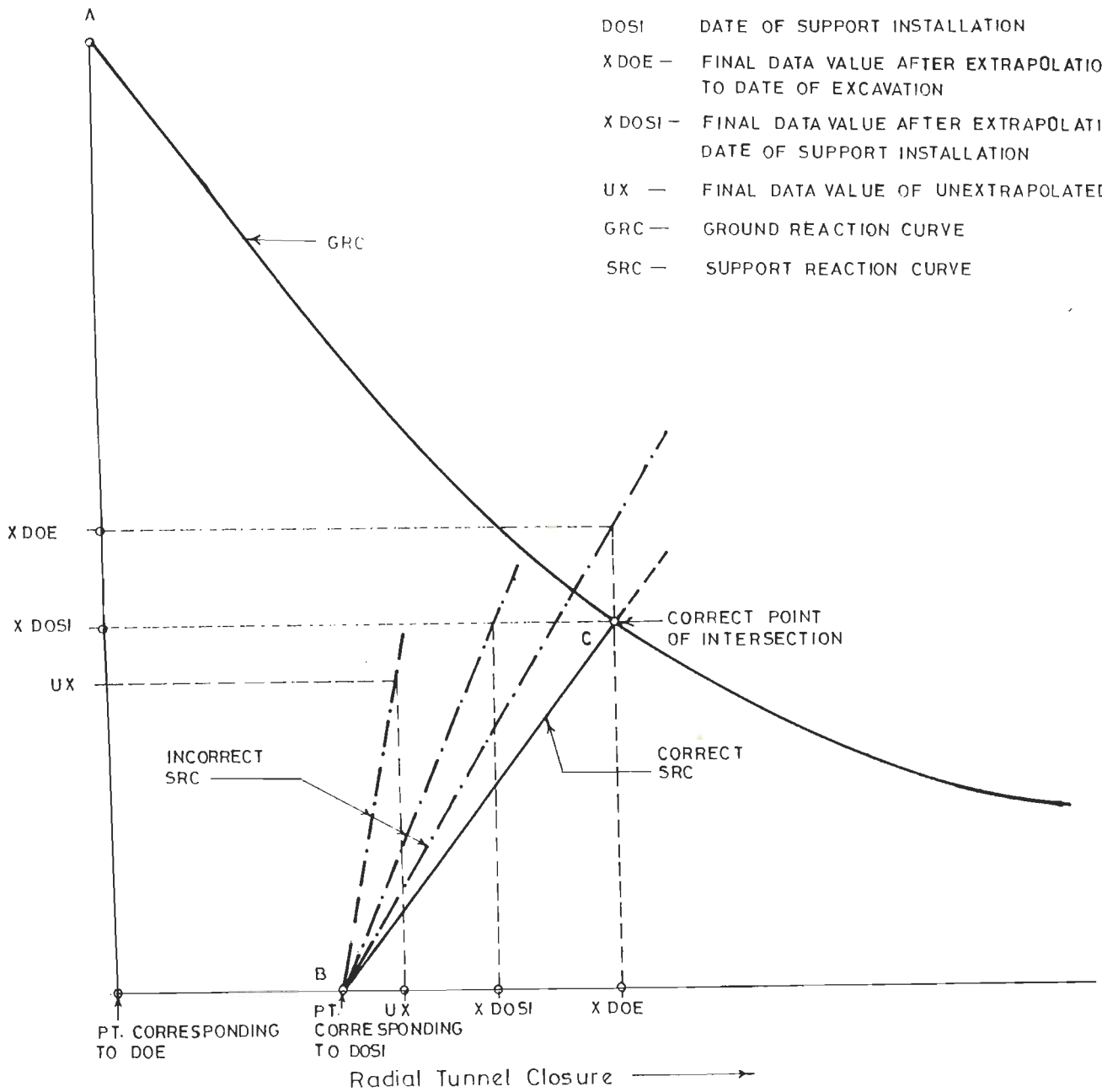
Fig.5.16 — Influence Of Unrecorded Data on Support Reaction Curve And Point of Intersection

the support reaction curve comes into picture only after the supports are installed (denoted by point 'B'). It would, therefore, be incorrect to extrapolate both the support pressure and the tunnel closure to the date of excavation to obtain the observed support reaction curve. Similarly, extrapolation of both the support pressure and the tunnel closure to the date of support installation would be incorrect. The support reaction curve obtained by using the 'unextrapolated' or, only the recorded data, (i.e., without considering the unrecorded observations) is also incorrect in the same way.

# CHAPTER 6

# CHAPTER 6

## DETERMINATION OF GROUND REACTION CURVE

### 6.1 GENERAL

Based on the analysis of the field data obtained from several Indian tunnels (Tables 5.1 and 5.2), an approach has been proposed in this chapter for determination of the ground reaction (response) curve for different ground conditions. Empirical correlations have also been suggested for prediction of the ground condition.

### 6.2 PREDICTION OF GROUND CONDITION

#### 6.2.1 Ground Conditions

Before performing the rock mass-tunnel support interaction analysis, it is important to know the ground condition in advance, since the ground behaviour and, consequently, the approach for determination of the ground reaction curve differs according to the ground condition.   In the following paragraphs, an approach has been proposed for prediction of the following three tunnelling conditions:

(i)   Self-supporting condition,

(ii) elastic ground condition, and

(iii) squeezing ground condition.

Out of these tunnelling conditions, the first two pertain to the elastic ground behaviour, whereas the third represents the elasto-plastic ground behaviour.   The difference between the

first two conditions is that in the self supporting condition, the tunnel does not require any support and attains stability after excavation with little closure. In the elastic ground condition, however, the tunnel attains stability with formation of chimney in the roof if no supports are installed. In the squeezing ground condition, failure of rock mass takes place alround the tunnel opening and even the tunnel walls tend to collapse if left unsupported.

### 6.2.2 Ground Conditions and Rock Mass - Tunnel Support Interaction

The above three conditions may be explained with the help of the rock mass-tunnel support interaction concept illustrated in Art.1.2. Fig.6.1 shows ground reaction curves for all the three conditions, and support reaction curves for the second and the third condition. It may be seen that in the case of the self-supporting tunnel, the ground reaction curve drops to $p_i=0$ (denoting stability) and the tunnel roof closure is less than the permissible closure. In the case of the elastic ground condition, however, the ground reaction curve would have dropped to a low value of support pressure only after attaining higher than the permissible closure if no supports were installed. To keep the tunnel closure within the permissible value, denoted by point C, the tunnel requires supports so as to achieve the point of intersection of the ground reaction and the support reaction curves at point F. Without support, the tunnel roof is, however, likely to collapse after the stand-up time is over. In the case of the squeezing ground condition, either a collapse or excessive

GRC - Ground Reaction
Curve

SRC - Support Reaction
Curve

SQ - Squeezing Ground
Condition

EL - Elastic Ground
Condition

SS - Self-supporting
Condition

$p_o$ - Insitu Stress
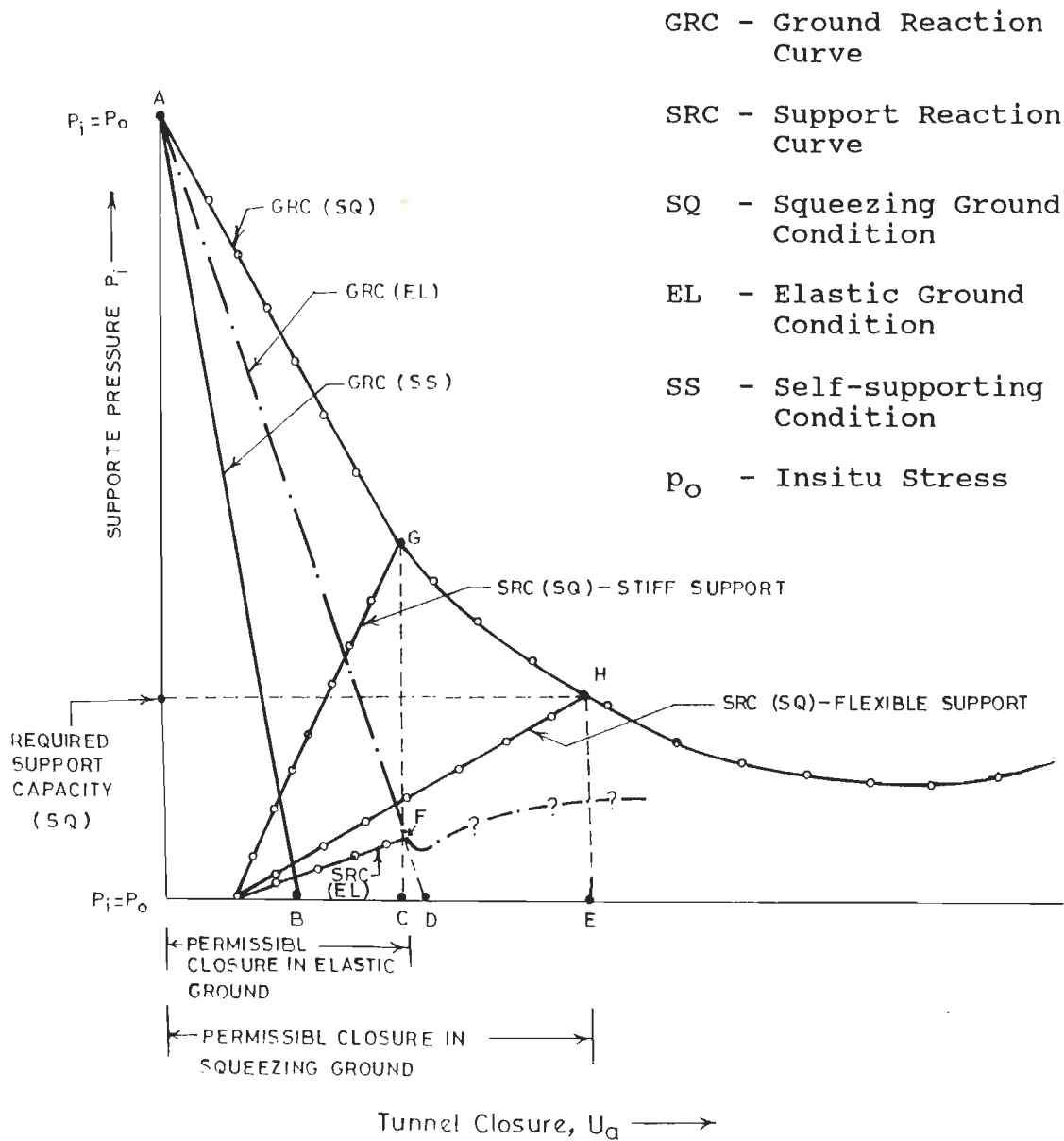
Fig.6.1 - Ground Reaction and Support Reaction Curves for
the Three Tunnelling Conditions

tunnel closure will take place. In this case, the supports are required to achieve the point of intersection of the ground reaction and the support reaction curves at point G. It may be seen that in this case, a stiffer support of higher capacity is required, than in the case of the elastic ground condition to keep the tunnel closure within the permissible limit. Since, the supports of such high capacity will be uneconomical, it is preferable to overexcavate the tunnel to increase the limit of the permissible closure (denoted by point E) and provide flexible supports in order to achieve the point of intersection at H and bring down the required support capacity.

### 6.2.3 Correlations for Ground Conditions

The data obtained from several Indian tunnels, both in squeezing and non-squeezing (elastic) ground conditions, and from some of the case-histories reported by Barton et al. (1974), were analysed. The analysis is presented in Fig.6.2 in the form of a log-log plot between Barton's Rock Mass Quality, $Q$, and $H(B-B_s)^{0.1}$, $H$ being the height of overburden in m, $B$ the tunnel span in m, and $B_s$ the self-supporting span in m given by Eq. 6.1a (Barton et al., 1974):

$$B_s = 2(ESR)Q^{0.4} \qquad (6.1a)$$

where, ESR is the excavation support ratio and is discussed in Art.3.7 . For tunnels, Barton et al. (1974) have suggested the value of ESR as 1.6. For tunnels, Eq.6.1 is, therefore, expressed as:

$$B_s = 3.2\ Q^{0.4} \qquad (6.1b)$$

In Fig.6.2, the points pertaining to the squeezing cases may be clearly separated from those belonging to the non-squeezing (elastic) cases by an inclined line. The equation of this line is given by:

$$H(B-B_s)^{0.1} = 483 \; Q^{1/3} \tag{6.2}$$

Therefore, for squeezing to occur, the left hand side of Eq.6.2 should be greater than the right hand side. Occurrance of a particular tunnelling condition may, therefore, be predicted by the following empirical correlations:

(i) $B-B_s < 0$       (for self-supporting condition)   (6.3)

(ii) $H(B-B_s)^{0.1} < 483 \; Q^{1/3}$ (for elastic ground condition)   (6.4)

(iii) $H(B-B_s)^{0.1} > 483 \; Q^{1/3}$ (for squeezing ground or       (6.5)
                                                rock burst condition)

In brittle, massive rocks, rock burst may take place instead of squeezing as predicted from Eq.6.5.

**Theoretical criterion for squeezing ground condition**

It may be mentioned here that theoretically the squeezing conditions around a tunnel opening are encountered if,

$$\sigma_\theta > q_c \tag{6.6a}$$

where $\sigma_\theta$ is the tangential stress and $q_c$ is the uniaxial compressive strength of the rock mass. Equation 6.6a may be written as follows for a circular tunnel under hydrostatic stress field:

$$2p_o > q_c \tag{6.6b}$$

where, $p_o$ is the magnitude of insitu stress.
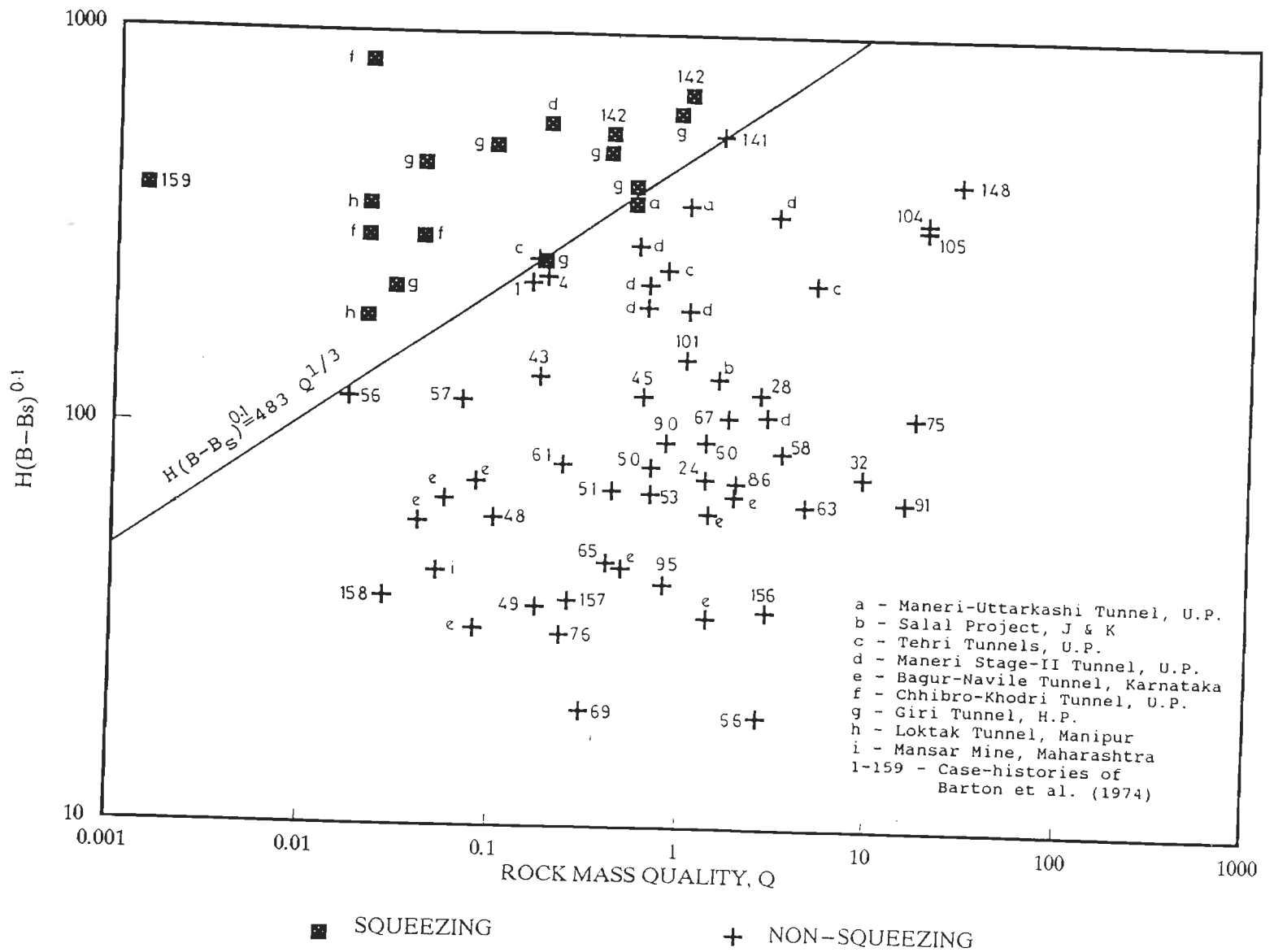
Fig.6.2 - Correlation for Prediction of Ground Condition

The figure is a scatter plot with the vertical axis labeled $H(B-B_s)^{0.1}$ ranging from 10 to 1000, and the horizontal axis labeled ROCK MASS QUALITY, Q ranging from 0.001 to 1000. A diagonal line labeled $H(B-B_s)^{0.1} = 483\ Q^{1/3}$ separates squeezing from non-squeezing conditions.

Legend:
a – Maneri-Uttarkashi Tunnel, U.P.
b – Salal Project, J & K
c – Tehri Tunnels, U.P.
d – Maneri Stage-II Tunnel, U.P.
e – Bagur-Navile Tunnel, Karnataka
f – Chhibro-Khodri Tunnel, U.P.
g – Giri Tunnel, H.P.
h – Loktak Tunnel, Manipur
i – Mansar Mine, Maharashtra
1-159 – Case-histories of
        Barton et al. (1974)

■ SQUEEZING      + NON-SQUEEZING

173

Use of the theoretical criterion for prediction of squeezing ground condition, given by Eq.6.6b, poses practical difficulties as the measurement of the insitu stress and the insitu compressive strength of rock mass is both expensive and time-consuming in developing countries. This problem can be overcome by using the empirical criterion for prediction of squeezing given by Eq.6.5.

## 6.2.4 The Design Chart

The results of the above analysis are presented in the form of a design chart in Fig.6.3 on log-log scale. It is clear from this chart that once the values of H and Q are known, the designer can pick up the critical value of B below which squeezing is not likely to occur. For doing so, the first step is to pick up the critical value of $(B-B_S)$ for given values of H and Q from the upper part of the design chart, which is based on Eq.6.2. The next step is to select the value of $B_S$ for this Q value from the lower part of the chart, which represents Eq.6.1b, and add this to the critical value of $(B-B_S)$ to arrive at the critical value of B.

Example

To illustrate the use of the chart, let Q be equal to 0.1, a value which fairly represents the average Q values in squeezing ground conditions, as observed in the lower Himalaya. It may be seen that the vertical line representing Q=0.1, meets the thick inclined line pertaining to H=200m at a value of $(B-B_S)$=3.13m. The values of $B_S$, which may be obtained from the lower part of

the chart, is 1.27m for this value of Q. Thus, a tunnel with a span $[=(B-B_S)+B_S]$ smaller than 4.4m (3.13m+1.27m) is not likely to experience squeezing under an overburden of 200m with Q equal to 0.1.

**Practical applications**

The above correlations have the following important practical applications:

(i) For performing the rock mass-tunnel support interaction analysis,it is necessary to know the ground condition as the approach for prediction of ground reaction curves is different in non-squeezing and squeezing cases.The ground conditions may be predicted approximately using Eqs.6.3 to 6.5. Thus, classifying a rock mass as a squeezing rock is not correct. Any rock mass may turn into squeezing rock condition at higher overburden.

For prediction of the squeezing ground condition, using the proposed correlation, there is no need to perform the expensive and time-consuming field measurements which are otherwise required if the theoretical criterion, given by Eq.6.6b, for prediction of the squeezing ground conditions is employed.

(ii) In case a tunnel is likely to experience squeezing ground condition, the tunnel alignment may possibly be changed to obtain a better rock mass quality (Q) or reduced overburden, or both, to avoid squeezing in order to eliminate/reduce the support problems. Similarly, an elastic ground condition may

Fig.6.3 - Design Chart for Selecting Tunnel Size for Given Tunnel Depth and Rock Mass Quality to Achieve Favourable Ground Condition

176
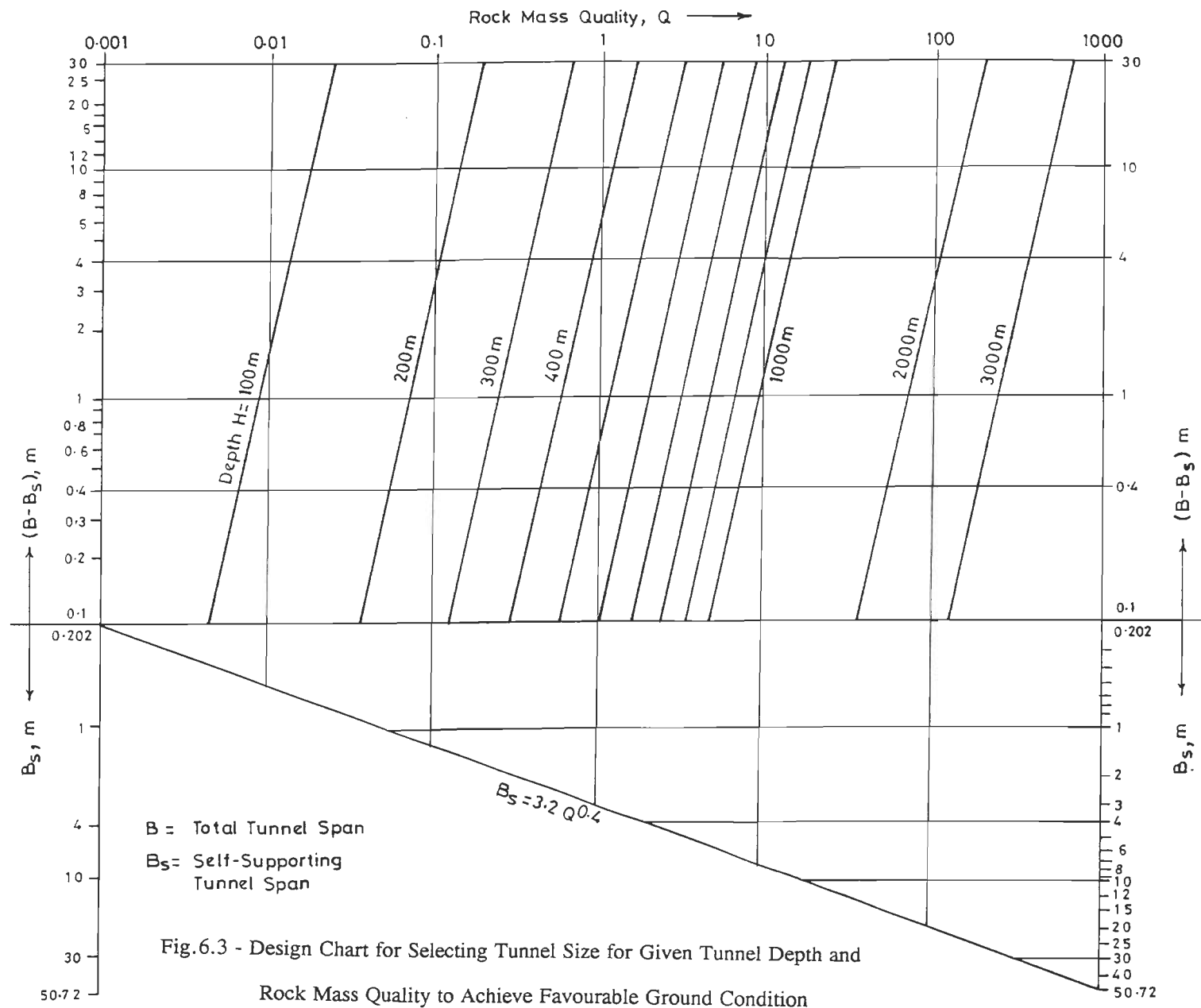
possibly be changed to the self-supporting condition by obtaining a better rock mass quality (Q) as a result of the changed tunnel alignment.

(iii) Alternatively, two or three smaller tunnels may be chosen instead of a larger tunnel to avoid squeezing ground conditions, thereby reducing the support problems and the construction time. **This was done in Chhibro-Khodri tunnel in Uttar Pradesh after it became extremely difficult to drive a 9m diameter tunnel through squeezing ground condition.**

Example

As an example, let us consider Q equal to 1 and the height of overburden equal to 400m. It is clear from Fig.6.3 that for Q=1 and H=400m, a tunnel of 9.8m span will encounter squeezing conditions. If, however, two smaller tunnels of 7m span each are constructed instead of a single tunnel of 9.8m span, none of these smaller tunnels will have squeezing problem.

Even when it is not possible to go in for two smaller tunnels due to design considerations, the information about the possibility of occurrence of squeezing will be helpful in making advance planning for tackling the increased construction problems and support requirements.

(iv) The above analysis shows why the observations in a pilot tunnel cannot represent the ground conditions in the main tunnel, which is not only bigger in size but also passes

under much greater height of overburden than the pilot tunnel.

Example

Let us take, for instance, the Q value of 0.1 which, as stated earlier, may be considered as representing the average Q value in squeezing ground condition in the lower Himalaya, and the height of overburden of 200m. It may be seen in Fig.6.3 that a tunnel of less than 4.4m span is not likely to experience squeezing ground condition, whereas a larger tunnel may encounter squeezing. A pilot tunnel, excavated for the purpose of observing the rock mass behaviour, is normally not more than 2m wide. Therefore, a pilot tunnel constructed in a rock mass with Q=0.1 and H=200m will not encounter squeezing. The main tunnel of a span of more than 4.4m will, however, come across squeezing ground condition. It is, therefore, inappropriate to predict the ground condition, support pressure, or tunnel closure for the main tunnel on the basis of observations made in the pilot tunnel. There have been instances in the lower Himalaya where elastic ground conditions were observed in the exploratory drifts and pilot tunnels, whereas the main tunnel experienced squeezing ground condition and much larger tunnel deformations than those observed in the pilot tunnel.

## 6.3 DETERMINATION OF GROUND REACTION CURVE

The next step is the determination of the ground reaction curve for the predicted ground condition.

## 6.3.1 Ground Reaction Curve for Self-supporting and Non-squeezing Ground Conditions

The ground reaction curve for the elastic ground condition (representing both the self-supporting and the non-squeezing conditions) may be obtained from the following equation, based on the theory of elasticity, for a circular opening driven through a homogeneous, isotropic and linearly elastic rock mass under hydrostatic stress field:

$$u_a/a = (1+\nu)(p_o-p_i)/E_d \qquad (6.7)$$

where,

$u_a$ = radial tunnel closure,

a = radius of tunnel opening,

$\nu$ = Poisson's ratio of rock mass,

$E_d$ = modulus of deformation of rock mass,

$p_o$ = in-situ stress magnitude, and

$p_i$ = required support pressure (short-term).

The ground reaction curve may be obtained by plotting $p_i/p_o$ against $u_a/a$. It may be seen from Eq.6.7 that the ground reaction curve is a straight line relationship for elastic ground condition.

### 6.3.1.1 Empirical correlation for determination of modulus of deformation of rock mass

The modulus of deformation in Eq.6.7 is normally obtained from expensive and time consuming uniaxial jacking tests whose results often have a large scatter. Therefore, the following simple empirical correlation has been obtained to determine the

modulus of deformation of dry rock masses, $E_d$:

$$E_d = f.10^{(RMR-20)/38} \quad GPa \qquad (6.8)$$

where,

RMR = Bieniawski's rock mass rating, and
f   = correction factor for the effect of depth.

The above correlation is based on the back analysis of the modulus of deformation from the data of support pressures and tunnel closures observed at several tunnel sections in elastic ground condition with RMR values ranging from 31 to 68. The back analysis was performed by using Eq.6.7 for which the observed values of $u_a$ and $p_i$, and assumed value of $\nu$ equal to 0.25 were used for different tunnel sections. Assumming a hydrostatic stress field, $p_o$ was considered equal to $\gamma H$ and its values for different tunnel sections were accordingly obtained. The back-analysed modulus of elasticity is plotted against RMR in Fig.6.4. The best-fit curve, represented by Eq.6.8, has a correlation coefficient of 91 percent.

Mehrotra (1992) also obtained nearly the same correlation with f=1 from uniaxial jacking tests on dry rock masses. Thus, one may use Eq.6.8 with confidence in poor rock conditions also.

Empirical correlations have been proposed earlier by Bieniawski (1978) and Serafim and Pereira (1983) between modulus of deformation, $E_d$ of the rock mass and RMR (Eqs.3.2 and 3.3 and Fig.3.3; Chapter 3). It is interesting to note the similarity of trends between the proposed $E_d$ versus RMR curve (Fig.6.4) and that obtained by Serafim and Pereira, (1983).

## 6.3.1.2 Effect of depth on modulus of elasticity of rock mass

The back analysed values of the modulus of deformation indicated its dependence on the height of overburden. To account for the effect of the height of overburden (or depth of tunnel), a correction factor, f, was introduced in Eq.6.8. the correction factor, $f(=E_d/10^{(RMR-20)/38})$ is plotted against the height of overburden, H in Fig.6.5, from which the following correlation has been obtained:

$$f = 0.3 \ H^{\alpha} \tag{6.9}$$

where $\alpha$ = 0.16 to 0.3, and H > 50m.

Eq.6.8 may, therefore, be written as:

$$E_d = 0.3 \ H^{\alpha}.10^{(RMR-20)/38} \ GPa \tag{6.10}$$

where, H is in meters.

**Discussions on effect of depth on modulus of deformation**

The case-histories, considered to arrive at Eq.6.10, pertain to poor to good rock mass quality (RMR = 31 to 68). It is quite likely that for rock masses having a higher RMR value than 68 (i.e., good to very good rock mass), the value of $\alpha$ is lower than 0.16, and for rock masses with a lesser RMR value than 31 (i.e., very poor to poor rock mass), the value of $\alpha$ is greater than 0.3. This argument originates from a growing evidence, mainly based on the laboratory experiments (Kulhawy, 1975; Santarelli and Brown, 1987; Brown,Bray and Santarelli,1989;Duncan Fama and Brown,1989), to suggest that - (a) the elasticity modulus increases with the confining pressure and has a relationship similar to Eq.6.9,and

(b) this pressure dependency, reflected in the value of $\alpha$, of the modulus of elasticity is more pronounced in the weaker rock materials and is almost absent in strong, brittle rock materials. Kulhawy (1975), for instance, proposed the following expression for modulus of elasticity of rock material, $E_r$, after examining a wide range of data:

$$E_r = E_o \sigma_3^{\alpha} \qquad (6.11)$$

where $\sigma_3$ is the minor principal stress, $E_o$ is the Young's modulus measured in a uniaxial compression test ($\sigma_3 = o$). The value of $\alpha$ varies between 0 and 1.

A similar expression was obtained by Santarelli and Brown (1987) on the basis of triaxial compression tests on hollow cylinders of Carboniferous sandstone. This is given by:

$$E_r = 15.08 \, \sigma_3^{0.195} \quad GPa \qquad (6.12)$$

where $\sigma_3$ is in MPa.

Other investigators have also obtained similar or slightly different expressions. The increase with confining pressure of the modulus of elasticity is, therefore, a well documented phenomenon, largely based on the laboratory tests. It is interesting, therefore, to observe the occurrance of this phenomenon in the field as indicated by Eq.6.10, which is based on the actual support pressure and tunnel closure measurements in tunnels.

The form of Eq.6.10 is such that $E_d \rightarrow 0$ as $H \rightarrow 0$, making the correlation inapplicable to situations where the height of overburden is less than say 50. Such situations, however, are
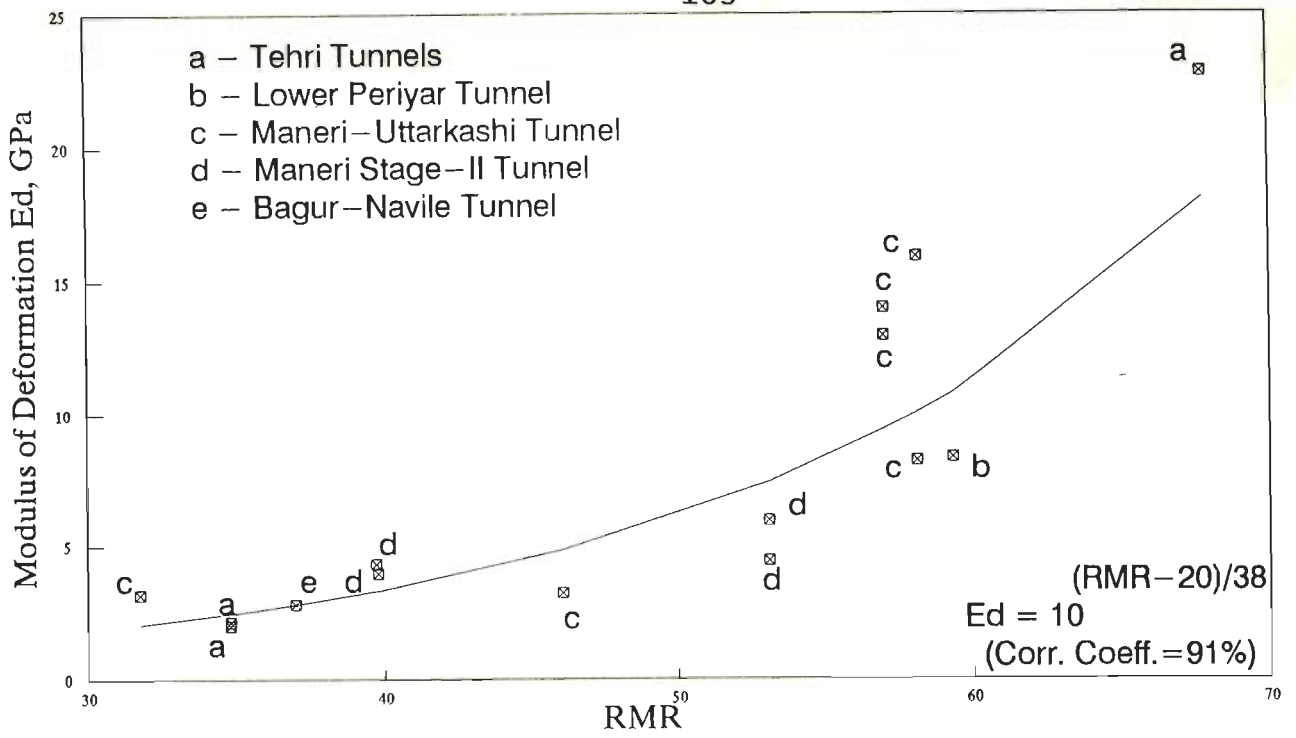
Fig.6.4 – Correlation Between RMR and Modulus of Deformation of Rock Mass
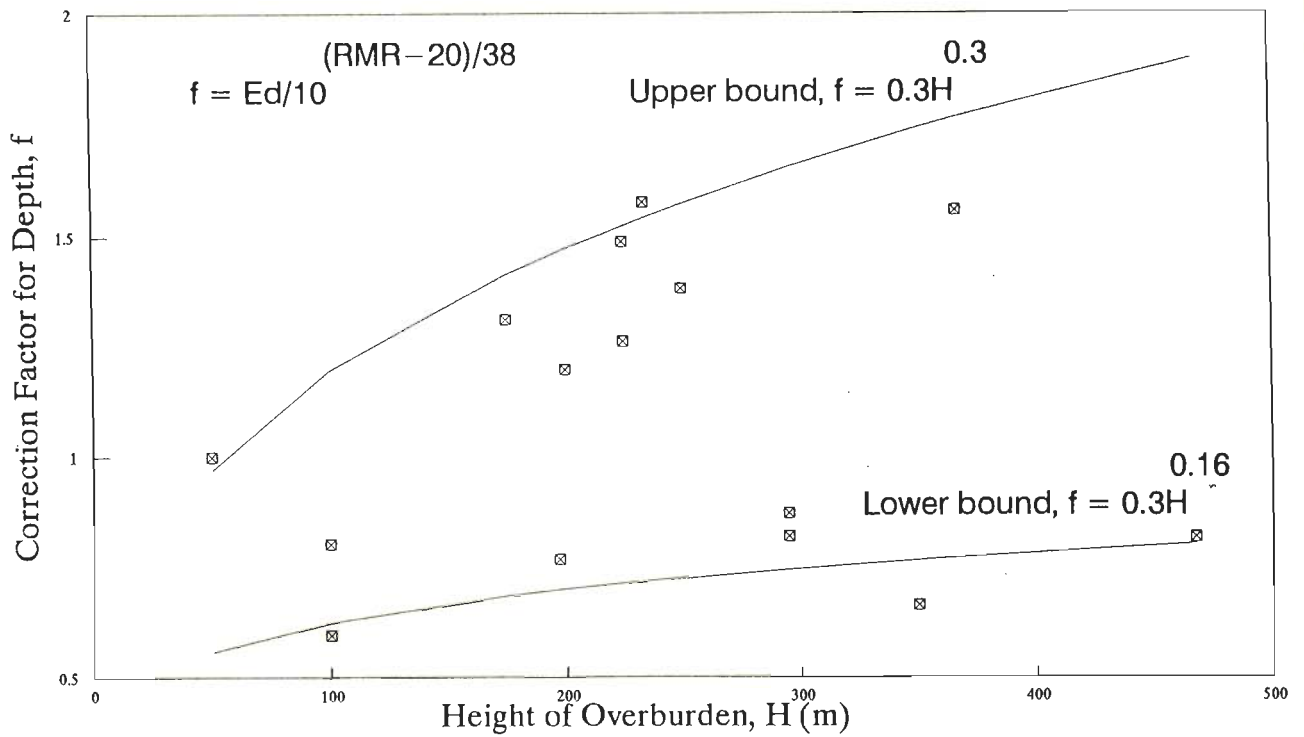


Fig.6.5 – Correction factor for Effect of Depth on Modulus of Deformation of Rock Mass

irrelevent in the context of the underground openings.

## 6.3.1.3 Correlation between RMR and modified Q

**Existing correlation between RMR and Q**

Application of Eq.6.10 requires the determination of RMR at site. If, however, one prefers to use the Q-system of Barton et al. (1974), one can obtain RMR from Q using the following empirical correlation, suggested by Bieniawski (1976):

$$RMR = 9 \ln Q + 44 \qquad\qquad (6.13)$$

The above correlation was further substantiated by Jethwa et al., 1982 (also reported by Bieniawski, 1989), with 12 Indian case-histories.

**Need for modifying Q**

It has been experienced that while estimating Q, determination of the Stress Reduction Factor (SRF) poses practical difficulties. This is because for 'competent and squeezing rock masses', the determination of SRF is based on $\sigma_1$, $\sigma_3$, $\sigma_c$ and $\sigma_t$ values (where $\sigma_1$ and $\sigma_3$ are major and minor principal stresses, $\sigma_c$ is unconfined compressive strength, and $\sigma_t$ is tensile strength based on point load test), and the suggested SRF values have large ranges (Barton et al., 1974). For the case of 'weakness zones intersecting excavation' also, a large range of reduction factor (for SRF) has been suggested if the shear zones only influence but do not intersect the excavation (Barton et al., 1974). To reduce this uncertainity, a modified Q is

proposed by eliminating SRF (or by keeping the value of SRF equal to 1).

## Proposed correlation

Based on 40 Indian case-histories and 27 NGI (Norwegian Geotechnial Institute) case-histories (reported by Barton et al., 1974 and Bieniawski, 1989), modified Q, i.e., $Q_m$ values have been plotted against RMR in Fig.6.6 and the following correlation has been obtained:

$$RMR = 10 \ln Qm + 36 \tag{6.14}$$

where, Qm = modified Q (with SRF=1).

This correlation has been found to have a better correlation coefficient of 91 percent.

## 6.3.2 Ground Reaction Curve for Squeezing Ground Condition

The squeezing ground condition in a tunnel is represented by the plastic failure of the rock mass around the tunnel periphery. Upon failure, an initially elastic rock mass enters the plastic stage under high stresses and the rock mass behaviour may, therefore, be called elasto-plastic. Theoretically, squeezing conditions are encountered around a tunnel when the tangential stress, which has the maximum value at the tunnel periphery, exceeds the uniaxial compressive strength of the rock mass. As a result of the rock mass failure, a broken zone (or, plastic zone) is formed around the tunnel periphery upto some distance, beyond which the rock mass exists in elastic state (Fig.6.7).

Fig.6.6 - Correlation Between RMR and Modified Q (with SRF=1)

$RMR = 10 \ln Q_m + 36$
(Corr. Coeff.=91%)
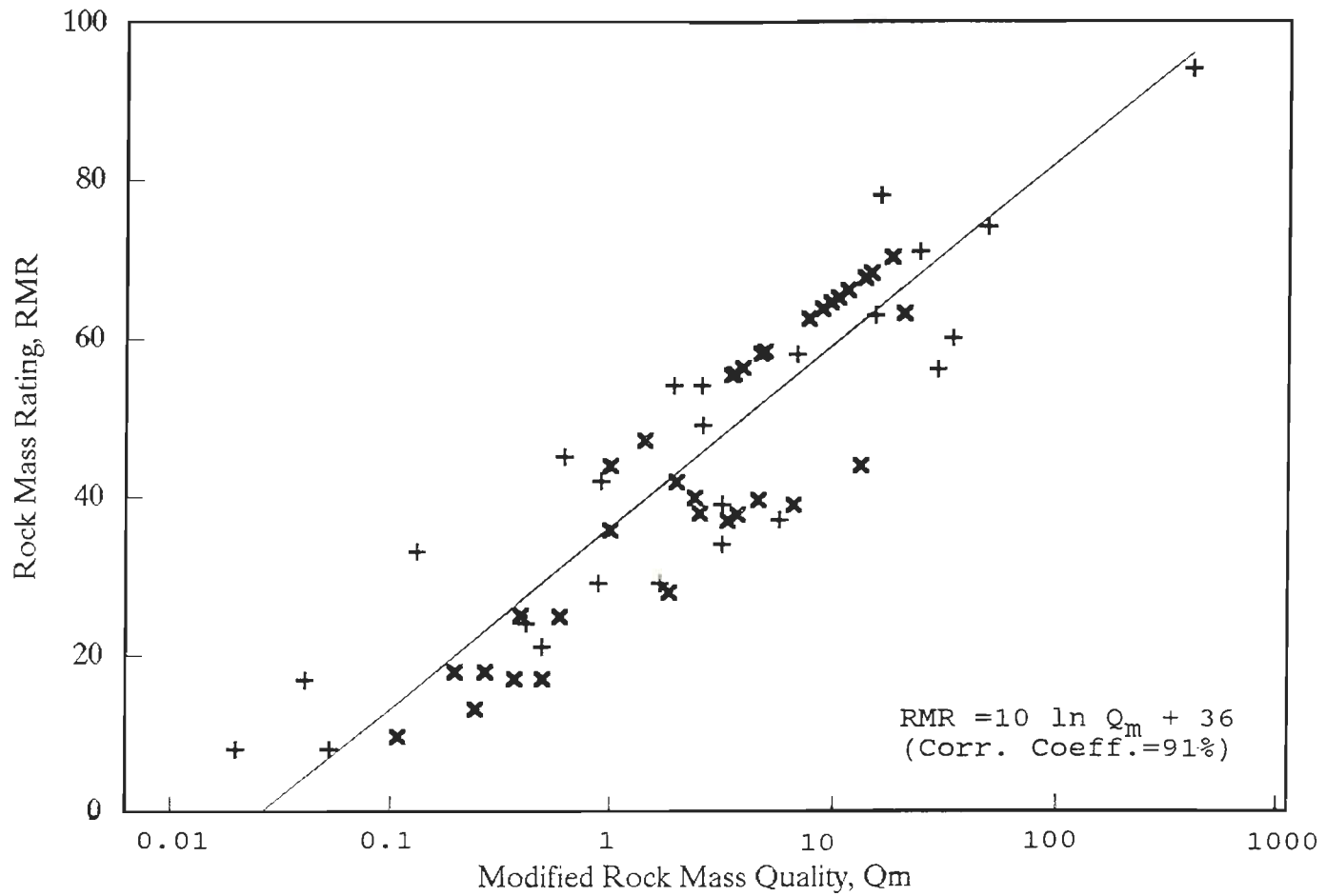
x Indian Case–histories    + NGI Case–histories
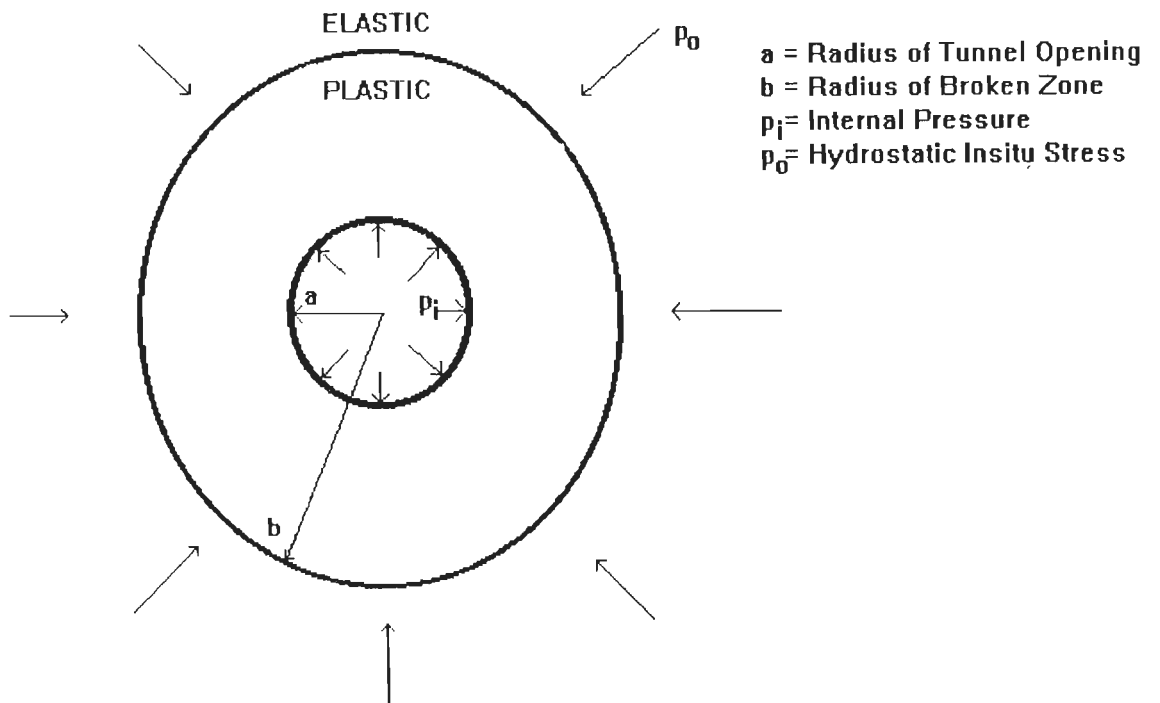
Fig.6.7 - Elastic and Plastic (Broken) Zones around a Tunnel under Hydrostatic Insitu Stress Field

As pointed out in Art.2.2 of Chapter 2, several authors have presented elasto-plastic analyses of tunnels (using either elastic-perfectly plastic or elastic-brittle-plastic or elastic-strain softening stress-strain model; Fig.2.1) to obtain solutions for stresses and displacements. One such elasto-plastic analysis was carried out by Daemen (1975). In the present study, a semi-empirical approach based on Daemen's analysis, has been proposed.

## 6.3.2.1 Basic assumptions in Daemen's analysis

Daemen's analysis (1975) is based on the following basic assumptions:

(i)    The tunnel is circular in shape. The length of the tunnel is such that the problem may be treated two-dimensionally. The tunnel section under consideration is far away from the tunnel face.

(ii)   The insitu stress field is hydrostatic and equal to the cover pressure.

(iii)  The rock mass is dry, homogeneous, isotropic and linear elastic and the elastic modulus does not depend on the confining pressure.

(iv)   The rock mass around the opening fails when the tangential stress exceeds its uniaxial compressive strength, and a homogeneous, isotropic cylindrical broken zone develops.

(v)    The rock mass follows the peak and residual Mohr-Coulomb

failure criteria.

(vi) The tunnel supports are in intimate contact with the failed rock mass.

(vii)The gravity is acting radially inwards in all the directions. Thus, the problem is treated as axisymmetric.

## 6.3.2.2 Daemen's equation for support pressure

Daemen (1975) proposed the following equation for short-term support pressure in circular tunnels under squeezing ground conditions:

$$p_i = [0.5(\sigma_{re} + \sigma_{\theta e})(1-\sin \phi_p) - c_p \cos \phi_p + c_r \cot \phi_r]M_\phi \qquad (6.15)$$
$$-c_r \cot \phi_r \pm \gamma(b-a)M_\gamma$$

in which $\sigma_{re}$ and $\sigma_{\theta e}$ are the radial and tangential stresses respectively on the elastic side of the elastic-plastic interface. Other terms are the same as in Eq.2.11. Daemen substituted $2p_o$ for the term $(\sigma_{re} + \sigma_{\theta e})$ for the case of hydrostatic insitu stress field, where $p_o$ is the insitu hydrostatic stress.

## 6.3.2.3 Daemen's equations for tunnel closure

Daemen (1975) assumed the rock mass to dilate (increase in volume) at failure and considered the following three variations of the volumetric expansion:

(i) Constant volume expansion throughout the broken zone,

(ii) volume change due to elastic relaxation of the broken zone

with the axial stress calculated from an elastic plane
strain assumption, and

(iii) volume change due to elastic relaxation of the broken zone
with the axial stress calculated from a plastic plane strain
assumption.

Daemen (1975) suggested Labasse's solution (1949) for the
first condition and derived expressions for the other two
conditions. The final expressions for radial tunnel closure (or,
tunnel-wall displacement), $u_a$, are given below as Eqs.6.16, 6.17,
and 6.18 respectively for the above three conditions:

(i) $\quad u_a = a - [a^2(1+e) - b^2 e - 2bu_b + u_b^2]^{1/2}$ $\qquad$ (6.16)

(ii) for $\sin \phi_r = 1/3$,

$$u_a = (b/a)u_b + \frac{(1+v)(1-2v)}{aE_d} [p_o(b^2-a^2) - p_i\{(b^3-a^3)/a\}$$

$$-3c_r \cos \phi_r \ b^2\{(b/a)-1\} \pm \tau\{(b^3-a^3)/3 - b^3\log(b/a)\}] \quad (6.17)$$

Similarly, expressions have been given by Daemen (1975) for
the conditions when $\sin \phi_r = o$ and $\sin \phi_r \neq o$, $\sin \phi_r \neq 1/3$.

(iii) for $\sin \phi_r = 1/3$,

$$u_a = (b/a)u_b + \frac{p_o(1-2v)(b^2-a^2)}{aE_d} - \frac{3 \ c_r \ \cos \phi_r(b-a)}{a^2E_d}$$

$$[(1-2v)b^2 + \frac{v(b^2+ab+a^2)}{9}] - \frac{1-2v+v/9}{aE_d}[p_i\{(b^3-a^3)/a\}$$

$$\mp \tau\{(b^3-a^3)/3 - b^3 \log(b/a)\}] \qquad (6.18)$$

Similarly, expressions have been given by Daemen (1975) for

the conditions when $\sin \phi_r = 0$ and $\sin \phi_r \neq 0$, $\sin \phi_r \neq 1/3$.

In the above equations,

a = radius of tunnel opening,

b = radius of broken zone,

e = coefficient of volumetric expansion for failed rock mass which is defined as the ratio of increase in volume of failed rock mass to its original volume,

$u_b$ = radial displacement of elastic-plastic boundary

$$= \frac{(1+\nu)p_0}{E_d} [p_0 \sin \phi_p + c_p \cos \phi_p] \qquad (6.19)$$

$p_0$ = insitu stress magnitude,

$E_d$ = modulus of deformation of rock mass,

$\phi_p$ = peak angle of internal friction of rock mass,

$c_p$ = peak cohesion of rock mass,

$\phi_r$ = residual angle of internal friction of rock mass,

$c_r$ = residual cohesion of rock mass,

$\nu$ = Poisson's ratio of rock mass, and

$\tau$ = unit weight of rock mass.

## 6.3.2.4 Determination of input parameters for Daemen's equations

The ground reaction curve may be obtained by Daemen's approach by calculating the values of support pressure, $p_i$, and radial tunnel closure, $u_a$, for different values of b/a ratio, using the equations given above (Eqs.6.15 to 6.19). The equations, however, contain several input parameters, some of which are difficult to determine. In particular, the modulus of deformation and the peak and residual values of cohesion and angle of internal friction of rock mass are required to be determined from expensive and time-consuming field tests. While a

correlation has already been proposed for determination of the modulus of deformation of the rock mass in this chapter (Eq.6.10), a semi-empirical relationship will now be proposed for determination of the value of the rock mass cohesion. That, however, is preceeded by a brief discussion on the existing correlation proposed by Bieniawski (1979).

## a) Bieniawski's approach for determination of the rock mass cohesion

A quick and easy way of estimating the rock mass cohesion was suggested by Bieniawski (1979) who related the Rock Mass Rating (RMR) with the cohesion and angle of internal friction of rock mass for rock slopes (Table 3.4, Chapter 3) based on the data compiled by Hoek and Bray (1977). The cohesion values, suggested by Bieniawski (1979), however, appear to be low for underground openings in the light of an apparant strength enhancement around the opening walls, experienced during laboratory tests on thick hollow cylinders by several investigators and during field observations. This is discussed later in the chapter.

## b) Proposed semi-empirical correlation for peak cohesion of rock mass

Daemen (1975) used the following constitutive equation for the unbroken rock mass at the periphery of the broken zone:

$$\sigma_{\theta e}(1-\sin \phi_p) = \sigma_{re}(1+\sin \phi_p) + 2c_p \cos \phi_p \qquad (6.20)$$

The following expression for $\sigma_{re}$ may be obtained from Eq.6.20:

$$\sigma_{re} = \frac{2p_o - q_{cr}}{1+K} \qquad (6.21)$$

where,

$q_{cr}$ = uniaxial compressive strength of rock mass in elastic zone,

= $2c_p \cos \phi_p / (1 - \sin \phi_p)$, and

$$K = \frac{1 + \sin \phi_p}{1 - \sin \phi_p}. \qquad (6.21a)$$

For squeezing to begin (or the rock mass to fail), $\sigma_{re}$ should be greater than zero. Therefore, at the instant when squeezing starts,

$$\sigma_{re} = o$$

or, from Eq.6.20, $\qquad p_o = (q_{cr}/2) \qquad (6.22)$

Now, from the empirical correlations (Eqs.6.4 and 6.5) for prediction of squeezing ground condition, it may be inferred that at the instant of the begining of squeezing,

$$H = \frac{483 \ Q^{1/3}}{(B-B_s)^{0.1}} \qquad (6.23)$$

Multiplying both sides of Eq.6.23 with $\gamma$ and substituting $\gamma H$ with $p_o$ for hydrostatic stress field,

$$p_o = \frac{483.\gamma.Q^{1/3}}{(B-B_s)^{0.1}} \qquad (6.24)$$

Since, Eqs.6.22 and 6.24 represent the same condition, these may be equated and the following expression for the mobilised cohesion, $c_{pm}$, obtained:

$$c_{pm} = \frac{483 \; \tau . Q^{1/3}}{(B-B_s)^{0.1}} \cdot \frac{(1-\sin \phi_p)}{\cos \phi_p} \qquad t/m^2 \qquad (6.25)$$

where, $\tau$ is in $t/m^3$

$\phi_p$ may be obtained from the block shear test or from RMR (Table 3.4), as suggested by Bieniawski (1979).

It may be recalled that the uniaxial compressive strength of rock core decreases with $d^{0.16}$ where d is the diameter of core (Hoek and Brown, 1980a). Similar size effect is also observed in Eq.6.25.

## c) Mobilised strength of rock mass around underground openings

Figure 6.8 shows a comparison between the mobilised cohesion, $c_{pm}$, and the cohesion, $c_p$, determined from Bieniawski's RMR, as well as that obtained by Mehrotra, for a tunnel of 9m diameter. The $c_p$ values given by Bieniawski (1979) are based on field test data on rock slopes compiled by Hoek and Bray (1977). Mehrotra (1992) obtained the shear strength parameters from block shear tests on dry rock mass blocks in the lower Himalayan region. The $c_{pm}/c_p$ ratio is plotted against RMR in Fig.6.9

It is clear from Fig.6.9 that there is definitely a need to account for a strength enhancement factor $(=c_{pm}/c_p)$, which increases with increasing RMR. The strength enhancement factor is recommended as 4 to 6 for practical application. This strength mobilisation around the underground openings, known as apparant strength enhancement, has been recorded by several investigators, such as, Hobbs (1966 b), Hoskins (1969), Daemen and Fairhurst

(1971), Santarelli and Brown (1987), Guenot (1989), and Fuenkajorn and Daemen (1992), during laboratory tests on thick-walled hollow cylinders. Daemen and Fairhurst (1971), for instance, found no indication of fracturing around the borehole when the external hydrostatic pressure applied to thick-walled hollow cylinders of Indiana limestone and concrete reached levels at which linear elastic analysis gives tangential stress at the borehole wall of at least four times the measured uniaxial compressive strength of the material. Final collapse occurred at even higher pressure. Guenot (1987) presented a survey of results of such laboratory tests on hollow cylinders conducted by ten authors on seven rock types. The ratio between the maximum (elastically) calculated compressive stress at which the failure occurs and the uniaxial compressive strength is typically about two. More recently, Fuenkajorn and Daemen (1992) obtained the following empirical equation from the biaxial borehole stability tests on cylindrical tuff samples :

$$\sigma_{\theta f} = 312.2 \exp(2.05\ \sigma_{H2}/\sigma_{H1}) \qquad \text{MPa} \qquad (6.26)$$

where,

$\sigma_{H2}, \sigma_{H1}$ = minimum and maximum applied boundary stresses, and

$\sigma_{\theta f}$     = tangential compressive stress at the borehole wall immediately before the fracture occurs

Fuenkajorn and Daemen (1992), however, acknowledged that Eq.6.26 might overestimate the rock mass strength around large boreholes due to the size effect and that the incorporation of this effect was not possible due to the lack of test data on large boreholes.
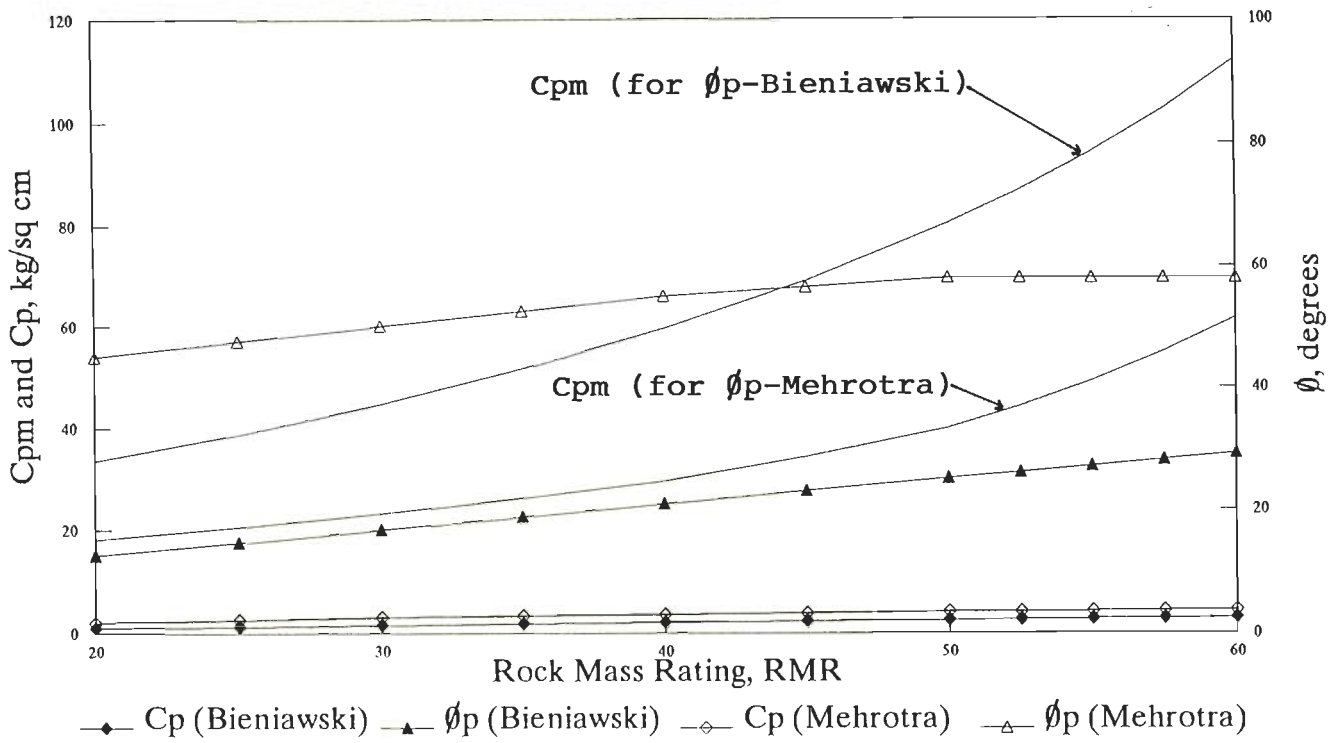
Fig.6.8 – Mobilised Cohesion (Eq.6.25) with respect
to RMR in a Tunnel of 9m Span
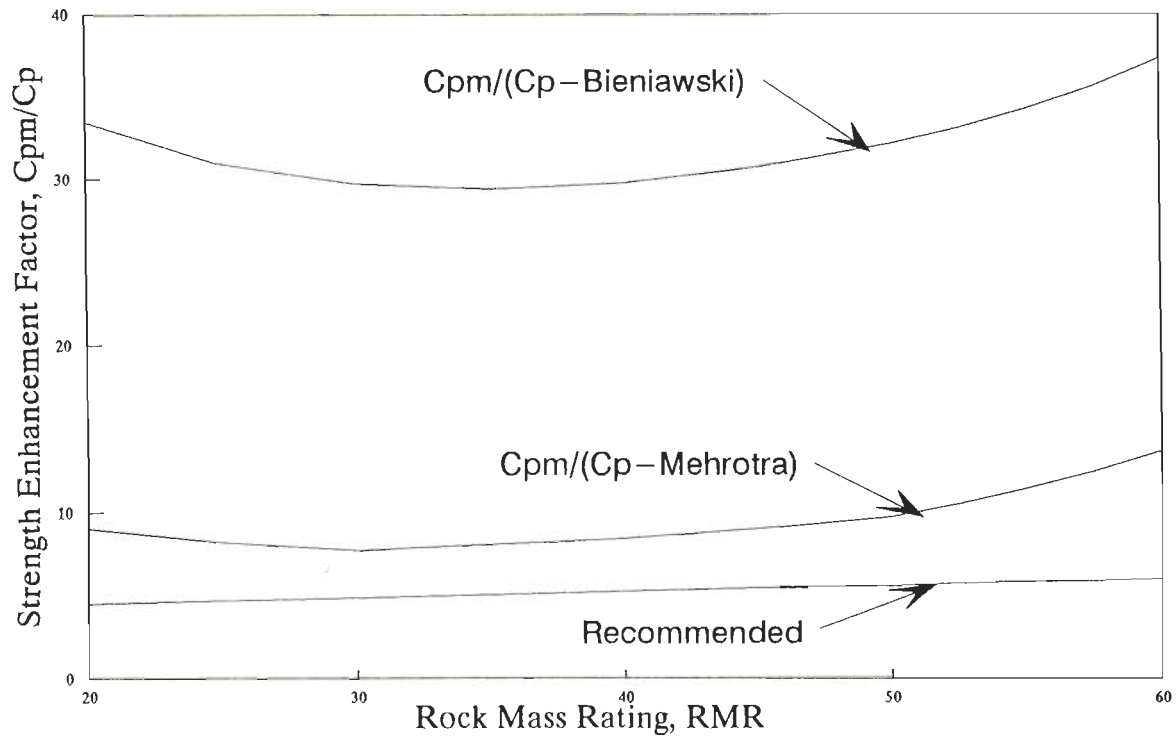


Fig.6.9 – Recommended Strength Enhancement Factor
for Cohesion Parameter from Block Shear Test

Eq.6.26 further suggests that the strength enhancement will be less in the case of non-hydrostatic insitu stress condition.

### d) Reasons for apparant strength enhancement around underground openings

The reason for the apparant strength enhancement is that the shear strength behaviour of the jointed rock mass is highly anisotropic (Hoek and Brown, 1980a). The RMR classification gives the lower limit of the strength parameter as obtained from failure of rock slopes. However, alround squeezing would not take place unless the tangential stress $(2p_0)$ exceeds the maximum limit of the uniaxial compressive stress of the rock mass. Hence, the mobilised cohesion $(c_{pm})$ may represent the upper limit of the cohesion of anisotropic rock mass.

Moreover, the uniaxial compressive strength is statistically varying from one element to another element of the same rock mass depending upon the distribution of fractures. Alround squeezing will not take place until the tangential stress exceeds the upper statistical limit of the uniaxial compressive strength of the rock mass.

It may also be noted that the rock mass quality (Q) is obtained from the visual inspection of the excavated face of the tunnel which is likely to be poorer than the rock mass quality in the elastic zone.

While agreeing with the recommended value of 4 to 6 of the strength enhancement factor, Hudson (1993) suggested that the apparant strength enhancement indicated by Fig.6.9 could be due

to the difference in the condition of shearing in the case of rock slopes, where full dilatancy is operative, and in the case of underground openings.

Another reason for the apparent strength enhancement around the underground openings appears to be the fact that the failure stresses are calculated assuming the classicial constant modulus linear elasticity, whereas the deformation modulus has been found to increase with increasing confining pressure (Eqs.6.10, 6.11, 6.12). There is a growing evidence to suggest that the linear elasticity approach can give misleading prediction of the onset and the extent of fracture, particularly in softer rocks (e.g. Guenot, 1987; Kaiser et al., 1985; Maury, 1987; Santarelli, 1987). Santarelli and Brown (1987) derived closed-form solution for the stresses and strains around an axisymmetric wellbore assumming a confining pressure dependent modulus of elasticity (given by Eq.6.11) and concluded that the tangential stresses at or near the wellbore wall could be much lower than those predicted by the theory of elasticity, and that the maximum tangential stress occurred some distance from the wellbore wall.

Santarelli and Brown (1987) obtained the following closed-form solutions for tangential and radial stresses assuming a confining pressure dependent modulus of elasticity:

a) Normalised tangential stress at elastic-plastic interface,

$$\sigma_{\theta e}/p_o = K_1(\sigma_{re}/p_o) - K_2(\sigma_{re}/p_o)^{\alpha} \tag{6.27}$$

b) Normalised radial stress at elastic-plastic interface,

$$\sigma_{re}/p_o = [\{(p_i/p_o)^{1-\alpha} - 1\}(b/a)^{(1-\alpha)K2} + 1]^{1/1-\alpha} \tag{6.28}$$

In Eqs. 6.27 and 6.28,

$$K_1 = [\nu(1-\alpha)-1]/[(1-\nu)(1-\alpha)], \text{ and} \qquad (6.29)$$

$$K_2 = [(2\nu-1)(1-\alpha)-1]/[(1-\nu)(1-\alpha)] \qquad (6.30)$$

Santarelli and Brown (1987) used Eqs.6.27 and 6.28 to show the variation of the tangential stress with the radial stress for different values of $\alpha$. This is shown in Fig.6.10 from which it is clear that the stress concentration factor is much below the value of 2.0, which is obtained when the constant modulus of elasticity ($\alpha=0$) is considered and that the maximum tangential stress occurs some distance away from the periphery.

### e) Suggestions for determining ground reaction curve

In Daemen's equation (Eq.6.15), the value of $\sigma_{re}+\sigma_{\theta e}$ should be picked up from Fig.6.10 according to the actual value of $\alpha$ and the radial pressure at the inner boundary of the elastic zone.

Further, the peak cohesion parameter, $c_p$, in Eq.6.15 should be substituted by $c_{pm}$ (recommended) from Fig.6.9 to account for the strength enhancement factor in the elastic zone.

The peak angle of internal friction may be taken from Table 3.4 (Bieniawski, 1979). The residual cohesion may be neglected. However, the residual angle of internal friction, $\phi_r$, may be taken equal to ($\phi_p-5°$) for the broken zone for (b/a)<5 (Jethwa, 1981).
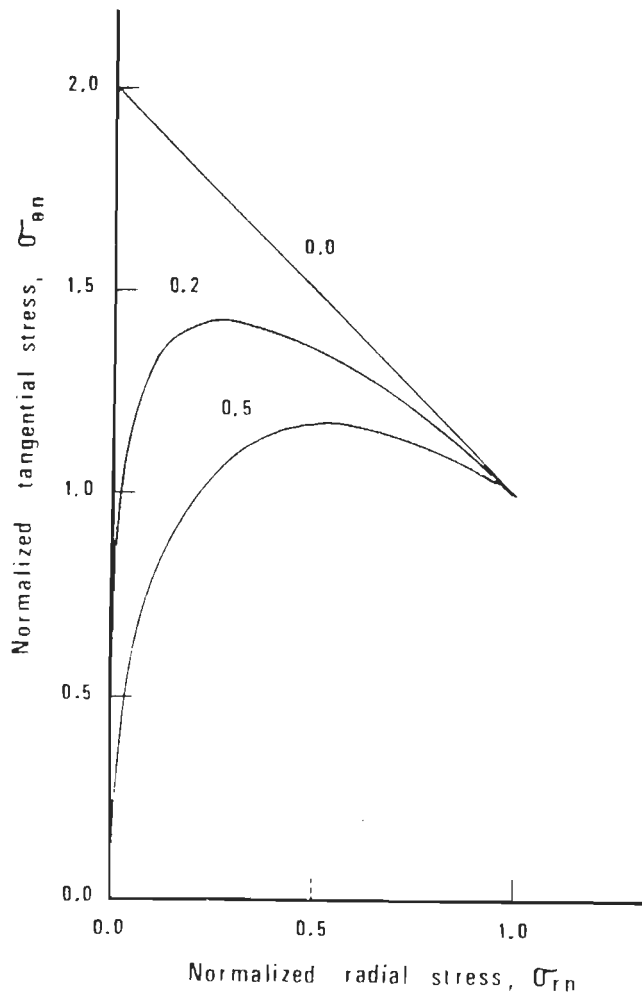
Fig.6.10 — Variation of Normalised Tangential Stress with the Normalised Radial Stress for Different Values of $\alpha$ (after Santarelli and Brown, 1987)

# CHAPTER  7

## CHAPTER 7

## DETERMINATION OF SUPPORT REACTION CURVE AND
## ROCK MASS-TUNNEL SUPPORT INTERACTION ANALYSIS

### 7.1 GENERAL

For the analysis of rock mass-tunnel support interaction, once the ground reaction (response) curve has been obtained, the next step is to determine the support reaction curve which denotes the relationship between the tunnel deformation and the support pressure available from the support system. Based on the analysis of data collected from several tunnels in India (Tables 5.1 and 5.2), the behaviour of the steel rib-backfill support system has been studied and an approach has been proposed for determination of the support reaction curve in this chapter. Some important aspects of the rock mass - tunnel support interaction also form the contents of the chapter.

### 7.2 DETERMINATION OF SUPPORT REACTION CURVE

As pointed out in Art.1.2 of Chapter 1, the support reaction curve depends on the stiffness of the support system. As illustrated in Fig.1.1 (Chapter 1), supports are usually installed after a certain amount of tunnel closure has already taken place. This initial closure is denoted by $u_{ao}$ in Fig.7.1 which shows an ideal support reaction curve. The stiffness of the support system is characterised by a stiffness constant k. From Fig.7.1, the radial tunnel deformation is given by:

$$u_a = u_{ao} + \frac{pi.a}{k} \qquad (7.1)$$

Equation 7.1 will be valid till the maximum support capacity is reached. Therefore, for obtaining the support reaction curve, the support stiffness as well as the maximum support capacity are required to be determined.

In the following paragraphs, an approach has been proposed for determination of the support reaction curve. The approach is based on the field instrumentation data collected from several Indian tunnels and it, therefore, pertains to the steel rib-backfill support system, as most of the tunnels in India are steel-supported.

## 7.2.1 Stiffness of Steel Rib-Backfill Support System

At a steel-supported tunnel section, the backfill is placed between the steel ribs and the rock mass and is meant to provide a contact between the two. The backfill itself is not designed to carry any load and its role is restricted to act as a packing between the rockmass and the steel ribs, which are the main load carrying elements of the support system. The stiffness of the backfill, however, plays an important role in determining the stiffness of the overall support system, as will be seen later.

The support system, comprising of the steel ribs and the backfill, may be assumed to be acting as two stiff springs connected in series. Therefore, the overall stiffness of the support system is given by:

$$1/k = 1/k_s + 1/k_b \qquad (7.2)$$

where,

k = overall stiffness of steel rib-backfill support system

$k_S$= stiffness of steel ribs, and

$k_b$= stiffness of backfill.

## 7.2.1.1 Stiffness of steel rib

Stiffness of the steel ribs may be obtained from the following expression for stiffness of a steel ring under an evenly distributed (external) pressure (Hoek and Brown, 1980):

$$k_S = \frac{E_S . A_S}{S.a} \tag{7.3}$$

where,

$E_S$ = modulus of elasticity of steel,

$A_S$ = cross-sectional area of steel rib,

S  = rib spacing, and

a  = tunnel radius.

## 7.2.1.2 Stiffness of backfill

Field instrumentation data, comprising of support pressures and tunnel deformations, obtained from several Indian tunnels (Tables 5.1 and 5.2, Chapter 5) were analysed and the support-reaction curves were plotted for each instrumented section according to the procedure outlined in Art.5.6. These 'observed' support reaction curves were then back-analysed to obtain the overall 'observed' support stiffness, k, using Eq. 7.1 by taking the observed $u_a$ and $p_i$ values from the support reaction curves and estimating the values of $u_{ao}$ according to the procedure explained in Art.5.5.2. The 'observed' stiffness of the

backfill, $k_b$, was then worked out using Eq. 7.2 from this overall support stiffness. For using Eq. 7.2, the value of the stiffness of steel ribs, $k_s$, was obtained from Eq. 7.3. From the values of the backfill stiffness, thus obtained, the following empirical correlation was arrived at:

$$k_b = \frac{1.16\ t_b E_b}{a^{1.05}} \qquad\qquad (7.4)$$

where,

$t_b$ = thickness of backfill in m,

$E_b$ = modulus of elasticity of backfill in kg/cm², and

$a$ = radius of tunnel opening in m.

Equation 7.4 resembles Eq. 7.3 which is desired theoretically.

### 7.2.1.3 An example of obtaining observed backfill stiffness from observed support reaction curve

Figure 7.2 shows an observed support reaction curve pertaining to a tunnel section at Ch.738.5m (D/S Maneri) in Maneri-Uttarkashi tunnel. The overall stiffness of the support system, k, may be obtained corresponding to any point of this curve using Eq. 7.1. One may take, for instance, the point A for which $u_a$=0.102 cm and $p_i$=0.345 kg/cm². The value of $u_{ao}$ is equal to 0.035cm and the tunnel radius, a, at this section is 290cm. Substituting these values in Eq. 7.1,

$$0.102 = 0.035 + [0.345)(290)/k]$$

from which, $\qquad\qquad$ k = 1493.28 kg/cm²
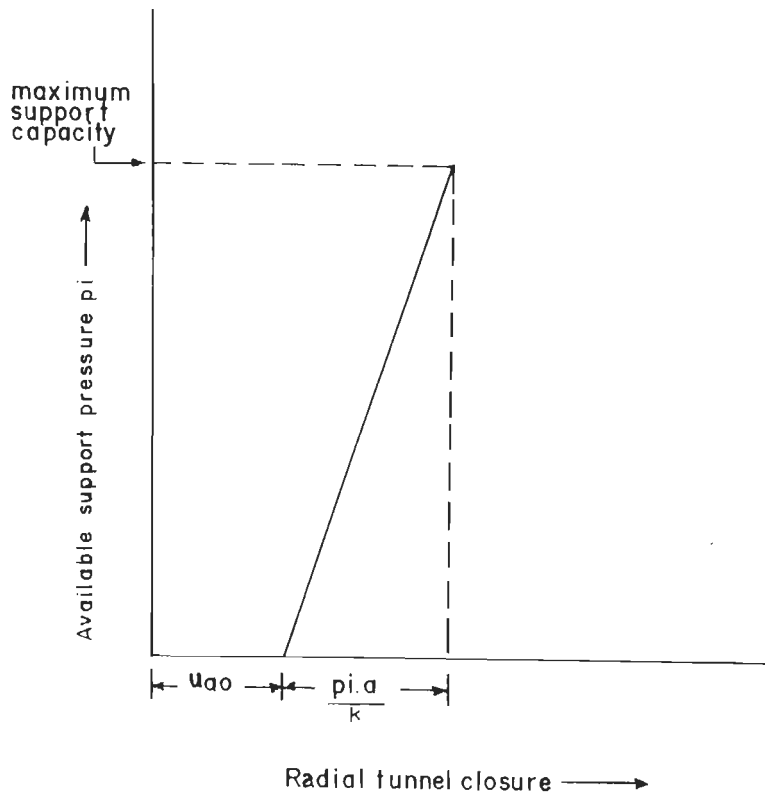
Fig.7.1 – A Linear Support Reaction Curve with a Constant Support Stiffness
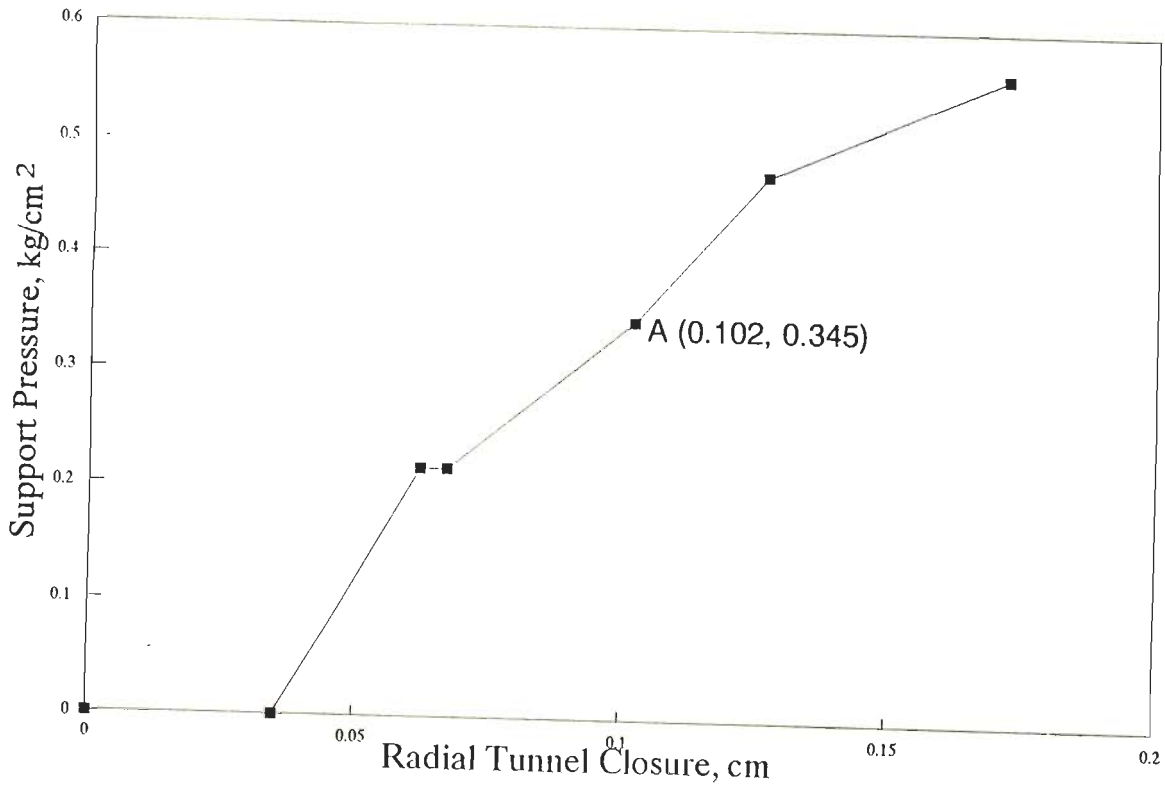


Fig.7.2 – Observed Support Reaction Curve for Ch. 738.5m (D/S Maneri) in Maneri – Uttarkashi Tunnel

At the section under consideration, steel ribs having $E_s = 2.1 \times 10^6$ kg/cm², $A_s = 38.98$ cm² and S=80 cm, have been used. Substituting these values in Eq. 7.3,

$$k_s = [(2.1 \times 10^6)(38.98)]/(80 \times 290) \quad kg/cm²$$

$$= 3528.36 \ kg/cm²$$

Substituting the values of k and $k_s$, thus obtained, in Eq. 7.2,

$$(1/1493.28) = (1/3528.36) + (1/k_b)$$

from which, $\qquad k_b = 2589.014 \ kg/cm²$

which is the observed stiffness of the backfill at point A on the observed support reaction curve. Similarly, the value of $k_b$ may be obtained all along the observed support reaction curve for different $p_i$ values. This was done for all the instrumented tunnel sections to evaluate the variation in the modulus of elasticity of the backfill (which is related to the backfill stiffness) with support pressure, as discussed in Art.7.2.1.4.

## 7.2.1.4 Variation of modulus of elasticity of back-fill with support pressure

The support reaction curves for all the instrumented sections were observed to be non-linear, unlike the conventional theoretical assumption of a linear support reaction curve. The reason for this could be attributed to the change in the modulus of elasticity of backfill, and, consequently, in the backfill stiffness, with increasing support pressure. While at most of the instrumented sections concrete was used as backfill, a few sections had gravel or tunnel-muck as backfills. This provided

an opportunity to study the behaviour of these different types of backfills under pressure. Figures 7.3 to 7.5 show the relationships between the modulus of elasticity of different backfills and the support pressure. From these figures, the following correlations may be obtained:

(i)  for concrete backfill –

$$E_b = 137 \ p_i^{0.77} \ \text{to} \ 926 \ p_i^{0.88} \quad \text{MPa} \tag{7.5}$$

(ii) for gravel backfill –

$$E_b = 10^{(pi+65.16)/41} \ \text{to} \ 10^{(pi+14.63)/9.26} \quad \text{MPa} \tag{7.6}$$

(iii) for tunnel-muck backfill –

$$E_b = 54 \ p_i^{0.215} \ \text{to} \ 97 \ p_i^{0.33} \quad \text{MPa} \tag{7.7}$$

In Eqs.7.5, 7.6 and 7.7, $p_i$ is in $kg/cm^2$.

For developing these correlations (Eqs. 7.4 to 7.7), the modulus of elasticity of the backfill was back calculated from the observed backfill stiffness for different values of support pressure, using the following expression for the stiffness of a thick wall cylinder:

$$k_b = \frac{E_b[a^2 - (a-t_b)^2]}{(1+\nu_b)[(1-2\nu_b)a^2 + (a-t_b)^2]} \tag{7.8}$$

where, $\nu_b$ is the Poisson's ratio of the backfill.

Equation 7.8 is based on the assumption of a closed ring of backfill (Fig. 7.6) and much of the backfill stiffness derives from the continuity of this ring.
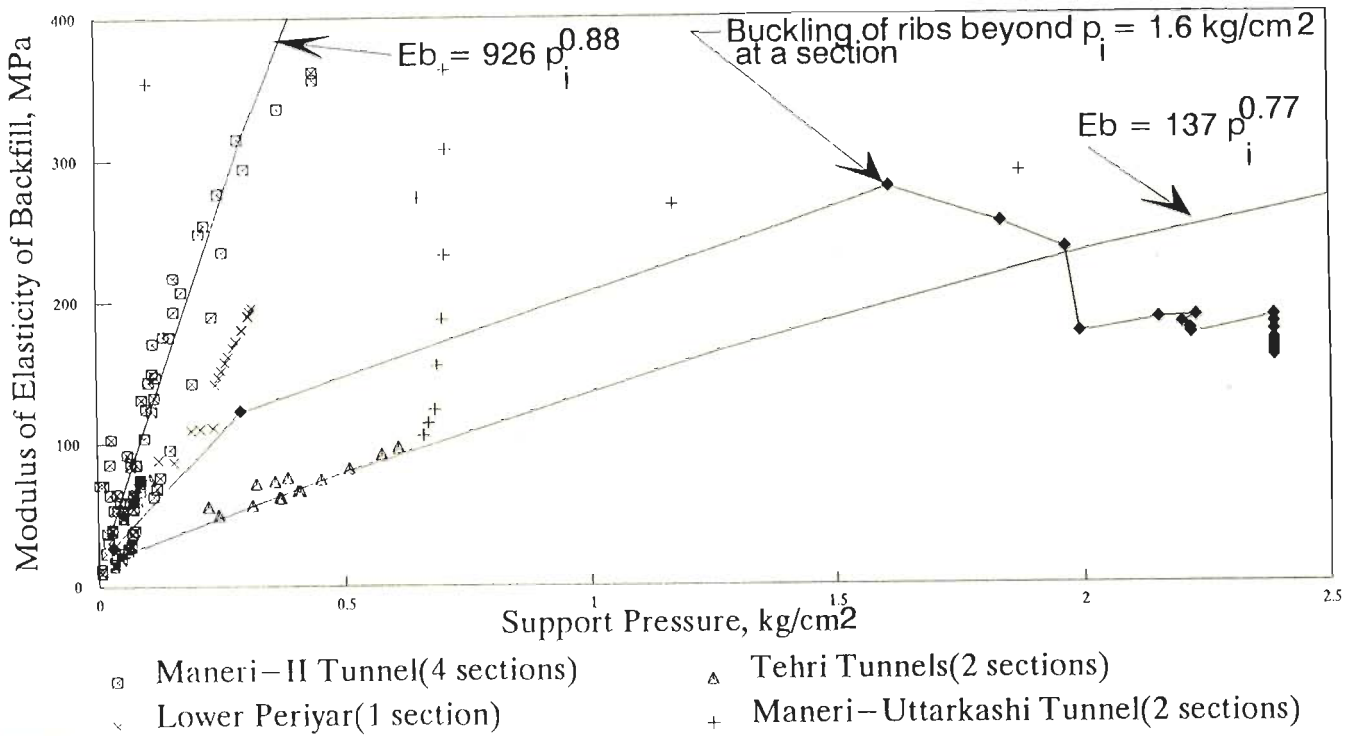
Fig.7.3 — Variation of Modulus of Elasticity of Concrete Backfill with Support Pressure
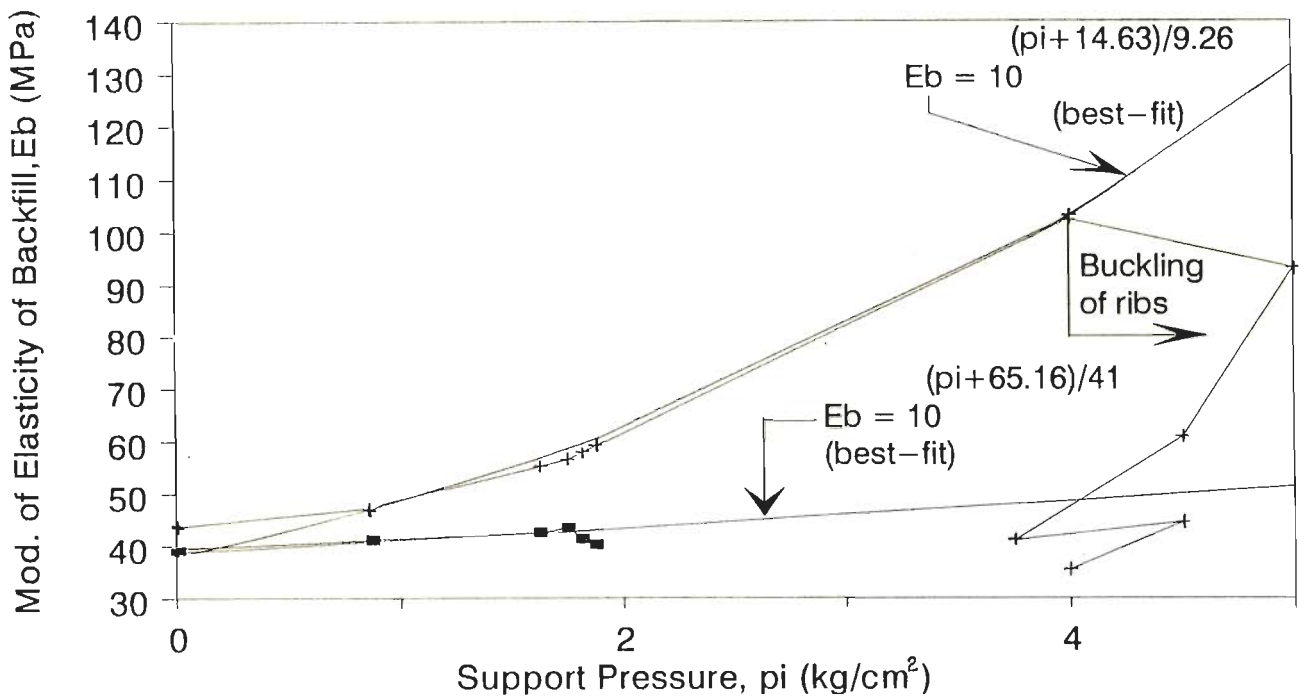


Fig.7.4 — Variation of Modulus of Elasticity of Gravel Backfill with Support Pressure at Two Locations in Giri Tunnel
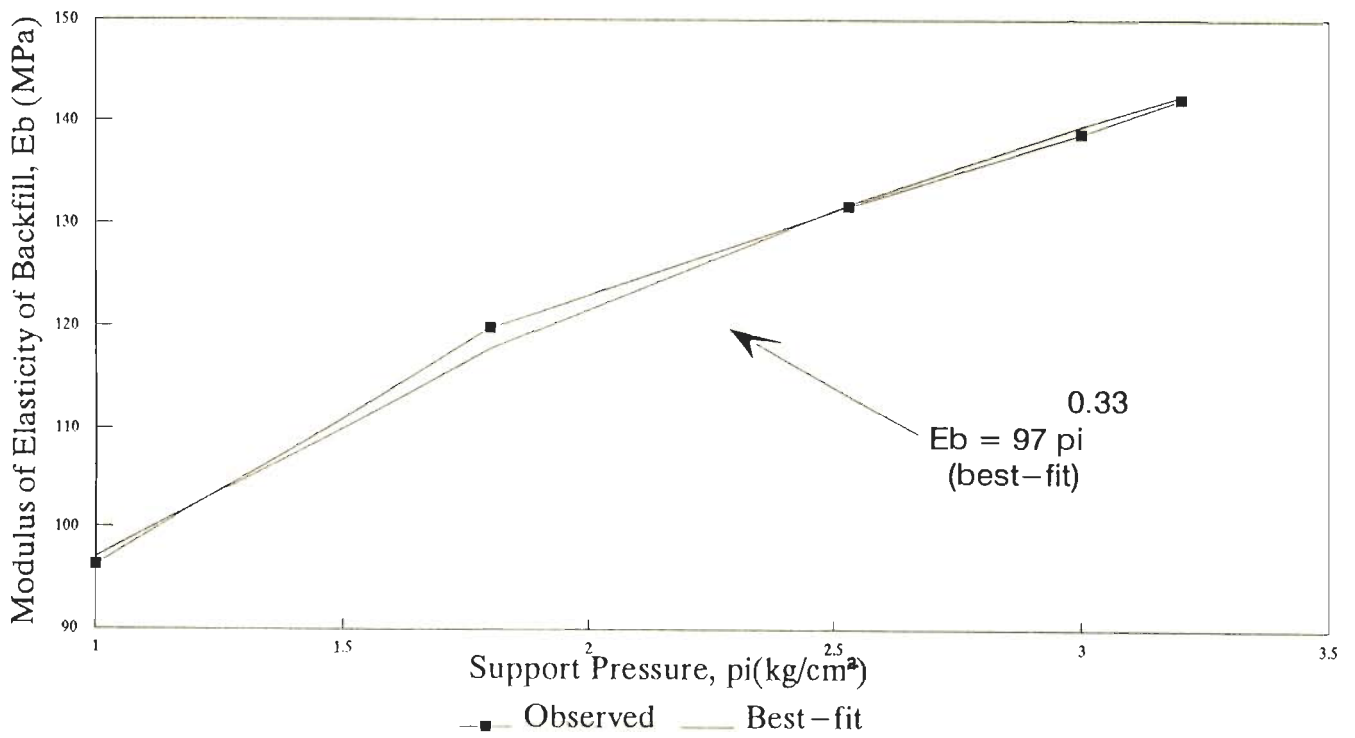
(a) Chhibro−Khodri Tunnel, Ch.2621m
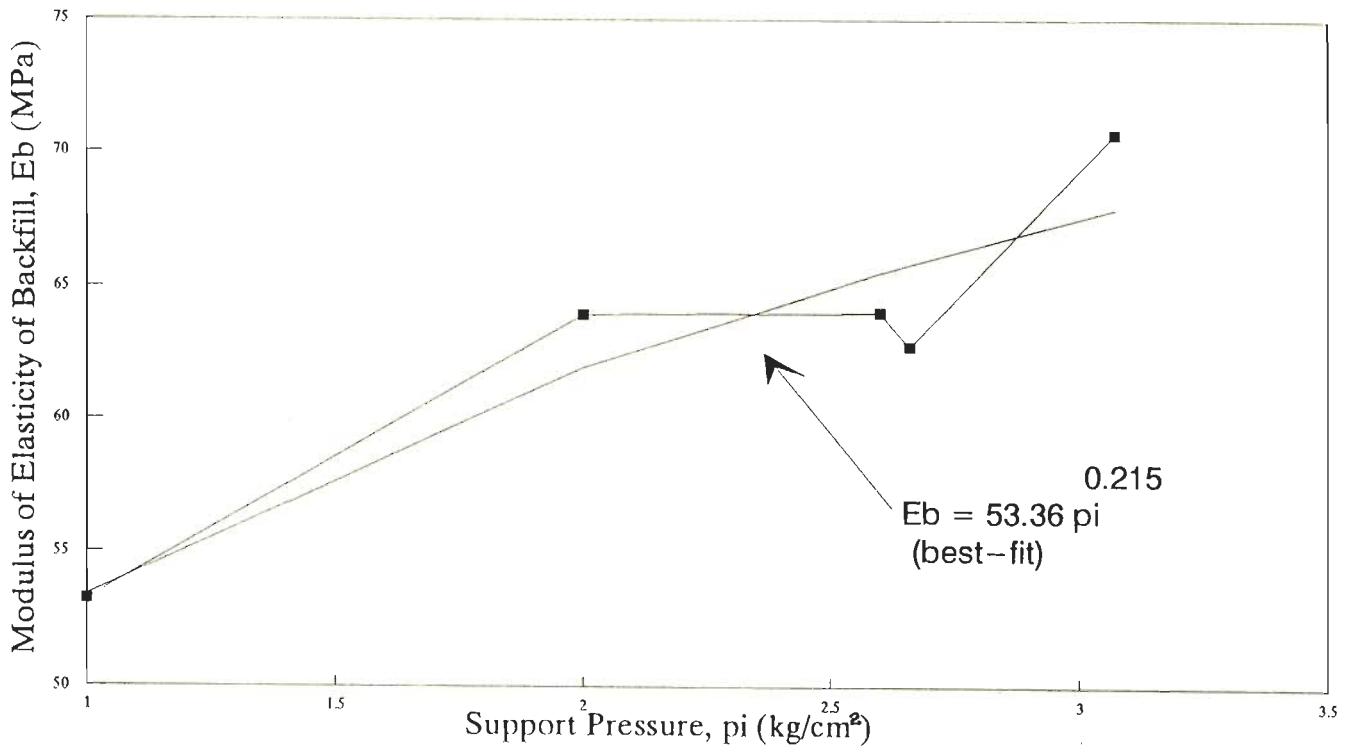


(b) Chhibro−Khodri Tunnel, Ch.2575m

Fig.7.5 − Variation of Modulus of Elasticity of Tunnel Muck with Support Pressure

## 7.2.2 Maximum support capacity of steel rib-backfill system

Although the backfill significantly influences the overall support stiffness, it does not contribute much to the load carrying capacity of the support system. It merely provides a contact between the ribs and the rock mass to facilitate the transfer of load (or support pressure) from the latter to the former. The maximum support capacity of the steel rib-backfill support system will, therefore, be governed by the maximum support capacity of the steel ribs, which is given by:

$$p_{imax} = \frac{\sigma_{ys} \cdot A_s}{S \cdot a} \tag{7.9}$$

where,

$p_{imax}$ = maximum support capacity of steel ribs, and

$\sigma_{ys}$ = yield strength of steel.

If the yield strength of steel is more than the buckling stress of the steel rib, $\sigma_{ys}$ should be replaced by the buckling stress in Eq. 7.9. The maximum support capacity will then be given by the following equation (Timoshenko and Gere, 1961):

$$p_{imax} = \frac{3E_s \cdot I_s}{a^3 \cdot S} \qquad \text{(for, } \sigma_{ys} > \text{buckling stress)} \tag{7.10}$$

where, $I_s$ is the moment of inertia of the steel rib.

The support reaction curve may, thus, be determined using Eqs. 7.2 to 7.7 for obtaining the support stiffness and Eqs. 7.9 and 7.10 for obtaining the maximum support capacity. The support reaction curve, thus obtained, will be non-linear, as indicated by Eqs. 7.5 to 7.7 which are based on actual field

observations. The earlier authors (Lombardi, 1970,1973; Ladanyi, 1974; Daemen, 1975; Hoek and Brown, 1980) did not consider the support pressure dependent modulus of elasticity of the backfill and, therefore, assumed the support reaction curves to be linear elastic.

## 7.2.3 Behaviour of different types of backfills

While studying the variation of the modulus of elasticity of different types of backfills with support pressure (Eqs. 7.5 to 7.7), some interesting observations were made regarding the backfill behaviour under pressure. These are as follows:

## (i)  Concrete backfill

Most of the instrumented sections had concrete as the backfill. An example of the typical behaviour of the concrete backfill, observed at the majority of such sections, is shown in Fig. 7.7 which is a plot between the modulus of elasticity of backfill and the support pressure at Ch.829m in HRT-3 of Tehri Project (Table 5.1). It may be inferred that the early stage concrete backfill cracks under low pressure, soon after it is placed behind the ribs, and looses its initial stiffness. The decrease in its stiffness continues for sometime until a stage is reached where the cracked backfill starts getting compacted with increasing support pressure. Consequently, its stiffness starts increasing. Another example of a similar trend is shown in Fig. 7.8 which pertains to Ch. 51m in Maneri Stage-II tunnel (Table 5.2). Sometimes, the initial decrease in the stiffness is rapid
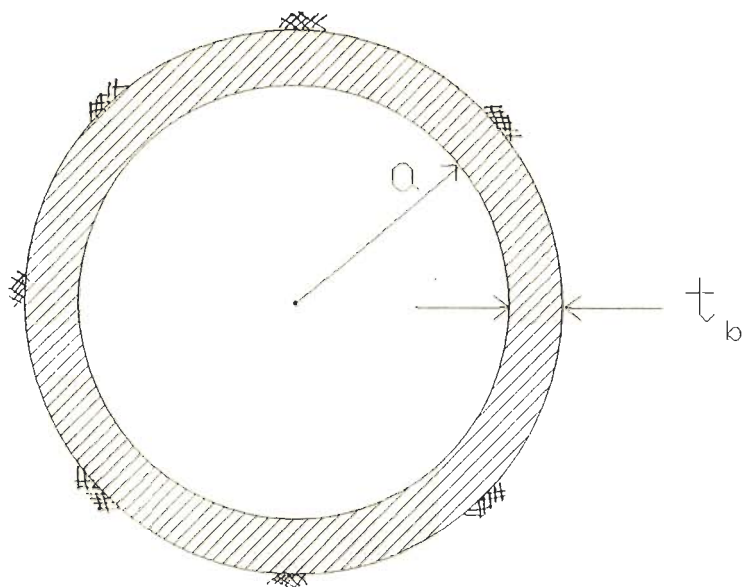
Fig.7.6 :   Closed Ring of Backfill
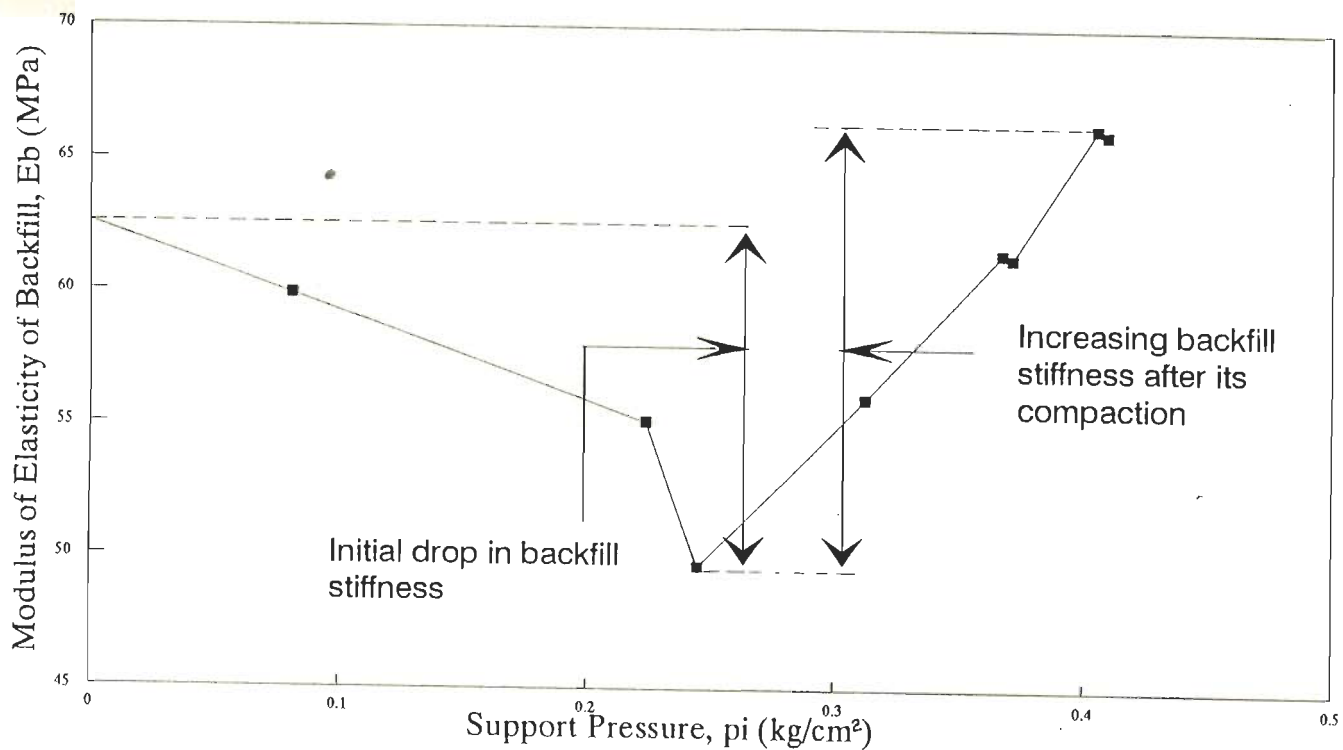


Fig.7.7 – Initial Drop in Concrete Backfill Stiffness at Ch.829m in HRT−3, Tehri Project

as illustrated in Fig. 7.9 which pertains to Ch. 1568.5m in the same tunnel. The overall trend was, however, observed to be similar at almost all the sections. At one of the sections (Ch.777m, U/S of Dhanarigad adit - Fig. 7.3) in Maneri Bhali Stage-II tunnel, the steel ribs buckled under high squeezing pressure (Fig.4.16, Chapter 4) resulting in a sudden loss of contact between the backfill and the rock mass. This is indicated by a sudden drop in the backfill stiffness after buckling of ribs. An outcome of this study is that the concrete, when used as backfill, almost immediately gets crushed and looses whatever strength it had gained during a very short time interval between its mixing and placing behind the ribs. Thereafter, it merely acts as a packing material which gains its stiffness from compaction of the crushed particles. It would, therefore, be more appropriate to call it as 'packing concrete' or 'blocking concrete' instead of just 'concrete'.

## (ii) Gravel backfill

The gravel backfill does not show any initial loss of stiffness under pressure, as illustrated through an example of Giri tunnel in Fig. 7.4. The stiffness increases with support pressure on account of increasing compaction of the backfill which, in the process, gradually becomes denser. This process continues till the equilibrium support pressure, or, as shown in Fig. 7.4 which pertains to a highly squeezing section, the maximum capacity of steel ribs is reached. In the former case, the opening stabilises and in the latter (Fig. 7.4), the steel supports buckle. The buckling of steel ribs under high pressure

results in a sudden loss of contact between the backfill and the rock mass. Consequently, the backfill stiffness drops sharply (Fig. 7.4).

### (iii) Tunnel-muck backfill

The tunnel-muck backfill has an initial stiffness similar to the gravel backfill. It also shows an increasing trend with increase in support pressure (Fig. 7.5; Chhibro-Khodri tunnel, Chs.2621m and 2575m). However, the build-up of backfill stiffness with increase in support pressure is slower than in the case of the gravel backfill.

### (iv) Comparative behaviour of backfills and suitability to different ground conditions

The concrete backfill, despite an initial loss of stiffness, provides a stiffer support as compared to the gravel and the tunnel-muck backfills. It may be seen from Eqs. 7.5 to 7.7 that for a support pressure of 1 kg/cm², the modulus of elasticity of concrete, tunnel-muck and gravel backfills ranges from 137 to 926, 54 to 97, and 41 to 49 MPa respectively. The concrete backfill is, therefore, preferable for elastic ground condition. The tunnel-muck backfill may be more suited to moderately squeezing ground condition, and the gravel backfill to highly squeezing ground condition, as the latter is more flexible. These two types of backfills are flexible initially and gradually become stiffer with increasing support pressure, thus accommodating large deformations, which occur in squeezing ground conditions, and permitting low support pressures.
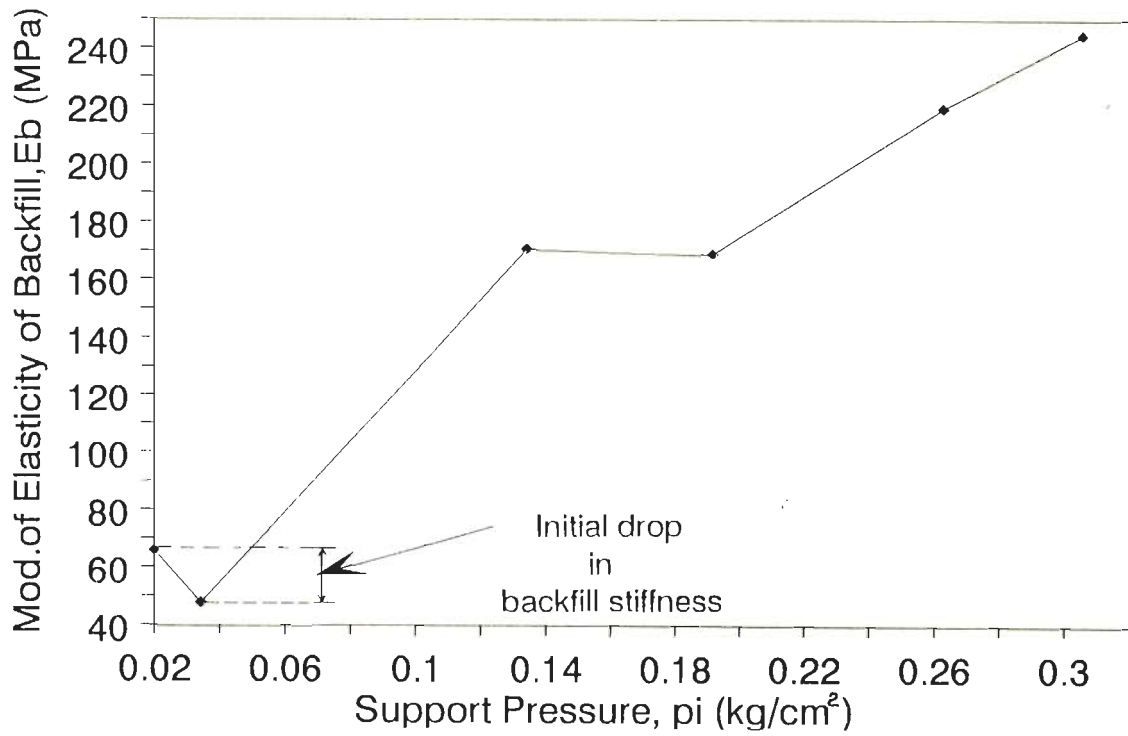
Fig.7.8 – Initial Drop in Concrete Backfill Stiffness
at Ch.51m in Maneri Stage II Tunnel
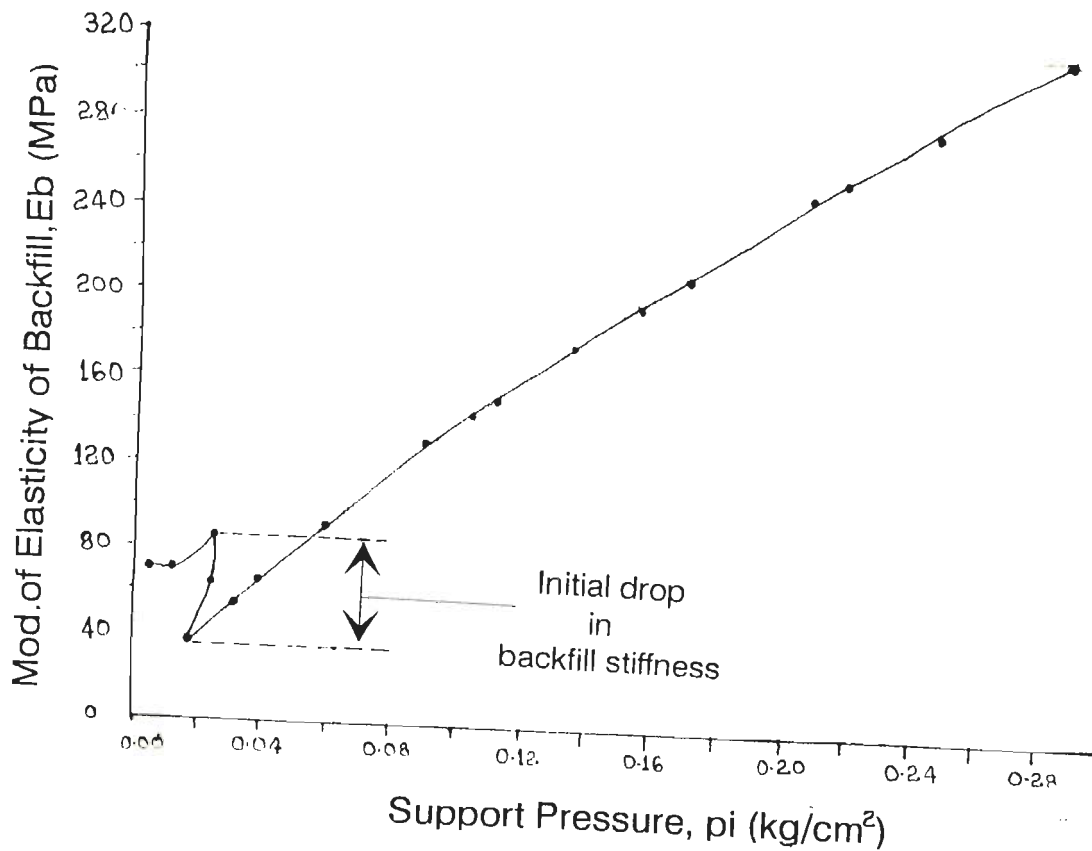


Fig.7.9 – Rapid Initial Drop in Concrete Backfill Stiffness
at Ch.1568.5m in Maneri Stage–II Tunnel

## 7.3 ROCK MASS - TUNNEL SUPPORT INTERACTION ANALYSIS

### 7.3.1 Proposed Approach for Non-squeezing and Squeezing Ground Conditions

Based on the data obtained from tunnels in India, approaches have been proposed for determination of the ground reaction and the support reactipon curves, the two essential components of the rock mass-tunnel support interaction analysis. The ground reaction curves may be obtained for the squeezing and non-squeezing (including the self-supporting condition) ground condition from the approaches suggested in Art. 6.3 of Chapter 6. This, together with the approach proposed in Art. 7.2 to obtain the support reaction curve, may be used to perform the rock mass-tunnel support interaction analysis.

### 7.3.2 A Simple Empirical Approach For Rock Mass-Tunnel Support Interaction Analysis in Squeezing Ground Condition

As an alternative to the proposed approach for rock mass - tunnel support interaction analysis for the squeezing ground condition, a simple empirical approach, discussed in the following paragraphs, may be used for the same purpose.

### 7.3.2.1 Empirical ground reaction curves

Singh et al. (1992) obtained an 'empirical' ground reaction curve for squeezing ground condition. This is shown in Fig. 7.10 for tunnel wall and in Fig. 7.11 for tunnel roof in the form of a plot between the normalised observed support pressure and the observed tunnel closure (as a percentage of the tunnel size). The normalised observed support pressure ($f'_w$ for tunnel wall and

$f'_r$ for tunnel roof) is defined as follows :

$$f'_w = \frac{p_w{}^{obsd}}{f.p_w} \qquad \text{and,} \qquad f'_r = \frac{p_r{}^{obsd}}{f.p_r} \tag{7.11}$$

where,

$p_w{}^{obsd}$ and $p_r{}^{obsd}$ = measured support pressure,

$$f \quad = \text{correction factor for overburden}$$
$$= 1+(H-320)/800 \geq 1 \tag{7.12}$$

$\qquad H \quad =$ height of overburden in meter, and

$p_w$ and $p_r$ = predicted short-term wall and roof support pressures using the approach of Barton et al. (1975)

Singh et al. (1992) first applied a correction factor, $f (= p_w{}^{obsd}/p_w$ or $p_r{}^{obsd}/p_r)$, for overburden to improve the relationship between the observed short-term support pressure and the short-term support pressure predicted by the approach of Barton et al. (1975). This resulted in the above relationship for 'f' (Eq.7.12) from instrumentation data of 20 tunnel sections in squeezing and non-squeezing ground conditions. The observed short-term support pressure was then normalised by incorporating 'f' and was plotted with the observed closure of tunnel wall and tunnel roof (Figs. 7.10 and 7.11). The data points in these figures represent eight tunnel sections from four different tunnels. The normalised support pressures are higher for low tunnel closures. The support pressures decrease when the tunnel closures increase and attain minimum value when the closures are approximately 5 percent. The normalised support pressures again rise beyond this point. Such a variation is in conformity with the ground reaction curve concept. The curves of
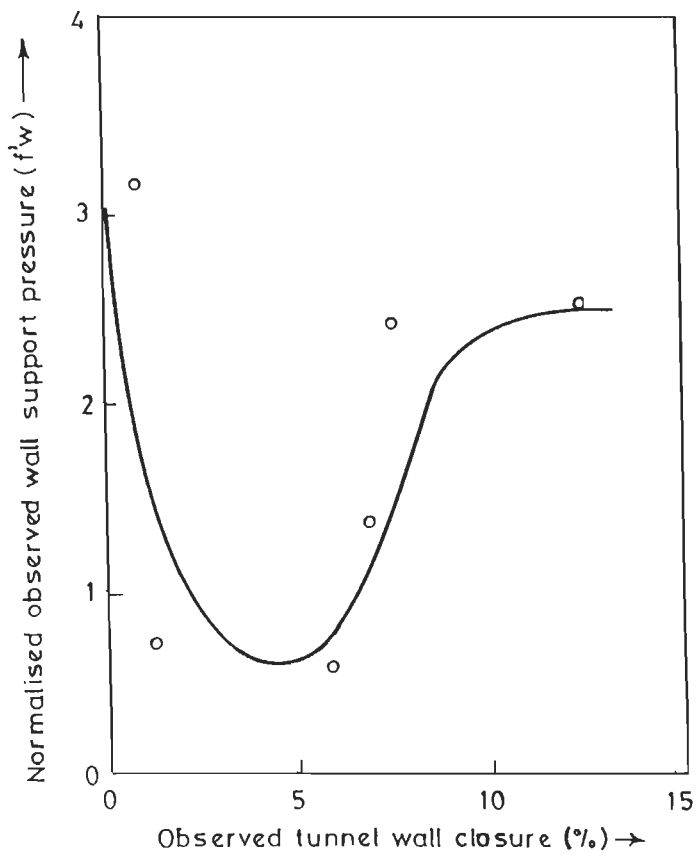
Fig.7.10 - 'Empirical' Ground Reaction Curve for Tunnel Wall in Squeezing Ground Condition (after Singh et al.,1992)
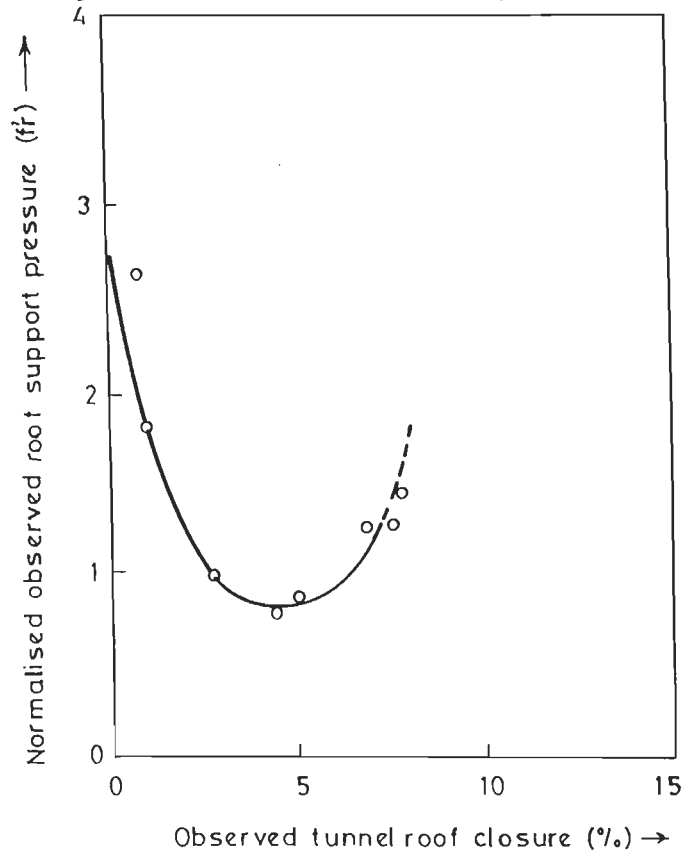


Fig.7.11 - 'Empirical' Ground Reaction Curve for Tunnel Roof in Squeezing Ground Condition (after Singh et al.,1992)

Figs. 7.10 and 7.11 may, therefore, be termed as 'empirical' ground reaction curves.

### 7.3.2.2 Rock mass - tunnel support interaction analysis using the empirical ground reaction curves

The curves of Figs. 7.10 and 7.11 may be used for performing the rock mass-tunnel support interaction analysis. The aim of this analysis is to locate the point of intersection of the ground reaction and the support reaction curves close to, but not beyond, the point of minimum support pressure. The preferable points of intersection are, therefore, A and B for tunnel wall and roof respectively, as shown in Fig. 7.12, in which the curves of Figs. 7.10 and 7.11 have been reproduced. The next step is to locate the starting point of the support reaction curve. This is marked as C in Fig. 7.12. The location of this point will depend upon the initial tunnel closrue, $u_{ao}$, expected to occur before the support installation. Monitoring of the tunnel closure during construction will help in determining reliable location of this point for subsequent tunnel sections. The last step is to choose a support system (i.e. steel rib section, and type and thickness of backfill) which gives a support reaction curve passing through C and A (for tunnel wall) using Eqs.7.1 to 7.10. Similarly, a support system may be chosen for tunnel roof.

It may be mentioned that many failures of the steel ribs in squeezing ground have taken place (Jethwa, 1981) due to very low stiffness in the horizontal direction as the struts were not provided in between the legs of the ribs. The secret of success

lies in ensuring minimum stiffness in the horizontal direction which can be easily achieved by providing the struts. This will also increase the support capacity in the horizontal direction. The inevitable loss in the rate of tunnelling due to muck clearance and installation of struts is worth tolerating as otherwise the tunnel may collapse completely. In the case of highly squeezing ground condition, selection of circular steel ribs, full face tunnelling, and small size (< 6m) of the tunnel, would be the ideal choice.

### 7.3.3 Effect of Charging of Water Conductor System on Support Pressure

When the water conductor system is charged, the rock mass gets saturated. As a result, an additional pressure builds up on the concrete lining. It is, therefore, important to consider this additional pressure while designing the lining. The rock mass-tunnel support interaction analysis can help in determining this additional support pressure.

Figure 7.13 shows schematically the ground reaction curves for both dry and saturated conditions in an elastic ground, alongwith the support reaction curve. Upon charging of the system, the modulus of deformation of the rock mass reduces due to saturation and the ground reaction curve shifts from the path AB to AC, putting an additional pressure, equal to the length BC, on the concrete lining. Using Eq.6.7 for both dry and saturated conditions of the rock mass, the following expression may be obtained for this additional pressure, $\Delta p_{isat}$:
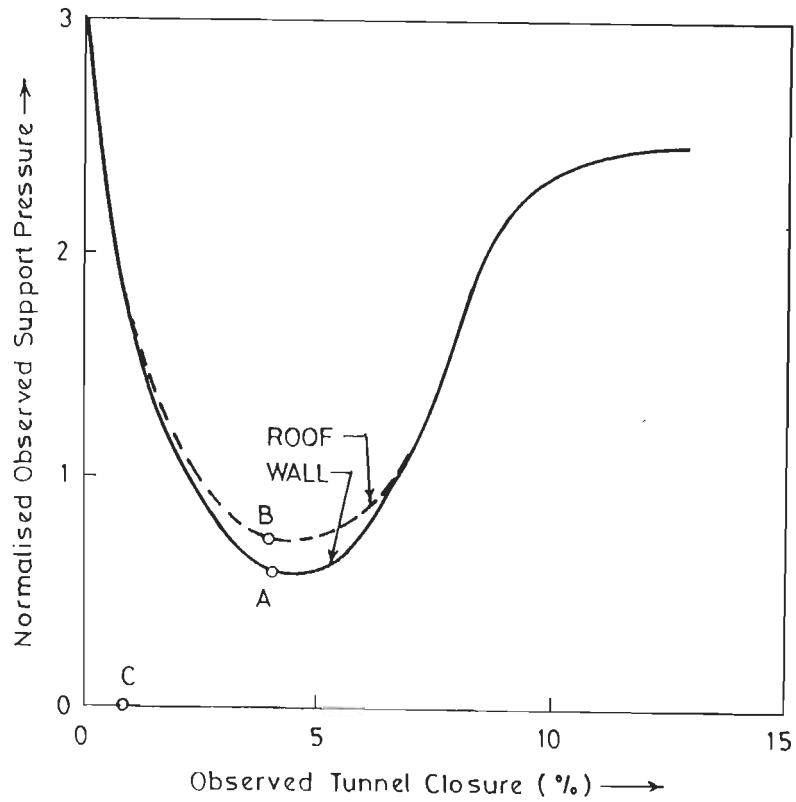
Fig.7.12 – Desirable Points of Intersection of Ground Reaction and Support Reaction Curves for Tunnel Wall and Roof

$$\Delta p_{isat} = (1 - \frac{E_{sat}}{E_{dry}}) \ (p_o - p_{idry}) \tag{7.13}$$

where,

$E_{sat}$ = modulus of deformation of saturated rock mass,

$E_{dry}$ = modulus of deformation of dry rock mass, and

$p_{idry}$= short-term support pressure in dry condition.

The derivation of Eq.7.13 is given in Appendix A.

It may be noted that the rock mass is assumed to be saturated everywhere after charging of the water conductor system. This assumption would be valid only if the internal water pressure head $(p_w/\gamma_w)$ is more than say three times the diameter of the tunnel. This is generally the case in hydroelectric projects.

According to Mehrotra (1992),

$$\frac{E_{sat}}{E_{dry}} = 0.016 \ RMR - 0.385 \quad \text{(for RMR = 41 to 60)} \tag{7.14a}$$

$$= 0.01 \ RMR - 0.1 \quad \text{(for RMR < 41 and rocks with water sensitive minerals)} \tag{7.14b}$$

Substitution of the above values of $E_{sat}/E_{dry}$ in Eq.7.13 for RMR > 30 in elastic ground condition, results in the following expression:

$$\Delta p_{isat}/p_o = 0 \text{ to } 0.8 \ (1-p_{idry}/p_o) \tag{7.15}$$

Equation 7.15 may be used to estimate the additional support pressure due to charging of the water conductor system in elastic

ground condition. The equation is presented in a graphical form in Fig. 7.14. It may be seen that for lower values of $p_{idry}/p_o$ ratio, the build-up of additional support pressure is high. Since, in practice, the $p_{idry}/p_o$ values are very low, $\Delta p_{isat}/p_o$ lies in a range of very high values, and the additional support pressure may be as high as about 80 percent of the insitu stress.

## 7.3.4 Expression for Support Pressure in Elastic Ground Condition and Effect of Tunnel Size

From the preceeding equations, the following expression may be obtained for the short-term support pressure or the support pressure at equilibrium, i.e., when the ground reaction and the support reaction curves intersect:

$$p_{if} = \frac{[(1+\nu)p_o/E_d - (u_{ao}/a)}{[(1+\nu)/E_d + (S.a/E_s.A_s) + (0.86\ a^{1.05}/t_b.E_{bf})} \qquad (7.16)$$

where,

$p_{if}$ = short-term support pressure (i.e., support pressure at equilibrium), and

$E_{bf}$ = modulus of elasticity of backfill at support pressure equal to $p_{if}$.

The derivation of Eq.7.16 is given in Appendix B.

Equation 7.16 may be used for evaluation of the effect of tunnel size on the short-term support pressure. It may be seen from Eq.7.16 that the short-term support pressure would be practically independent of the tunnel size if $A_s/S$ and $t_b$ are increased in direct proportion to the tunnel size. This is illustrated in Fig.7.15 for a flexible and a stiff support system, using assumed input data.
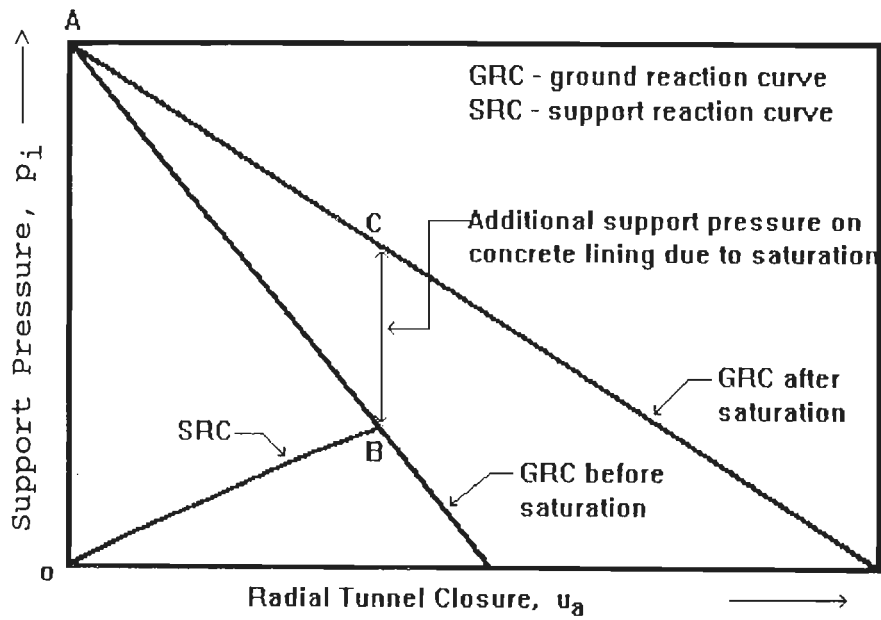
Fig. 7.13- Effect of Rock Mass Saturation on Support Pressure
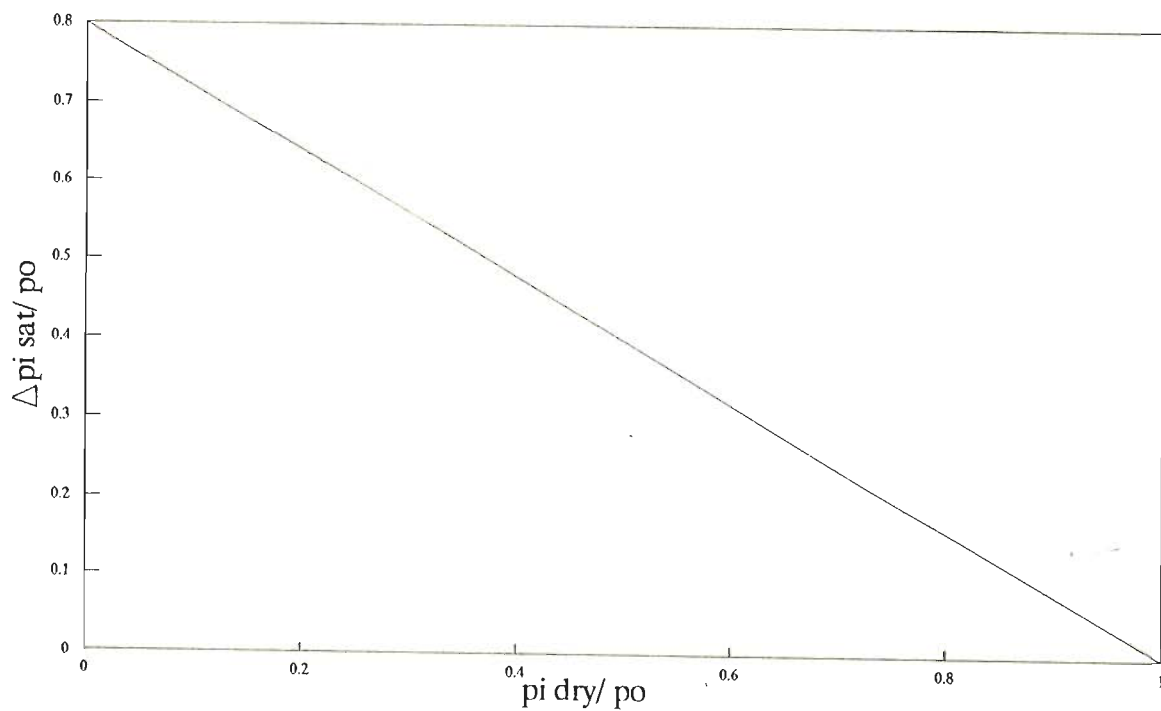


Fig.7.14 — Additional Support Pressure ($\Delta$ pi sat) due to saturation of rock mass as a Function of Pre—saturation Support Pressure (pi dry)

Equation 7.16 may be generalised to include the effect of the anisotropy of the rock mass, additional support pressure due to charging of the water conductor system, and the seepage pressure. The generalised equation is as follows:

$$p_{if} = \frac{[(1+\nu)p_o/RF.E_{min}] - u_{ao}/a}{[(1+\nu)/RF.E_{min}]+(S.a/E_s.A_s)+(0.86\ a^{1.05}/t_b.E_{bf})} + p_{isat} + p_w \quad (7.17)$$

where,

RF = reduction factor, which together with Emin, accounts for anisotropy of rock mass,

$E_{min}$= smaller of the two moduli of deformation of rock mass in horizontal and vertical directions, and

$p_w$ = seepage pressure on tunnel lining.

The value of the reduction factor, RF, is derived by analyzing the numerical model of a lined tunnel (Kumar and singh, 1990). The whole approach is based on a continuum characterisation of anisotropic rock mass, in which elastic properties of the rock mass are reduced depending upon the discontinuity description and their spacing. This continuum model was derived by Singh (1973). The variation of RF with $G/E_{min}$ for different values of $E_1/E_2$ is plotted in Fig.7.16, where G is the shear modulus of rock mass and $E_1, E_2$ are the moduli of deformation of rock mass in the horizontal and vertical directions respectively. This is also given in a tabular form in Table 7.1.

Table 7.1 - Reduction Factor for Anisotropic Rock Mass

| $E_{min}$ (kg/cm²) | $E_1/E_2$ | $G/E_{min}$ | RF |
|---|---|---|---|
| 10000 | 2.0 | 0.3636 | 1.000 |
| 10000 | 2.0 | 0.3000 | 0.9653 |
| 10000 | 2.0 | 0.1500 | 0.6744 |
| 10000 | 2.0 | 0.0500 | 0.4036 |
| 20000 | 1.0 | 0.4167 | 0.9741 |
| 20000 | 1.0 | 0.3000 | 0.8196 |
| 20000 | 1.0 | 0.1500 | 0.5606 |
| 20000 | 1.0 | 0.0500 | 0.3050 |
| 50000 | 1.0 | 0.4167 | 0.9737 |
| 50000 | 1.0 | 0.3000 | 0.8168 |
| 50000 | 1.0 | 0.0500 | 0.3057 |

## 7.3.5 Expression for Support Pressure in Squeezing Ground Condition and Effect of Tunnel Size

The expression for short-term support pressure in squeezing ground condition may be obtained by equating the radial tunnel closures obtained from the ground reaction and the support reaction curves, since these two values are equal at the point of intersection of the two curves. This results in the following expression for the case of a constant volume expansion throughout the broken zone (refer Art.6.3.2, Eq.6.16):

$$p_{if} = \frac{1-[(1+e)-(b_f/a)^2 e - 2(b/a)u_b + (u_b/a)^2]^{1/2} - (u_{ao}/a)}{(S.a/A_s.E_s) + (0.86 \, a^{1.05}/t_b.E_{bf})} \qquad (7.18)$$

where, $b_f$ is the radius of broken zone corresponding to $p_i=p_{if}$ and may be obtained in terms of $p_{if}$ from Eq.2.11 (Chapter 2), which may be rewritten as follows for $p_i=p_{if}$ and $b=b_f$:

$$p_{if} = [p_o(1-\sin \phi_p) - c_p \cos \phi_p + c_r \cot \phi_r](a/b_f)^\alpha - c_r \cot \phi_r$$
$$\pm \, \tau.a.[(1-\sin \phi_r)/(1-3\sin \phi_r)][(a/b_f)^{\alpha-1}-1] \qquad (7.19)$$
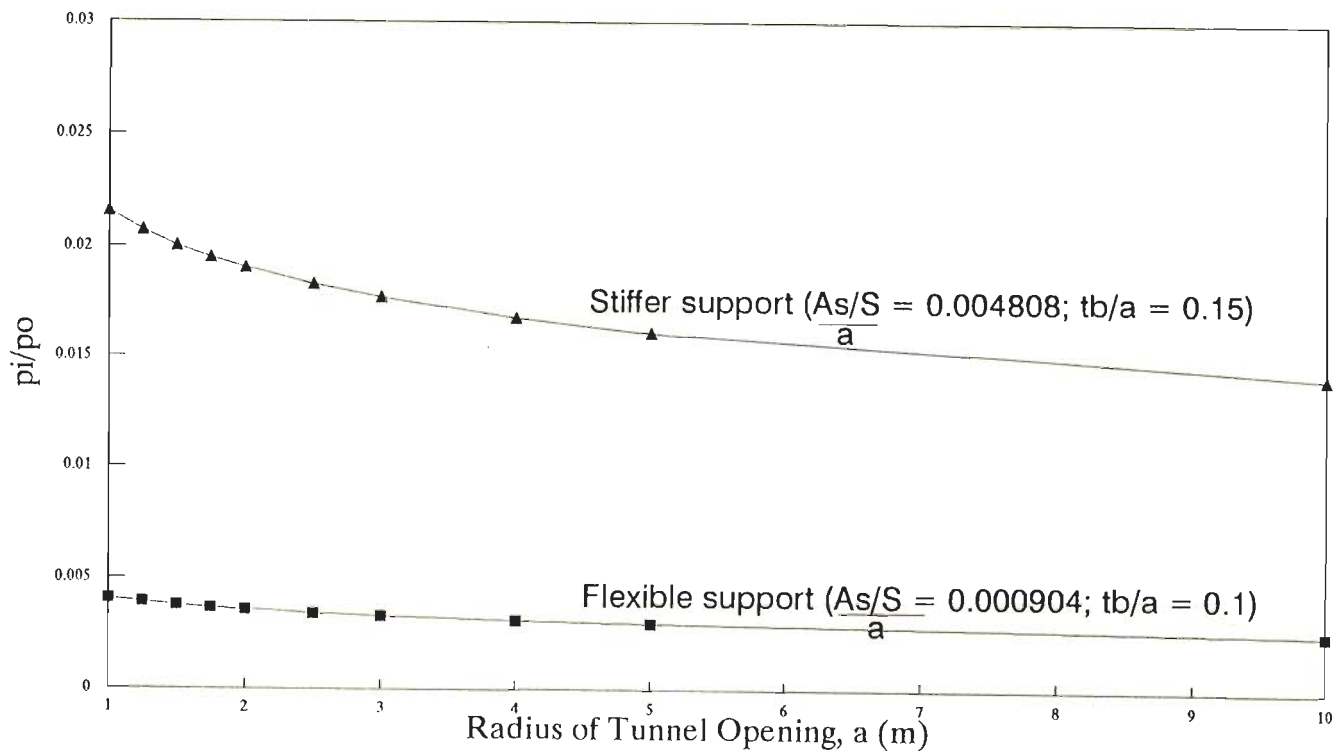
Fig.7.15 — Effect of Tunnel Size on Equilibrium Support Pressure in Elastic Ground Condition for Constant (As/S)/a and tb/a Values
(assumed rock mass data: $\nu=0.25$, $E=11400$ kg/sq cm, po$=50$ kg/sq cm)
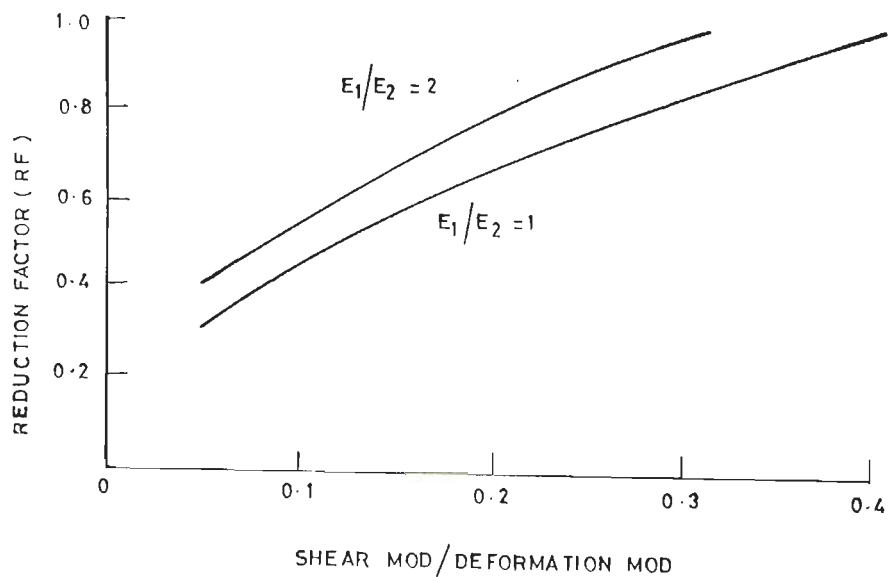


Fig. 7.16 — Reduction Factor For Anisotorpic Rock Mass
(After Kumar And Singh, 1990)

The nature of Eqs. 7.18 and 7.19 is such that the value of $p_{if}$ has to be obtained by iterative process using Eq. 7.18.

The derivation of Eq.7.18 is given in Appendix C.

Eq.7.18 may be used for evaluation of the tunnel size on the short-term support pressure. It may be seen from Eq. 7.18 that the short-term support pressure is practically independent of the tunnel size if $A_S/S$ and $t_b$ are increased in direct proportion to the tunnel size.

Like the case of elastic ground condition (Eq.7.17), Eq.7.18 may also be generalised, and written in the following form (Eq.7.20 and 7.21), to incorporate the effect of the anisotropy of the rock mass.

$$p_{if} = \frac{1-[(1+e)-(b_f/a)^2 e-2(b/a)u_b+(u_b/a)^2]^{1/2}-(u_{ao}/a)}{(S.a/A_S.E_S) + (0.86\ a^{1.05}/t_b.E_{bf})} \quad (7.20)$$

where,

$$u_b = \frac{(1+\nu)p_o}{RF.E_{min}}[p_o \sin \phi_p + c_p \cos \phi_p] \quad (7.21)$$

(obtained from Eq. 6.19 by replacing E with $RF.E_{min}$)

## 7.3.6 Empirical Correlation for Stand-up Time

It is important to know the time period for which a tunnel section can stand on its own without supports. Knowledge of this time gap helps in determining the time by which installation of the supports may be delayed and the initial displacement, $u_{ao}$, which may be permitted. This time period is called the stand-up

time and its concept was introduced by Lauffer (1958, Art.3.4).

## 7.3.6.1 Need for a correlation for stand-up time

Bieniawski (1989) related the stand-up time with RMR and roof span and plotted the results in the form of a chart (Fig.3.2). For a given roof span and RMR value, one can determine the stand-up time from this chart. Bieniawski (1989), however, did not suggest any correlation for determination of the stand-up time. Further, the chart does not consider the effect of the excavation shape and gives the same value of stand-up time for a given opening size and RMR, regardless of the shape of the opening. The excavation shape is likely to influence the stand-up time as shown schematically by Lauffer (1958, Fig.7.17).

To overcome the above problem, Bieniawski's data (1989, pp.207-217) were analysed to arrive at an empirical correlation for stand-up time. The mining and the tunnelling (including chambers) cases were separated for this purpose as these normally have different excavation shapes - flat roof and arch roof respectively.

## 7.3.6.2 Effect of RMR on stand-up time

An analysis of Bieniawski's data base has revealed that RMR has a dominating influence on the stand-up time. The following correlations between the stand-up time and RMR (Figs. 7.18 and 7.19) have been obtained from regression analysis for underground openings with arch and flat roofs (i.e., tunnelling and mining cases respectively):
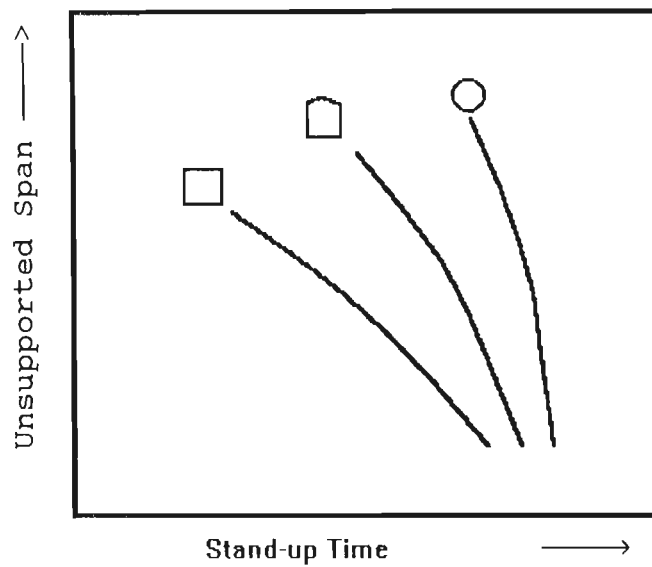
Fig. 7.17 - Effect of Shape of Underground Opening on Stand-up Time
*[Schematically After Lauffer, 1958]*

The plot shows "Stand-up Time, hrs" on the vertical (logarithmic) axis ranging from 0.1 to 100000, and "Rock Mass Rating, RMR" on the horizontal axis ranging from 0 to 100.

$$t_{arch} = 10^{(RMR-20)/15}$$

(Corr.Coeff. = 81 %)
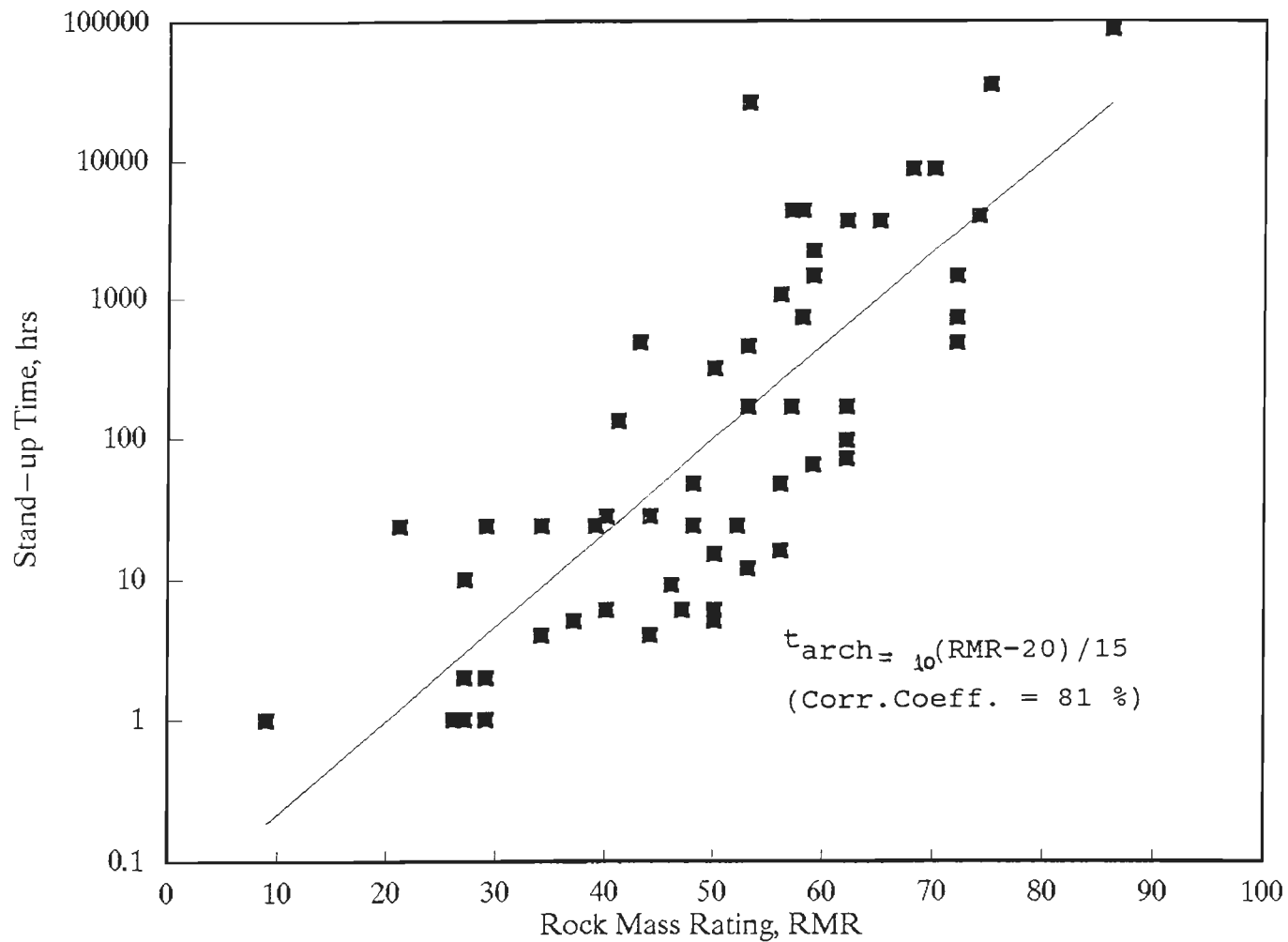
Fig.7.18 - Correlation Between Stand-up Time and RMR
for Underground Openings with Arch Roof

$$t_{flat}=10^{(RMR-23)/14}$$

(Corr.Coeff. = 96 %)
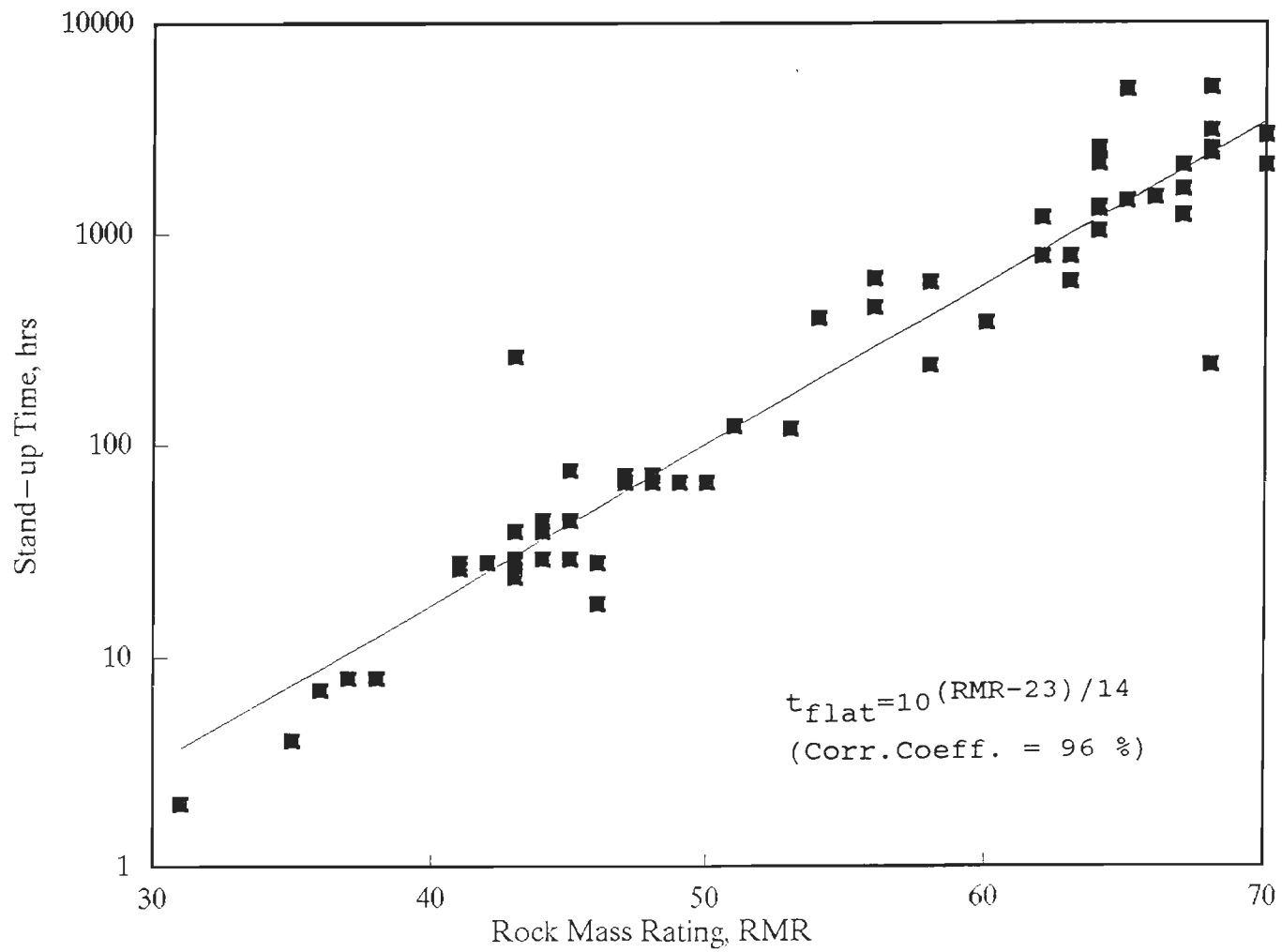
Fig.7.19 - Correlation Between Stand-up Time and RMR
for Underground Openings with Flat Roof

$$t_{arch} = 10^{(RMR-20)/15} \text{ hrs} \tag{7.22}$$

(Correlation coefficient = 81%)

$$\text{and, } t_{flat} = 10^{(RMR-23)/14} \text{ hrs} \tag{7.23}$$

(Correlation Coefficient = 96 %)

where, $t_{arch}$ and $t_{flat}$ = stand-up time for openings with arch roof and flat roof respectively.

### 7.3.6.3 Effect of opening size and overburden height on stand-up time

To study the effect of the opening size, correction factors $f_{arch}$ and $f_{flat}$ (for arch and flat roof respectively) were incorporated in Eqs. 7.22 and 7.23 in the following manner :

$$t_{arch}^{obsd} = f_{arch} \ 10^{(RMR-20)/15} \text{ hrs} \tag{7.24}$$

$$\text{and, } t_{flat}^{obsd} = f_{flat} \ 10^{(RMR-23)/14} \text{ hrs} \tag{7.25}$$

where, $t_{arch}^{obsd}$ and $t_{flat}^{obsd}$ = observed stand-up time for openings with arch roof and flat roof respectively.

The correction factors may, therefore, be expressed as:

$$f_{arch} = \frac{t_{arch}^{obsd}}{10^{(RMR-20)/15}} \tag{7.26}$$

and

$$f_{flat} = \frac{t_{flat}^{obsd}}{10^{(RMR-23)/14}} \tag{7.27}$$

The regression analysis yielded the following correlations for the correction factors calculated from Eqs. 7.26 and 7.27:

$$f_{arch} = B^{-(0.004H-0.21)} \tag{7.28}$$

and

$$f_{flat} = B^{-(0.0014H-0.24)} \tag{7.29}$$

Substitution of $f_{arch}$ and $f_{flat}$ from Eqs. 7.28 and 7.29 into Eqs. 7.26 and 7.27 respectively, gives the following correlations for the stand-up time:

$$t_{arch} = 10^{(RMR-20)/15} . B^{-(0.004H-0.21)} \quad hrs \tag{7.30}$$

and

$$t_{flat} = 10^{(RMR-23)/14} . B^{-(0.0014H-0.24)} \quad hrs \tag{7.31}$$

where, B and H are in meters.

It may be seen from Eqs. 7.30 and 7.31 that the stand-up time decreases with increase in the opening size. Further, the size effect depends upon the height of overburden. The size effect is more pronounced in deeper openings than those located at shallow depths.

### 7.3.6.4 Correction factors for obtaining $t_{arch}$ from $t_{flat}$ and effect of opening shape

Equations 7.30 and 7.31 further indicate that the opening size influences the stand-up time more in the case of the arch roof openings than in the case of the flat roof openings. This, however, does not appear to be correct. This anamoly in Eqs. 7.30 and 7.31 has its roots in the fact that the stand-up time depends on the active span of the opening and not on its total span as considered in the equations. The active span (unsupported span) is defined as the distance of the last support from the tunnel face, and the tunnel span, whichever is less (Fig.7.20). The data reported and used (for plotting the chart given as Fig.3.2) by Bieniawski (1989, pp. 207-217), shows the
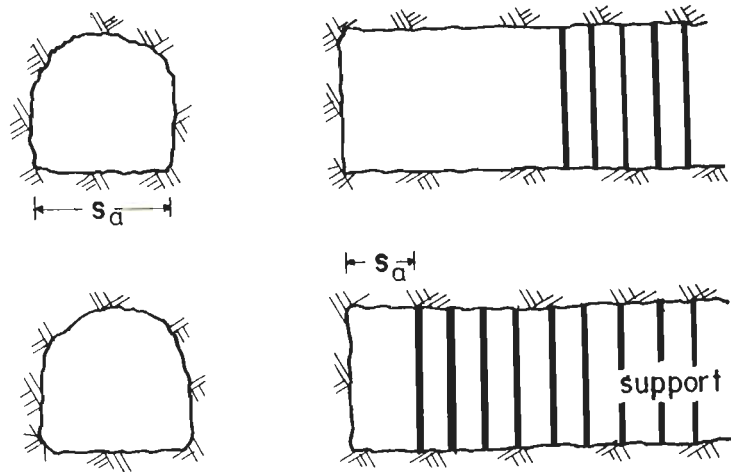
Fig.7.20 – Definition of Active Span, $S_a$



correction factor, $f_t = t_{arch}/t_{flat}$

$\geq 1$
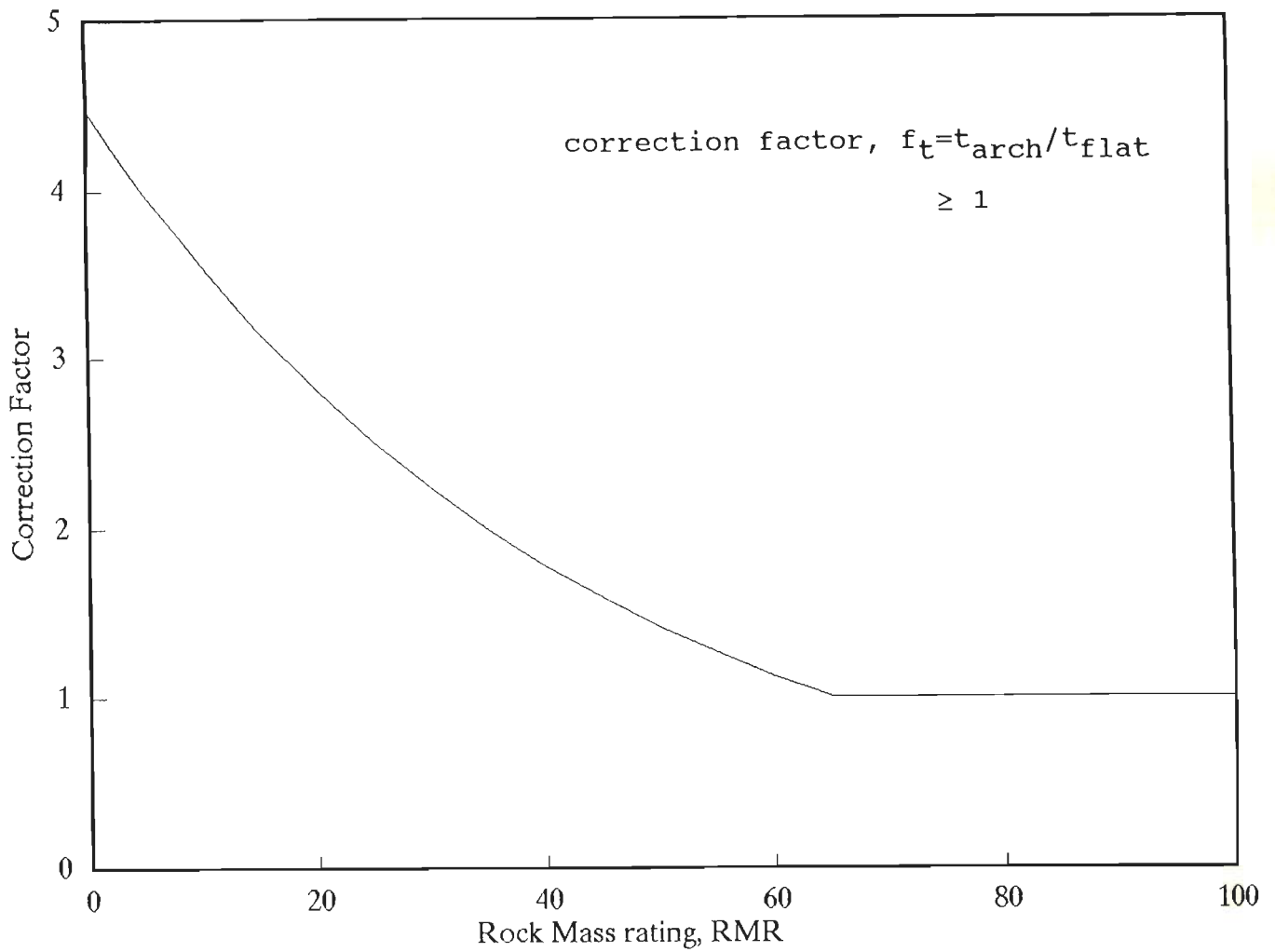
Fig.7.21 – Variation of Correction factor (Ratio of Stand-up
Times of Arch and Flat Openings) with RMR

total span of the opening and not its active span. It is, therefore, futile to seek a correlation for the stand-up time incorporating the effect of the opening size from the data given by Bieniawski (1989). The Eqs. 7.30 and 7.31, therefore, may not be used directly for estimating the stand-up time.

The analysis revealed that the correlation coefficients of Eqs. 7.30 and 7.31 are only marginally better than those of Eqs. 7.22 and 7.23. In the light of this, Eqs. 7.22 and 7.23 may be used to determine the ratio of stand-up time of the arch roof openings to that of the flat roof openings. This is given as:

$$f_t = 10^{-(RMR-65)/100} \geq 1 \qquad\qquad (7.32)$$

where, $f_t = t_{arch}/t_{flat}$

$f_t$ may be used as the correction factor for obtaining $t_{arch}$ from the following equation :

$$t_{arch} = f_t \cdot t_{flat} \qquad\qquad (7.33)$$

For using Eq. 7.33, $t_{flat}$ may be obtained from Fig.3.2 (Bieniawski, 1989) and $f_t$ may be picked up from Fig.7.21.

Equation 7.33 shows the effect of the shape of the underground opening on the stand-up time. it may be seen from Fig.7.21 that this effect is more pronounced in openings driven through relatively poor rock masses (i.e., with low RMR values), and goes on reducing with the improvement in the rock mass quality. This effect finally becomes non-existant for RMR value of 65 and above.

# CHAPTER  8

# CHAPTER 8

## CONCLUSIONS AND RECOMMENDATIONS FOR FUTURE RESEARCH

### 8.1 CONCLUSIONS

1. The overall aim of the present study is to propose a practical approach for prediction of the ground reaction and the support reaction curves for different ground conditions in order to perform the rockmass-tunnel support interaction analysis. The first logical step in this direction is to predict the ground condition, for which empirical correlations have been proposed (Art.6.2.3) on the basis of observations from instrumented tunnels. From these correlations, it can be concluded that:

(i) It is possible from Eqs.6.3 to 6.5 and Fig.6.3 to predict occurrance of squeezing, non-squeezing, or self-supporting condition on the basis of Q, height of overburden, and tunnel size.

(ii) The supporting problems may be reduced or eliminated by bringing the squeezing condition to the non-squeezing condition, and the non-squeezing condition to the self-supporting condition, by changing the tunnel alignment to obtain a better rock mass quality, or a reduced overburden, or both.

Alternatively, two or three smaller tunnels may be chosen instead of a larger tunnel to avoid squeezing ground condition, thereby reducing supporting problems and the construction time. This was done in Chhibro-Khodri tunnel after it became extremely difficult to drive a 9m diameter tunnel through squeezing ground condition.

(iii) Due to the effect of tunnel size and height of overburden, the observations in a pilot tunnel may not truely represent the ground condition likely to occur in the main tunnel, which is not only larger in size but also passes under much greater height of overburden than the pilot tunnel.

2. An empirical correlation has been proposed for prediction of the deformation modulus of dry rock masses (Eq.6.10, Art.6.3.1), which is required to be determined for obtaining the

ground reaction curve. The correlation indicates that:

(i)   The deformation modulus of the rock mass increases with increase in RMR and the tunnel depth.

(ii)  This depth dependency of the deformation modulus is likely to be more pronounced in weaker rock masses and almost absent in strong, brittle rock masses, due to the effect of the confining pressure.

3.    A semi-empirical correlation has been proposed for estimating the the cohesion of rock mass (Eq.6.25, Art.6.3.2), which is required for determination of the ground reaction curve for squeezing ground condition. The correlation has revealed that:

(i)   Mobilisation of a much higher cohesion takes place around underground openings, than the values suggested by Bieniawski (1979) on the basis of the field test data on rock slopes compiled by Hoek and Bray (1977). This indicates a strength enhancement around underground openings due to increased restraint in the freedom of propagation of fractures. As such, the cohesion parameter from block shear test needs to be multiplied with a strength enhancement factor of about 4 to 6 for determination of the ground reaction curve in the squeezing ground condition.

(ii)  The observation of this 'apparant strength enhancement' on the basis of field instrumentation data, is well supported by a number of laboratory tests conducted by several investigators on thick-walled hollow cylindrical samples.

4.    In order to propose an approach for determination of the support reaction curve, the behaviour of the steel rib-backfill support system has been studied at a number of tunnel sections. Expressions have been obtained for estimating the stiffness of the support system with different types of backfills. The study shows that:

(i)   The backfill stiffness depends on its thickness and modulus

of elasticity and on the tunnel size according to Eq.7.4. The backfill stiffness keeps on changing with increase in the support pressure on account of a pressure-dependent modulus of elasticity of the backfill. The backfill modulus of elasticity has a non-linear relationship with the support pressure.

(ii) The early stage concrete backfill cracks under low support pressure soon after it is placed behind the ribs and shows an initial loss of stiffness. The cracked concrete backfill starts getting compacted after sometime and thereafter gains stiffness with time and increasing pressure according to Eq.7.5. The gravel and the tunnel-muck backfills do not show any initial loss of stiffness. The stiffness of these backfills also increases with the support pressure (Eqs.7.6 and 7.7).

(iii) The concrete backfill, despite the initial loss of stiffness, provides a stiffer support as compared to the gravel and the tunnel-muck backfills. The concrete backfill is, therefore, preferable for elastic ground condition. The tunnel-muck backfill may be more suited to moderately squeezing ground condition and the gravel backfill to highly squeezing ground condition, as the latter is more flexible. These two types of backfills are flexible initially and gradually become stiffer with increasing support pressure, thus accommodating large deformations, which occur in squeezing ground conditions, and permitting low support pressures.

5. Effect of charging of the water conductor system on support pressure has been studied. The study has revealed that:

(i) Charging of the water conductor system creates an additional pressure (Eq.7.15) on the concrete lining due to reduction in the deformation modulus after saturation of the rock mass.

(ii) This additional suppoprt pressure may be as high as 80 percent of the insitu stress in elastic ground condition.

6. The following conclusion may be drawn from the expressions obtained for short-term support pressure in elastic and squeezing ground conditions:

The short-term support pressure is practically independent of the tunnel size if the $A_s/S$ and $t_b$ values are increased in direct proportion to the tunnel size, where $A_s$ is the

cross-section area of the steel rib, S is the rib spacing and $t_b$ is the backfill thickness.

7. Empirical correlations have been proposed for determination of the stand-up time for underground openings with arch and flat roof shapes. The correlations indicate that:

(i) The stand-up time of an underground opening depends on its span, RMR, and height of overburden. Out of these parameters, RMR has the most dominating influence on the stand-up time. Effect of the active (unsupported) span on the stand-up time could not be ascertained due to non-availability of data.

(ii) The influence of size of the opening on the stand-up time depends on the height of overburden. The size effect is more pronounced in openings located at deeper depths as compared to the shallow openings.

(iii) The stand-up time is also influenced by the shape of the underground opening according to Eq.7.32 and Fig.7.21. An opening with an arch roof has a better stand-up time than that with a flat roof for a given value of RMR. The difference in the stand-up times of the two types of openings decreses with increase in RMR and ceases to exist for RMR $\geq$ 65.

## 8.2 RECOMMENDATIONS FOR FUTURE RESEARCH

The field of tunnel mechanics is a broad one which is yet to be fully understood and perfected. There are, therefore, several possibilities for research. In this field many aspects of geology, construction engineering and rock mechanics are involved and the research may proceed along several directions. In the present study, an attempt has been made to close some of the gaps. There is, however, scope for further research work for which the following suggestions are offered.

(i) The modulus of deformation of the rock mass depends on tunnel depth, as indicated by the empirical correlation proposed for its determination. The correlation has tunnel

depth as a parameter with an exponent α whose value varies from 0.16 to 0.3. The correlation is based on field instrumentation data at locations where the RMR values lie between 31 and 68. It is likely that the value of α is more than 0.3 for RMR<31 (i.e., for very poor to poor rock masses) and less than 0.16 for RMR>68 (i.e., for good to very good rock masses). This, however, needs to be verified by further field studies and analysis of data with RMR values outside the above range. Ideally, the value of α should have a range from 0 to 1. Similar correlation is needed for saturated rock masses also.

(ii) The behaviour of steel rib-backfill support system with different types of backfills has been studied and correlations have been proposed for determination of the support reaction curves on the basis of the field instrumentation data. similar data should be collected from the rock bolt-shotcrete supported tunnels to develop an approach for determining the support reaction curve for this type of support system also. Although, tunnels in India are expected to continue to be largely steel-supported for a few years to come, a gradual switch-over to the rock bolt-shotcrete support system is very much likely due to its numerous advantages over the conventional support system. It is likely that the modulus of elasticity of shotcrete in the early stage is much lower than at its matured stage. The behaviour in the early stage will perhaps determine the support pressure.

(iii) The study indicates that upon charging of the water conductor system, additinal support pressure builds up on the concrete lining in the elastic ground condition. This needs to be verified by actual measurement of support pressure in the field before and after charging of the water conductor system.

(iii) The correlations obtained for determining the stand-up time of openings with arch roof and flat roof are based on the total tunnel span. There is a need to incorporate the active tunnel span in the correlations for evaluating its influence on the stand-up time of both types of openings, which will substantially enhance the practical utility of the correlations.

(iv) The effect of time-dependent behaviour of the rock mass and the support system should be taken into account for determination of the ground reaction and the support reaction curves. Since the steel supports do not show the creep effect, the support pressures are likely to be more in the case of visco elastic-plastic rock mass.

# REFERENCES

Auden, J.B. (1939), Rec. Geological Survey of India, 78.

Auden, J.B. (1934), Geology of the Krol Belt, Rec. Geol. Surv. of India, Vol.76, Pt.IV.

Auden, J.B. (1942), A Geological Investigation of Tunnel Alignment for Yamuna Hydroelectric Scheme, Rec. Geol. Surv. of India, vol. 78, Pt.II.

Barton, N., Lien, R. and Lunde, J. (1974), Engineering Classification of Rock Masses for the Design of Tunnel Supports, Rock Mechanics, Vol.6, No.4, pp. 189-236.

Barton, N. Lien, R. and Lunde, J. (1975), Estimation of Support Requirements for Underground Excavations, Proc. 16th Symposium on Rock Mechanics, University of Minnesota, Minneapolis, U.S.A., pp. 163-177.

Bieniawski, Z.T. (1973), Engineering Classification of Jointed Rock Masses, Transactions, South African Institution of Civil Engineers, Vol.15, No.12, pp.335-344.

Bieniawski, Z.T. (1975), Case Studies - Prediction of Rock Mass Behaviour by the Geotechnical Classification, 2nd Australia - New Zealand Conference on Geomechanics, Brisbane, pp.36-41.

Bieniawski, Z.T. (1975), Case Studies - Prediction of Rock Mass Behaviour by the Geomechanical Classification, 2nd Australia - New Zealand Conference on Geomechanics, Brisbane, pp.36-41.

Bieniawski, Z.T. (1976), Rock Mass Classifications in Rock Engineering, Proc. Symposium on Exploration for Rock Engineering, ed. Z.T. Bieniawski, A.A. Balkema, Rotterdam, pp. 97-106.

Bieniawski, Z.T. (1978), Determining Rock Mass Deformability, Experience from Case Histories', International Journal of Rock Mechanics and Mining Sciences, Vol.15, pp. 237-247.

Bieniawski, Z.T. (1979), The Geomechanics Classification in Rock Engineering Applications Proc. 4th Congress of International Society for Rock Mechanics, Montreux, Vol.2, pp. 51-58.

Bieniawski, Z.T. (1984), Rock Mechanics in Mining and Tunnelling, A. A. Balkema, Rotterdam, 272 p.

Bieniawski, Z.T. (1989), Engineering Rock Mass Classifications, John Wiley & Sons, 251 p.

Boisen, B.P. (1990), Applied Underground Instrumentation, Proc. ISRM International Symposium on Static and Dynamic

Considerations in Rock Engineering, Swaziland, September 10-12, pp. 41-47.

Bray, J.W. (1967), A Study of Jointed and Fractured Rock, Part-II-Theory of Limiting Equilibrium, Rock Mechanics and Engineering Geology, Vol.5, No.4, Vienna, Austria, pp. 197-216.

Brekke, T.L. and Howard, T.R. (1972), Stability Problems Caused by Seams and Faults, Proc. North American Rapid Excavation and Tunnelling Conference, Chicago, ed. by Lane and Garfield, AIME, Vol.1, pp. 25-41.

Brown, E.T., Bray, J.W., Ladanyi, B. and Hoek, E. (1983), Ground Response Curves for Rock Tunnels, Journal of Geotechnical Engineering, ASCE, Vol. 109, No.1, pp. 15-31.

Brown, E.T., Bray, J.W. and Santarelli, F.J. (1989), Influence of Stress-Dependent Elastic Moduli on Stress and Strains Around Axisymmetric Boreholes, Rock Mechanics and Rock Engineering, Vol.22, pp. 189-203.

Carter, J.P. and Booker, J.R. (1990), Sudden Excavation of a Long Circular Tunnel in Elastic Ground, International Journal of Rock Mechanics and Mining Sciences, Vol.27, No.2, pp. 129-132.

Carvalho, O. and Kovari, K. (1977), Displacement Measurements as a Means for Safe and Economical Tunnel Design, Proc. International Symposium on Field Measurements in Rock Mechanics, Zurich, Vol.2, pp.

Cecil, O.S. (1970), Shotcrete Support in Rock Tunnels in Scandinavia, Civil Engineering, ASCE, pp. 74-79.

Chang, W.C. (1990), Application and Limitation of Extensometer for Tunnel Monitoring, Proc. 31st U.S. Symposium on Rock Mechanics Contributions and Challanges, Golden, June 18-20, pp. 421-428.

Choudhury, A.K. and Chattopadhyay, B. (1982) Geological Set-up and Prediction of Tunnelling Problems Along Tunnel Alignment, Loktak Hydel Project, Manipur, India, Proc. 4th International Congress of International Association of Engineering Geology, New Delhi, Dec. 10-15, Vol.IV, pp.IV 93- IV 100.

Corbetta, F., Bernaud, D. and Minh, D.N. (1991), Contribution to the Convergence-Confinement Method by the Principle of simlitude (in French), Rev Fr Geotech, No.54, pp. 5-11.

Cording, E.J. and Deere, D.U. (1972), Rock Tunnel Supports and Field measurements, Proc. North American Rapid Excavation and Tunnelling Conference, ed. by Lane and Garfield, AIME, Chicago, Vol.1, pp. 601-622.

Cording, E.J., Hendron, A.J. and Deere, D.U. (1971), Rock Engineering for Underground Caverns, Symposium on Underground Chambers, ASCE, Phoenix, Arizona, pp. 567-600.

Daemen, J.J.K. (1975), Tunnel Support Loading Caused by Rock Failure, Technical Report MRD-3-75, Missouri River Division, U.S. Corps of Engineers, Omaha, Neb.

Daemen, J.J.K. (1977), Problems in Tunnel Support mechanics, Underground Space, Vol.1 No.3, pp. 163-172.

Daemen, J.J.K., and Fairhurst, C. (1971), Influence of Failed Rock Properties on Tunnel Stability, Dynamic Rock Mechanics, Proc . 12th Symposium on Rock Mechanics, AIME, New York, N.Y., pp. 855-875.

Dayal, H.M. and Mandwal, N.K. (1969), Progress Report No.5 on the Construction Stage Geological Investigations for Giri-Bata Link Project Stage I, Giri Valley Hydel Scheme, Himachal Pradesh, Unpubl. Rep. of Geol. Surv. of India.

Deere, D.U. (1964), Technical Description of Rock Cores for Engineering Purposes, Rock Mechanics and Engineering Geology, Vol.1, No.1, pp. 17-22.

Deere, D.U., Peck, R.B., Parker, H., Monsees, J.E. and Schmidt, B. (1970), Design of Tunnel Support Systems, Highway Research Record, No.339, pp. 26-33.

Detournay, E. and Fairhurst, C. (1987), Two-dimensional Elastoplastic Analysis of a Long, Cylindrical Cavity under Non-hydrostatic Loading, International Journal of Rock Mechanics and Mining Sciences, Vol.24, No.4, pp. 197-211.

Diest, F.H. (1967), A Nonlinear Continuum Approach to the Problem of Frcture Zones and Rockbursts, Journal of the South African Institute of Mining and Metallurgy, Vol. 65, No.10, Johannesburg, South Africa, pp.502-522.

Douglas, T.H. and Alexander, R.J. (1989), Dinorwig Power Station - Results of Long Term Monitoring, Proc. Conference on Instrumentation in Geotechnical Engineering, Nottingham, April 3-5, Vol.I, pp. 301-318.

Dube, A.K. (1979), Geomechanical Evaluation of Tunnel Stability Under Failing Rock Conditions in a Himalayan Tunnel, Ph.D. Thesis, Deptt. of Civil Engg., University of Roorkee, Roorkee, India.

Duddeck, H. (1980), On the Basic Requirements for Applying the Convergence-Confinement Method Underground Space, Vol.4, No.4, pp. 241-247.

Duncan Fama, M.E. and Brown, E.T. (1989), Influence of Stress Dependent Elastic Moduli on Plane Strain Solution for Boreholes, Proc. International Symposium on Rock at Great Depth, Pau, France, 28-31 August, vol.2, pp. 819-826.

Dutro, H.B. and Perry, D.J. (1987), Measuring up for Tunnel Construction, Tunnels and Tunnelling, Vol.19, No.6, June, pp.47-51

Dunnicliff, C.J. and Schmidt, B. (1974), An Engineering Approach to Monitoring the Performance of Soft ground Tunnels under Construction. Proc. Rapid Excavation and Tunnelling Conference, AIME, New York, pp. 377-396.

Egger, P. (1974), Gebirgsdruck im Tunnelbau and Stutzwirkung der Ortsburst bei Uberschreiten der Gebirgsfestigkeit, Advances in Rock Mechanics, Proc. 3rd Congress of the International Society for Rock Mechanics, Vol.2, Part B, National Academy of Sciences, Washington, D.C., pp.1007-1011.

Egger, p. (1980), Deformations at the Face of the Heading and Determination of the Cohesion of the Rock Mass, Underground Space, Vol.4, No.5, pp.313-318.

Einstein, H.H. and Schwartz, C.W. (1979), Simplified Analysis for Tunnel Supports, Journal of the Geotechnical Engineering Division, ASCE, GT4, April, pp. 499-518.

Eisenstein, Z. and Branco, P. (1991), Convergence-Confinement Method in Shallow Tunnels, Tunnelling and Underground Space Technology, Vol.6, No.3, pp. 343-346.

Fairhurst, C. (1964), On the Validity of the Brasilian Test for Brittle Materials, International Journal of Rock Mechanics and Mining Sciences, Vol.1, pp. 535-546.

Fenner, R. (1938), Untersuchungen zur Erkenntnis des Gebirgsdruckes, Gluckauf, Vol.74, Essen, Germany, pp.681-695 and 705-715.

Florence, A.L., and Schwer, L.E. (1978), Axisymmetric Solution of a Mohr-Coulomb Medium Around a Circular Hole, International Journal for Numerical and Analytical Methods in Geomechanics, Vol.2, No.4, pp.367-379.

Fritz, P. (1982), Modelling Rheological Behaviour of Rock, Proc. 4th International Conference on Numerical Methods in Geomechanics, Edmonton, June.

Fritz, P. (1984), An Analytical solution for Axisymmetric Tunnel Problems in Elasto-Viscoplastic Media, International Journal for Numerical and Analytical Methods in Geomechanics, Vol.8, pp. 325-342.

Fuenkajorn, K. and Daemen, J.J.K. (1992), Borehole Stability in Densely Welded Tuffs, Report No. NUREG/CR-5687, Deptt. of Mining and Geological Engg., University of Arizona, Tucson, USA, 58 p.

Geological Survey of India (1977), Longitudinal Cross-section of Giri Hydel Tunnel, Northern Region, D.O. No. 295-9-77.

Geological Survey of India (1979),

Gesta, P., Kerisel, J., Londe, P. Louis, C. and Panet, M. (1980), General Report: Tunnel Stability by the Convergence-Confinement Method, Underground Space, Vol.4, No.4, Feb., pp.225-232.

Ghosh, S.K. (1970), Progress Report of Giri-Bata Tunnel, Field Session 1969-70, Unpublished Report of Geological Survey of India.

Gill, D.E. and Ladanyi, B (1983), The Characteristic Line Concept of Lining Design in Creeping Ground, Proc. CIM Symposium on Underground Support Systems, Sudbury, Ontario, CIM Special Volume.

Gill, D.E. and Ladanyi, B. (1987), Time-dependent Ground Response Curves for Tunnel Lining Desgin, Proc. 6th International Congress on Rock Mechanics, Vol.2, Theme 4, pp.917-921.

Golser, J. (1973), Praktishe Beispiele Empirischer Dimensionieung von Tunneln, Rock Mechanics, Suppl. 2, Springer, pp.225-241.

Grosvener, N.E. and Abel, J.F. (1966), Measurement on the Pilot Bore for Straight Creek Tunnel, Highway Research Board Record No.135.

Guenot, A. (1987), Contraintes et Ruptures Autour de Forages Petroliers, Proc. 6th Congress of International Society for Rock Mechanics, Montreal, Vol.1, pp. 109-118.

Guenot, A. (1989), Borehole Breakouts and Stress Fields, International Journal of Rock Mechanics and Mining Sciences, Vol.26, No.3, pp. 185-195.

Haimson, B.C. and Edl, J.N. (1972), Hydraulic Fracturing of Deep Wells, Soc. Petrol. Engrs. Paper No. 4061.

Hendron, A.J. and Aiyer, A.K. (1972), Stresses and Strains Around a Cylindrical Tunnel in an Elasto-Plastic Material with Dilatancy, Technical Report No.10, Missouri River Division, U.S. Corps of Engineers, Omaha, Neb.

Hills, S.F., Szalay, K.A., Rourke, J.E. and Smith, D.(1974), Instrumentation of Tarbela Dam Tunnels, Proc. of Rapid Excavation and Tunnelling Conference, San Francisco, California, Vol.2, pp.1275-1303.

Histake, M., Cording, E.J., Ito, T., Sakurai, S. and Phien-Weja, N. (1989), Effects of Non-linearity and Strength Reduction of Rocks on Tunnel Movements, Proc. International Symposium on Rock at Great Depth, Pau, France, 28-31 August, vol.2, pp. 553-560.

Hobbs, D.W.(1966a), A Study of the Behaviour of Broken Rock under Triaxial Compression and Its Application to Mine Roadways, International Journal of Rock Mechanics and Mining Sciences, Vol.3, pp.11-43.

Hobbs, D.W. (1966b), The Strength of Coal under Biaxial Compression, Colliery Engg. 39, pp. 285-290.

Hoek, E. and Bray, J.W. (1977), Rock Slope Engineering, Revised Second Edition, Institution of Mining and Metallurgy, London.

Hoek, E. and Brown, E.T. (1980 a), Underground Excavations in Rock, The Institution of Mining and Metallurgy, London, England.

Hoek, E. and Brown, E.T. (1980 b), Empirical Strength Criterion for Rock Masses, Journal of the Geotechnical Engineering Division, ASCE, Vol.106, No.GT9, Proc. Paper 15715, pp.1013-1035.

Hoskins, E.R. (1969), The Failure of Thick Walled Hollow Cylinders of Isotropic Rock, International Journal of Rock Mechanics and Mining Sciences, Vol.6, pp.99-125.

Hudson, J. A. (1993), Personal Discussion on January 20 at University of Roorkee, Roorkee, India.

Indraratna, B. and Kaiser, P.K. (1990), Design for Grouted Rock Bolts Based on the Convergence Control Method, International Journal of Rock Mechanics and Mining Sciences, Vol. 27, No.4, pp. 269-281.

Jain, M.S., Andotra, B.S. and Sondhi, S.N. (1975), Note on Geological Features of the Chhibro-Khodri Tunnel and Occurences of Subathu Shales, Unpubl. Re.of Geol. Surv. of India.

Jain M.S., Jaitle, G.S., Sondhi, S.N. and Rajagopalan, G. (1976), Geotechnical Note on Alternative Alignments Between Heena and Tiloth Adits, Memo XIV Meeting, Board of Consultants, Maneri Stage-I Project.

Jethwa, J.L. (1981), Evaluation of Rock Pressures in Tunnels through Squeezing Ground in Lower Himalayas, Ph.D. Thesis, Deptt. of Civil Engg., University of Roorkee, Roorkee, India, 272 p.

• Jethwa, J.L., Dube, A.K., Singh, B. and Mithal R.S. (1982), Evaluation of Methods of Tunnel Support Design in Squeezing Rock Conditions, Proc. 4th International Congress of International Association of Engineering Geology, New Delhi, Dec.10-15, Vol.5, pp. A101-A109.

Jethwa, J.L., Goel, R.K., Verman, M., Prabhakar, B. and Singh, B. (1988), A report on Ground Control Problems and Rock mechanics Instrumentation of Bagur-Navile Tunnel, Hemavathy Project, Karnataka, October.

Kaiser, P.K. (1980), Effect of Stress History on the Deformation Behaviour of Underground Openings, Underground Rock Engineering, Proc . 13th Canadian Rock Mechanics Symposium, The Canadian Institute of Mining and Metallurgy, Montreal, Canada, pp. 133-140.

Kaiser, P.K. (1981), A New Concept to Evaluate Tunnel Performance-Influence of Excavation Procedure, Rock Mechanics from Research to Application, Proc. 22nd U.S. Symposium on Rock Mechanics, Massachusetts Institute of Technology, Cambridge, Mass., pp. 264-271.

Kaiser, P.K., Guenot, A. and Morgenstern, N.R. (1985), Deformation of Small Tunnels-IV, Behaviour During Failure, International Journal of Rock Mechanics and Mining Sciences, Vol.22, pp.141-152.

Kastner, H (1949), Uber den echten Gebiergsdruck beim Bau tiefliengender Tunnel, Osterreich Bauzeitschrift, Vol.10, No.11, Vienna, Austria.

Kennedy, T.C. and Lindberg, H.E. (1978), Tunnel Closure for Nonlinear Mohr Coulomb Functions, Journal of the Engineering Mechanics Division, ASCE, Vol.104, No.EM6, Proc. Paper 14245, Dec., pp.1313-1326.

Korbin, G.E. (1976), Simple Procedure for the analysis of Deep Tunnels in Problematic Ground, Site Characterisation, Pre-print-Proc. 17th U.S. Symposium on Rock Mechanics, W.S. Brown, S.J. Green and W.A. Hustrulid, eds, University of Utah, Salt Lake City, Utah, pp. 1A-3-1-1A3-7.

Kovari, K., Amstad Ch. and Grob, H. (1974), Displacement Measurements of High Accuracy in Underground Openings, Proc. 3rd International Congress of the International Society for Rock Mechanics, Denver, September 1-7, Vol.II, Part A, pp. 445-450.

Krishnaswami, V.S. (1967), A Geological Review of the Construction and Post-construction Problems Anticipated in the Crossing of the Krol-Nahan Intra-thrust Zone by Tons-Yamuna Tunnel of Stage II, Phase II, Yamuna Hydel Scheme, U.P., Unpubl.Re.of Geol. Surv. of India.

Krishnaswami, V.S. and Jalote, S.P. (1968), A Geological Note on the Exploration of the Alternative Layouts for the Tons-Yamuna Tunnel, Yamuna Hydel Scheme, Stage II, Part II, U.P. Unpubl. Rep. of Geol.Surv. of India.

Kulhawy, F.H. (1975), Stress Deformation Properties of Rock and Rock Discontinuities,Engineering Geology, Vol.9, pp.327-350.

Kumar, P. and Singh, Bhawani (1990), Design of Reinforced Concrete Lining in Pressure Tunnels Considering Thermal Effects and Jointed Rockmass, Tunnelling and Underground Space Technology, Vol.5, No.1/2, pp.91-101.

Labasse, H. (1949), Les Pressions de Terrains dans les Mines de Huiles, Revue Universelle des Mines, Liege, Belgium, Series 9, Vol.5, No.3, pp.78-88.

Ladanyi, B. (1974), Use of the Long-Term Strength Concept in the Determination of Ground Pressure on Tunnel Linings, Advances in Rock Mechanics, Proc. 3rd Congress of the International Society for Rock Mechanics, Vol.2, Part B, National Academy of Sciences, Washington, D.C., pp.1150-1156.

Ladanyi, B. (1980), Direct Determination of Ground Pressure on Tunnel Lining in a Non-linear Visco-elastic Rock, Proc. 13th Canadian Rock mechanics Symposium, Montreal, pp. 126-132.

Ladanyi, B. and Gill, D.E. (1984), Tunnel Lining Design in a Creeping Rock, Proc. ISRM Symposium on Design and Performance of Underground Excavations, Cambridge, U.K., Vol.I, pp. 19-26.

Lane, K.S. (1957), Effect of Lining Stiffness on Tunnel Loading, Proc. 4th Int. Conf. on SMFE, Vol.2, pp.223-227.

Lane, K.S. (1975), Field Test Sections Save Cost in Tunnel Support, American Society of Civil Engineers, October, 59 p.

Lauffer, H. (1958), Gebirgsklassifizierung fur den Stollenbau, Geologie und Bauwesen, Vol.24, No.1, pp. 46-51.

Lo, K.Y. and Ramsay, J.A. (1991), The Effect of Construction on Existing Subway Tunnels - a Case Study from Toranto, Tunnelling and Underground Space Technology, Vol.6, No.3, pp. 287-297.

Lombardi, G. (1966), `Discussion', Proc. Ist Congress of the International Society of Rock Mechanics, Lisbon, Theme 7, Vol.3, pp.525-526.

Lombardi, G. (1970), Influence of Rock Characteristics on the Stability of Rock Cavities, Tunnels and Tunnelling, vol.2, No.1, Jan-Feb., London, England, pp.19-22, Vol.2, No.2, Mar.-Apr., pp.104-109.

Lombardi, G. (1973), Dimensioning of Tunnel Linings with Regard to Constructional Procedure, Tunnels and Tunnelling, Vol.5, pp. 340-351.

Lombardi, G. (1977), Long-Term Measurements in Underground Openings and their Interpretation with Special Consideration to the Rheological Behaviour of Rock, Proc. International Symposium on Field Measurements in Rock Mechanics, Zurich, K. Kovari, ed., Vol.2, A.A. Balkema, Rotterdam, Holland, pp. 839-858.

Lombardi, G. (1980), Some Comments on the Convergence-Confinement Method, Underground Space, Vol.4, No.4, Jan-Feb., pp.249-258.

Lu, J. (1986), Elastoplastic Analysis of Rock Masses Surrounding Circular Opening Considering Strain Hardening, Proc. Intdrnational Symposium on Large Rock Caverns, Helsinki, 25-28 August, Vol.2, pp. 1329-1335.

Madhavan, K. (1982), Tunnelling in Rock with High In-situ Stresses, Proc. 4th International Congress of International Association of Engineering Geology, New Delhi, Dec. 10-15, Vol.V, pp. V79-V84.

Malhotra, R.K., Tyagi, G.D. and Sharma, K.S. (1982), NATM for Tunnel Boring at Loktak H.E. Project, Proc. Symposium on Tunnelling, 52nd Board Session of the Central Board of Irrigation and Power, New Delhi, June 8-10, pp.35-58.

Maury, V. (1987), Observations, Recherches et Resultats Recents sur les Mecanismes de Ruptures Autour Galeries Isolees, Proc. 6th Congress of International Society for Rock Mechanics, Montreal, Vol.2, pp. 1119-1126.

Mehrotra, V.K. (1992), Estimation of Engineering Parameters of Rock Mass, Ph.D. Thesis, Department of Civil Engineering, University of Roorkee, Roorkee, India.

Merrit, A.H. (1972), Geologic Prediction for Underground Openings, Proc. North American Rapid Excavation and Tunnelling Conference, Chicago, ed. by Lane and Garfield, AIME, Vol.1, pp. 115-133.

Minh, N.D. and Berest, P. (1979), Etude de Ia Stabilite des Cavites Souteraines avec un Modele de Comportement Elastoplastique Radoucissant, Proc. 4th Congress of the International Society for Rock Mechanics, Vol.1, A.A.Balkema, Rotterdam, Holland, pp. 249-256.

Mitri, H.S. and Hassan, F.P. (1990), Structural Characteristics of Coal Mine Steel Arch Supports, International Journal of Rock Mechanics and Mining Sciences, Vol.27, No.2,pp.121-127.

Morrison, R.G.K. and Coates, D.F. (1955), Soil Mechanics Applied to Rock Faulure in Mines, The Canadian Mining and Metallurgical Bulletin, Vol.48, No.523, Montreal, Canada, pp.701-711.

Pacher, F. (1964), Deformations Messungen im Versuchsstollenals Mittel zur Erorschung des Gebirgsverhaltens and zur Bemessung des Ausbaues, Felsmechanik and Ingenieurgeologie, Supplementum IV, pp.149-161.

Pacher, F., Rabcewicz, L. and Golser, J. (1974), Zum der seitigen Stand der Gebirgsklassifizierung in Stollen-und Tunnelbau, Proc. XXII Geomechanics Colloquium, Salzburg, pp. 51-58.

Panet, M. (1976), Analyse de la Stabilite d'un Tunnel Creuse dans un Massif Rocheux en Tenant Compte du Comportement apres la Rupture, Rock Mechanics, Vienna, Austria, Vol.8, No.4, pp.209-233.

Pant, G., Kumar, V. and Gupta, U.P. (1982), Tunnelling Experience at Tehri Dictates the Choice of Layout and Support Methodology of Underground Power House, 4th Congress of International Association of Engineering Geology, Dec.10-15, New Delhi, India, pp. IV 83 - IV 87.

Rabcewicz, L.V. (1964), The New Austrian Tunnelling Method, Water Power Vol.16, No.11, Part 1, pp.453-456, Vol.16, No.12, Part 2, pp.511-515.

Rabcewicz, L.V. (1969), Stability of Tunnels under Rock load, Water Power, June, pp.225-229; July, pp.266-273; August, pp.297-302.

Rajvanshi, U.S. (1985), Undermining of Overt Lining of Diversion Tunnels of Tehri Dam Project - A Case Study, Proc. 3rd Symposium on Rock Mechanics, Roorkee, Nov. 16-18, pp.V47-V55.

Ray, S. (1968), A Geological Report on Loktak Hydroelectric and Reclamation Project, Manipur, Unpubl. Rep. of Geol. Surv. of India.

Richter, R. (1966), Das Mittelbare Ingleichgewich thal ten bei Untertagigen Hohlraumen, Proc. 1st Congress of the International Society of Rock Mechanics, Lisbon, Vol.2, pp.375-378.

Sakurai, S. (1970), Stability of Tunnel in Viscoelastic-plastic Medium, Proc. 2nd Congress of International Society for Rock Mechanics, Vol.2, pp. 521-529.

Sakurai, S. (1983), Displacement Measurements Associated with the Design of Underground Openings, Proc. International

Symposium on Field Measurements in Geomechanics, Zurich, September 5-8, Vol.2, pp. 1163-1178.

Salencon, J. (1969), Contraction Quasistatique d'une Cavite a Symetrie Spherique ou Cylindrique dans un Milieu Elastoplastique, Annales des Ponts et Chaussees, No.4, Paris, France, July-Aug., pp. 231-236.

Sanchez-Trejo, Roberto and Moreno-Fernandez, Andres (1983), Behaviour of a Tunnel Excavated through Soft Ground by Means of a Shield and Compressed Air Chambers, Proc. International Symposium on Field Measurements in Geomechanics, Zurich, September 5-8, Vol.2, pp. 1179-1189.

Santarelli, F.J. (1987), Theoretical and Experimental Investigation of the Stability of the Axisymmetric Wellbore, Ph.D. Thesis, University of London.

Santarelli, F.J. and Brown, E.T. (1987), Performance of Deep Wellbores in Rock with a Confining Pressure-Dependent Elastic Modulus, Proc. 6th Congress of International Society for Rock Mechanics, Montreal, Vol.2, pp. 1217-1222.

Senseny, P.E., Lindberg, H.E. and Schwer, L.E. (1989), Elastic-Plastic Response of a Circular Hole to Repeated Loading, International Journal for Numerical and Analytical Methods in Geomechanics, Vol.13, pp. 459-476.

Serafim, J.L. and Pereira, J.P. (1983), Considerations of the Geomechanics Classification of Bieniawski. Proc. International Symposium on Engineering Geology and Underground Construction, LNEC, Lisbon, Portugal.

• Serata, S. (1964), Theory and Model of Underground Opening and Support System, Proc. 6th Symposium on Rock Mechanics, University of Missouri, Rolla, pp.260-292.

Sharma, V.M. (1985), Prediction of Closure and Rock Loads for Tunnels in Squeezing Ground, Ph.D. Thesis, Indian Institute of Technology, Delhi, 254 p.

Shome, S.K., Andotra, B.S. and Jain, M.S. (1973), Review of Failure Patterns in the Stage II Tunnels of Yamuna Hydroelectric Scheme, Dehradun District, Symposium on Rock Mechanics and Tunnelling Problems, Kuruskshetra Univ., Vol.1, pp. 70-79.

Shome, S.K. and Dayal, H.M. (1965), The Progress Report No.2 on the Pre-construction Stage Geological Investigations for the Giri Valley Hydel Scheme, Stage I,II and III, Sirmur, H.P., Unpubl. Rep. of Geol. Surv. of India.

Shome, S.K. and Dayal, H.M. (1966), On the significance of Recent Faulting in the Siwaliks to the Location of Majri Power House Site, Giri Valley Scheme, Stage I, Sirmur, H.P., Proc.

3rd Symposium on Earthquake Engg., Roorkee University, India.

Shome, S.K. and Dayal, H.M. (1967), Progress Report No.3 on the Pre-construction Stage Geological Investigations for Giri Valley Hydel Scheme, Stage I, Sirmur, H.P., Unpubl. Rep. of Geol. Surv. of India.

Shome, S.K. and Kumar, V. (1979), Geology and Foundation Treatment of Tehri Dam Project, U.P., India, Proc. Workshop on Tehri Dam Project, Dec. 4-6 Vol.-1, pp.1-21.

Singh, Bhawani (1973), Continuum Characterisation of Jointed Rockmass, International Journal of Rock Mechanics and Mining Sciences, Vol.10, pp.311-349.

Singh, Bhawani and Jethwa, J.L. (1993), Unpublished Paper.

Singh, R. N. and Aziz, N., I. (1983), Instrumentation for Stability Evaluation of Coal Mine Tunnels and Excavations, Proc. International Symposium on Field Measurements in Geomechanics, Zurich, September 5-8, Vol.2, pp. 1191-1204.

Singh, R.P. and Choudhury, A.K. (1975), A Note on the Geological Set-up along the Tunnel Route and its Influence on Tunnelling Conditions at Loktak Hydel Project, Manipur, Rep. of Geol. Surv. of India.

Singh, Bhawani, Jethwa, J.L., Dube, A.K. and Singh B. (1992), Correlation Between Observed support pressure and Rock Mass Quality, Tunnelling and Underground Space Technology, Vol.7, No.1, pp.59-74.

Sirieys, P.M. (1964), Champs de Contraintes Autour des Tunnels Circulaires en Elastoplasticite, Felsmechanik und Ingenieurgeologie, Vol.II/1, pp.62-75.

Stillborg, B., Pekkari, M. and Pekkari, R. (1983), An Advanced Rock Mechanics Monitoring System, Proc. International Symposium on Field Measurements in Geomechanics, Zurich, September 5-8, Vol.2, pp. 1215-1227.

Stille, H., Holmberg, M. and Nord, G. (1989), Support of Weak Rock with Grouted Bolts and Shotcrete, International Journal of Rock Mechanics and Mining Sciences, Vol. 26, No.1, pp. 99-113.

Stimpson, B. (1991), Simplified Rock Mass-Bolt Interaction Analysis for Horizontally Layered Strata, Geotech Geol Engg., Vol.9, No.1, March, pp. 27-51.

Stini,I.(1950), Tunnelbaugeologie, Springer-Verlag, Vienna 336 p.

Takino, K., Kimura, H., Kamemura, K. and Kawamoto, T. (1983), 3-Dimensional Ground Behaviour at Tunnel Intersections, Proc. International Symposium on Field Measurements in Geomechanics, Zurich, September 5-8, Vol.2, pp. 1237-1246.

Tattersall, F., Wakeling, T.R.M. and Ward, W.H. (1955), Investigations into the Design of Pressure Tunnels in London Clay, Proc. Inst. of Civil Engineers, London, Paper No. 6027, Vol. 4, Part I, pp.400-471.

Terzaghi, K. (1919), Die Erddruckerschinungen, Oesterr. Wochenschr. Oeffentl. Baudienst, Heft 17, pp. 194-199; H. 18, pp. 206-210; H.19, pp. 218-233.

Terzaghi, K. (1925), Erdbaumechanik auf Bodenphysikalischer Grundlage, Franz Deuticke, Vienna, Austria, pp. 212-214.

Terzaghi, K. (1942), Shield Tunnels of the Chicago Subway, Journal of the Boston Society of Civil Engineers, Vol.28, pp.163-210.

Terzaghi, K. (1943), Theoretical Soil Mechanics, John Wiley and Sons Inc., New York, pp.202-215.

Terzaghi, K. (1946), Rock Defects and Load on Tunnel Supports, Introduction to Rock Tunnelling with Steel Supports by Proctor, R.V. and White, T.L., Commercial Shearing and Stamping Co., Youngstown, Ohio, U.S.A.

Timoshenko, S.P. and Gere, J.M. (1961), Theory of Elastic Stability, 2nd ed., McGrew Hill Book Co.

Ueng, T., Kao, C., Chi, B. and Huang, T. (1983), Field Instrumentation of Minghu Underground Powerplant Excavation, Proc. International Symposium on Field Measurements in Geomechanics, Zurich, September 5-8, Vol.2, pp. 1247-1256.

Unal, E. (1983), Design Guidelines and Roof Control Standards for Coal Mine Roofs. Ph.D. Thesis, The Pennsylvania State University.

Varshney, R.S. (1988), Tunnelling in Squeezing Rock, Proc. International Symposium on Tunnelling for Water Resources and Power Tunnels, New Delhi, January, pp. 37-47.

Verma, M.S. and Rajvanshi, U.S. (1988), Analysis of Supports for Diversion Tunnels of Tehri Dam Project - A comparative Study, Proc. International Symposium on Underground

Engineering, New Delhi, April 14-17, Vol. I, pp.131-137.

Verman, M., Jethwa, J.L. and Goel, R.K. (1993), Estimation of Wall Support Requirements for Underground Power House Cavern of Sardar Sarovar Project in India, to be published in Proc. of International Congress 'Options for Tunnelling', Amsterdam, April 19-22.

Verman, M., Jethwa, J.L. and Singh, B. (1991), Monitoring of a Large Underground Power House Cavity, Proc. 7th International Congress of International Society for Rock Mechanics, Aachen, pp. 1233-1236.

Ward, W.H. (1955), Techniques for Field Measurements of Deformation and Earth Pressures, Trans. of Inst. of Civil Engineerrs, London, pp. 338-358.

Ward, W.H. and Chaplin, T.K. (1957), Existing Stresses in Several Old London Underground Tunnels, Proc. 4th International Conference on SMFE, pp.256-260.

Ward, W.H., Coates, D.J. and Tedd. P. (1976), Performance of Tunnel Support Systems in the Four Fathom Mudstone, Proc. "Tunnelling'76", Institution of Mining and Metallurgy, London, pp. 329-340.

Ward, W.H. and Thomson, H.S.H. (1965), The Development of Earth Loading and Deformation in Tunnel in London Clay, Proc. 6th Int. Conf. on SMFE, Montreal, pp. 432-437.

Whittaker, B.N., Hassani, F.P., Bonsall, C.J. and White M.J. (1983), Investigation into the Development of Rock Yield Zones Around Mining Tunnels, Proc. International Symposium on Field Measurements in Geomechanics, Zurich, September 5-8, Vol.2, pp. 1257-1266.

Wickham, G.E., Tiedmann, H.R. and Skinner, E.H. (1972), Support Determinations Based on Geologic Predictions, Ist North Americam Rapid Excavation and Tunnelling Conference, Chicago, Vol.1, Am.Inst. Min. Met. and Pet. Engr. Inc., New York.

Wickham, G.E. Tiedmann, H.R. and Skinner, E.H. (1974), Ground Support Prediction Model-RSR Concept, North American Rapid Excavation and Tunnelling Conference, San Francisco, California, Vol.1, pp. 691-708.

Yashimura, H., Yuki, T., Yamada, Y. and Kokubun, N. (1986), Analysis and Monitoring of the Miyana Railway Tunnel Constructed Using the New Austrian Tunnelling Method, International Journal of Rock Mechanics and Mining Sciences, Vol.23, pp.68-75.

## APPENDIX A

## ADDITIONAL SUPPORT PRESSURE DUE TO
## CHARGING OF WATER CONDUCTOR SYSTEM

From Eq.6.7 for elastic ground condition,

$$u_a = (1+\nu)(p_o-p_i)/E_d \tag{A.1}$$

Rewriting Eq.A.1 for dry and saturated rock mass conditions (i.e., before and after charging of the water conductor system), and equating the right hand sides of the resulting equations (tunnel closure is the same for both the conditions - Fig.7.13),

$$(1+\nu)(p_o-p_{idry})/E_{dry} = (1+\nu)(p_o-p_{isat})/E_{sat} \tag{A.2}$$

where, $p_{isat}$ = short-term support pressure in saturated condition.

From Eq.A.2,

$$p_{isat} = p_o[(1-(E_{sat}/E_{dry})] + p_{idry}(E_{sat}/E_{dry})$$

or, $\Delta p_{isat} = p_o[(1-(E_{sat}/E_{dry})] - p_{idry}[(1-(E_{sat}/E_{dry})] \tag{A.3}$

where, $\Delta p_{isat} = p_{isat}-p_{idry}$

Eq.A.3 may be written as,

$$\Delta p_{isat} = [(1-E_{sat}/E_{dry})](p_o-p_{idry}) \tag{A.4}$$

which is the same as Eq.7.13.

## APPENDIX B

### EXPRESSION FOR SUPPORT PRESSURE IN ELASTIC GROUND CONDITION

From Eq.6.7 for ground reaction curve in elastic ground condition,

$$u_{ag} = (1+v)(p_o-p_{ig})/E \qquad (B.1)$$

From Eq.7.1 for support reaction curve,

$$u_{as} = (u_{ao}/a) + (p_{is}/k) \qquad (B.2)$$

where the subscripts 'g' and 'a' refer to the ground reaction and the support reaction curves respectively.

At the point of intersection of the two curves, $u_{ag}=u_{as}$. At this point, therefore, the right hand sides of Eqs.B.1 and B.2 may be equated. This, together with the substitution of $p_{ig}$ and $p_{is}$ with $p_{if}$ for the point of intersection, results in the following equation:

$$(1+v)(p_o-p_{if})/E_d = (u_{ao}/a) + (p_{if}/k) \qquad (B.3)$$

or, $\qquad p_{if}[(1+v)/E_d + (1/k)] = [(1+v)p_o/E_d - (u_{ao}/a)]$

or, $\qquad p_{if} = \dfrac{[(1+v)p_o/E_d - (u_{ao}/a)]}{[(1+v)/E_d + (1/k)]} \qquad (B.4)$

Substituting for 1/k in Eq.B.4 from Eqs.7.2, 7.3 and 7.4,

$$p_{if} = \dfrac{[(1+v)p_o/E_d - (u_{ao}/a)]}{[(1+v)/E_d] + (S.a/E_s.A_s) + (0.86\ a^{1.05}/t_b.E_{bf})} \qquad (B.5)$$

which is the same as Eq.7.16.

## APPENDIX C

### EXPRESSION FOR SUPPORT PRESSURE
### IN SQUEEZING GROUND CONDITION

From Eq.6.16 for ground reaction curve in squeezing ground condition,

$$u_{ag}/a = 1 - [(1+e) - (b/a)^2 e - 2(b/a)u_b + (u_b/a)^2]^{1/2} \qquad (C.1)$$

From Eq.7.1 for support reaction curve,

$$u_{as}/a = (u_{ao}/a) + (p_{is}/k) \qquad (C.2)$$

where the subscripts 'g' and 'a' refer to the ground reaction and the support reaction curves respectively.

At the point of intersection of the two curves, $u_{ag}=u_{as}$. At this point, therefore, the right hand sides of Eqs.C.1 and C.2 may be equated. This, together with the substitution of b with $b_f$ and $p_{is}$ with $p_{if}$ for the point of intersection, results in the following equation:

$$1-[(1+e)-(b_f/a)^2 e-2(b_f/a)u_b+(u_b/a)^2]^{1/2} = (u_{ao}/a)+(p_{if}/k) \qquad (C.3)$$

$$\text{or,} \ p_{if} = \frac{1-[(1+e)-(b_f/a)^2 e-2(b_f/a)u_b+(u_b/a)^2]^{1/2} - (u_{ao}/a)}{1/k} \qquad (C.4)$$

Substituting for 1/k in Eq.C.4 from Eqs.7.2, 7.3 and 7.4,

$$p_{if} = \frac{1-[(1+e)-(b_f/a)^2 e-2(b_f/a)u_b+(u_b/a)^2]^{1/2}-(u_{ao}/a)]}{(S.a/A_s.E_s)+(0.86 \ a^{1.05}/t_b.E_{bf})} \qquad (C.5)$$

which is the same as Eq.7.18.